IAEA-TECDOC-1238

Gas turbine power conversion systems for modular HTGRs

Report of a Technical Committee meeting
held in Palo Alto, United States of America, 14–16 November 2000

INTERNATIONAL ATOMIC ENERGY AGENCY

August 2001

The originating Section of this publication in the IAEA was:

Nuclear Power Technology Development Section
International Atomic Energy Agency
Wagramer Strasse 5
P.O. Box 100
A-1400 Vienna, Austria

GAS TURBINE POWER CONVERSION SYSTEMS FOR MODULAR HTGRs

IAEA, VIENNA, 2001
IAEA-TECDOC-1238
ISSN 1011–4289

Printed by the IAEA in Austria
August 2001

FOREWORD

The IAEA has been fostering the exchange of information and co-operative research on gas cooled reactor technology with the guidance and support of the International Working Group on Gas Cooled Reactors since 1978. During the 1980s, interest and activities in Member States related to gas cooled reactor technology development shifted from the earlier large high temperature gas cooled reactor (HTGR) plant design using prestressed concrete reactor vessels to small modular designs using steel reactor vessels.

The modular HTGR concept originated in Germany in 1979, based primarily around the concept that by limiting thermal power and allowing sufficient heat losses from the reactor vessel, the key safety function of removal of residual heat could be accomplished without the need for active systems. The economic viability of the concept is based on the presumption that cost savings from system simplification can offset the small unit size. All of the early modular HTGR designs were based on a Rankine cycle with steam conditions similar to modern fossil plants, except without steam reheat. As the designs advanced, more detailed cost estimates indicated that the steam cycle modular HTGR may not be cost competitive. Optimization studies in the 1990s indicated that considerable cost savings could result from application of a closed A brayton cycle using advances in technology for open cycle gas turbines, compact heat exchangers, manufacturing and electronics. While the resulting gas turbine modular HTGR designs are based on existing technology, the specific configurations and operating environment differ considerably from existing applications. These differences introduce uncertainties and issues that must be understood and addressed in the course of development and deployment of the gas turbine modular HTGR concept.

The information presented in this report was developed from an IAEA Technical Committee Meeting (TCM) on Gas Turbine Power Conversion Systems for Modular HTGRs, held 14–16 November in Palo Alto, California, United States of America. The meeting was hosted by the Electric Power Research Institute and included participants from national organizations and industries in Member States. The TCM provided a forum for participants to discuss and share the status of their individual programmes associated with the design and analysis of systems and components for gas turbine modular HTGR power conversion systems.

The IAEA officer responsible for this publication was J.M. Kendall of the Division of Nuclear Power.

EDITORIAL NOTE

This publication has been prepared from the original material as submitted by the authors. The views expressed do not necessarily reflect those of the IAEA, the governments of the nominating Member States or the nominating organizations.

The use of particular designations of countries or territories does not imply any judgement by the publisher, the IAEA, as to the legal status of such countries or territories, of their authorities and institutions or of the delimitation of their boundaries.

The mention of names of specific companies or products (whether or not indicated as registered) does not imply any intention to infringe proprietary rights, nor should it be construed as an endorsement or recommendation on the part of the IAEA.

The authors are responsible for having obtained the necessary permission for the IAEA to reproduce, translate or use material from sources already protected by copyrights.

CONTENTS

SUMMARY

1. OVERVIEW AND PURPOSE

The Technical Committee Meeting (TCM) on Gas Turbine Power Conversion Systems for Modular HTGRs was held 14–16 November 2000 in Palo Alto, California, United States of America. The meeting was hosted by the Electric Power Research Institute, and was convened by the IAEA on the recommendation of its International Working Group on Gas Cooled Reactors (IWGGCR). The meeting was attended by 27 participants from 9 Member States (Argentina, China, France, Japan, Netherlands, Russian Federation, South Africa, United Kingdom and the United States of America). In addition to presentations on relevant technology development activities in participating Member States, 16 technical papers were presented covering the areas of:

- Power conversion system design
- Power conversion system analysis
- Power conversion system component design.

Following the papers, a panel discussion was held on technology issues associated with gas turbine modular HTGR power conversion systems and the potential for international collaboration to address these issues. A summary of the presentations, discussions and recommendations will be prepared for use along with the papers presented in a TECDOC on the subject. A detailed report on the meeting is available.

The purpose of this Technical Committee Meeting was to foster the international exchange of information and perspectives on gas turbine power conversion systems and components for modular HTGRs. The overall objectives were to provide:

- A current overview of designs under consideration
- Information on the commercial availability or development status of key components
- Exchange of information on the issues involved and potential solutions
- Identification of further development needs for both initial deployment and longer term performance enhancement, and the potential for addressing needs through international collaboration.

2. GAS TURBINE MODULAR HTGR NATIONAL DEVELOPMENT ACTIVITIES

The technology for open cycle gas turbines, applied primarily to the combustion of oil and natural gas, has advanced rapidly over recent years, driven by cost and performance competition and supported by advances in high temperature materials, fabrication techniques, engineering design tools, etc. Concurrent application of similar technological advances to heat exchangers has resulted in compact, low cost gas-to-gas units for an expanding range of applications. Advances in electronics support the development of magnetic bearings and introduce the possibility of other innovations, such as a high-speed turbo-generator with high power frequency converter. While these are proven technologies already in commercial application, they have not been combined as a system under the environmental conditions and design constraints relevant to a modular HTGR.

Modular HTGRs utilising closed cycle gas turbines for generation of electricity are a source of considerable current interest and activity among several IAEA Member States. Designs under consideration incorporate recent developments in high temperature materials, electronics, heat exchangers, gas turbine technology, etc. These features are used in conjunction with modular HTGR concepts that have been under development for two decades with an emphasis on passive safety characteristics. Proponents of these designs expect that the simplification of systems from the passive safety characteristics and the reduction in total equipment relative to a steam cycle will allow for an economically competitive nuclear power generation option in the 100 to 300 MW(e) net unit power rating range.

Representatives from each of the participating Member States reported on relevant national activities, as summarized below:

Argentina — Innovative reactor development efforts are focused mainly on the CAREM integral PWR, but some economic assessment work is under way regarding modular HTGRs

China — Loading of fuel in the HTR-10 test reactor was expected to begin in mid November 2000, with initial criticality planned for December. Hot commissioning testing to reach full power is expected to take about one year. Irradiation testing of fuel spheres made in China for the HTR-10 is under way in the Russian Federation, with positive initial results. An evaluation of future directions for development of the modular HTGR in China, assuming successful operation of HTR-10, is under way with consideration of both steam turbine and gas turbine cycles.

France — Most of the activity in France is associated with the European Commission 5th Framework program. The EC work currently addresses fuel technology, reactor physics and fuel cycle, and materials development. Work is in progress on recuperator design in advance of anticipated activities on power conversion system components in the 5th Framework.

Japan — The power ascension testing of the HTTR is continuing, having reached a level of about 10 MWt. Gas turbine modular HTGR feasibility studies addressing both pebble and prismatic block fuel over a core power range of 300–600 MWt are under way. The gas turbine modular HTGR is being considered in a national review of the long-term nuclear energy development program, expected to be completed in December 2000. The Japan Atomic Industrial Forum has requested that the government perform a feasibility study on commercialisation of modular HTGRs. The possibility of locating nuclear power stations in the Tokyo Bay area was raised by the Tokyo metropolitan governor. In related discussions, PBMR was raised as one of the candidates.

Netherlands — A study of PBMR deployment in the Netherlands after demonstration in South Africa is being conducted for Dutch utilities. Work is underway to study the failure of SiC coatings under mechanical loading as a part of studies on long-term waste behaviour of coated particle fuel. Additional supporting activities are being conducted for the PBMR project.

Russian Federation — Work is continuing on the preliminary design of the GT-MHR. Fuel development efforts have produced about 200 g of plutonium kernels for subsequent use in fabrication of coated particles. A test programme for components of the GT-MHR Power Conversion Unit is under development.

South Africa — The PBMR project is proceeding with the addition in recent months of BNFL and Exelon Generation Co. (formerly elements of PECO Energy and Commonwealth Edison) as partners. The detailed PBMR feasibility study is underway, an environmental impact assessment (EIA) has been submitted and the review is in progress, and a safety analysis report has been submitted to the National Nuclear Regulator (NNR) for review. The reviewing Government organisations have agreed to target dates for completion. Assuming a favourable outcome of the EIA, a construction license from NNR, shareholder approval and Government consent, construction activities could commence by the first half of 2002.

United Kingdom — Continued supporting technology development and operation of the Magnox and AGR reactors are producing relevant experience and data. BNFL is playing an active role as a partner in the PBMR project. Organisations in the UK also involved in the PBMR project as contractors include AEA Technologies on graphite internals, GEC Alsthom on the turbo-generator, and Heatrix on the heat exchangers.

United States of America — Several activities on modular HTGR development are in process in the USA. The US Department of Energy has an ongoing project with General Atomics and Oak Ridge National Laboratory, in collaboration with organisations in the Russian Federation, for the development of the GT-MHR concept, and several DOE Nuclear Energy Research Initiative projects are related to HTGR technology. Exelon Generation Company and BNFL/Westinghouse are active participants in the PBMR project, while a co-operative effort of MIT and INEEL is developing a plant concept based in part on the PBMR design. Also, EPRI has initiated an HTGR programme covering a range of specific issues considered important to the success of the technology.

An important aspect of modular HTGR technology development is the emerging trend toward multinational projects. For example, the GT-MHR project involves participants from France, Japan, the Russian Federation and the United States of America. The PBMR project involves partners and contractors from France, Germany, Netherlands, the Russian Federation, South Africa, the UK and the USA. While this trend enhances international exchange of information within the projects, as the technology approaches deployment commercial considerations are beginning to restrict exchange of information outside the projects. This is more the case with power conversion system technology because it primarily involves adaptation of existing commercial technology. Information exchange and co-operative activities in the reactor technology area, as illustrated by activities related to the start-up and operation of the HTTR and HTR-10 test reactors, is less affected.

3. TECHNICAL PRESENTATIONS

As noted earlier, technical presentations were grouped into the subject areas of system design, system analysis, and component design. The information presented in these three areas is very briefly summarized below and copies of the papers are provided later in this report, with the exception of Argentina and the United States of America, which did not provide their presentation material in paper form.

3.1 Power conversion system design

Presentations on the subject were made by participants from Argentina, China, the United States of America, Japan and the Russian Federation:

Argentinean approach of GT reactor technology — Argentina technology development is centered around the CAREM integral PWR design. An economic assessment of GT modular HTGR technology was performed to identify cost targets. Using a higher contingency factor based on Argentina's views of the uncertainty in the costs of this technology, it was concluded that a cost target of US $30–40 million for a plant in the 200-300 MWth size range would be needed.

Study on coupling a gas turbine cycle to the HTR-10 test reactor — The original design of the HTR-10 included provision for replacing the steam generator, to be installed initially, with a heat exchanger for process heat or indirect cycle gas turbine testing. Design studies have been performed for both a direct and indirect gas turbine cycle in future HTR-10 operations. It is anticipated that future operations will include testing of a gas turbine, but a decision on the cycle to be used has not been taken at present.

US history of direct cycle gas turbine HTGRs — US experience included early design and prototype projects beginning with open cycle gas turbines for the ANP project in the late 1950s. Closed cycle designs were developed in the 60's and a large HTGR design was developed in the late 1970s. The evolution of the modular HTGR and its coupling with a gas turbine in the early 1990s was reviewed, including the large number of configuration options considered in the selection of the current design configuration.

Selection of JAERI's HTGR-GT concept — A feasibility study for a gas turbine modular HTGR design has been underway at JAERI since 1996. The study has included both pebble bed and prismatic block concepts and established temperatures and power levels considered optimum for each option. Designs have been developed for a 400 MWt/182 MW(e) pebble bed and a 600 MWt/284 MW(e) prismatic block plant. Power conversion system layout options have included configurations equivalent to the PBMR and GT-MHR designs as well as a JAERI version with horizontal turbomachinery. Evaluation of the designs is continuing, with a final selection expected in the near future

Features of adapting gas turbine cycles and heat exchangers for HTGRs — OKBM optimisation studies for the GT-MHR power conversion unit have been conducted to determine design layout and operating conditions. A reactor inlet temperature of 490°C, limited by reactor vessel material considerations, resulted in an optimum reactor outlet temperature of 850°C. Other parameters studied included reactor pressure, PCU pressure ratio, intermediate conditions and component configuration. A single shaft turbomachine was selected to provide protection against overspeed on a loss of electrical load.

The necessity of achieving competitive economics and balancing of projected cost and technological risk were common themes of the papers. As noted in the US paper, gas turbines have been considered for nuclear power generation for over 40 years, with a major increase in interest and activity in the past decade. Considerable variation in power conversion system layouts (e.g. single vs. multiple shaft, vertical vs horizontal orientations) remains in the designs currently under development.

3.2 Power conversion system analysis

Presentations on the subject were made by participants from the Netherlands and South Africa:

Dynamics of a small direct cycle pebble bed HTR — The ACACIA 40 MWt cogeneration design was analyzed for safety related transients. Loss of coolant and loss of flow events were analyzed along with other events. A long-term low load transient without limits on reactor vessel exit temperatures resulted in the highest fuel temperatures due to reactivity insertions from xenon decay.

Dynamic modelling of a cogenerating nuclear gas turbine plant — A dynamic model of the ACACIA 40 MWt cogeneration design was developed to study response to operational transients for various design options. The model structure and simplifying assumptions were described along with analytic results. The system response for various ratios of heat and electrical output were studied to identify effects of design options and control system parameters. The closed loop responses showed that good set-point tracking for the electricity production and good disturbance-rejection for the recuperator temperature can be achieved.

PBMR dynamic/transient operation and performance prediction — The theory behind the off design and transient modelling of the PBMR design, development of a computer simulation model, and the selection of the PBMR control scheme was described. Areas addressed in the performance review included material selection, modular design, testing and commissioning, prediction of plant performance and controllability, and control system design. Two primary control schemes studied were heat source bypass and inventory control, with the selection of inventory control for efficient changes at moderate speed, and heat source bypass for high-speed changes with short duration.

The papers demonstrated that the analytical capability to perform transient analysis of the power conversion system for safety, equipment protection, and control purposes is well developed. However, because of the complexity of dynamic component behaviour and interactions among components, empirical data on full-scale components and systems is necessary to accurately predict performance with high confidence.

3.3 Power conversion system component design

Presentations on the subject were made by participants from Japan, the Netherlands, France, the UK and the USA:

Study of fission product release, plate-out and maintenance in helium turbomachinery — The generation, release, transport and deposition of ^{137}Cs and ^{110m}Ag was studied for a 600 MWt prismatic design and a 300 MWt pebble bed design. Fission product distribution calculations were based on available empirical data adjusted for the temperature and heat transfer conditions of the designs studied. The local activities were used to estimate allowable time for maintenance of the turbine rotor. The results were considered to have high uncertainties, but times were reported as 11 minutes for the prismatic block and 5.5 hours for the pebble bed. It was concluded that measures to reduce the dose levels for both cases is desired, and a ceramic coating on the turbine blades was identified as the leading candidate.

Fission product transport in the primary system of a pebble bed high temperature reactor — Fission product transport and deposition in the ACACIA 40 MWt pebble bed reactor with a combined heat and power configuration was investigated. Four radionuclides were identified for investigation based on their volatility and radiotoxicity: ^{137}Cs, ^{90}Sr, ^{110m}Ag,

and ^{131}I. Fission product release and distribution in the primary system was calculated as a function of time for normal operation, and for a core heatup incident with damaged fuel.

Compact heat exchanger technologies for HTR recuperator applications — Industrial compact heat exchanger technologies for possible application in the recuperator of a helium gas turbine cycle were investigated. Design categories reviewed included plate, spiral, plate and shell, plate-fin, microchannel, matrix, and flat tube and fin heat exchangers. All of the options identified were assessed for their range of operating parameters relative to the conditions for a recuperator in a modular HTGR closed cycle gas turbine circuit. Diffusion bonded microchannel heat exchangers were identified as the most promising concept for this application.

High temperature alloys for the HTGR gas turbine: Required properties and development needs — Potential high temperature alloys were reviewed for application in the turbine blades and disks of a gas turbine modular HTGR. Turbine materials development for HTGR application was reviewed along with advances in materials for open cycle gas turbines, with consideration of failure modes due to thermal and environmental effects in modular HTGR applications. Nickel based superalloys are being considered for both blades and disks in the current GT-MHR design. Future materials development, and mechanical testing and life modelling requirements were also addressed.

Nuclear graphite for high temperature reactors — Graphite components for cores and reactor internals of both prismatic and pebble bed reactors were reviewed in terms of design conditions and issues. Graphite component manufacturing processes and feed materials were also reviewed along with effects on product microstructure and material properties. Issues and important parameters for reliable service were identified and a proposed specification for HTR graphite was provided.

Auxiliary bearing design considerations for gas cooled reactors — Options for auxiliary bearings to serve as backup to the magnetic bearings employed in the gas turbine modular HTGR designs were reviewed. Existing design configurations along with design considerations and the experience base were addressed for both radial and axial bearings. While the radial auxiliary bearing technology appears well in hand, the heavy loads and vertical orientation of most gas turbine modular HTGR designs present challenges for the axial bearings.

Transportation and deposition of fission products in the form of particulate accumulation or vapour condensation is important from the standpoint of system and component maintenance. Although considerable testing has been done, relatively large uncertainties remain for a given plant concept due to system geometry, operating conditions, and surface and material property variations. Options for mitigation include in-line filters and component surface coatings. Many varieties of compact heat exchangers are in commercial service, with a limited subset having the capability to meet modular HTGR service conditions, but needing further product development for this application. Considerations of low long term creep to maximize service intervals, avoidance of blade cooling to simplify design, and the modular HTGR chemical environment present challenges for turbine component design utilizing existing open cycle turbine technology. Temperature and fluence history are the primary factors driving the design of graphite components, with uncertainties in service life warranting design for replacement wherever practical. Advances in electronics and rapidly expanding operating experience indicate that magnetic bearing technology is generally well in hand, but considerable

uncertainties remain in the design of backup mechanical bearings, particularly thrust bearings, to deal with failure of a magnetic bearing.

4. CONCLUSIONS AND RECOMMENDATIONS

The following conclusions and recommendations were identified as a result of the discussions at the meeting:

1. International review and collaboration is of interest for China and Japan in the planning and conduct of their test programs:
   - Both the HTTR and HTR-10 reactor projects are exploring scale model testing of a gas turbine, with the HTTR project considering a 7 MWt gas heated loop, and HTR-10 a direct or indirect cycle connected to the reactor.
   - The HTR-10 is considering a series of safety demonstration tests to be conducted following completion of the power ascension testing phase.
2. The IAEA Co-ordinated Research Project on Evaluation of HTGR Performance was noted as a possible vehicle for discussion of HTTR and HTR-10 plans.
3. Increasing restrictions on availability of technical information as the technology comes closer to commercial application were noted. The potential commercial advantages of restricting availability of information must be weighed against the added risk due to reduced information exchange and design review inputs. The general consensus was that in several areas of power conversion system design and technology development the uncertainties are sufficient that the benefits of information exchange are likely to outweigh the benefits of commercial advantage to the developers.

BACKGROUND AND SYSTEM DESIGN

(Session 1)

IAEA HIGH TEMPERATURE GAS COOLED REACTOR ACTIVITIES

J.M. KENDALL
International Atomic Energy Agency,
Vienna

Abstract:

IAEA activities on high temperature gas cooled reactors are conducted with the review and support of Member States, primarily through the International Working Group on Gas Cooled Reactors (IWGGCR). This paper summarises the results of the IAEA gas cooled reactor project activities in recent years along with ongoing current activities through a review of Co-ordinated Research Projects (CRPs), meetings and other international efforts. A series of three recently completed CRPs have addressed the key areas of reactor physics for LEU fuel, retention of fission products, and removal of post shutdown decay heat through passive heat transport mechanisms. These activities along with other completed and ongoing supporting CRPs and meetings are summarised with reference to detailed documentation of the results.

1. INTRODUCTION

International interest in HTGR technology has been increasing in recent years due to a growing recognition of the potential of HTGR designs to provide high efficiency, cost effective electricity generation appropriate for the conditions in developing countries, and in the longer term to provide a source of high temperature process heat. The international exchange of information and co-ordination of HTGR research through the IAEA has helped to establish the foundation for the future development and deployment of HTGR technology. The gas cooled reactor activities of the IAEA are conducted with the active participation and advice of the International Working Group on Gas Cooled Reactors. An overview of the IAEA gas cooled reactor activities, modular HTGR technology, and full text versions of IAEA technical documents are available on the Internet at http://www.iaea.org/inis/aws/htgr/index.html.

2. INTERNATIONAL WORKING GROUP ON GAS COOLED REACTORS

The International Working Group on Gas Cooled Reactors is a continuing working group within the framework of the International Atomic Energy Agency with the purpose of advising the Director General of the IAEA and promoting the exchange of technical information in the field of gas cooled reactors. The first meeting of the IWG-CGR was held in 1978, with the most recent meeting (16th) held in June 2000. The focus of interest of this working group is on helium-cooled thermal reactors utilized in steam cycle or direct cycle nuclear plants for electricity and/or heat production, but the scope also includes carbon-dioxide-cooled thermal reactors and, to the extent not already covered by other international organisations, gas-cooled fast reactors.

The IWG-GCR currently includes participants from the following countries:

China	France	Germany
Indonesia	Japan	Netherlands
Poland	Russian Federation	South Africa
Switzerland	United Kingdom	United States of America

The IWG-GCR meets approximately every 18 months to exchange information regarding ongoing and planned activities related to gas cooled reactor technology in participant countries. The results and recommendations of IAEA meetings and Co-ordinated Research Projects related to gas cooled reactor technology held since the previous meeting are presented and reviewed. Other issues and activities of current interest to the Member States are discussed along with recommendations regarding future plans for the IAEA gas cooled reactor project.

3. CO-ORDINATED RESEARCH PROJECTS

Research efforts supported by the IAEA are normally carried out within the framework of Co-ordinated Research Projects (CRPs). CRPs are developed in relation to a well defined research topic on which a number of institutions agree to collaborate, and represent an effective means of bringing together researchers in both developing and industrialised countries to solve a problem of common interest. Each CRP is essentially a network of 5–15 national research institutions mandated to conduct the research within the countries concerned, each being represented by a chief scientific investigator (CSI). A network of institutions is thus established which works within an operational framework for research with a similar and well defined global or regional thematic or problem focus.

Advanced HTGR designs currently being developed are predicted to achieve a high degree of safety with substantially reduced safety related demands on plant operations and licensing oversight through reliance on inherent safety features. These anticipated benefits derive largely from the ability of the ceramic coated fuel particles to retain fission products under normal and accident conditions, the neutron physics behaviour of the core, the chemical stability of the core and the ability of the design to dissipate decay heat by natural heat transport mechanisms without reaching excessive temperatures. In support of licensing and commercial deployment of advanced HTGRs, these features must be demonstrated under experimental conditions representing realistic reactor conditions, and the methods used to predict the performance of the fuel and reactor must be validated against experimental data. Three recently completed CRPs which have been directed toward these considerations are summarised below. Another recently completed and an ongoing CRP directed toward maximising the value of the test programs of the two new experimental HTRs (HTTR and HTR-10) are also summarised. A new CRP directed toward the conservation and application of HTGR technology is under development.

3.1. CRP on validation of safety related physics calculations for low enriched HTGRs

This CRP was formed to address core physics needs for advanced gas-cooled reactor designs. It was focused primarily on development of validation data for physics methods used for core design of HTGRs fuelled with low enriched uranium. Experiments were conducted for graphite moderated LEU systems over a range of experimental parameters, such as carbon-to-uranium ratio, core height-to-diameter ratio, and simulated moisture ingress conditions, which were defined by the participating countries as validation data needs. Key measurements performed during the CRP provide validation data relevant to current advanced HTGR designs including measurements of shutdown rod worth in both the core and side reflector, effects of moisture on reactivity and shutdown rod worth, critical loadings, neutron flux distribution and reaction rate ratios. Countries participating in this CRP included China, France, Germany, Japan, the Netherlands, Poland, the Russian Federation, Switzerland, and the United States of America. Work under the CRP has been completed and a final report is expected to be completed in late 2000.

3.2. CRP on validation of predictive methods for fuel and fission product behaviour in gas cooled reactors

This CRP was formed to review and document the experimental database and predictive methods for HTGR fuel performance and fission product behaviour under normal operation and accident conditions, and to verify and validate methodologies for the prediction of fuel performance and fission product transport. Areas addressed included HTGR fuel design and fabrication, TRISO fuel performance under normal operation, fuel performance and fission product behaviour during heatup under both non-oxidising and oxidising conditions, ex-core fission product transport during normal and accident conditions, and prospects for advanced fuel development. Countries participating in this CRP included China, France, Germany, Japan, Poland, the Russian Federation, the United Kingdom and the United States of America. The results have been documented and published as an IAEA-TECDOC [1].

3.3. CRP on heat transport and afterheat removal for gas-cooled reactors under accident conditions

Within this CRP, the participants addressed the inherent mechanisms for removal of decay heat from GCRs under accident conditions. The objective was to establish sufficient experimental data at realistic conditions, and validated analytical tools to confirm the predicted safe thermal response of advance gas cooled reactors during accidents. The scope included experimental and analytical investigations of heat transport by natural convection, conduction and thermal radiation within the core and reactor vessel, and afterheat removal from the reactor vessel. Code-to-code and code-to-experiment benchmarks were performed for verification and validation of the analytical methods. Countries participating in this CRP included China, France, Germany, Japan, the Netherlands, the Russian Federation and the United States of America. Work under the CRP has been completed and a final report in the form of an IAEA-TECDOC [2] is available for downloading from the GCR Project web site.

3.4. CRP on Design and evaluation of heat utilisation systems for the high temperature test reactor (HTTR*)*

The high temperature capability of HTGR technology has long been recognised as offering the potential for extending the application of nuclear power to a broad range of current and future industrial process heat needs. This CRP was formed to advance the understanding and development of this potential through the examination of specific high temperature process heat applications and identification of prospective experimental programmes on heat utilisation systems which could be carried out by the HTTR. Heat utilisation systems addressed included steam reforming of methane for the production of hydrogen and methanol, carbon dioxide reforming of methane for the production of hydrogen and methanol, thermochemical water splitting for hydrogen production, combined coal liquefaction and steam generation and high temperature electrolysis of steam for hydrogen production. Countries participating in this CRP included China, Germany, Indonesia, Israel, Japan, the Russian Federation and the United States of America. Work under the CRP was completed in 1999, and the results will be documented in a final report in the form of an IAEA-TECDOC.

3.5. CRP on evaluation of high temperature gas cooled reactor performance

The 30 MWt prismatic fuelled HTTR in Japan and the 10 MWt pebble bed fuelled HTR-10 in China will be conducting experimental programmes in support of HTGR development. The primary objectives of this CRP are to evaluate HTGR analytical and experimental

performance models and codes in conjunction with the start-up, steady state and transient operating conditions of the HTTR and the HTR-10, to validate the results achieved in earlier CRPs related to reactor safety, and to assist in the development, performance and evaluation of benchmark code-to-experiment research activities in support of the testing programmes for the HTTR and HTR-10. Utilisation of these test reactors affords an opportunity to validate the analytical findings of the earlier CRPs and represents the next logical step in HTGR technology development. Countries participating in this CRP included China, France, Germany, Indonesia, Japan, the Netherlands, the Russian Federation, South Africa and the United States of America. Work under the CRP is continuing, with completion scheduled for 2002.

3.6. Pending CRP on conservation and application of HTGR technology

During the past several meetings, the IWG-GCR has been concerned with preservation of HTGR technology developed in earlier programmes (e.g. in Germany, the United Kingdom and the United States of America), and its application in support of future programmes (e.g. in China, Japan, and South Africa). Formation of a new CRP is in process to address the recommendations of the IWG-GCR and related consultancy meetings regarding these concerns. The objective the CRP will be to identify research needs and exchange information on advances in technology for a limited number of topical areas of primary interest to HTR development, and to establish, within these topical areas, a centralised co-ordination function for the conservation of HTGR know-how and for international collaboration, utilising electronic information exchange, data acquisition and archiving methods. The topical areas identified include high temperature control rod development, research and irradiation testing of graphite for operation to 1000ºC, R&D on very high fuel burnup, including plutonium, qualification of pressure vessel steels to 500ºC, R&D and component testing of high efficiency recuperator designs, and materials development for turbine blades up to 900ºC for long life creep. The CRP is under development, with results to be documented in a final report in the form of an IAEA-TECDOC.

4. TOPICAL MEETINGS ON HTGR TECHNOLOGY

In addition to long term efforts associated with CRPs, the IAEA fosters the international exchange of information on HTGRs through the organisation of topical meetings on subjects of interest to Member States. When appropriate, the results of these exchanges are documented in reports issued by or with the support of the IAEA. Several meetings held in recent years and their resulting reports are briefly summarised below.

4.1. Uncertainties in physics calculations for gas cooled reactor cores

A Specialists Meeting was held on the subject of uncertainties in physics calculations for GCR cores at the Paul Scherrer Institute in Switzerland in May 1990. The meeting was attended by representatives from Austria, China, France, Germany, Japan, Switzerland, the Russian Federation and the United States of America. A total of 19 papers were presented in the topical areas of comparison of predictions with results from existing HTGRs; predictions of performance of future HTGRs; and critical experiment planning and results. The papers were compiled and published as an IAEA document [3] on the proceedings of the meeting.

4.2. Behaviour of gas cooled reactor fuel under accident conditions

A Specialists Meeting was held on the subject of behaviour of GCR fuel under accident conditions at the Oak Ridge National Laboratory in the United States of America in November 1990. The meeting was attended by representatives from France, Germany, Japan, the Russian Federation, Switzerland, the United Kingdom and the United States of America. A total of 22 papers were presented in the topical areas of current research and development programmes for fuel; fuel manufacture safety requirements and quality control; modelling of fission product release; irradiation testing/operational experience with fuel elements; and behaviour at depressurisation, core heat-up, power transients and steam/water ingress. The papers were compiled and published as an IAEA document [4] on the proceedings of the meeting.

4.3. The status of graphite development for gas cooled reactors

A Specialists Meeting was held on the subject of graphite development for gas cooled reactors at the Japan Atomic Energy Research Institute in September 1991. The meeting was attended by representatives from France, Germany, Japan, the Russian Federation, the United Kingdom and the United States of America. A total of 33 papers were presented in the topical areas of graphite design criteria, fracture mechanisms and component tests; graphite materials development and properties; and non-destructive examinations, inspections and surveillance of graphite materials and components. The papers were compiled and published as an IAEA-TECDOC [5] on the proceedings of the meeting.

4.4. High temperature applications of nuclear energy

A Technical Committee Meeting on the subject of high temperature applications of nuclear energy was held at the Japan Atomic Energy Research Institute in October 1992. The meeting was attended by representatives from China, France, Germany, Japan, Poland, the Russian Federation, Venezuela, the United Kingdom and the United States of America. A total of 17 papers were presented in the topical areas of industrial/user needs, potential applications of high temperature nuclear process heat and system economics; reactor and heat utilisation system technology and safety; and component and system design, development and testing. The papers were compiled and published as an IAEA-TECDOC [6] on the proceedings of the meeting.

4.5. Response of fuel, fuel elements and gas cooled reactor cores under accidental air or water ingress conditions

A Technical Committee Meeting on the subject of response of fuel, fuel elements and gas cooled reactor cores under accidental air or water ingress conditions was held at the Institute for Nuclear Energy Technology in China in October 1993. The meeting was attended by representatives from China, France, Germany, Japan, the Netherlands, Switzerland, the Russian Federation, the United Kingdom and the United States of America. A total of 19 papers were presented in the topical areas of experimental investigations of the effects of air and water ingress; predicted response of fuel, graphite and other reactor components; and options for minimising or mitigating the effects of air or water ingress. The papers were compiled and published as an IAEA-TECDOC [7] on the proceedings of the meeting.

4.6. Development status of modular HTGRs and their future role

A Technical Committee Meeting on the subject of development status of modular HTGRs and their future role was held at the Netherlands Energy Research Foundation in November 1994. The meeting was attended by representatives from China, France, Germany, Indonesia, Japan, the Netherlands, Switzerland, the Russian Federation and the United States of America. A total of 33 papers were presented in the topical areas of status of national GCR programmes and experience from operation of GCRs; advanced HTR designs and predicted performance; and future prospects for advanced HTRs and the role of national and international organisations in their development. The papers were compiled and published as an ECN report [8] on the proceedings of the meeting.

4.7. Graphite moderator lifecycle behaviour

A Specialists Meeting on the subject of graphite moderator lifecycle behaviour was held in Bath, United Kingdom in September 1995. The meeting was attended by representatives from France, Germany, Japan, Lithuania, the Russian Federation, the United Kingdom and the United States of America. A total of 27 papers were presented addressing a range of topics including irradiation behaviour, graphite performance assessment methodologies, oxidation effects, material properties and development of new materials. The papers were compiled and published as an IAEA-TECDOC [9] on the proceedings of the meeting.

4.8. Design and development of gas cooled reactors with closed cycle gas turbines

A Technical Committee Meeting on the subject of design and development of gas cooled reactors with closed cycle gas turbines was held at the Institute for Nuclear Energy Technology in China in August 1996. The meeting was attended by representatives from China, France, Germany, Japan, the Netherlands, the Russian Federation, South Africa and the United States of America. A total of 16 papers were presented in the topical areas of summaries of national and international activities in gas cooled reactors; design of HTGRs with closed cycle gas turbines; licensing, fuel and fission product behaviour; and gas-turbine power conversion system development. The papers were compiled and published as an IAEA-TECDOC [10] on the proceedings of the meeting.

4.9. High temperature gas cooled reactor technology development

A Technical Committee Meeting on the subject of HTGR technology development was held in Johannesburg, South Africa in November 1996. The meeting was attended by representatives from China, France, Germany, Indonesia, Japan, the Netherlands, the Russian Federation, South Africa, the United Kingdom and the United States. A total of 32 papers were presented covering a large range of topics including GCR programme development; GCR safety and management; development of the pebble bed modular reactor plant in South Africa; HTR plant system and component design; and technical developments in GCR design. The papers were compiled and published as an IAEA-TECDOC [11] on the proceedings of the meeting.

4.10. Technologies for gas cooled reactor decommissioning, fuel storage and waste disposal

A Technical Committee Meeting on technologies for gas cooled reactor decommissioning, fuel storage and waste disposal was held at Forschungszentrum Jülich, Germany in September

1997. The meeting was attended by representatives from China, France, Germany, Japan, the Netherlands, the Russian Federation, Slovakia, Spain, Switzerland, South Africa, the United Kingdom and the United States of America. A total of 25 papers were presented in the topical areas of status of plant decommissioning programmes; fuel storage, status and programmes; and waste disposal and decontamination practices. The papers were compiled and published as an IAEA-TECDOC [12] on the proceedings of the meeting.

4.11. High temperature gas cooled reactor applications and future prospects

A Technical Committee Meeting on HTGR applications and future prospects was held at the Netherlands Energy Research Foundation in November 1997. The meeting was attended by representatives from China, France, Germany, Japan, the Netherlands, the Russian Federation, South Africa, the United Kingdom and the United States of America. A total of 21 papers were presented in the topical areas of status of GCR programmes, HTGR applications, and HTGR development activities. The papers were compiled and published as an ECN report [13] on the proceedings of the meeting.

4.12. Safety related design and economic aspects of high temperature gas cooled reactors

A Technical Committee Meeting on safety related design and economic aspects of HTGRs was held at the Institute for Nuclear Energy Technology in China in November 1998. The meeting was attended by representatives from China, France, Germany, Indonesia, Japan, the Netherlands, the Russian Federation, South Africa, the United Kingdom and the United States of America. A total of 24 papers were presented in the general topical areas of status of design and development activities associated with safety related and economic aspects of HTGRs; and identification of pathways which may provide the opportunity for international co-operation in addressing these issues. Publication of the proceedings of the meeting as an IAEA-TECDOC is in process.

4.13. Gas turbine power conversion systems for modular HTGRs

This Technical Committee Meeting, scheduled for November 2000, is intended to foster the international exchange of information on gas turbine power conversion systems and components for modular HTGRs. The overall objectives are to provide a current overview of designs under consideration, information on the commercial availability or development status of key components, exchange of information on the issues involved and potential solutions, identification of further development needs for both initial deployment and longer term performance enhancement, and the potential for addressing needs through international collaboration. The proceedings of the meeting will be published as an IAEA-TECDOC.

5. OTHER IAEA ACTIVITIES IN SUPPORT OF HTGR TECHNOLOGY DEVELOPMENT AND APPLICATION

In addition to the CRP and meeting activities discussed previously, the IAEA has supported the development of HTGR technology through production of additional documents and establishment of a database for irradiated graphite as summarised below. An important new activity is the application of IAEA nuclear safety standards to HTGRs.

5.1. Hydrogen as an energy carrier and its production by nuclear power

This report [14], developed under contract to the IAEA, documents past activities as well as those currently in progress by Member States in the development of hydrogen as an energy carrier and its corresponding production through the use of nuclear power. It provides an introduction to nuclear technology as a means of producing hydrogen or other upgraded fuels and to the energy carrier hydrogen and its main fields of applications. Emphasis is placed on high-temperature reactor technology which can achieve the simultaneous generation of electricity and the production of high-temperature process heat.

5.2. Irradiation damage in graphite due to fast neutrons in fission and fusion systems

This report was developed with the joint support of the IAEA and the United Kingdom Health and Safety Executive to document information that has been accumulated and understanding that has been gained from research on the subject of radiation damage in graphite. Topical areas addressed include fundamentals of radiation damage in graphite due to energetic neutrons; the structure and manufacture of nuclear graphite; dimensional changes in graphite and the thermal expansion coefficient; stored energy and the thermo-physical properties of graphite; mechanical properties and irradiation creep of graphite; the electronic properties of irradiated graphite; pyrocarbon in high temperature nuclear reactors; and radiolytic oxidation in graphite. An IAEA-TECDOC [15] is available for downloading from the GCR Project web site.

5.3. International database on irradiated nuclear graphite properties

In conjunction with support from Japan, South Africa and the United Kingdom, the IAEA is establishing an international database on irradiated nuclear graphite properties. The objective of the database is to preserve existing knowledge on the physical and thermo-mechanical properties of irradiated nuclear graphites, and to provide a validated data source for all participating Member States with interest in graphite-moderated reactors or development of high-temperature gas cooled reactors, and to support continued improvement of graphite technology for applications. The database is currently under development and includes a large quantity of irradiated graphite properties data, with further development of the database software and input of additional data in progress. Development of a site on the internet for the database, with direct access to unrestricted data, is also currently in progress.

5.4. Application of IAEA nuclear safety standards to HTGRs.

In July 2000, the IAEA Nuclear Safety Department, in conjunction with CEA (France), held a workshop on Safety and Licensing Aspects of Modular High Temperature Gas Cooled Reactors. A consultancy held in parallel with the workshop, and additional meetings planned for 2001 are intended to provide a general approach for the design and safety assessment of modular HTGRs, including methods of analysis and criteria, implementation of defence in depth, and achievement of the fundamental safety functions and their implication on the safety classification of structures, systems and components. Existing experimental data and analytical methods and results of relevance to the safety assessment of modular HTGR designs, and existing licensing experience and applicable precedents will be summarized, and the applicability of the existing IAEA Safety Standards to HTGRs will be assessed.

REFERENCES

[1] IAEA-TECDOC-978, "Fuel Performance and Fission Product Behaviour in Gas Cooled Reactors, November 1997

[2] IAEA-TECDOC-1163, "Heat Transport and Afterheat Removal for Gas Cooled Reactors Under Accident Conditions", 2000

[3] IWGGCR/24, "Uncertainties in Physics Calculations for Gas Cooled Reactor Cores", April 1991.

[4] IWGGCR/25, "Behaviour of Gas Cooled Reactor Fuel Under Accident Conditions", November 1991.

[5] IAEA-TECDOC-690, "The Status of Graphite Development for Gas Cooled Reactors", February 1993.

[6] IAEA-TECDOC-761, "High Temperature Applications of Nuclear Energy", August 1994.

[7] IAEA-TECDOC-784, "Response of Fuel, Fuel Elements and Gas Cooled Reactor Cores Under Accidental Air or Water Ingress Conditions", January 1995.

[8] ECN-R-95-026, "Development Status of Modular HTGRs and Their Future Role", September 1995.

[9] IAEA-TECDOC-901, "Graphite Moderator Lifecycle Behaviour", August 1996.

[10] IAEA-TECDOC-899, "Design and Development of Gas Cooled Reactors with Closed Cycle Gas Turbines", August 1996.

[11] IAEA-TECDOC-988, "High Temperature Gas Cooled Reactor Technology Development", December 1997.

[12] IAEA-TECDOC-1043, "Technologies for Gas Cooled Reactor Decommissioning, Fuel Storage and Waste Disposal", September 1998.

[13] ECN-R-8-004, "High Temperature Gas Cooled Reactor Applications and Future Prospects", September 1998.

[14] IAEA-TECDOC-1085, "Hydrogen as an Energy Carrier and Its Production by Nuclear Power", May 1999.

[15] IAEA-TECDOC-1154, "Irradiation Damage in Graphite Due to Fast Neutrons in Fission and Fusion Systems", 2000

DEVELOPMENT HISTORY OF THE GAS TURBINE MODULAR HIGH TEMPERATURE REACTOR

H.L. BREY
Vail, Colorado,
United States of America

Abstract:

The development of the high temperature gas cooled reactor (HTGR) as an environmentally agreeable and efficient power source to support the generation of electricity and achieve a broad range of high temperature industrial applications has been an evolutionary process spanning over four decades. This process has included ongoing major development in both the HTGR as a nuclear energy source and associated power conversion systems from the steam cycle to the gas turbine. This paper follows the development process progressively through individual plant designs from early research of the 1950s to the present focus on the gas turbine modular HTGR.

1. INTRODUCTION

This report traces the world-wide development of the HTGR through individual plant designs and selected facilities from initial research to the present focus on the modular HTGR coupled to the gas turbine. This developmental path has followed an evolutionary process spanning the last half of the twentieth century and, with some discretionary latitude, can be divided into the following five general areas:

- Gas cooled reactor (GCR) development and early HTGR research
- HTGR prototype plants
- HTGR demonstration plants and large plant designs
- Modular HTGR steam cycle plant development
- Modular HTGR gas turbine plant development.

This maturing process has often been quite successful, but also tempered with developmental set-backs. However, one constant throughout this evolution has been the continuing pursuit for HTGR improvement as a safer, more efficient, environmentally acceptable and economically realistic source of nuclear energy for society.

A graphical presentation and the design characteristics of selected HTGRs are provided as Appendix A and B, respectively, at the end of this report.

2. GAS COOLED REACTOR (GCR) DEVELOPMENT AND EARLY RESEARCH

Gas-cooled reactor history effectively begins with the startup in November 1943 of the graphite-moderated, air-cooled, 3.5-MW, X-10 reactor in Oak Ridge, Tennessee. The X-10 was the pilot plant for the water-cooled, plutonium production reactors at Hanford, Washington, and used open-circuit cooling (that is, the air coolant was drawn from and exhausted to the atmosphere). Commercial gas-cooled nuclear power began in 1953 when the United Kingdom decided to combine plutonium production with electric power generation, and work was started on the four-unit power station at Calder Hall.

These first power reactors were graphite moderated with natural-uranium metal rods and cooled by forced circulation of carbon dioxide at a pressure of 0.8 MPa and at an outlet temperature of 335°C (635°F). The Calder Hall reactors became operational in 1956, and continue to produce a combined electrical power of 270 MW. The UK's extensive commitment to GCR technology has included construction of 26 Magnox reactors (20 remain in operation) and 14 advanced gas-cooled reactors (AGRs), which deliver steam at the modern conditions of 538°C (1000°F) and 16.5 MPa (2400 psi).

France's early interest in the GCR aided development in the UK In 1951, the 2-MW research reactor at Saclay, which began operating with nitrogen coolant and later switched to carbon dioxide, was the first gas-cooled reactor to use closed circuit, pressurized cooling. These experiments, coupled with the experience of the air-cooled, open-circuit, G1 plutonium production reactor, formed the basis for France's GCR program. Although similar to the U.K's program in coolant, moderator, and fuel, the French program introduced the use of the prestressed concrete reactor vessel (PCRV), which the United Kingdom adopted for its later Magnox reactors and all of its AGRS.

The first nuclear power reactor in Japan, which started commercial operation in July 1966, was the carbon dioxide-cooled, 166 MW(e) Tokai station located 80 miles northeast of Tokyo. The plant design generally followed the design of the U.K's Magnox reactors; however, because of population concerns, its containment design provided a partial third barrier for a postulated release of coolant by sealing after pressure decay. In 1969, the Japan Atomic Energy Research Institute (JAERI) initiated studies on the very high temperature gas-cooled reactor (VHTR) in recognition that a nuclear process heat source of 900°C or higher would find use in coal gasification and hydrogen and methanol production [1].

Development of the HTGR began in the 1950s to improve upon GCR performance. HTGRs utilize ceramic fuel particles surrounded by coatings and dispersed in a graphite matrix, along with a graphite moderator. Either prismatic type graphite moderator blocks (block type reactor) or spherical fuel elements (pebble bed type reactor) are employed. Helium is used as the coolant to permit an increase in the operating temperature, and flows through coolant holes in the block type elements, or through the interstices present in the pebble bed core. HTGRs can operate at very high core outlet coolant temperatures because of the use of an all ceramic core [3].

3. HTGR PROTOTYPE PLANTS

The initial HTGRs included the Dragon reactor experiment, the Arbeitsgemeinshaft Versuchsreaktor (AVR) and Peach Bottom (No. 1). Common among these plants were the utilization of steel vessels to contain the primary system and the attainment of high core outlet temperatures culminating in the AVR achieving extended operation at 950°C.

3.1 Dragon Reactor Experiment

The Dragon reactor in the UK was the first HTGR prototype. It began in 1959 as an international project of the European Organization for Economic Cooperation and Development [4]. The initial objective of this project was to demonstrate the feasibility of the HTGR and to launch the development of a technology which had already begun at a low level in various national laboratories. Simultaneously with the initiation of the Dragon project, interest in Germany and the US led to the 15 MW(e) AVR at Julich and the 40 MW(e) HTGR at Peach Bottom, respectively.

The Dragon Reactor Experiment first operated at power in July 1965 and reached its full-power operation of 20 MW(t) by April 1966. The reactor had a steel pressure vessel, graphite fuel elements with high-enriched uranium-thorium carbide coated fuel particles, and a helium coolant. Exit helium at 750°C (1382°F) was circulated through primary heat exchangers and returned at 350°C (electric power generation was not a feature of this prototype.) The reactor operated for long periods at full power and demonstrated the successful operation of many components, e.g., the helium circuit purification system, the control rod drives, the fuel handling equipment, the gas-bearing circulators, and the reactor fuel. As a test bed, it provided much information on fuel and material irradiation tests and component tests under high-purity helium conditions. The reactor operated until March 1976, at which time the project was terminated [5].

3.2 The AVR

In August 1959, the order was placed with the German partnership of BBC/Krupp for the construction of an experimental nuclear power plant with a high temperature reactor of 46 MW(t)/15 MW(e). Construction work on the plant at the KFA Nuclear Research Center in Juelich began in 1961. Initial reactor criticality occurred in August 1966, and on 17 December 1967 electricity was supplied to the public supply grid for the first time. In February 1974, the mean gas outlet temperature, which had initially been set at 850°C, was increased to 950°C. Operation of the AVR continued until December 1988. In completing 21 years of service, the plant had accumulated more than 122,000 hours of operation with a 66.4% overall availability and had generated 1.67 billion kwhr of electricity [3].

The design of the AVR included a steel containment vessel and used particle fueled, graphite spheres 6 cm in diameter that traveled downward through the core. Although the AVR initially included a core outlet temperature of 850°C, this was subsequently raised to 950°C without decrease in plant performance. The AVR was the main fuel development tool for the pebble bed concept, and it and supplementary laboratory fuel testing became the major support of Germany's position that an LWR-type containment barrier was not needed for future HTGRs [6].

The core of the reactor consisted of a pebble bed containing 100,000 fuel spheres in a graphite reflector pot. The steam generator was located above the core and shielded against radiation from the core by a 50 cm thick top reflector made of graphite and two additional 50 cm thick layers of carbon bricks. The coolant was helium, pressurized to 10 bar and circulated by two blowers located in the lower section of the reactor vessel. The helium was heated in the core from 270°C to 950°C and then flowed through the steam generator, where it transferred the energy to the water/steam circuit. The generated steam had a pressure of 73 bar and a temperature of 505°C. The core, steam generator and blowers were surrounded by two concentrically arranged reactor vessels. The interspace between the vessels was filled with helium at a pressure slightly above the coolant gas pressure.

In addition to continuous component testing and the collection of operating experience and results, the plant was also used during its operating period for the implementation of several experiments. In particular, these included the testing of various types of fuel elements, investigations of fission product behavior in the circuit, experiments on the chemistry of coolant gas impurities and the performance of several tests related to HTGR safety.

During the last few years, the operating mode of the AVR was increasingly oriented to performing test programs related to HTGR performance and safety. During 1988, operations

were centered almost exclusively on tests related to the safety of HTGRs and, in particular, to the performance of simulated loss of coolant accidents [3].

3.3 Peach Bottom (No. 1)

Peach Bottom Unit 1 was the first prototype HTGR in the USA The 40 MW(e) plant, owned and operated by the Philadelphia Electric Company, was built as part of the US Atomic Energy Commission (USAEC) Power Reactor Demonstration Program and the High Temperature Reactor Development Associates (HTRDA) Program to demonstrate the feasibility of a high performance, helium cooled, nuclear power plant.

The reactor achieved initial criticality on March 3, 1966, and the plant went into commercial operation in June 1967. It operated successfully with a gross capacity factor of 74% and an overall availability of 88% (exclusive of planned shutdowns for R&D programs) from June 1967 until October 31, 1974, when it was shut down for decommissioning. Decommissioning was a planned economic decision, based on the additional costs associated with satisfying revised USAEC safety requirements. Accumulated operation totaled 1,349 effective full-power days, for a total of 1,385,919 gross electrical megawatt hours generated.

Peach Bottom provided a valuable demonstration of the high-temperature reactor concept by confirming the core physics calculations, verifying the design analysis methods, and providing a data base for further design activities in the following areas: reactor core; mechanisms in high-temperature helium; helium purification systems; and steam generator tube materials.

Two reactor cores were utilized in the operation of Peach Bottom. The fuel particles in Core 1 were coated with a single layer of anisotropic carbon. Fast-neutron-induced dimensional changes resulted in fracture and distortion of the coatings, which eventually resulted in 90 cracked fuel element sleeves out of 804. Plant operation, however, was not impaired; reactor operation continued, and primary circuit activity reached a maximum of 270 Ci, well below the design activity level of 4,225 Ci. Core 1 accumulated 452 equivalent full power days before it was replaced with Core 2. Core 2, which provided buffer isotropic pyrolytic carbon (BISO) coatings on the fuel particles, operated with no fuel failures for its full design lifetime of 897 equivalent full power days. The primary circuit activity averaged only 0.5 Ci during this period.

Throughout the operation of Peach Bottom, excellent agreement was found between the predicted and the actual plant design characteristics, verifying the methods used and providing a reference data base for application to larger HTGR plants. The overall plant control system functioned exceptionally well, and the plant was operated in a load-following manner during the majority of its lifetime, demonstrating the ability of the HTGR to function in this manner [5].

4. HTGR DEMONSTRATION PLANTS AND LARGE PLANT DESIGNS

Early international development of the HTGR focused on two basic core designs recognized specifically by their fuel element structure. The German core design has generally followed a core design incorporating spherical fuel elements (pebble bed), whereas, beginning with Fort St. Vrain (FSV), the US core design included ceramic coated fuel particles imbedded within rods placed in large hexagonal shaped graphite elements. The other major HTGR designer during this period was Russia with their VG series of plant designs which incorporated the pebble bed core.

The HTGR plants that followed the successful AVR and Peach Bottom included construction of FSV and the Thorium High Temperature Reactor (THTR-300). A major shift occurred with these plants including primary systems enclosed within PCRVs rather then steel vessels, and accompanied by significant increases in plant power level.

These two features were to be dominant throughout HTGR development of the 1970s and early 1980s. Although the general focus of the HTGR plant designers was on the development of large steam cycle units, including the first significant design for a closed cycle gas turbine plant, these designs did not materialize into the commissioning of a nuclear plant. This was primarily attributed to the nuclear industry being in a general state of decline in those countries with national HTGR development programs.

Performance of the THTR-300 and FSV in validating reactor safety characteristics and the TRISO coated fuel particle was very good. However, FSV was beset with inconsistent operation and a corresponding low capacity factor throughout its life. The THTR-300 was also plagued with problems primarily associated with changing regulatory requirements that contributed to delays that eventually ended up with a construction period of ~14 years. Corresponding financial concerns by the operating utilities led to the premature shutdown of both these plants in the 1988-1989 time frame.

4.1 Fort St. Vrain (FSV)

The FSV HTGR was operated by Public Service Company of Colorado as part of the United States Atomic Energy Commission's Advanced Reactor Demonstration Program. This plant was designed with several advanced features including; a.) A PCRV containing the entire primary coolant system, b.) A core of hexagonal, graphite block fuel elements and reflectors with fuel in the form of ceramic coated (TRISO) particles, c.) Once-through steam generator modules producing 538°C superheated main and reheat steam, and d.) Steam-turbine-driven axial helium circulators. At its rated capacity, the FSV plant generated 842 MW(t) to achieve a net output of 330 MW(e).

The steam cycle was essentially conventional, utilizing a standard reheat turbine, except that the steam flow was from the high-pressure turbine exhaust to the helium circulator turbines before being reheated and returned to the intermediate pressure turbine. The steam conditions were comparable to those of modern fossil units.

Initial electric power generation was achieved at FSV in December 1976, and 70% power was reached in November 1977. Full-power operation was achieved in November 1981 [5]. Although ~5.5 billion kwhr of electricity was generated at FSV, the plant operated at low availability primarily because of excessive downtime due to problems with the water-lubricated bearings of the helium circulators.

In spite of this low availability, the plant was a valuable technology test-bed, successfully demonstrating the performance of several major systems, including the reactor core with TRISO coated fuel particles in hexagonal graphite blocks, reactor internals, steam generators, fuel handling and helium purification [1].

4.2 Thorium High Temperature Reactor (THTR-300)

The THTR-300 nuclear power plant included a steam cycle for the generation of electric power with a net output of 296 MW. The heat generated in the reactor core of the helium cooled, graphite moderated high temperature reactor was transported via the helium gas

coolant circuit (primary system) to the steam generators where it was transferred to the steam-feedwater circuit (secondary system) and then transported to the turbine generator. The secondary system was cooled by means of a 180 m high natural draught dry cooling tower [3].

The THTR-300 power plant was sponsored by the Federal Republic of Germany and Nordrhein Westfalen (NRW). Construction of this 300 MW(e) plant began in 1971, but primarily due to increasing licensing requirements, the plant was not completed until 1984. This pebble bed reactor plant was connected to the electrical grid of the utility Hochtemperatur-Kernkraftwerk GmbH (HKG) in November 1985. In August 1989, the decision was made for the permanent shutdown of the THTR-300. This action was not due to technical difficulties associated with the plant, but was the result of an application by HKG for early decommissioning based on a projected short fall in funding and contractual changes in the allocation of decommissioning costs between the FRG, NRW and HKG that would take effect upon the termination of the demonstration phase in 1991. Operation of the THTR-300 was successful in validating the safety characteristics and control response of the pebble bed reactor, primary system thermodynamics and the good fission product retention of the fuel elements [2]. The plant operated over 16,000 hrs. and generated 2.891 billion kwhr of electricity [20].

4.3 Large HTGR Steam Cycle Plant Designs [2]

The primary focus of international HTGR designers in the 1970s and early 1980s was associated with the development of large HTGR units. Continued interest in development of larger steam cycle HTGR plants included the German HTR-500, the Russian VG-400 and the United States' HTGR-Steam Cycle (SC) plants.

In the USA, the focus in the early 1970s was on HTGR-Steam Cycle designs of 770 to 1,160 MW(e). Contracts to General Atomics from US utilities included 10 plants that did not materialize due primarily to the 1973 oil crisis and corresponding economic setback and collapse of the US nuclear power market of 1975. These plants incorporated cores of hexagonal graphite blocks with TRISO coated fuel particles similar to FSV.

The HTR-500 made considerable use of the technology development for the THTR-300, with simplifications and optimizations based on practical experiences with the THTR-300 [3]. This plant featured a simple design with the primary system components located within a single cavity PCRV, and included a pebble bed reactor power level of 1,390 MW(t) to produce 550 MW(e) of electricity.

The Russian HTGR development program included the VG series of plants primarily developed at OKBM in Nizhny Novgorod. Of these, the VG-400 design incorporated a pebble bed reactor with a final power level of 1,060 MW(t) for co-generation applications of electricity generation and process heat production for steam reforming of methane. The reactor was designed for a core helium outlet temperature of 950°C. During the preliminary phases of the design development both the pebble bed and prismatic fuel block variants of the core were analyzed. As a result of the design and engineering analysis, the pebble bed core was chosen for further development due to considerations of simplified fuel element manufacturing technology and possibility of full scale testing in experimental reactors, utilization of a simplified core refueling mechanism and the possibility of core refueling during on-load reactor operation. Also considered was a gas turbine cycle/VG-400 reactor plant.

4.4 Early Gas Turbine HTGR Assessment

A promising approach for making good use of the high temperature capability of the HTGR is to use the primary helium coolant to drive a gas turbine in a direct closed cycle arrangement. In the 1970s, this was extensively studied in the USA, Germany, the UK and France. At that time, the concept was based on enclosing a large (2,000 to 3,000 MW(t)) reactor core and the gas turbine power conversion system within a prestressed concrete reactor vessel [19]. One of the early gas turbine designs was the HTGR-GT by General Atomics. This plant was projected to have the potential for high plant efficiencies (40%) under dry cooling conditions and achievement of even higher efficiencies (50%) when bottoming cycles were incorporated. An assessment of this plant was subsequently conducted in ~ 1980 with the focal point for the assessment being the potential commercial HTGR-GT plant having the following characteristics:

- Size 2000 MW(t)/800 MW(e)
- Core outlet temperature 850°C
- Number of heat transport turbine loop 2

T'he principal findings of the assessment (in the early1980s) were as follows: (1) the HTGR-GT is feasible, but with significantly greater development risk than that associated with the HTGR-SC; (2) at the level of performance corresponding to the reference design, no incremental economic incentive can be identified for the HTGR-GT to offset the increased development costs and risk relative to those for the HTGR-SC (this was true over the range of cooling options investigated); (3) the relative economics of the HTGR-GT and HTGR-SC are not significantly affected by dry cooling considerations; and (4) although the reduced complexity of the cycle may ultimately result in a reliability advantage for the HTGR-GT, the value of that potential advantage could not be quantified.

Although these (early 1980s) findings did not provide the basis for the HTGR-GT as the preferred lead commercial plant (for General Atomics), the HTGR-GT continued to engender interest from participating utilities. This interest stemmed from the potential of the HTGR-GT for improved efficiencies at high core outlet temperatures, the basic simplicity of the gas turbine cycle (low maintenance, high capacity factors), low water use requirements and attractive co-generation characteristics [5].

In retrospect, this plant, although significantly different in general configuration compared to the current modular HTGR/gas turbine designs, the basic cycle remain unaltered throughout these past twenty years. Figures 1 and 2 provide the HTGR-GT configuration and basic cycle diagram, respectively.

5. MODULAR HTGR STEAM CYCLE PLANT DEVELOPMENT

The overall good safety characteristics of all HTGRs are due to: the high heat capacity of the graphite core; the high temperature capability of the core components; the chemical stability and inertness of the fuel, coolant, and moderator; the high retention of fission products by the fuel coatings, the single phase characteristics of helium coolant; and the inherent negativetemperature coefficient of reactivity of the core. Figure 3 provides a graphic overview of maximum accident core temperatures for US HTGR designs.

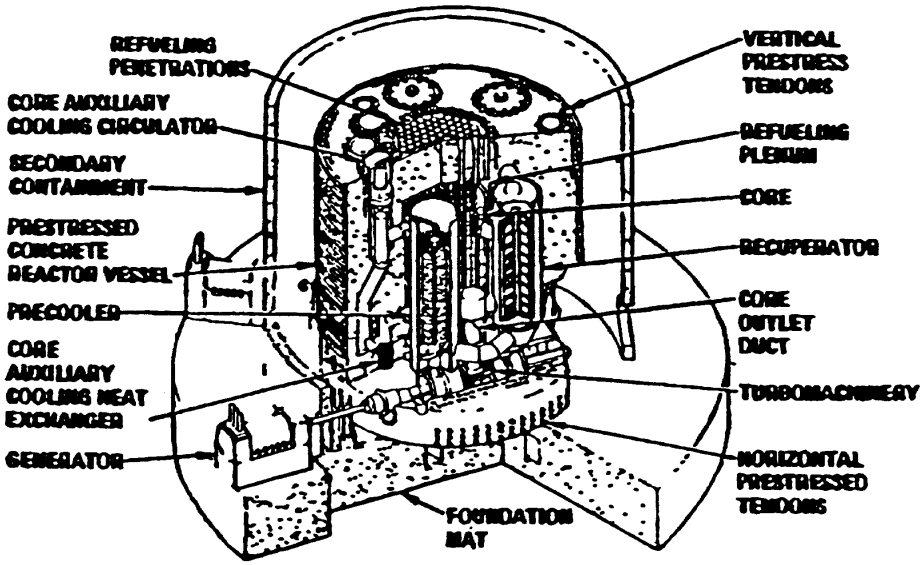

FIG. 1: HTGR-GT system [5].

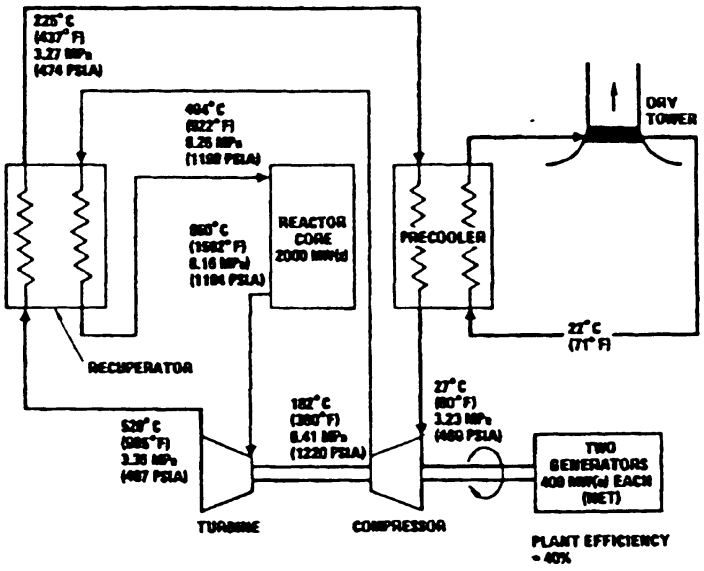

FIG. 2: HTGR-GT cycle diagram [5].

The modular HTGR adds the unique characteristic of being able to cool the reactor entirely by passive heat transfer mechanisms following postulated accidents without exceeding the failure temperature of the coated particles. This characteristic has been achieved by deliberately decreasing the core power level and configuring the reactor so that natural heat removal processes can limit fuel temperatures to levels at which the release of fission products from the reactor system to the environment is insignificant for postulated accidents. Even for extreme accidents having very low probabilities of occurrence, the cumulative fission product release at the site boundary is estimated to be below those acceptable under defined protective action guidelines [2].

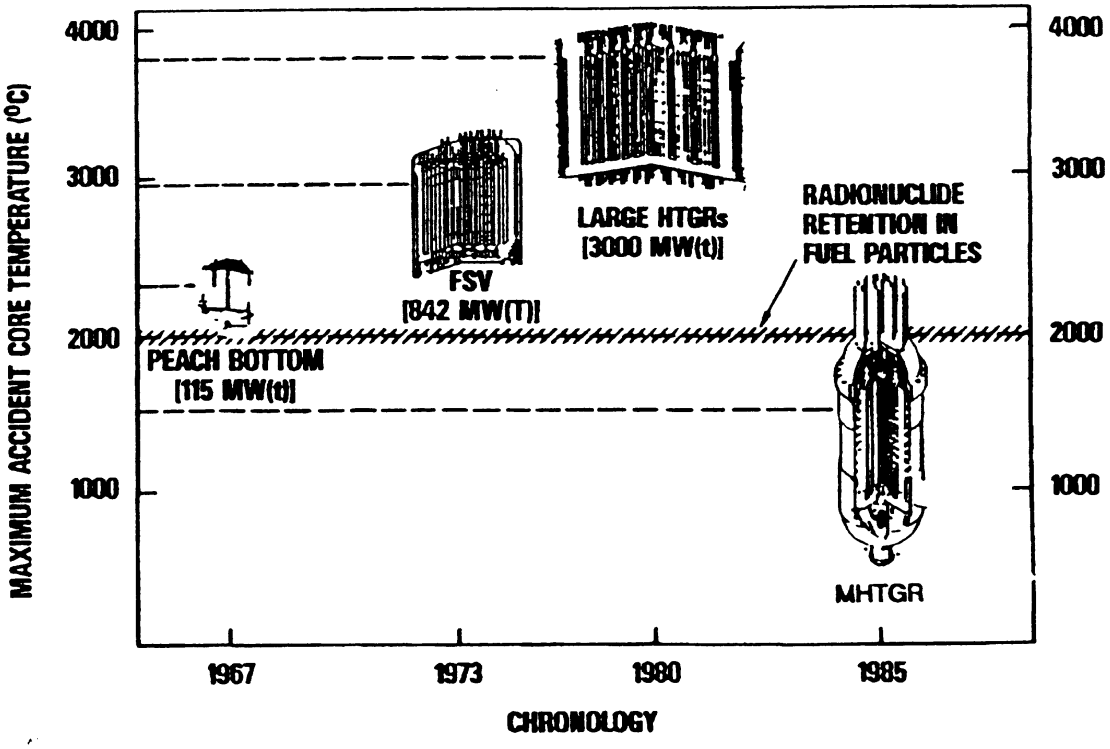

FIG. 3: Maximum accident core temperature depicted chronologically for US HTGR designs [1].

5.1 HTR-MODULE [3]

The 80 MW(e) HTR module (HTR-MODULE) concept, developed by Siemens/Interatom, was the first small, modular type HTGR concept to be proposed. Although initially developed in the early 1980s for industrial process heat applications, the passive safety features of the side-by-side concept, coupled with the other attractive characteristics of the modular concept, soon led to the proposed electricity generation application. Work on a generic, site independent safety assessment of the HTR module was initiated with the filing, in 1987, of the safety analysis report in the State of Lower Saxony. The HTR module safety concept is characterized by comprehensive protection of the environment by passive system characteristics even under extreme, hypothetical accident conditions.

The safety features of the HTR module were based on the design condition that, even in the case of failure of all active cooling systems and complete loss of coolant, the fuel element temperatures would remain within limits such that there is virtually no release of radioactive fission products from the fuel elements. Such a condition guaranteed that the modular HTR power plant would not cause any hazard to the environment either during normal operation or in the case of an accident.

A small core diameter (~3 m) stems from the requirement for reactor shutdown from all operating conditions using only free falling control rods in reflector borings. The requirement to keep the maximum fuel element temperature for all possible accidents inherently below 1600°C, a temperature at which all radioactive fission products are contained within the fuel elements, leads directly to a mean power density of 3 MW/m^3. In order to gain as much power as possible from the core, the core height was chosen as large as possible.

5.2 HTR-100

With the objective that nuclear power plants utilizing small HTGRs can provide economic, environmentally favorable and reliable electricity and heat for community and industrial purposes, Brown, Boveri und Cie and Hochtemperatur-Reacktorbau initiated the design of the HTR-100 pebble bed plant. This design featured a 285 MW(t) HTGR with a net electrical output of 100 MW on the basis of the AVR concept and utilized the advanced technologies of THTR-300 components and systems. The primary system included the reactor, steam generator and helium circulator in a single, vertical steel pressure vessel. The reactor core included 317,500 spherical elements of TRISO type particles and a power density of 4.2 MW/m^3. In the equilibrium cycle, 55% of the spherical elements were fuel, with the remainder being graphite. The basic design for this plant incorporated two HTR-100 units with overall capability of producing 170 to 500 t/hr of industrial steam at 270°C and 16 bar, with 100 to 175 MW(e) gross output [9].

5.3 VGM

Analysis of the heat energy market in Russia revealed a need for the development of small nuclear power energy sources whose power utilization factor and high degree of safety could meet the requirements of high availability and capacity factors and potential close-in siting required by industrial plants. The VGM modular HTGR, with a power output of 200 MW(t) and a design configuration very similar to the HTR-MODULE which was being developed in Germany, was selected as a low power pilot unit after considering several different designs. The power required by large industrial complexes would be reached by the use of several such modules, permitting also the necessary reserves for both high availability and high capacity factors.

5.4 MHTGR

In 1983, the US organization representing utility/user interests in the HTGR program, the Gas Cooled Reactor Associates, conducted a survey to determine the utility nuclear generation preference for the future. This survey resulted in a strong interest for smaller generation increments. This was an important input leading to the evaluation and subsequent selection of the modular HTGR in 1985 [1]. Following a detailed evaluation in the spring and summer of 1985, a side-by-side concept similar in configuration to a German module design was chosen as the reference concept for further design and development by the US program. The basic module was designed to deliver superheated steam at 17.3 MPa and 538°C. An initial module power level of 250 MW(t) was selected, but subsequent detailed safety analyses showed that this power level could be increased with the hexagonal graphite block core design without compromising margins. Adopting an annular core allowed the power level to be increased initially to 350 MW(t). Other reactor design changes and analysis refinements subsequently allowed the power to be increased to 450 MW(t), while maintaining adequate margins to component and safety limits [8].

Central to the Modular HTGR (MHTGR) passive safety approach was the annular reactor core of prismatic fuel elements within a steel reactor vessel. A low-enriched uranium, once-through fuel cycle was used. For a standard steam cycle MHTGR plant, the steam output from each of the four modules was connected to an individual turbine generator. The four module plant consists of two separate areas, the nuclear island and the energy conversion area.

The most fundamental characteristic of the MHTGR that separated it from previous reactor designs was the unique safety philosophy embodied in the design [7]. First, the philosophy requires that control of radionuclides be accomplished with minimal reliance on active systems or operator actions; the approach to safety is to rely primarily on the natural processes of thermal radiation, conduction, and convection and on the integrity of the passive design features. Arguments need not center on an assessment of the reliability of pumps, valves, and their associated services or on the probability of an operator taking various actions, given the associated uncertainties involved in such assessments.

Second, the philosophy requires control of releases by the retention of radionuclides primarily within the coated fuel particle rather than reliance on secondary barriers (such as the primary coolant boundary or the reactor building). Thus, ensuring that the safety criteria are met is the same as ensuring that the retention capability of the coated fuel particles is not compromised.

The assessment of the capability of the MHTGR to control accidental radioactivity releases shows that the doses are a small fraction of the US10CFR100 requirements even for the bounding analyses which consider only the systems, structures and components that require neither operator action nor other than battery power. In fact, the exposures are so low that the protective action guidelines would require no evacuation or sheltering plans for the public as specified in the utility/user requirements. The evaluation confirms that accident dose criteria can be met with a containment system that places primary emphasis on fission product retention within the fuel barriers.

Consistent between the modular HTGR designs of the HTR-MODULE, MHTGR and the VGM are side-by-side steel vessels housing the reactor and the helium circulator and steam generator in a common configuration. Figures 4 and 5 depict the US MHTGR and German HTR-MODULE, respectively. The VGM is similar with the inclusion of another vessel housing an auxiliary cooling system.

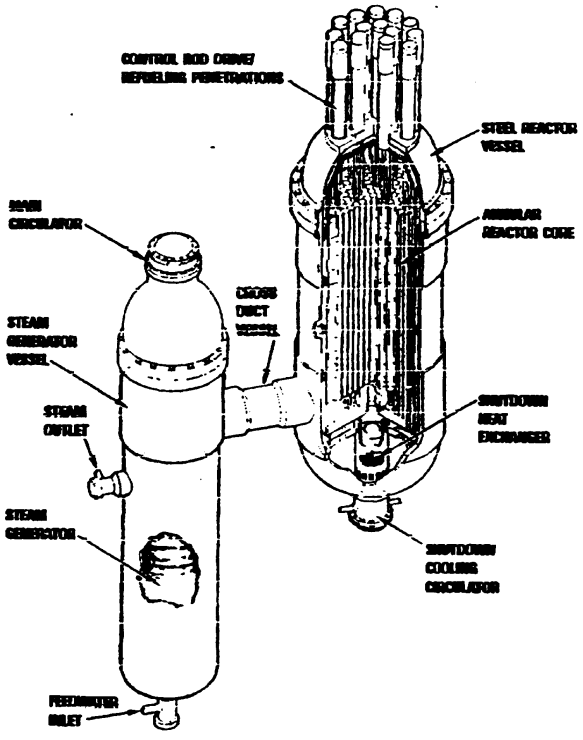

FIG. 4: MHTGR arrangement [1].

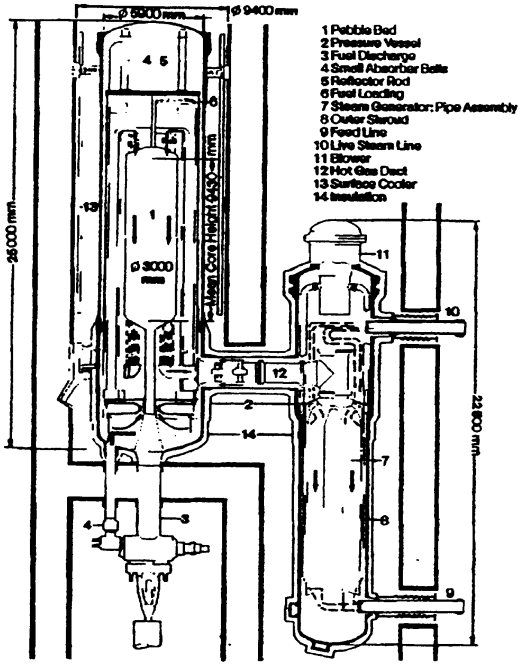

FIG. 5: HTR-MODULE arrangement [3].

It was the development of the above mentioned modular HTGR steam plants that provided the key emphasis to initiation of the HTGR coupled to a gas turbine power conversion system. With few exceptions, it is the German HTR-MODUL and the HTR-100 reactor designs that are being utilized by ESKOM as the base for the PBMR. The MHTGR, with its annular core arrangement within a steel vessel, forms the basis for the GT-MHR reactor design [2].

Also, it was during the 1980s and early 1990s that a major focus of the international HTGR community was directed towards investigation of the industrial heat applications and co-generation capabilities provided by the modular HTGR. Investigation of the capabilities of this nuclear energy source to support high temperature process heat applications as well as the need to evaluate the safety and technological features of the HTGR were contributing factors in the decisions by JAERI and China's Institute of Nuclear Energy Technology (INET) to construct the High Temperature Engineering Test Reactor (HTTR) and High Temperature Gas Cooled Reactor Test Module (HTR-10), respectively.

6. MODULAR HTGR GAS TURBINE PLANT DEVELOPMENT

It has long been recognized that substantial gains in the generation of electricity from nuclear fission can be achieved through the direct coupling of a gas turbine to a HTGR. This advanced nuclear power plant is unique in its use of the Brayton cycle to obtain a net electrical efficiency approaching 50% [10]. This plant provides a promising alternative for the utilization of nuclear energy to produce electricity. Although evaluation of this concept was initiated over twenty years ago, it was terminated due to the technical risks primarily in the component areas of magnetic bearing, compact plate-fin heat exchanger and turbo machinery development. Subsequent technological advancements in the design and operation of these components, coupled with the international capability for their fabrication and testing has resulted in renewed interest in this HTGR concept [11].

6.1 Development of the Gas Turbine Plant

In order to be competitive, the thermal efficiency of nuclear power had to be markedly improved to compete with modern, high efficiency fossil plants. HTGR technology has always held the promise for electricity generation at high thermal efficiency by means of a direct Brayton cycle and fortuitously, technological developments during the past decade provided the key elements to realize this promise. These key elements are as follows:

- The HTGR reactor size had been reduced in developing the passively safe module design. At the same time, the size of industrial gas turbines had increased. The technology was now available for a single turbo-machine to accommodate the heat energy from a single HTGR module.

- Highly effective compact recuperators had been developed. Recuperator size and capital equipment cost are key economic considerations. Highly effective plate-fin recuperators are much smaller than equivalent tube and shell heat exchangers, provide for substantially less complexity and capital cost, and are a key requirement for achieving high plant efficiency.

- The technology for large magnetic bearings had been developed. The use of oil lubricated bearings for the turbo-machine with the reactor coolant directly driving the turbine was problematic with regard to the potential coolant contamination by the oil. The availability of magnetic bearings eliminates this potential problem [12].

A major requirement was for the plant to become substantially simplified in order to provide a significant reduction in the capital expenditure for new capacity additions. Figures 6 and 7 provide a comparison of nuclear power plant efficiencies and a graphic simplification that can be achieved in moving from the HTGR steam cycle to the basic direct gas turbine cycle, respectively.

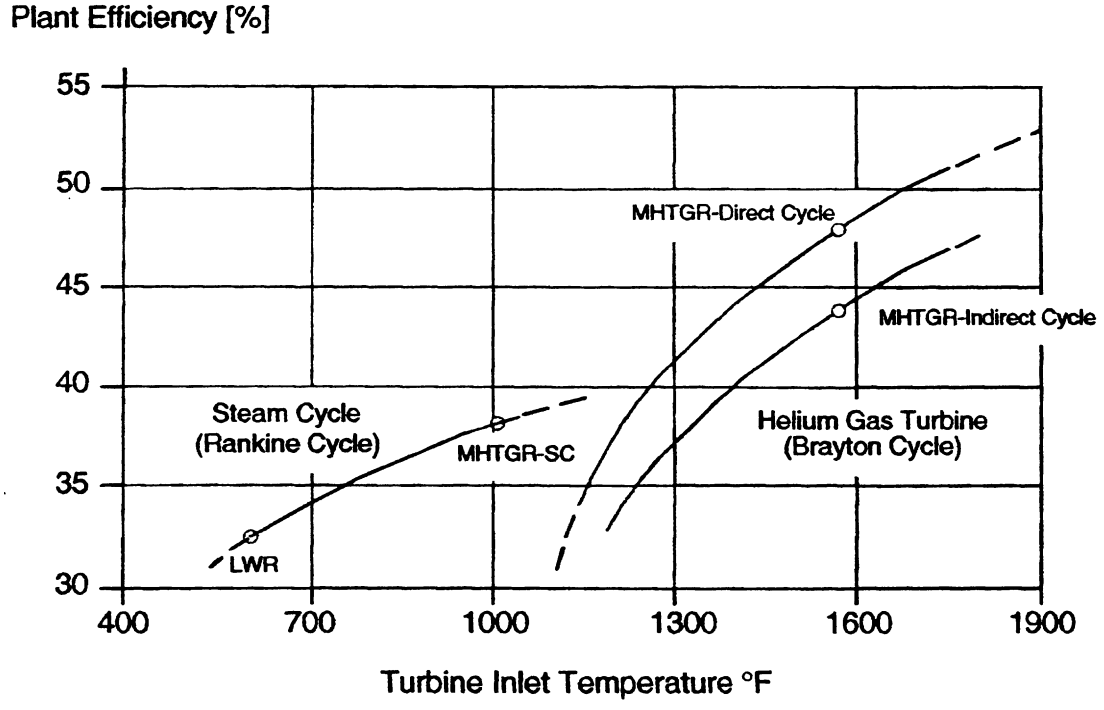

FIG. 6: Plant efficiency comparison [1].

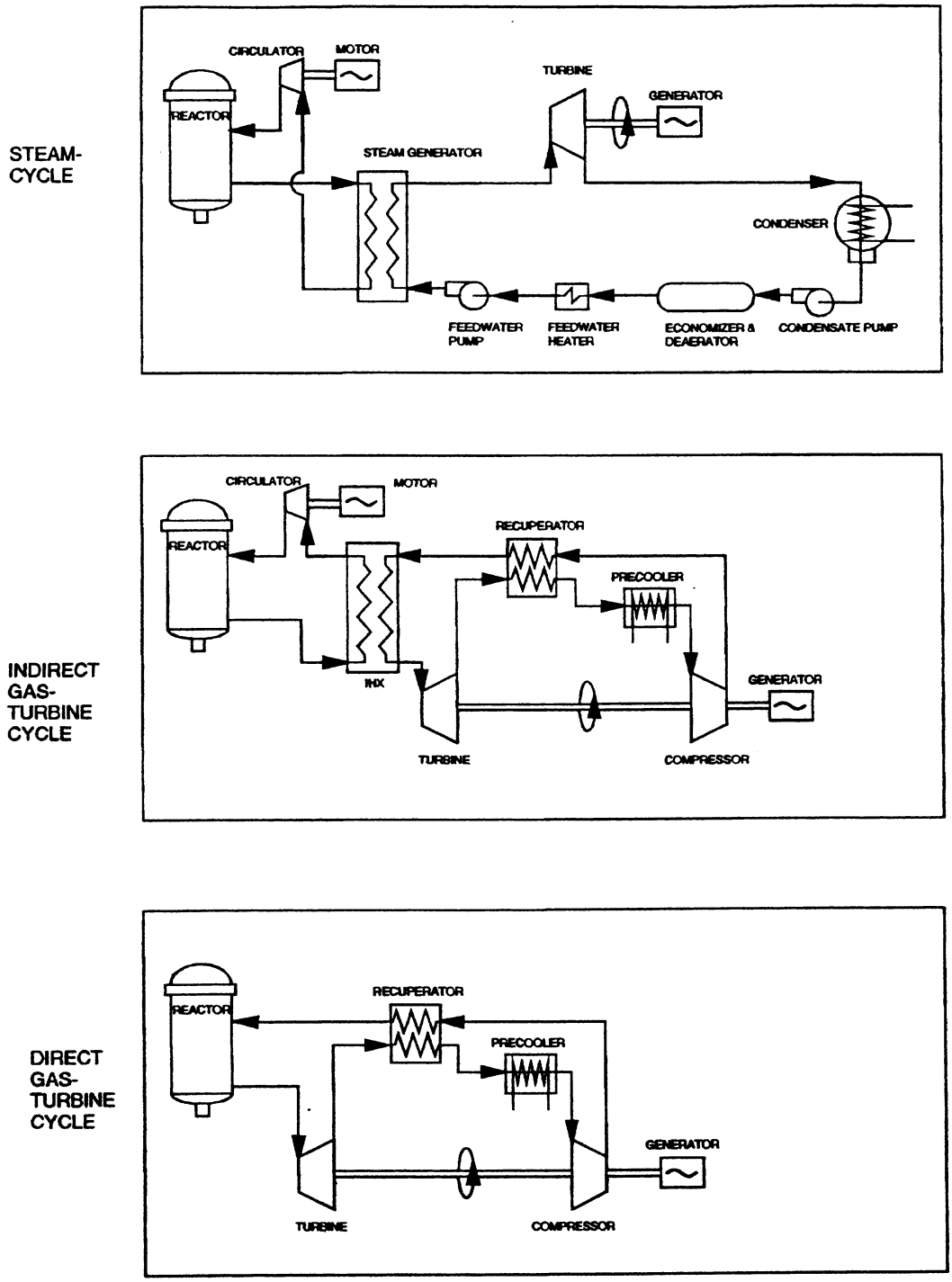

FIG. 7: System simplification, steam cycle to the closed cycle gas turbine plant [1].

The possibilities presented by the gas turbine modular HTGR for substantial improvement in nuclear power plant efficiency coupled with the potential for significant gains in lowering capital and operating costs due to plant simplification have brought about an increasing interest by international research organizations and plant developers. Overviews of the most prominent among the designs currently being investigated are provided in the following sub-sections.

6.2 Pebble Bed Modular Reactor (PBMR)

The PBMR was first identified by ESKOM in 1993 as an option for expansion of their electrical generation capacity. Subsequently, ESKOM contracted with Integrators of System Technology to perform a technical and economic study of the feasibility of the PBMR for the generation of electricity. This study, which was completed in early 1997, supported the continued development of the PBMR. Reactor development follows the HTR-MODULE pebble bed which was previously licensed in Germany for commercial operation.

A series of internal reviews by ESKOM and subsequent independent reviews of this feasibility study by international entities have generally acknowledged that the PBMR is technically and economically capable of meeting the requirements originally set by ESKOM for commercialization. These requirements included: a.) New generation capacity capable of being located where the load growth is taking place in South Africa (coastal regions); b.) Small, modular increments of electrical generation capacity corresponding to system growth needs; c.) Reduced exposure to negative environmental issues such as carbon dioxide emissions and capable of providing a strategy for economic mitigation of greenhouse gas reductions; d.) Generating plants placed where there would be a limited need for extensive transmission system additions, and; e.) Cost of capital and plant operation to be within those costs presently being achieved at ESKOM's largest coal fired stations (with targets of capital cost less than US$ 1,000/installed kw and overall generation, transmission and distribution costs of utility operations within 2.0 cents/kwhr [13]. ESKOM, in conjunction with British Nuclear Fuel, the US utility PECO Energy and the Industrial Development Corporation of South Africa, is currently in the process of performing the final evaluation for the introduction of this advanced nuclear power reactor coupled to a closed cycle gas turbine as additional generation capacity on their electric grid and for commercialization in the international market place [2].

6.3 Gas Turbine-Modular Helium Reactor (GT-MHR)

Renewed interest in the nuclear powered closed cycle gas turbine system within the US resulted in the present GT-MHR developmental program beginning in early 1993. Subsequent discussions with organizations of the Russian Federation resulted in GA and MINATOM entering into a Memorandum of Understanding to cooperate on the development of the GT-MHR with the goal, following design and development, to construct, test and operate a prototype in Russia [14]. FRAMATOME joined this program in 1996 with Fuji Electric becoming a participant and sponsor in 1997.

The conceptual design is now completed on this 600 MW(t)/293MW(e) plant which is currently under development for the destruction of weapons plutonium, but with the longer term goal of commercial development. The next stage of development is in preliminary design of the plant to begin in 1999. Most of the design work on the GT-MHR is being performed within the nuclear organizations of the Russian Federation with financial and management/technical support from all members of the consortium.

A recent significant development in the advancement of the GT-MHR is the authorization of financial support by the US government on a matching resource basis with MINATOM for the destruction of weapons plutonium. Although the GT-MHR is initially to utilize a plutonium fuel cycle which has the capability of achieving a burn-up approaching 95%, the versatility and flexibility of this core will allow for the application of a wide range of diverse

fuel cycles. Fuel derived from uranium, thorium and a variety of plutonium grades is under consideration for long term applications in the GT-MHR [13].

6.4 Other Gas Turbine and Modular HTGR Co-generator Designs [13]

6.4.1 ECN's ACACIA Plant

ECN Nuclear Research is developing a conceptual design of an HTGR for the combined generation of heat and power for industry within the Netherlands as well as for possible export. The ACACIA plant utilizes a 40 MW(t)h pebble bed HTGR to produce 14 MW of electricity and 17 tonnes of 10 bar, 220°C. steam per hour [15]. The electric generation system utilizes a basic closed cycle gas turbine which receives helium from the HTGR at 800°C and 2.3 MPa. After the recuperator, a secondary helium loop removes heat from the primary system via an intermediate heat exchanger (precooler) which then transfers energy to the steam/feedwater system for industrial use.

6.4.2. Japan's HTGR Gas Turbine Designs

A number of HTGR gas turbine plant designs are currently under development within Japan. These plants are primarily under development by JAERI within the framework of the Japanese HTGR-GT feasibility study program, and include gas turbine cycle units with reactors of 400 MW(t), 300 MW(t), and two variations with a power level of 600 MW(t). In order to provide an indication of the diversity of application under consideration in Japan, two of these designs are discussed as follows:

The 300 MW(t) Plant: The 300 MW(t) pebble bed annular reactor of this plant provides a core outlet temperature of 900°C. to the turbine of a single shaft machine. The design is coordinated by JAERI and includes developmental support from Japanese industry. The flexibility of this plant includes the co-generation application of electricity production and the capability to provide 283 tons of desalinated water per hour through the use of an additional heat exchanger between the recuperator and precooler. The net thermal efficiency for this plant is anticipated at 48.2% [16].

The GTHTR 300 Plant: This plant incorporates a 600 MW(t) hexagonal fuel block core. The power conversion system includes a vertical heat exchanger vessel and a horizontal turbo-machine vessel to allow for bearing support and stable rotor operation. The cycle configuration has been simplified in comparison to the GT-MHR by elimination of a compressor unit and the corresponding intercooler. The overall net plant efficiency for this simplified unit is 45.4% [17].

6.4.3 MIT and INEEL's MPBR Plant

The development of the MPBR is being addressed based on preliminary research into future energy options by MIT student work beginning in 1998. It was concluded that this technology provided the best opportunity to satisfy the safety, economic, proliferation, and waste disposal concerns that face all nuclear generating technologies. The areas of research for this project are aimed at addressing some of these fundamental concerns to determine whether the small 110 MW(e) modular gas-cooled pebble bed plant can become the next generation of nuclear technology for worldwide deployment [18].

MIT and INEEL have utilized the reference design from the ESKOM PBMR, but with a significantly different balance of plant. The HTGR is of pebble bed design with a power level of 250 MW(t). Primary coolant helium from the reactor flows through an intermediate heat exchange providing a transfer of energy to the secondary coolant (air). The secondary loop consists of a high pressure turbine which drives three (high, medium and low pressure) compressors with two stages of intercooling. A second shaft incorporates the low pressure turbine and electric generator. High temperature coolant air leaves the IHX to drive the compressors via the high pressure turbine. After exiting this turbine, the coolant then enters the low pressure turbine to expand and drive the generator. From this turbine, the secondary coolant path includes the recuperator, precooler and compressors/intercoolers. The MPBR utilizes conventional oil bearings rather then magnetic bearings on its turbomachines.

6.4.4 INET's MHTGR-IGT

This design features an indirect gas turbine system coupled to a 200 MW(t) pebble bed HTGR. Although the HTGR can provide heat at 950°C with the attributes of outstanding safety and gas turbine cycle efficiency in the range of 47%, the possible radioactivity deposition on the turbine blades and thus the increase in maintenance difficulties suggests that the indirect gas turbine cycle should be applied initially in the development process to help solve these problems.

In this design, the helium out of the intermediate heat exchanger (IHX) is extracted to a RPV cooling system. The gas flows through a small RPV recuperator and is cooled. It then is used to cool the RPV. The whole primary circuit is integrated in a single pressure vessel with the core inlet/outlet temperatures 550°C/900°C, which can supply heat of ~850°C on the secondary side. The heat source would be used to drive a nitrogen gas turbine cycle with a busbar electricity generation efficiency of about 48%. The 200 MW(t) pebble bed reactor core is located at the lower position of reactor pressure vessel with a geometry similar to that of the Siemens 200 MW HTR-MODULE. The straight tube IHX is located at the upper position of the RPV and connected with the core through a gas duct. Similar to the AVR, the control rod system is installed at the bottom of the RPV and all rods are inserted upward into the side reflector. The main helium blower and an auxiliary blower for shutdown cooling are located at the top of the RPV. A reactor vessel cooling system recuperator and cooler are installed respectively in annular regions outside of the IHX and blowers [2].

7. CONCLUSIONS

The HTGR development process has been subjected to many significant changes from the initial Dragon plant to the present gas turbine designs. Major among these changes are the following:

- Dragon, Peach Bottom and the AVR were commissioned in the 1960s primarily to develop and demonstrate the feasibility of HTGR technology. The plants were generally quite successful in achieving the individual goals set for them. This was particularly evident with the AVR in demonstrating extended reactor operation at an average core outlet temperature of 950°C, and for validation of the UO_2 kernel TRISO coated fuel particle. This fuel represents the foundation for the safety and environmental aspects of the HTGR, and is now used exclusively in all modular HTGR designs.

- FSV and the THTR-300 were then commissioned to be the next milestones in HTGR development. The primary goal for these plants was to demonstrate the commercial

capabilities of the HTGR as the fore-runners to achieving marketability of the large follow-on plant designs. These plants were not successful in accomplishing this goal. Commonalties shared by FSV and the THTR-300 were size (each ~300 MW(e)) and the utilization of a PCRV rather then steel vessels to contain the primary coolant system. Of note is that these plants were valuable in demonstrating the attributes of the HTGR, including the TRISO coated fuel particle.

- The modular steam cycle HTGR became the next focus for plant designers. This was influenced by utilities and designers to evaluate small nuclear power sources that would have added safety characteristics including the potential for being located at industrial sites. This resulted in the adoption of the modular HTGR with its safety attribute of passive heat transfer resulting in plant simplification and associated economic advantages. Modular HTGR designs of this era reverted back to the steel vessel, generally in a side-by-side configuration, and the reactor took on an annular configuration. Although the generation of electricity was the preferred product for this plant, an ever increasing interest, primarily by many national research organizations, was the development of co-generation and industrial applications afforded by its capability to achieve high core outlet temperatures. .

- The major emphasis of HTGR development into the 1990s continued with the modular plant, but now with an annular reactor core and coupled to a gas turbine power conversion system rather then the steam cycle. These changes are anticipated to contributed substantially to the goals of reduced capital and operating costs by further plant simplification and a significant improvement in cycle efficiency over existing nuclear plant designs.

The gas turbine plant continues to be the primary focus of international HTGR development. However, of note is that the constituency of partners in this development has changed significantly in the past decade. This is particularly evident with the PBMR and GT-MHR where international partnerships now include major nuclear plant developers and utilities. The reasons for this are obvious; a design that shows promise for significant improvements in nuclear plant economics and attendant plant efficiency, with the long term prospect of achieving substantial marketability and associated financial reward. However, the task ahead for commercialization of this plant has to overcome significant hurdles including: 1.) A modular HTGR has never before been constructed, 2.) The size and environmental application of major components such as plate-fin recuperators and turbomachines fitted with magnetic bearings has yet to accomplished, and 3.) The licensing process has yet to be completed for a nuclear power plant of this configuration.

Yet, successful commercial deployment of this plant has the potential of significantly advancing nuclear power as a world-wide primary energy source for the future with corresponding financial reward to the investors willing to take the risks associated with its development.

REFERENCES

1. WILLIAMS, P.M., et al., “MHTGR Development in the United States”, Progress in Nuclear Energy, ISSN 0149-1970, Vol. 28, No. 3, (1994), pp.265-346.
2. BREY, H.L., (Ed), “Current Status and Future Development of Modular HTGR Technology”, IAEA-TECDOC-TBD, Vienna, 2000.

3. INTERNATIONAL ATOMIC ENERGY AGENCY, Gas Cooled Reactor Design and Safety, Technical Report Series No. 312, IAEA, Vienna (1990).
4. RENNIE, C.A., Achievements of the Dragon Project, Ann. Nuclear Energy 5 (8) (1978), pp.305-320.
5. MOORE, R.A., et al., "HTGR Experience, Programs, and Future Applications", Nuclear Engineering and Design 72 (1982), pp. 153-174.
6. KROGER, W., et al., "Safety Characteristics of Modern High-Temperature Reactors: Focus on German Designs", Nuclear Safety, Vol. 29, No. 1, (1988) pp. 36-48.
7. SILADY, F.A., PARME, L.L., "The Safety Approach of the Modular High Temperature Gas-Cooled reactor (MHTGR)", 11th International Conference on the HTGR, Dimitrovgrad, USSR, (13-16 June, 1989).
8. SILADY, F.A., GOTSCHALL, H., "The 450 MW(t) MHTGR: More Power with the Same High Level of Safety", Third International Seminar on Small and Medium Sized Nuclear Reactors, New Dehli, India (26-28 August, 1991)
9. BRANDES, S., KOHL, W., "HTR 100 Industrial, Nuclear Power Plant for Generation of Heat and Electricity", IAEA-TECDOC-436, Vienna, 213-234, (1987)
10. INTERNATIONAL ATOMIC ENERGY AGENCY, "Design and Development of GCRs with Closed Cycle Gas Turbines", Vienna, IAEA-TECDOC-899, August 1996.
11. INTERNATIONAL ATOMIC ENERGY AGENCY, "High Temperature Gas Cooled Reactor Technology Development", IAEA-TECDOC-988, Vienna, December 1997.
12. LA BAR, M.P., SIMON, W.A., "International Cooperation in Developing the GT-MHR", IAEA-TECDOC-988, Vienna, December 1997, 59-71.
13. BREY, H.L. (Ed), "Helium Gas Turbine Reactor Technical Challenges; A Characterization for Use in Focusing R&D Resources", EPRI document TP-114690, Palo Alto, California, January 2000
14. SIMON, W.A., SHENOY, A.S., "International Cooperation in Developing the GT-MHR, Evolution and Program Status", proceedings on the IAEA Technical Committee Meeting on High Temperature Gas Cooled Reactor Applications and Future Prospects, ECN-R-98-004, Petten, the Netherlands, 10-12 November 1997.
15. HAVERKATE, B.R.W, VAN HEEK, A.I., KIKSTRA, J.F., "An HTR Cogeneration System for Industrial Applications", proceedings of a Technical Committee Meeting, Beijing, China, 2-4 November 1998, IAEA-TECDOC (to be published)
16. MUTO, Y, "Present Activity of the Design and Experimental Works for HTGR-GT System in JAERI", EPRI Helium Gas Turbine Reactor Workshop, Palo Alto, California, December 7-8, 1999
17. YAN, X., SHIOZAWA, S., KUNITOMI, K., MUTO, Y., MIYAMOTO, Y., "Design of Gas Turbine High Temperature Reactor-GTHTR 300", EPRI Helium Gas Turbine Reactor Workshop, Palo Alto, California, December 7-8, 1999
18. MASSACHUSETTS INSTITUTE OF TECHNOLOGY and IDAHO NATIONAL ENGINEERING & ENVIRONMENTAL LABORATORY, "Modular Pebble Bed Reactor Project", First Annual Report, (June 1999).
19. CLEVELAND, J., LEWKOWICZ, I., "Status of the IAEA Coordinated Research Programme on Design and Evaluation of Heat Utilization Systems for the HTTR", Presented at the 2nd International Conference on Multiphase Flow, Kyoto, Japan, (April 1995)
20. BAUMER, R., KALINOWSKI, I., "THTR Commissioning and Operating Experience", Energy, Vol. 16, No.1/2, (1991), pp.59-70

He Cooled HTGR in World
ВТГР с гелиевым охлаждением в мире

Dragon, 1964
(GB)

20 MW(t)
750/350°C
2.0 MPa
U-Th

Peach Bottom, 1966
(USA)

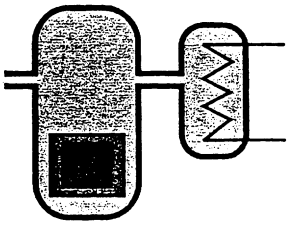

115 MW(t) 2.0 MPa
40 MW(e) U-Th
750/350°C

AVR, 1966
(FRG)

49 MW(t)
15 MW(e)
850-950/175°C
1.0 MPa
U-Th/U
4.0 MPa
U-Th
Pebble bed

FSV, 1976
(USA)

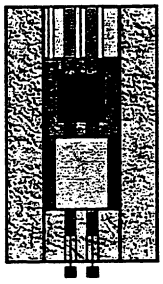

835 MW(t)
330 MW(e)
735/350°C
5.0 MPa
U-Th

THTR-300, 1982
(FRG)

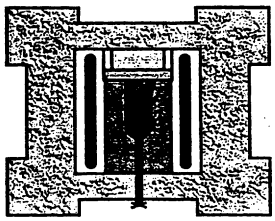

750 MW(t) 4.0 MPa
300 MW(e) U-Th
750/260°C Pebble bed

HTTR, 1998
(Japan)

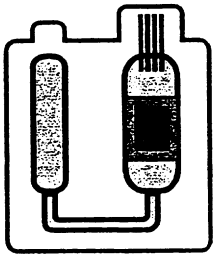

30 MW(t) 4.0 MPa
850-950/260°C U

GT-MHR,
Conceptual design 1998
(Russia, USA, France, Japan,)

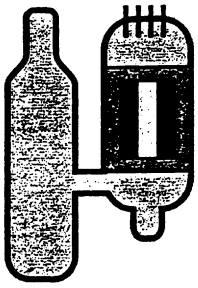

600 MW(t)
286 MW(e)
850/490°C
Gas Turbine
5.0 MPa
U

HTR-10, Construction
(China)

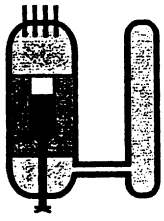

10 MW(t)
850/300°C
1.0 MPa
U
Pebble bed

PBMR, Conceptual design
1998 (SAR)

250 MW(t) Gas Turbine
110 MW(e) 7.0 MPa, U
900/300°C Pebble bed

HTGRs in the world
Courtesy of:
V. Grebennik, Kurchatov Institute

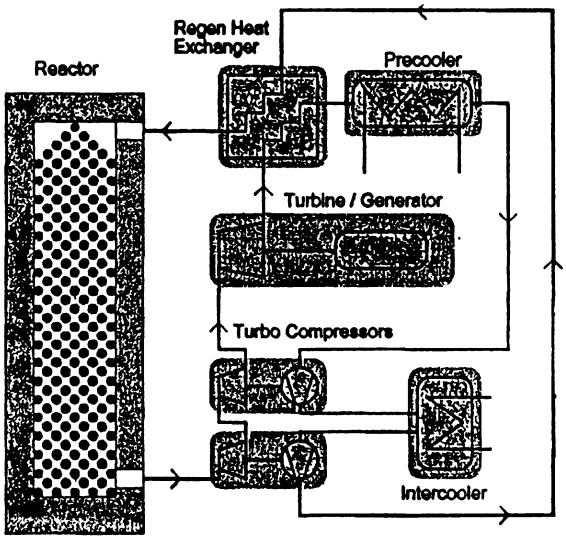

PBMR System Arrangement

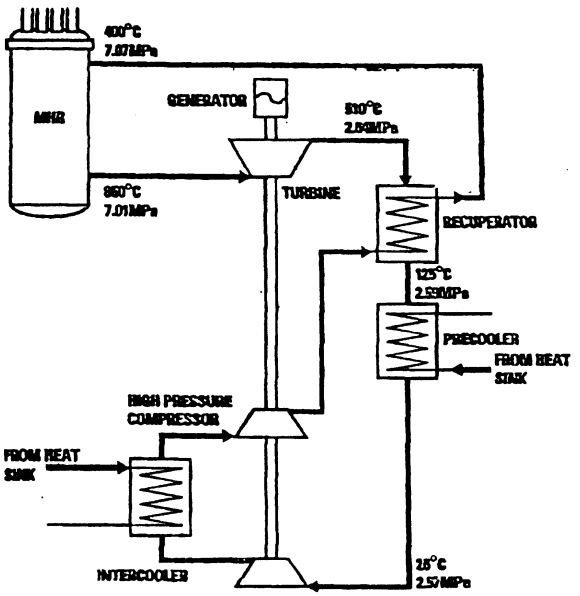

GT-MHR System Arrangement

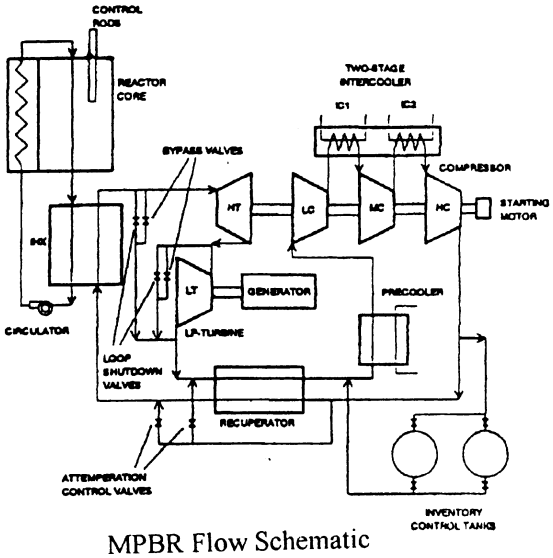

MPBR Flow Schematic

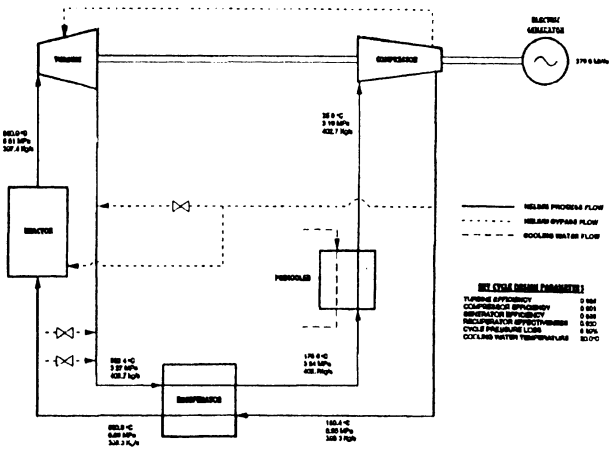

System arrangement of GTHTR-300

System Arrangements for Selected Modular HTGR Gas Turbine Plant Designs

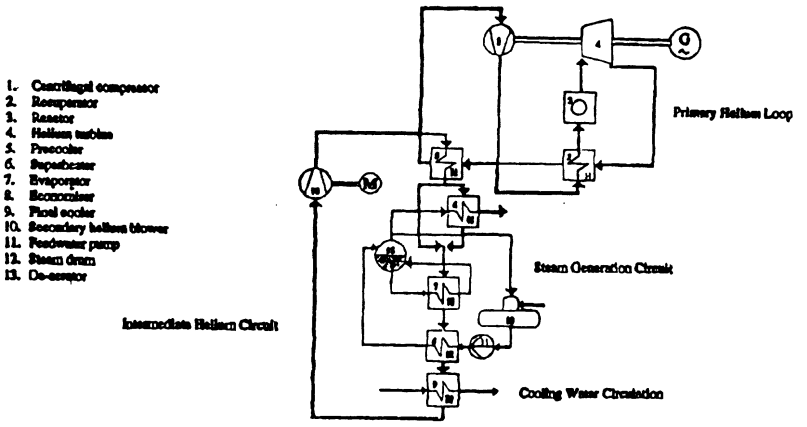

Flow Diagram of ACACIA Co-generation Plant

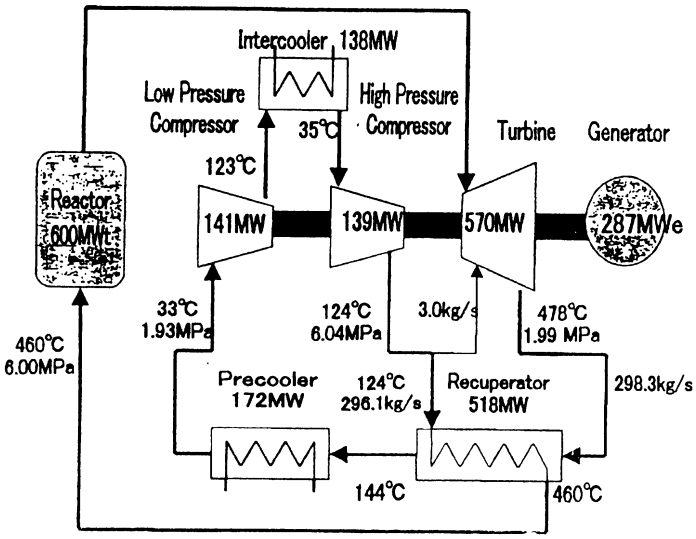

System Arrangement of 600 MW HTGR-GT

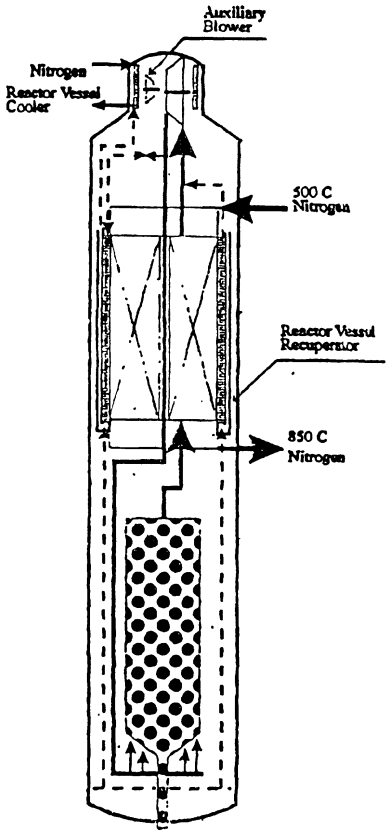

Primary System Layout of MHTGR-IGT

System Arrangements
For
Selected Modular HTGR Gas Turbine Plant Designs

Appendix B

Characteristics of Selected Steam Cycle HTGRs

	AVR	Peach Bottom	Ft. St. Vrain	THTR-300	HTR-500	VGM-400	HTR-Module	MHTGR
Country/Origin	Germany	USA	USA	Germany	Germany	Russia	Germany	USA
Thermal Pwr, MW(t)	46	115	842	750	1,390	1,060	200	350
Net Elec. Pwr, MW(e)	13	40	330	300	550	Co-Gen.	80	139
Pwr Density, MW/m^3	2.5	8.3	6.3	6.0	6.6	6.9	3.0	5.9
Core Out Temp, °C	950	725	775	750	700	950	700	686
Helium Pres, MPa	1.1	2.25	4.8	3.9	5.5	5.0	6.6	6.4
Steam Temp. °C	505	538	538/538	530/530	530	535	530	538
Elec. Gen., MWh	~ 1,670	~ 1,380	~ 5,500	~ 2,890	N/A	N/A	N/A	N/A
Reactor Type	Pebble	Sleeve	Block	Pebble	Pebble	Pebble	Pebble	Block
Fuel Enrichment	Various	HEU	HEU	HEU	LEU	LEU	LEU	LEU
Fuel Composition	Oxide	Carbide	Carbide	Oxide	Oxide	Oxide	Oxide	Ox-Carb
Fuel Coating	Various	BISO	TRISO	BISO	TRISO	TRISO	TRISO	TRISO
Vessel Material	Steel	Steel	PCRV	PCRV	PCRV	PCRV	Steel	Steel

Characteristics of selected modular htgr gas turbine plants

	GT-MHR	PBMR	MHTGR-IGT	ACACIA	GTHTR-300	600 MW-HTGR-GT	MPBR
Country/Origin	USA, Russia	S. Africa	China	Netherlands	Japan	Japan	USA
Thermal Pwr, MW(t)	600	265	200	40	600	600	250
Net Ele Pwr, MW(e)	278	116	~ 96	Co-Gen.	273	287	112
Pwr. Den, MW/m^3	6.5	4.3	3.0	----------	---------	5.77	--------
Core Out Temp, °C	850	900	900	800	850	850	850
Helium Pres, MPa	7.15	7.0	6.0	2.3	6.8	6.0	7.9
Cycle Type	Direct	Direct	In-Direct	Direct	Direct	Direct	In-Direct
Core Type	Block	Pebble	Pebble	Pebble	Block	Pin/Block	Pebble
Fuel Enrichment	HE-Pu	LEU	LEU	LEU	LEU	LEU	LEU
Fuel Composition	PuO	Oxide	Oxide	Oxide	Oxide	Oxide	Oxide
Fuel Coating	TRISO	TRISO	TRISO	TRISO	TRISO	TRISO	TRISO
Vessel Material	Steel	Steel	Steel	Steel	Steel	Steel	Steel

STUDY ON COUPLING A GAS TURBINE CYCLE TO THE HTR-10 TEST REACTOR

YULIANG SUN, YINGUANG ZHANG, YUANHUI XU
Institute of Nuclear Energy Technology,
Beijing, China

Abstract:

Currently, a 10MW helium cooled high temperature test reactor (HTR-10) using spherical fuel elements is being constructed. The test reactor facility is now under commissioning and will reach its first criticality soon. The test reactor is now coupled with a steam turbine cycle through a steam generator, but it is planned that in the second phase of the project, a gas turbine cycle shall be coupled to the reactor to carry out R&D programmes on the gas turbine power generation technology. Different possibilities of coupling a gas turbine cycle to the HTR-10 test reactor are discussed taking into account of conditions given by the existing facility. If an intermediate heat exchanger is implemented into the current system configuration, indirect gas turbine cycles can be coupled to the HTR-10 reactor. The presence of the intermediate heat exchanger also allows some room for the choice of gas turbine working fluid. Two options are discussed in the paper: nitrogen and helium as the working fluid of the gas turbine cycle. For the nitrogen option, the gas turbine cycle is inter-coupled with the existing steam cycle through a residual heat recover, while for the helium option, the helium cycle and the steam cycle are not inter-coupled. The helium cycle is a recuperated, inter-cooled Brayton cycle. As another possibility, the option of coupling a direct gas turbine cycle without steam cycle is shortly discussed. The materialization of reasonably coupling a gas turbine cycle to HTR-10 would help acquire R&D experience of nuclear power generating technology using the combination of high temperature reactor and gas turbine.

1. INTRODUCTION

In the Institute of Nuclear Energy Technology of Tsinghua University at Beijing, a pebble bed helium cooled high temperature test reactor is under construction. The test reactor is termed as HTR-10, as its thermal power is 10MW. The construction work started in 1995. Currently, commissioning work is being carried out. First core loading and initial criticality will take place very soon.

The HTR-10 test reactor project is state-supported through the National High Technology Research and Development Programme. In the first phase of the test reactor project, a steam turbine cycle is coupled to the reactor. Electrical power and space heating heat are produced as co-generation application of nuclear heat. It has been planned that a second phase of the test reactor project shall be carried out after 2000, which will focus more on the R&D of application technology of higher temperature heat from helium cooled reactors. The first R&D item would be gas turbine technology. Application has been made to the government for the establishment of a gas turbine facility coupled with the HTR-10 test reactor. In the following sections, preliminary considerations and studies on the possibility and feasibility of coupling a gas turbine cycle to HTR-10 are discussed.

2. HTR-10 EXISTING SYSTEM CONFIGURATION

The HTR-10 in its current system configuration consists of the 10MW pebble bed reactor, the steam generator (SG) and the steam turbine-generator system, as shown in FIG. 1. Primary helium works under the nominal pressure of 3.0MPa. Helium average temperatures at reactor inlet and outlet are respectively 250°C and 700°C. Nominal helium mass flow rate is 4.3 kg/s. On the steam cycle side, the feed water temperature is 104°C and the main steam parameters at turbine inlet are 435°C/3.43 MPa. Water/steam flow rate is 3.49 kg/s. The electrical power output of the turbine-generator is 2.5 MW.

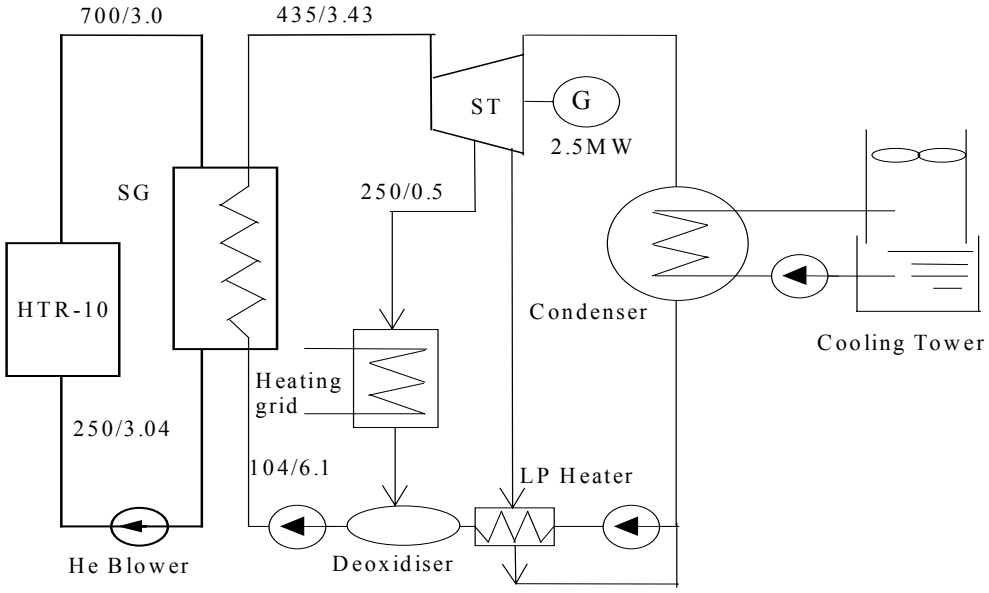

FIG. 1 Flow Diagram of the HTR-10 Steam Turbine Cycle

The HTR-10 reactor design represents the features of modular HTGR design. The reactor core and the steam generator are housed in two carbon steel pressure vessels which are arranged in a side-by-side way (FIG. 2). These two vessels are connected to each other by a connecting vessel in which the hot gas duct is designed. All these steel pressure vessels are in touch with the cold helium of about 250°C coming out from the circulator which sits over the steam generator tubes in the same vessel. The structural design of the test reactor allows that the primary helium can be heated to 700-950°C.

The steam generator is composed of a number of modular helical tubes which are arranged in a circle between two insulation barrels inside the steam generator pressure vessel. The place inside the inner barrel is reserved for an intermediate heat exchanger (IHX) which might be installed for future R&D tasks. Inlet/outlet nozzles for the secondary fluid of IHX are also in place on the steam generator pressure vessel.

3. COUPLING AN INDIRECT GAS TURBINE CYCLE TO HTR-10

As described in the previous section, it is foreseen that an IHX would be installed for later R&D purposes. Considering coupling a gas turbine cycle through the IHX would result in an indirect cycle. This option allows some room for selecting the working fluid on the secondary side of the IHX. Preliminary studies have been made on two options: nitrogen and helium as the secondary working fluid.

Nitrogen as working fluid. Selecting nitrogen as gas turbine working fluid has the advantage that much experience can be used from conventional gas turbine and aeroengine technology, and less challenge is expected on the power conversion part. The process flow of this option is shown in FIG. 3.

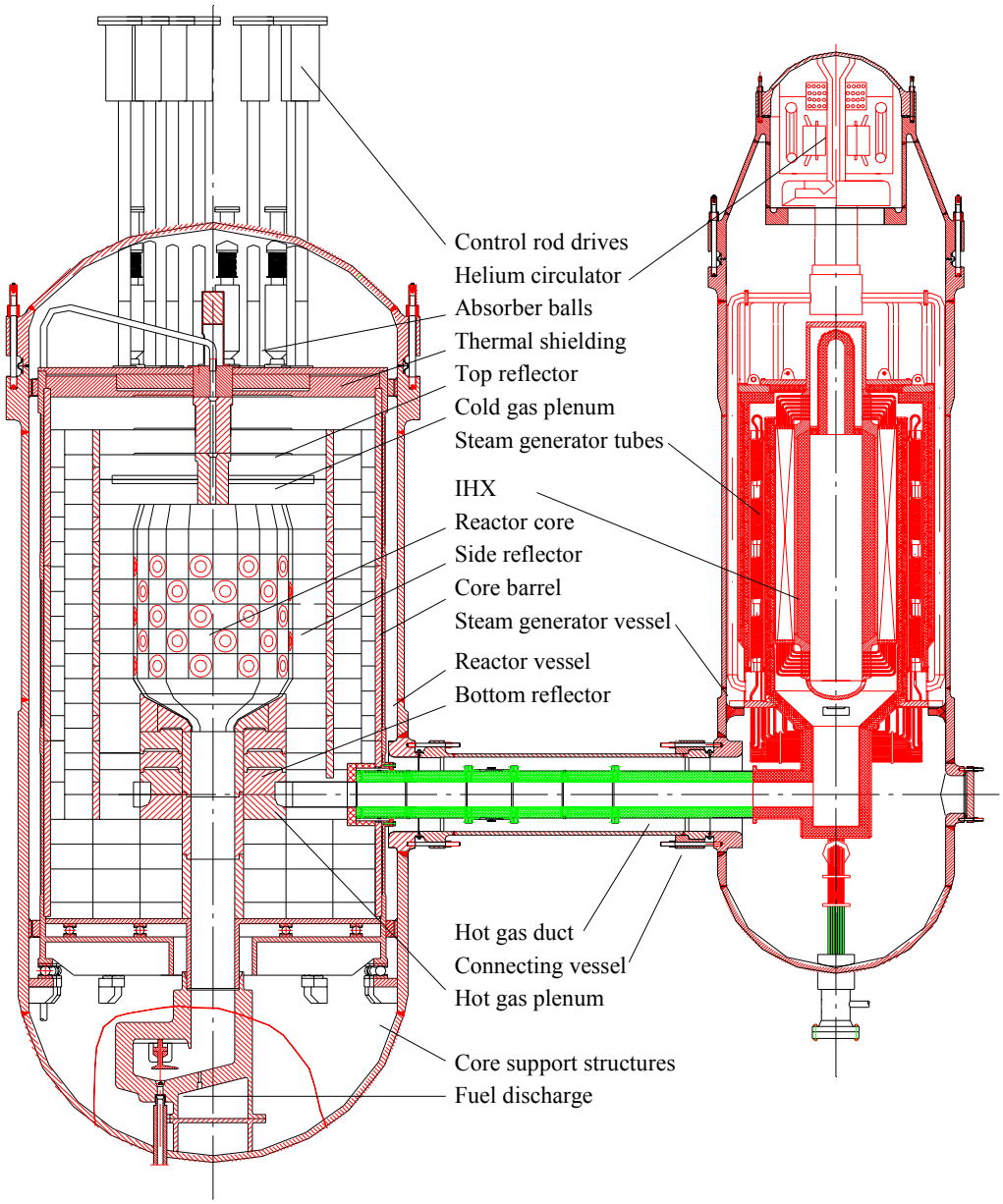

FIG. 2 HTR-10 Reactor and Steam Generator

In this option, the primary helium temperature at reactor outlet is supposed to be 950°C. It is cooled down in the IHX by the secondary nitrogen to 486°C and enters into the steam generator where it is further cooled down by water/steam to about 287°C. Primary helium enters the reactor core with about 300°C. This results that 70% of the reactor power goes to IHX and 30% to SG. The gas cycle and the steam cycle are inter-coupled through a residual heat recover (RHR), which has a power of 5.56 MW. From the viewpoint of the gas cycle part, the RHR takes the places of recuperator and pre-cooler. No inter-cooler is foreseen. On the steam cycle part, more heat is put into the cycle through RHR than through SG.

Preliminary design parameters are listed in Table 1 for further design studies on the nitrogen turbine and compressor.

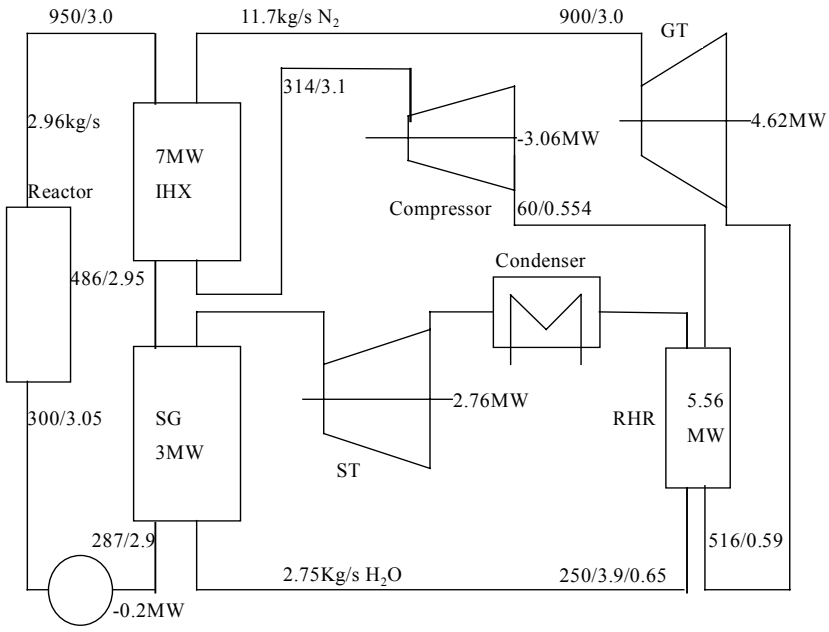

FIG. 3 Flow Diagram of Coupling a Nitrogen Turbine to HTR-10

Table 1: Key design input parameters for nitrogen turbine and compressor

	Turbine	Compressor
Inlet temperature	900 °C	60 °C
Inlet pressure	3.0MPa	0.554MPa
Outlet temperature	~516 °C	60 °C
Outlet pressure	0.594MPa	3.1MPa
Mass flow rate	11.7kg/s	

Studies have been made on the design of the turbine and compressor. It seems that detailed design work could be based on some existing machine models and much R&D work would not be necessary. The question of whether this option will be adopted should be answered before basic and detailed designs start.

Helium as working fluid. Helium turbine represents much interest to the present gas cooled reactor community. Coupling an indirect helium turbine cycle to the HTR-10 test reactor would enable the establishment of a nuclear gas turbine facility allowing much R&D work to be carried out. The process flow of this option is shown in FIG. 4.

In this process proposal, helium temperatures at reactor inlet and outlet are respectively 300°C and 900 °C. Sixty percent of the reactor power goes to IHX and forty percent to SG. This results in that primary helium leaves IHX and enters SG with a temperature of 540 °C. The gas cycle on the high temperature part and the steam cycle on the lower temperature part are not inter-connected. The helium cycle is an inter-cooled, recuperated Brayton cycle. Secondary helium of IHX enters turbine with 850°C and leaves turbine with 531°C. Listed in Table 2 are the key design parameters preliminarily chosen for further studies of the gas cycle turbo-components.

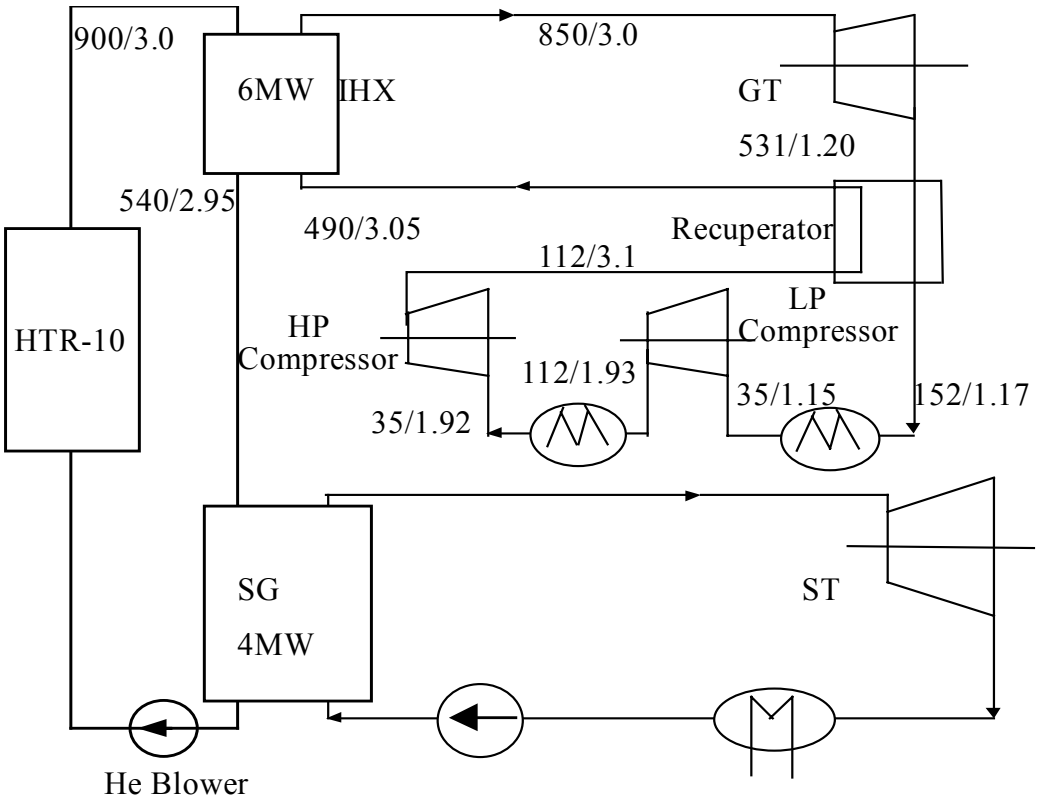

FIG. 4 Flow Diagram of Coupling an Indirect He Turbine to HTR-10

Table 2: Key design parameters requirement on indirect helium turbine cycle

	Turbine	LP Compressor	HP Compressor
Inlet temperature	850°C	3 °C	35°C
Inlet pressure	3.0 MPa	1.16 MPa	1.92 MPa
Outlet temperature	531°C	112°C	112°C
Outlet pressure	1.2 MPa	1.93 MPa	3.1 MPa
Mass flow rate	2.97 kg/s		

Simplified one dimensional studies are made on the helium turbo-machines. Design studies are also made on the heat exchanging components. It is proposed that turbine and compressors are put on a single shaft which has a rotating speed of 18, 000 rpm. The turbine shaft and generator shaft are connected through a gear-box to allow a 3, 000rpm rotating speed of the generator shaft. It is calculated that the generator has a power output of about 2.5 MW.

For nitrogen or helium gas turbine in indirect cycle configuration, the cycle components could be installed in the reactor hall above the reactor and steam generator cavity. In the strength design of the building, consideration was already given to the realization of the second phase of the project, namely, to the arrangement of additional components on the floor of the reactor hall.

4. COUPLING A DIRECT HELIUM TURBINE CYCLE TO HTR-10

Direct helium turbine cycle coupled with high temperature gas-cooled reactor is presently the technical concept of several countries, for example, the PBMR and GT-MHR projects. Direct cycle configuration simplifies significantly the plant system design and should bring considerable cost benefit. Coupling a direct helium cycle to the HTR-10 test reactor would be another attractive proposal to the second phase of the test reactor project.

This coupling proposal would basically require the dismantling of the existing steam generator and helium circulator, probably even the steam generator pressure vessel. It is also to be taken into account that the design temperature of the HTR-10 carbon steel pressure vessel system should not be higher than 350^{o}C. This basically limits the helium inlet temperature to about 300^{o}C.

One of the proposals under consideration is shown in FIG. 5. In this proposal, the gas turbine cycle is again a recuperated, inter-cooled Brayton cycle. The high pressure turbine drives the two compressors with a speed of 18, 000rpm and the power turbine drives the generator with the speed of 3000rpm. Helium flows through the reactor with a pressure of about 1.76 MPa. Listed in Table 3 are cycle parameters preliminarily chosen for further design studies.

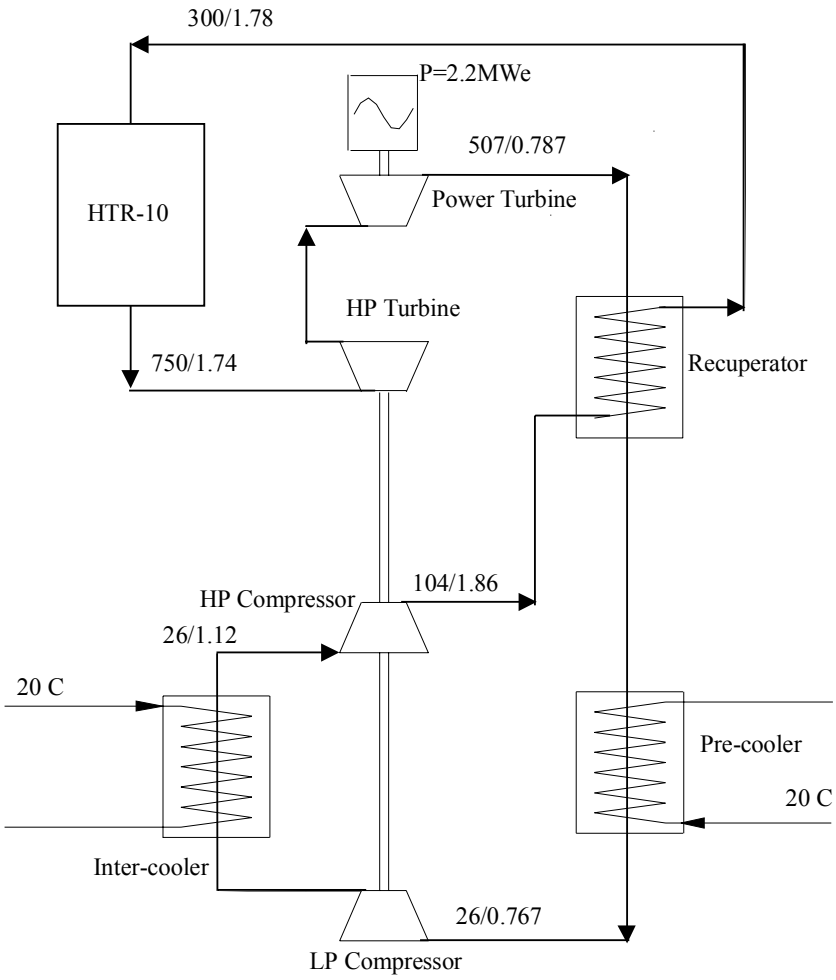

FIG. 5 Flow Diagram of Coupling a Direct He Turbine Cycle to HTR-10

Table 3: Preliminary parameters of direct helium turbine cycle

	HP Turbine	Power Turbine	HP Compressor	LP Compressor
Inlet temperature	750 °C	610 °C	26 °C	26°C
Inlet pressure	1.74 MPa	1.13 MPa	1.12 MPa	0.767 MPa
Pressure ratio	1.541	1.437	1.627	1.476
Rotating speed	18, 000 rpm	3000 rpm	18,000 rpm	18, 000 rpm
Mass flow rate	4.28 kg/s			

5. SUMMARY

It is planned to couple a gas turbine cycle later to the HTR-10 test pebble bed reactor which is now under construction and will soon reach its first criticality. Though the current HTR-10 design allows the installation of an intermediate heat exchanger in the existing steam generator pressure vessel, no decision has been made regarding the system configuration of the gas cycle to be coupled with HTR-10. Both indirect and direct cycles are possible options. Different options are under consideration as discussed in the previous sections. The materialization of reasonably coupling a gas turbine cycle to HTR-10 would help acquire R&D experience of nuclear power generating technology using the combination of high temperature reactor and gas turbine.

SELECTION OF JAERI'S HTGR-GT CONCEPT

Y. MUTO, S. ISHIYAMA, S. SHIOZAWA
Japan Atomic Energy Research Institute,
Oarai-machi, Ibaraki-ken, Japan

Abstract:

In JAERI, a feasibility study of HTGR-GT has been conducted as an assigned work from STA in Japan since January 1996. So far, the conceptual or preliminary designs of 600, 400 and 300 MW(t) power plants have been completed. The block type core and pebble-bed core have been selected in 600 MW(t) and 400/300 MW(t), respectively. The gas-turbine system adopts a horizontal single shaft rotor and then the power conversion vessel is separated into a turbine vessel and a heat exchanger vessel. In this paper, the issues related to the selection of these concepts are technically discussed.

1. INTRODUCTION

In JAERI, a feasibility study of HTGR-GT has been conducted since January 1996 under the sponsorship of the Science and Technology Agency in Japan [1-3]. This paper was prepared based on the results of this study. So far, the designs of 600, 400 and 300 MW(t) power plants have been carried out.

There are two types of core, that is, block type and pebble bed type. The former is considered to have an advantage in the larger core capacity and the latter has a higher availability and smaller fission products plate out. Then, in the 600 MW(t) plant, the block type core was employed. On the other hand, pebble bed type core was employed for the 300 and 400 MW(t) plants. In the reactor design, the design of reactor pressure vessel (RPV) is one of the most important issues. Then, some discussions are made in this subject.

There are three types of turbomachinery system, that is, GA [4], ESKOM [5] and JAERI [6,7] are proposed at present. GA's system is a vertical single shaft rotor and all the power conversion components are accommodated in the one pressure vessel. ESKOM's system is a vertical multi-rotor configuration and each rotor is housed in each vessel. In the former design, many difficulties are expected such as shaft seals, shaft vibration behavior, capacity of axial catcher bearing and structural design exposed to high temperature and large pressure difference. In the latter design, there exists an over-speed problem at the time of load rejection in generator. Complicated flow pass may cause associated difficulties in the pressure seal and reliability in the structural design. In JAERI's design, all the components can be designed based on the existing technology and its reliability is sufficiently high. The replacement, inspection and reassembling of turbomachinery are possible mainly by means of remote control devises. These design items are discussed precisely.

2. DESIGN PARAMETERS AND REACTOR VESSEL DESIGN

2.1 Design parameters

There are well-known two types of reactor. One is the core with block type fuel elements and the other is the pebble-bed core. In the framework of the above feasibility study, both the designs have been conducted to examine and clarify their characteristics.

In case of block type, the modest reactor outlet gas temperature of 850℃ has been employed because the restriction of the maximum fuel temperature at the normal operation is most critical.

The structure in the upper reactor plenum becomes relatively complex due to the more number of control rods and the insertion of fuel exchange machine compared with the pebble bed. Then, the simple reactor vessel structure without insulation or cooling and then, 9Cr-1Mo-V steel is employed and the inlet gas temperature was reduced a little from the cyclically optimum temperature to obtain the high enough material strength needed to achieve the maximum vessel diameter. Then, the main parameters are determined as follows:

Reactor thermal power 600 MW

Reactor outlet gas temperature 850℃

Reactor inlet gas temperature 460℃

Helium gas pressure 6 Mpa

Figures 1 and 2 show the flow diagram and the vertical and horizontal cross-sections of the reactor.

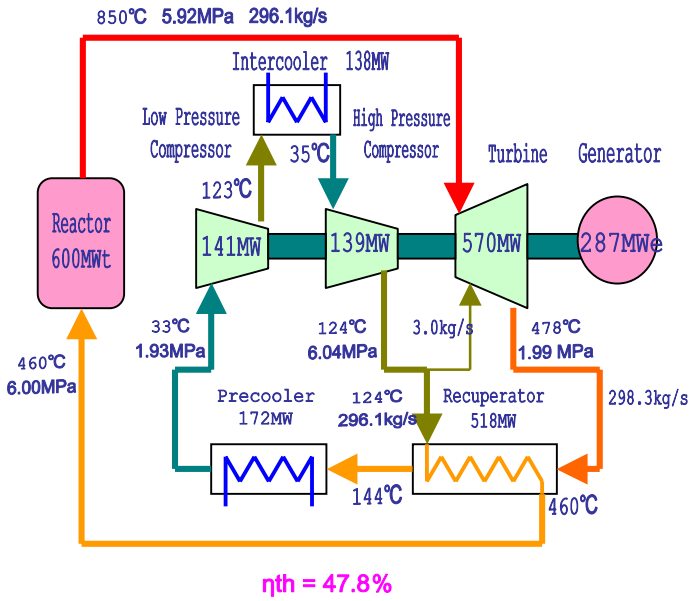

Fig. 1. Flow diagram for the 600 MW(t) plant.

In case of pebble-bed core, the higher reactor outlet gas temperature of 900℃ could be achieved easily at the normal operation. In this type of core, the maximum temperature at the depressurization accident is most critical. Due to the lower power density requested to prevent the excessive core pressure drop, the vessel diameter is obliged to become larger than that of the block type core. The original core structure developed by HTR-module in Germany is suitable to adopt the thermal insulation inside the reactor pressure vessel to reduce the vessel temperature. Then, the reactor inlet gas temperature to coincide with the optimum value from the aspect of cycle thermal efficiency and at the same time the LWR pressure vessel material of SA533 can be employed. The main design parameters are as follows:

Reactor thermal power 300 to 400 MW

Reactor outlet gas temperature 900℃

Reactor inlet gas temperature 550℃

Helium gas pressure 6 Mpa.

Regarding the thermal power, 300 MW was employed first and increased up to 400 MW in the second step. Naturally, 400 MW will be more desirable from the economic aspect. Figures 3 and 4 show the flow diagram and the vertical and horizontal cross-sections of the reactor.

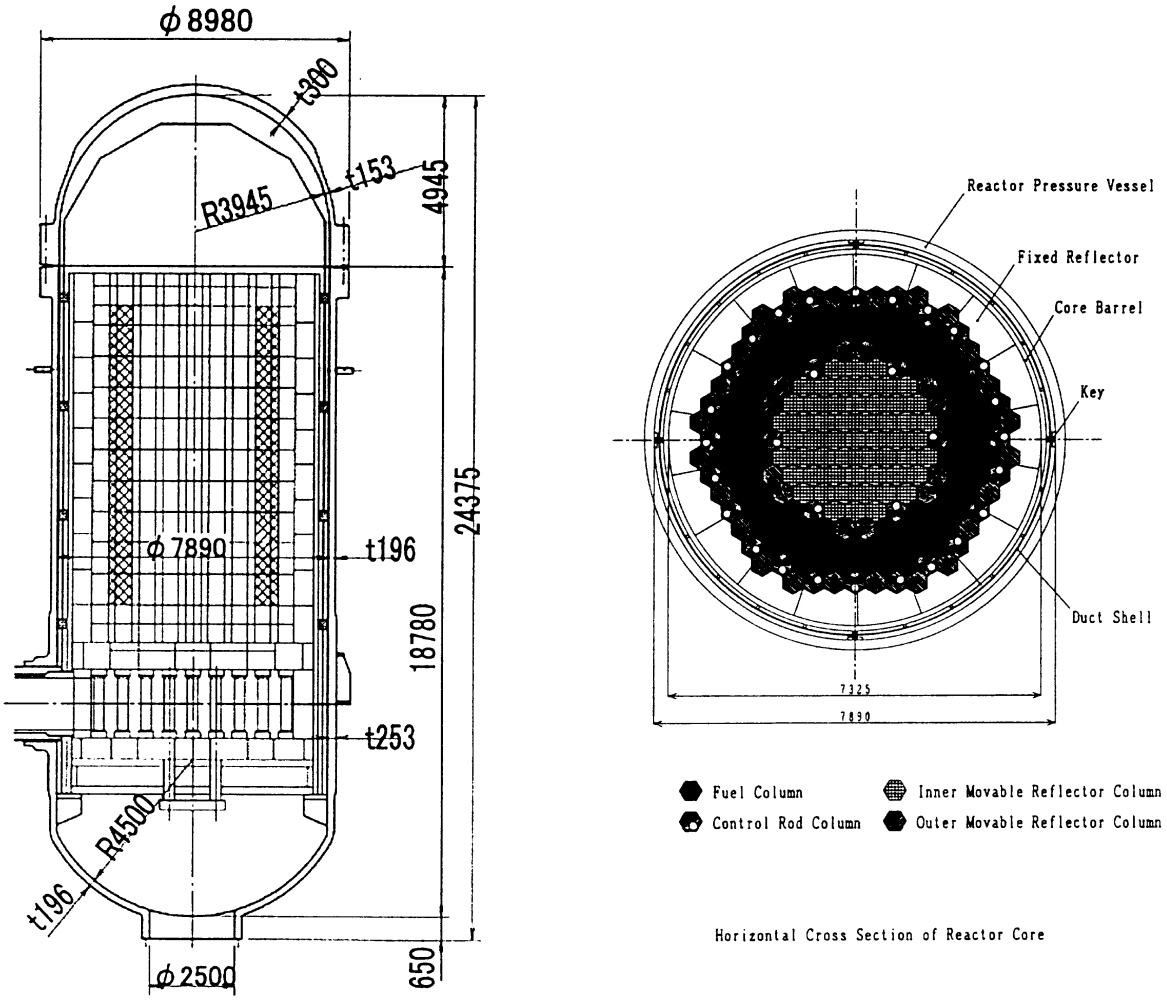

Fig. 2. Vertical and horizontal cross sections of the 600 MW(t) reactor.

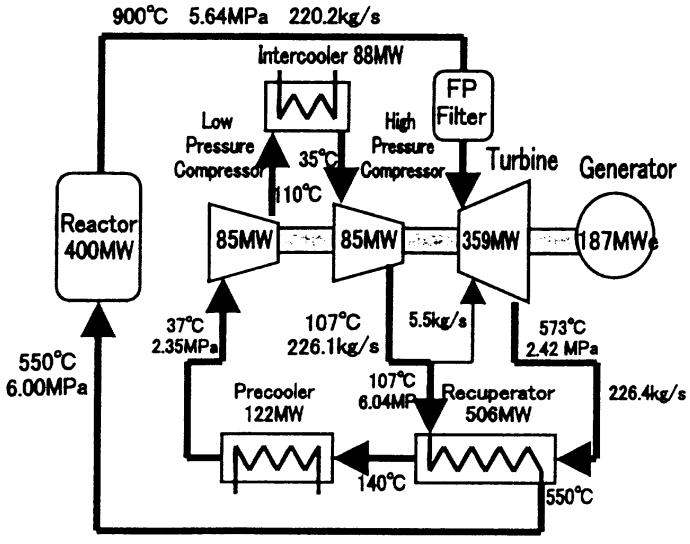

Fig. 3. Flow diagram of 400 MW(t) plant.

2.2 Reactor vessel design

The reactor vessel design is very important issue because this requires high reliability and at the same time its cost occupies a significant ratio in the total construction cost and moreover it influences on the achievable reactor power or cycle thermal efficiency. There are three design options are proposed as follows:

1) High RPV temperature and 9Cr-1Mo-V steel
2) Cooling by the compressor outlet He gas and SA533 steel
3) Week inner insulation of RPV and SA533 steel.

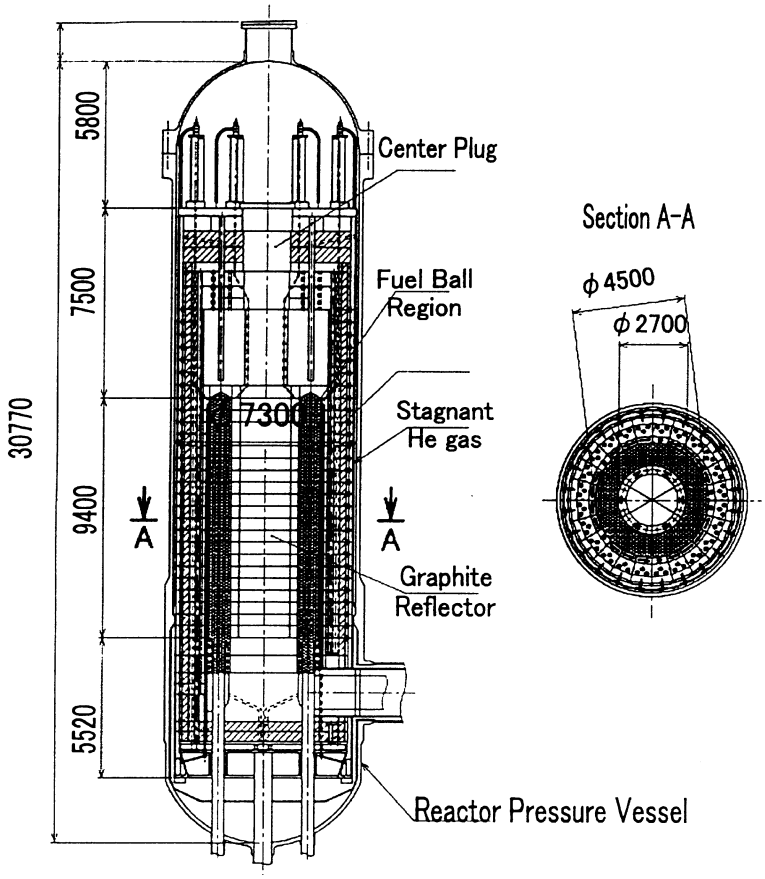

Fig. 4. Vertical and horizontal cross section of 400 MW(t) reactor.

The first option is the simplest, but the material strength of 9Cr-1Mo-V steel at 500℃ is not high enough to achieve the large reactor power and cycle thermal efficiency. In addition, this material is not yet authorized as the class 1 vessel material, which is required in the licensing procedure.

The second option has great advantage to be able to adopt SA533, which is the RPV material for the light water reactors. However, the cooling of RPV by the cold He means that the flow passes for the reactor inlet gas and the cooling gas should be separated. This requires additional space within the RPV and may affect the maximum temperature at the time of depressurization accident. In addition, the cooling passage is obliged to become complicated.

The third option is similar to the second one. The difference is that in this case, cooling pass is not influenced but, the high reliability of the internal insulation structure is required.

2.3 JAERI's decision

The major characteristics of 600 MW(t) block type core and 400 MW(t) pebble bed type core are compared in Table 1. It is not easy to judge which type is superior, but it should be pointed out that there is no manufacturing design and fabrication experiences in the pebble bed reactor in Japan and this fact is an additional critical factor in the selection. At the end of this fiscal year, we will have data of both the construction cost and power generation cost estimated for these plants. In addition, some studies will be implemented for the RPV design. Then, we could make the selection in these options in near future..

3. ARRANGEMENT OF POWER CONVERSION SYSTEM

Firstly, the power conversion system is classified into a vertical rotor and a horizontal rotor. The second option is a single rotor or a multi rotor. The third option is a single vessel type or a multi-vessels type. As there is no possibility of the combination of the horizontal rotor and the single vessel, a number of probable cases will be 6. Among them, three designs are actually implemented, that is, Case A (GA/MINATOM type), Case B (PBMR type) and Case C (JAERI's type), which are shown in Figs 5 to 6 schematically.

Before comparing them, we had better to remind the fundamental features of the helium gas turbine. Firstly, the long rotor length is needed because more number of stages is needed in the helium turbine than that in the existing thermal gas turbine and usually two compressors are needed to achieve sufficiently high efficiency. This means that the rotor dynamics behavior becomes very important related to the adoption of magnetic bearings. The second is that the coolant is the primary helium gas and the seal mechanism for the helium is much more difficult than the air or steam. Therefore, a submerged structure with magnetic bearings is desired to arrange all the rotating components. The third is that there are vast ranges both in the temperature and in the pressure. This means that the integral arrangement becomes very difficult. The forth is the existence of radioactivity in the turbine, recuperator and piping due to the plate-out of fission products such as Cs-137 and Ag-110m. Then, the maintenance by remote control method is needed. These are summarized as follows though they are mutually implicated and then very complicated:

1) Rotor dynamics behavior is important,
2) Submerged arrangement with magnetic bearings,
3) Rotating seal and absorption of thermal expansion,
4) Necessity of remote control maintenance.

Regarding the above-mentioned options, we have selected first a combination of "horizontal" rotor and "multi-vessel". Where the multi-vessel means separation of rotating machines and heat exchangers though only the intercooler is accommodated together with rotating machines due to the strong connections with the compressors. This selection was considered to be most desirable to solve the above problems and all the existing thermal gas turbines are horizontal type and then this is effective to minimize the research and development works. Secondly, a single rotor was employed to protect the over speed of rotor at the time of electrical load rejection.

Regarding the other types, we didn't implement the design and we have no reliable data. However, rough comparisons are tried. The results are shown in Table 1. Case A becomes most compact and then it is most desirable from the economic aspect. However, it will be very difficult to achieve good rotating seal, sufficiently high support stiffness to achieve the acceptable rotor dynamics behavior. The size of axial magnetic bearing and its associated catcher bearing becomes very large compared with the state-of-the-art technology. In addition,

TABLE 1. COMPARISON OF THE PLANT DESIGNS WITH BLOCK TYPE CORE AND PEBBLE BED TYPE CORE

Reactor Type	Block Fuel's Core	Pebble Bed Core
Power and Efficiency		
Thermal Power	600 MW(t)	400 MW(t)
Electrical Power	284 MW(e)	182 MW(e)
Cycle Thermal Efficiency	48.4%	47.3%
Net Thermal Efficiency	46.2%	45.5%
Main Gas Conditions		
Reactor Outlet Helium Gas Temperature	850℃	900℃
Reactor Inlet Gas Temperature	460℃	550℃
Helium Gas Pressure	6 MPa	6 MPa
Mass Flow Rate	296.4 kg/s	220.2 kg/s
Fuel		
Enrichment	15% (Packing fraction = 35% and 30%)	10%
Average Burn-up	110 GWd/tonU	100 GWd/tonU
Fuel cycle	450 day	903 day
Fuel Exchange Working Time	82 day (Including reflector exchange)	On power loading
Core		
Equivalent Diameter	3.70 m (Inner Dia.) 5.48 m (Outer Dia.)	2.70 m (Inner Dia.) 4.50 m (Outer Dia.)
Effective Height	8.1 m	9.4 m
Average Power Density	5.77 MW/m3	4.2 MW/m3
Pressure Drop	1.42%	6.09%
Maximum Fuel Temperature at Normal Operation	1286℃	1165℃
Maximum Fuel Temperature at Accident	1575℃	1520℃
Reactor Vessel		
Inner Diameter	7.89 m	7.30 m
Height	24.4 m	32.4 m
Weight	398 ton (Upper Part) 92 3 ton (Lower part)	134 ton (Upper Part) 975 ton (Lower part)
Material	9Cr-1Mo-V steel	SA533
Dose Rate due to FP Plate out on the Turbine Rotor	160 mSv/h	5.44 mSv/h

TABLE 2. COMPARISON OF THREE TYPES OF ARRANGEMENT OF THE POWER CONVERSION SYSTEM

Design Items	Types of Power Conversion System		
	Case A (GA)	Case B (PBMR)	Case C (JAERI)
Aerodynamic design	No problem	No problem	No problem
Rotor dynamics	There exist more than two bending modes under the rated speed. The high enough support stiffness is difficult to be achieved.	As the rotor length is shorter in the sprit shaft design than the single shaft design, the problem is mitigated.	By means of insertion of diaphragm coupling, the rotor can be divided into the connection of simple rotors.
Magnetic bearing	The axial bearing and its catcher bearing become larger and then exceed the state-of-the-art technology.	Due to the smaller capacity and sprit shaft design, this problem is mitigated, but still not so easy.	Some developments are needed regarding a control of flexible rotor, catcher bearing and power amplifier.
Over-speed of generator	No problem	In case of sprit shaft design, the over speed becomes higher than 110% at the time of load rejection.	No problem
Alignment	Maybe possible	Maybe possible	Possible but the access to turbine is needed at the time of assembling.
Field balance	Difficult	Maybe possible	Possible
Rotor replacement	Possible, but tentative fixation of rotor and casing is needed.	Possible, but tentative fixation of rotor and casing is needed.	Possible, but extraction space is needed.
Seal among components	Some leakage is inevitable	Not clear	No problem
Thermal expansion and insulation	Careful design and some countermeasure are needed.	Maybe possible	No problem
Building area	Smallest	Small	Larger than other cases due to the horizontal layout.

the high temperature surrounding the turbine rotor is worried about to realize the necessary thermal insulation for the magnetic bearings and to minimize the thermal expansions between components. In Case B, similar problems can be pointed out. However, the effects are mitigated than the Case A due to the smaller capacity and shorter rotor length due to multi-rotors. The most worried problem is the over speed protection in which the Electricity Enterprise Law in Japan requires the maximum over speed less than 111%. In addition, the complex structures are worried about in the unexpected thermal distortion and larger helium gas leakage.

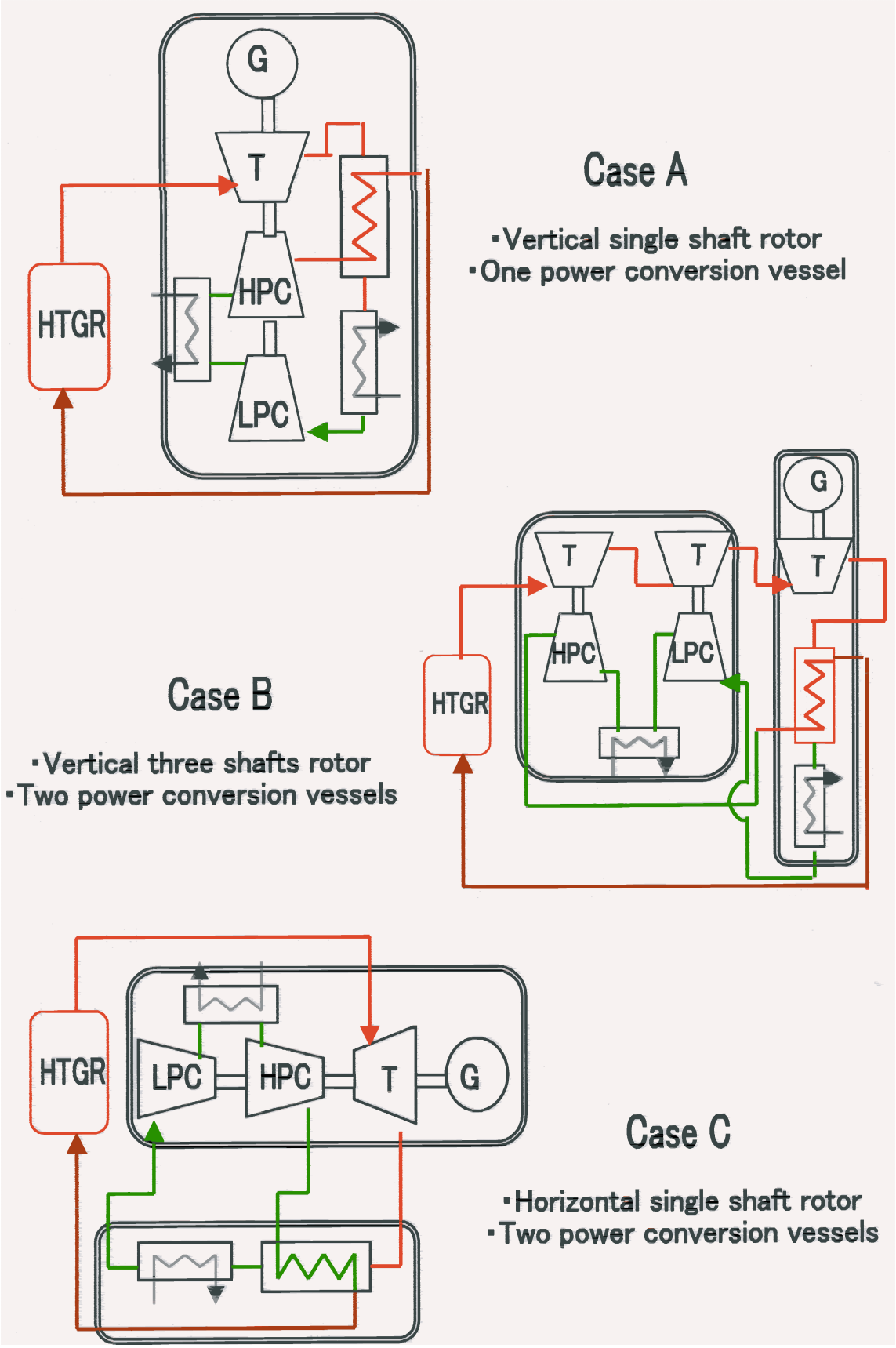

Fig. 5. Three types of arrangement for the power conversion system.

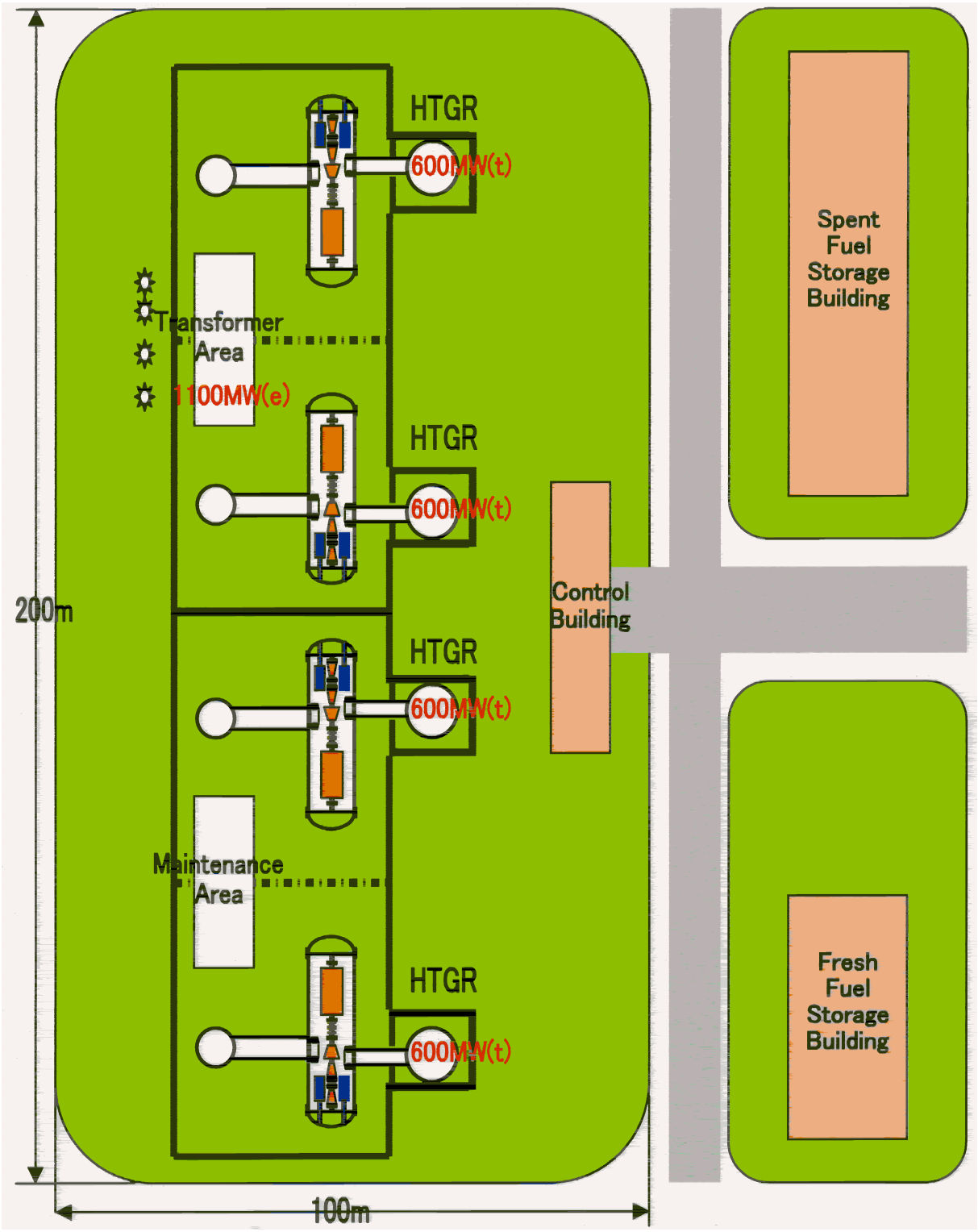

Fig. 6. Plot plan of HGTR-GT power plant.

The drawback of our design is the larger building area for the horizontal turbine vessel and associated rotor extraction space. The length of the turbine vessel is 32m. The lengths of the gas turbine rotor and the generator rotor are 13.6 m and 12.9 m, respectively. Though both the rotors should be extracted from the turbine vessel, only the length of 16m is needed because the generator rotor can be moved aside laterally after its extraction. In the real plant, more than 4 units, that means more than 1000 MW(e), will be placed at the same site in Japan. Then, such an extraction space and a maintenance area can be used commonly. Therefore, the total space could be saved as shown in Fig. 8 than seemingly expected.

Regarding the type of power conversion system, no controversy exists in JAERI except for small options. In the demonstration plant, the horizontal single shaft rotor and the two separated power conversion vessels will be selected without doubt. However, some studies regarding the vertical shaft design will be continued to clarify its technical feasibility.

4. SUMMARY

In the feasibility study of HTGR-GT power plant in JAERI, some selections in the design parameters or decision have been made. Those are the reactor type, the reactor power, the outlet and inlet gas temperature, gas pressure, reactor vessel design, the rotor orientation and the arrangement of power conversion system components. The reasons of selections are described. Regarding the reactor type, both the block type core and the pebble bed type core are designed and the final decision will be made in near future. The system parameters are 850℃, 460℃ and 6 MPa for the 600 MW(t) plant and 900℃, 550℃ and 6 MPa for the 400 MW(t) plant, respectively. The decision of reactor vessel design will be made in near future. The rotor orientation is horizontal though some further design work will be continued for the vertical rotor to improve the economic aspect. The power conversion system components are housed in the two vessels, that is, the turbine vessel and the heat exchanger vessel in accordance with their functions.

REFERENCES

[1] Muto, Y., Y. Miyamoto and S. Shiozawa, “Present Status of the Feasibility Study of HTGR-GT System”, IAEA Technical Committee Meeting, Petten, Netherlands, 10-12 November 1997.

[2] Muto, Y., Y. Miyamoto and S. Shiozawa, “Present Activity of the Feasibility Study of HTGR-GT System”, IAEA Technical Committee Meeting, Beijing, China, 2-4 November 1998.

[3] Muto, Y., “Present Activity of the Design and Experimental Works for HTGR-GT System in JAERI”, Helium Gas Reactor Workshop, Palo Alto, USA, 7-8 December 1999.

[4] Neylan, A. J. et al., “Status of GT-MHR with Emphasis on the Power Conversion System”, IAEA-TECDOC-899, pp.55-66 (August 1996).

[5] Eskom, “Eskom sees a nuclear future in the pebble bed”, Nuclear Engineering International, pp.12-16 (December 1998).

[6] Muto, Y. et al., “Design Study of Helium Turbine for the 600 MWt HTGR-GT Power Plant”, Proc. International Gas Turbine Congress 1999 Kobe, pp.313-320 (November 1999).

[7] Muto, Y. et al., “Design Study of Helium Turbine for the 300 MW HTGR-GT Power Plant”, ASME Paper 2000-GT-159 (May 2000).

FEATURES OF ADAPTING GAS TURBINE CYCLE AND HEAT EXCHANGERS FOR HTGRs

V.F. GOLOVKO, I.V. DMITRIEVA,
N.G. KODOCHIGOV, N.G. KUZAVKOV
OKB Mechanical Engineering, Nizhny Novgorod,
Russian Federation

A.G. CHUDIN
Ministry of the Russian Federation for Atomic Energy, Moscow,
Russian Federation

A. SHENOY
General Atomics, United States of America

Abstract:

Problems of adaptation of the closed direct gas turbine cycle to nuclear power plant with HTGRs for producing electricity with high efficiency and safety are considered. It should be noted that only in such combination advantages of HTGR producing high-temperature heat with outlet helium temperature of up to 1000°C could be realized, in comparison with other reactor plants. As for reactor plants with steam turbine cycle, there are no problems with transients and disconnection of Power Conversion Units (PCU) at abnormal situations since there is substantial experience in operation of such plants (nuclear engineering was based on steam-turbine cycle from the very beginning) and experience in steam turbine units design. In similar situations, HTGRs with gas turbine cycle rise more problems concerning PCU control and serviceability and, in particular, risk of turbomachine overspeeding, serviceability of heat exchanges and so on. Also, a difficulty to be resolved is normal start-up of reactor plant together with turbomachine, compressors of which supply the core with gas flow. For competitiveness of reactor plants with gas-turbine cycle in comparison with other NPPs and conventional power plants on fossil fuel, heat exchange equipment of gas turbine cycle should have unique performances to provide for plant efficiency of up to 50%. For this purpose, heat exchangers should have high compactness and minimal pressure losses to allow assembling within vessels with limited dimensions and should operate under significant pressure differences between circuits (up to 5 MPa) and at high temperatures of up to 600°C. Approaches to the solution of the noted problems are reflected in the report with reference to the modular helium reactor with gas turbine (GT-MHR) developed in the international cooperation.

1. GAS TURBINE CYCLE PLANT PERFORMANCES

Capabilities and advantages of HTGR, due to the helium temperature at reactor outlet of up to 1000^{o}C, can be used for supplying high temperature technologic processes with heat or for electricity production using the direct closed gas-turbine cycle.

Gas-turbine cycle efficiency of such NPPs that is up to 50%, together with considerable simplification and smaller number of available equipment and systems (turbine building, including steam generator, steam pipes, condenser, deaerator, etc.) make them competitive in the field of electricity production in comparison with NPPs with steam cycle or conventional power plants on fossil fuel.

On early stage of development and creation of HTGRs, when it was necessary to confirm their reliable operation, HTGRs were applied with mastered and developed steam-turbine cycle for electricity production. Operating experience of such HTGRs has confirmed their reliability, however, their economical indexes are lower than those of conventional NPPs. The economical reasons have led to cancellation of HTGR programs in the

development countries and to shutdown of prototype reactors Fort St. Vrain (USA) and THTR-300 (Germany) commissioned in the second half of the 1970s with electric capacity of 340 and 300 MW(e), respectively.

There is no experience in usage of NPPs with HTGR and gas-turbine cycle in the world, and the advantages of such NPPs are based on experimental and analytical research and development of similar NPPs and experimental plants/1/.

At present, the international project of the 600 MWt commercial GT-MHR plant with a modular reactor is being developed in Russia for electricity production using gas turbine cycle /2/.

The optimal parameters of gas-turbine cycle for NPPs with HTGR, that ensure the maximal plant efficiency, are defined by allowable reactor outlet and inlet temperatures. In experimental reactors of small power, the core outlet helium temperature is up to 950^{o}C. The level of temperature depends on power, type of core, layout and safety assurance concepts. It is known, that NPPs of higher power have better economical indices in comparison with smaller power ones, provided other conditions are equal, therefore it is expedient to use in NPP a reactor with the highest possible power.

At present, all of the modern HTGR designs are based on the modular concept providing for increased safety because of inherent self-protection properties and passive cooldown. The powers of reactors with a pebble bed core and annular active core of prismatic fuel blocks are limited by 215 and 600 MWt, respectively. These values are determined by allowable fuel temperature (<1600^{O}C) at residual heat removal through the reactor vessel to the reactor cavity cooling system in case forced cooling of the core is lost. Evidently, higher power is required to improve economical indices of NPPs. In the core of prismatic fuel blocks, higher power is ensured by better heat removal conditions in the annular blocks and their denser structure, and also due to reduced temperature at reactor outlet of up to 850^{O}C, that is lower than 950^{O}C in the pebble bed core case. Reactor outlet helium temperature of up to 850^{O}C is sufficient to reach maximal gas-turbine cycle efficiency under limited reactor inlet helium temperature of 490^{O}C (to be shown below), and it also creates better temperature conditions and extends service life of cross duct, core support structure, turbine inlet metal elements and turbine materials.

There is an essential dependence of cycle efficiency on recuperator effectiveness to validate reactor outlet helium temperature of 850^{O}C (at the turbine inlet) mentioned above (Fig. 1). The modern technologies of compact heat exchanger development give foundations for creation of a recuperator with high effectiveness of up to 95% with allowable sizes and pressure losses. Decrease in recuperator effectiveness by every 5% results in decrease in plant efficiency by ~2-5% in the optimal range of cycle pressure ratio from 2 to 3,5. Thus, for helium temperature 850^{O}C and recuperator effectiveness in cycle of 0.95, the efficiency is from 47% to 49% for the optimal range of pressure ratio.

As follows from Figure 2, increase or decrease in outlet temperature of 850^{O}C by every 50^{O}C results in respective change of ultimate plant efficiency by 1,75-2%. These plots also demonstrate that the optimal pressure ratios providing for the maximal plant efficiency depends on cycle recuperation effectiveness and does not practically depend on reactor outlet helium temperature (at the turbine inlet). So, optimal pressure ratio is ~ 2,3 for recuperator effectiveness of 0.95, for recuperator effectiveness 0.85 it extends to up to ~ 3.1. In turn, increase in pressure ratio results in increase in number of stages and, accordingly, in overall turbine and compressors dimensions, which also leads to reduction in their efficiencies, that are the most important parameters affecting the cycle efficiency. Optimization of turbine and compressor efficiencies that depend on pressure ratio and many other parameters (power, dimensions, speed, volume flow rate, technology of manufacturing, etc.) is a special, interdependent problem. Therefore, for cycle parameters optimization, turbines efficiency is

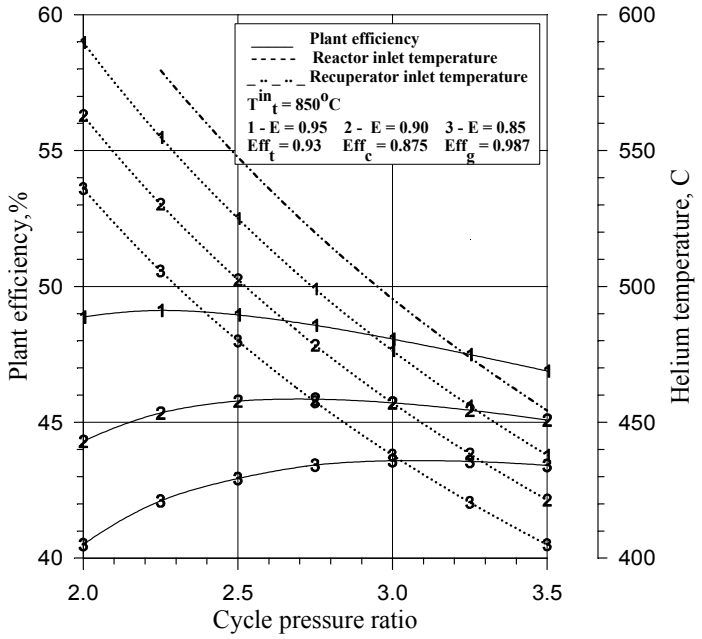

Fig.1. Influence of pressure ratio and recuperator effectiveness on plant efficiency, reactor and recuperator inlet helium temperature.

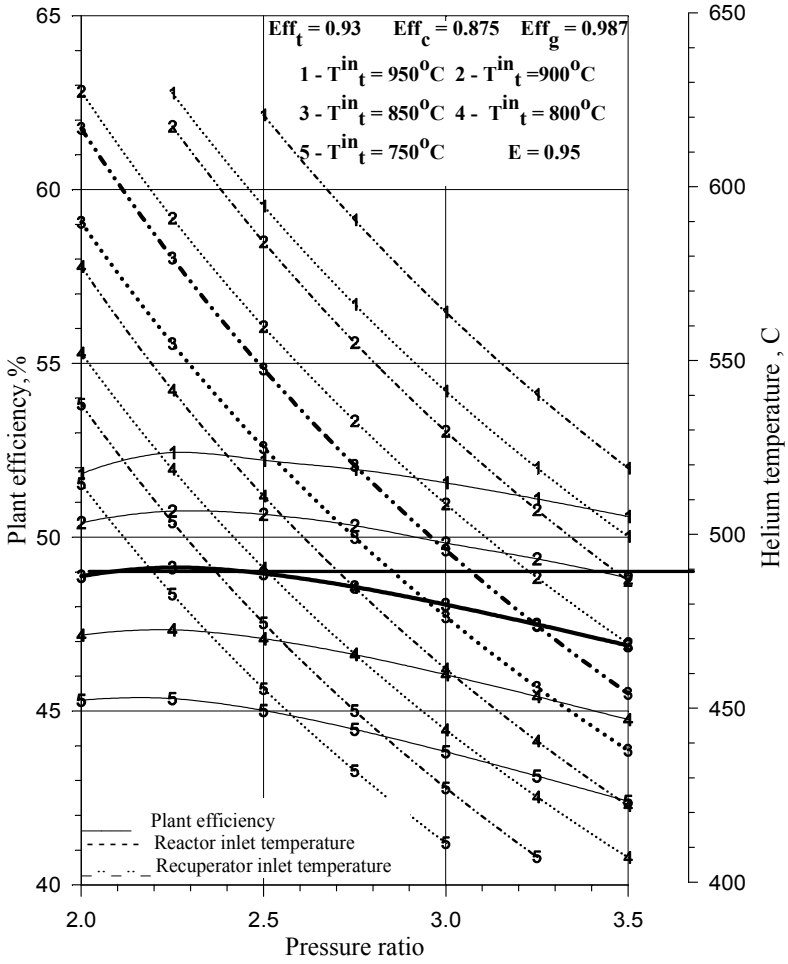

Fig.2. Impact of reactor outlet helium temperature (at the turbine inlet) on plant efficiency, reactor and recuperator inlet helium temperature

assumed to vary from 94% to 90% and compressors efficiency - from 89% to 86%, which corresponds to the considered range of pressure ratio from 2.0 to 3.5 (data for the plots are computed for turbine efficiency of 93% and compressors efficiency of 87,5%).

However, as it is seen from Figures 1 and 2, there is an essential influence of pressure ratio on reactor inlet helium temperature and recuperator inlet temperature.

Reactor inlet helium temperature is constrained by the temperature of the reactor vessel metal, that must ensure long service life. For vessel of perlitic steel, admissible temperature of helium is up to ~350^{O}C, for vessel of high-chromium steel - up to ~490 ^{O}C. With admissible reactor inlet temperature of 850 ^{O}C and adopted recuperator efficiency of 0.95, the optimal pressure ratio ensuring maximal plant efficiency of 49% is equal to ~2,3.

However, temperature of helium at the reactor inlet is 550^{O}C at this pressure ratio. Admissible helium temperature at the reactor inlet of 490^{O}C is ensured by increase in pressure ratio up to ~2.865, with respect to the optimal value, and, respectively, by decrease in plant efficiency from 49% to 48.36% (Fig. 2). Decrease in reactor inlet helium temperature from 550^{OC} to 490^{O}C can be achieved by decreasing reactor outlet helium temperature and cycle recuperation effectiveness, however it decreases the plant efficiency more than in case of increasing of pressure ratio.

Applying vessels of perlitic steel requiring decrease in reactor inlet temperature down to 350 C is non-optimum for the turbine cycle. Such temperature requires both increase in pressure ratio and decrease in reactor outlet helium temperature and recuperation efficiency, which, in total, results in decrease of cycle efficiency to 30%-35%. It should be noted that decreasing of reactor inlet helium temperature can be more optimally achieved by decreasing reactor outlet helium temperature and maintaining the higher recuperation efficiency, because it helps achieve greater cycle efficiency. However, under reactor inlet helium temperature of up to 350^{O}C, efficiency of gas turbine cycle is lower than that of steam-turbine cycle with reactor outlet helium temperature of 850 C and inlet temperature of 350 C.

Using intercooled or non- intercooled helium cycle has a strong influence on complication of the turbomachine design and its layout when arranging it in the limited space of the Power Conversion Unit (PCU). Figure 3 shows the design of the GT-MHR plant PCU.

Implementation of coolers results in lengthening of the turbomachine shaft. It may require an additional radial bearing and additional cross gas ducts within PCU which will increase hydraulic losses and leaks in helium circuit and also will complicate turbomachine installation and dismantling in case of replacement or repair. At the same time, as seen from Figure 4, arrangement of two intercooling stages considerably raises cycle efficiency from 44% up to 50%, and the highest increase (~4.5%) takes place when one stage is added. Despite of drawbacks, such increase in efficiency is a weighty reason to include at least one intercooling stage.

The selection of primary system pressure is based on a trade study involving influence of the pressure on wall thickness of the reactor and power conversion vessels, on the primary coolant system pressure losses and the size of the components located within the two vessels. Higher helium pressure results in smaller component sizes and less considerable pressure loss, but increases the vessel wall thickness. Lower helium pressure results in thinner reactor and power conversion vessels walls, which reduces the cost of the materials, conversely, higher volumetric flow rate increases the height of the turbine blades and efficiency of turbines and compressors, but simultaneously requires larger components under the set pressure loss. The maximal helium pressure for more than 100 MW plants is optimal at level of 7-7,5 MPa. At lower plant power and sizes of turbine (compressors) blade systems, specific decrease of blade height adversely affects their efficiency. This influence can be reduced by increasing volumetric flow rate at lower primary system helium pressure.

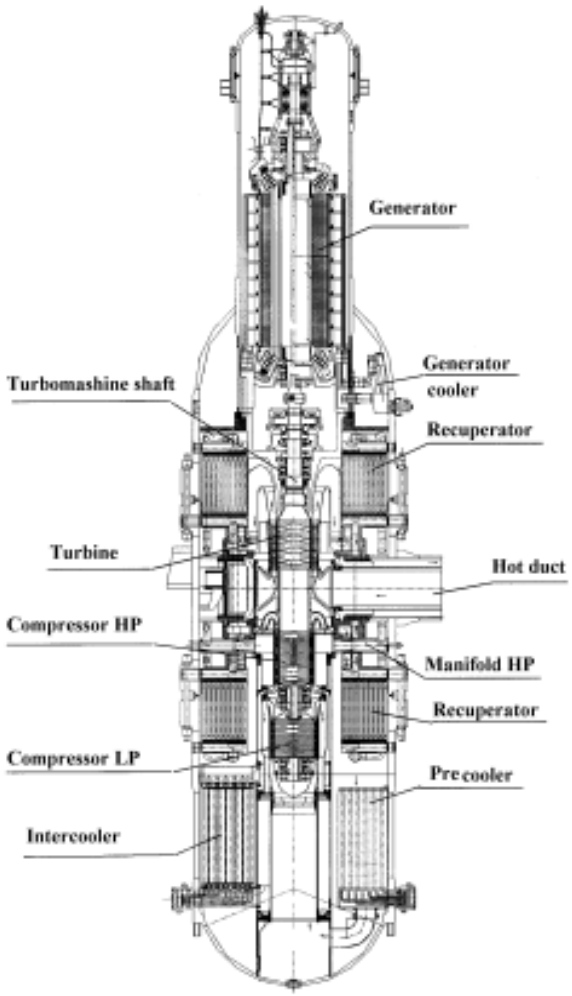

Fig.3. Power conversion unit.

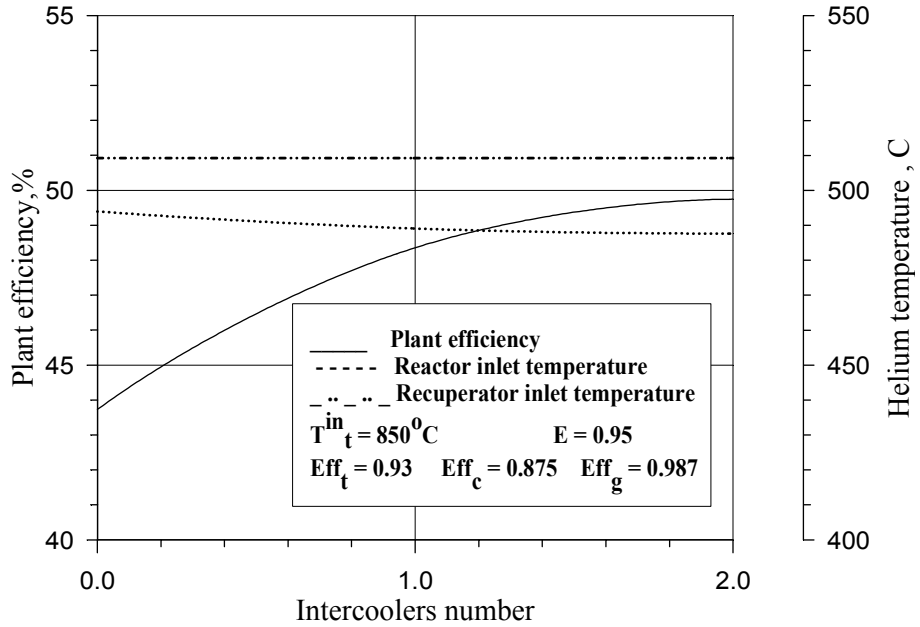

Fig.4. Impact of intercoolers number on plant efficiency, reactor and recuperator inlet helium temperature.

Thus, the performed analysis shows that for HTGR of up to 600 MW power with accessible and admissible reactor outlet helium temperature of up to 850^{O}C and inlet temperature of up to 490^{O}C, the following gas turbine cycle performances, that provide the maximal plant efficiency, can be taken:

Recuperator efficiency	0.95
Number of helium intercoolers	1
Compressors pressure ratio	2.865.

2. CONTROL, DESIGN OF TURBOMASHINE AND HELIUM CIRCUIT

The requirements for efficiency and maneuverability of reactor plants with HTGR and gas-turbine cycle intended for electricity production should be based on superiority and competitiveness of such plants in comparison with conventional power plants on fossil fuel and other types of NPPs.

The common requirements imposed by operating organizations on the power system of Russia, are as follows: daily monitoring of electrical load in the range from 100% to 50% and from 50% up to 100% with the rate of 0.6% /min; rapid change of load in the control range from 100% to 30% with the rate of up to 6%/min; rapid increasing and rejection of power on the 20% level with the rate of up to 10%/min at grid failures; grid frequency monitoring followed by the change of electric load in the range of ±5% with the rate of 2%/min, etc.

Therefore, aside from reliable and safe operation, HTGR plant with gas-turbine cycle in, shall ensure the following during normal operation and accidents:

- Startup and shutdown of the plant;
- Stable and effective operation of the plant on 100% electrical load within the required range of its changes;
- Required rate of transferring from one power load to another;
- Off-schedule shutdown for repair and planned shutdown for refueling;
- Plant load rejection to house load level and avoiding of turbomachine overspeeding under abrupt generator disconnection from the grid, its maintenance during defined time and recovery up to the demanded level;
- Rapid and safe trip of reactor and turbomachine in case of loss of offsite power and internal failures in the turbomachine and its systems, resulting in increased vibration, pressure and flowrate fluctuations, overheating of individual elements, etc. above the permissible limits. Fulfillment of these requirements and, at the same time, maximal plant efficiency significantly influence selection of the optimal design of turbomachine, helium circuit and plant control principles. This selection should also be based on the features of similar plants, which were detected, in particular, while designing the GT-MHR plant:
- Rate of removal and restoration of helium inventory of ~6%/min; if helium is removed from the circuit to the inventory tank through the purification system, the rate of removal is up to 1%/min, that is determined by admissible number and sizes of openings in PCU vessel and sizes of external systems, pipe lines and valves;
- Limitations on the rate of helium temperature variation in the circuit, that shall not result in «thermal hammering» and should be within the limits from 100^{o}C/hr up to 300^{o}C/hr and eliminate increasing of temperature differences affecting metal structure by more than 30^{o}C-50 ^{o}C;
- Inadmissibility thermocyclic loading of metal structures due to temperature fluctuations in helium flow resulting in decrease of their lifetime below established value.

Problems related to plant control are tied to the problems of selection of turbomachine overspeeding protection options requiring its rapid trip.

The control of electrical load with the help of variation of helium mass in the circuit and reactor power ensures the greatest efficiency on partial loads and is feasible for any layout and design concepts of PCU, but such control does not ensure demanded rates of electrical load variation and emergency trip of the turbomachine. Therefore, the simplest solution of the complete set of the enumerated requirements and limitations at the current design stage can be carried out by varying helium mass in the circuit and reactor power and by bypassing helium from the high-pressure compressor outlet to the turbine outlet at the single shaft design concept of a turbomachine (Fig. 5).

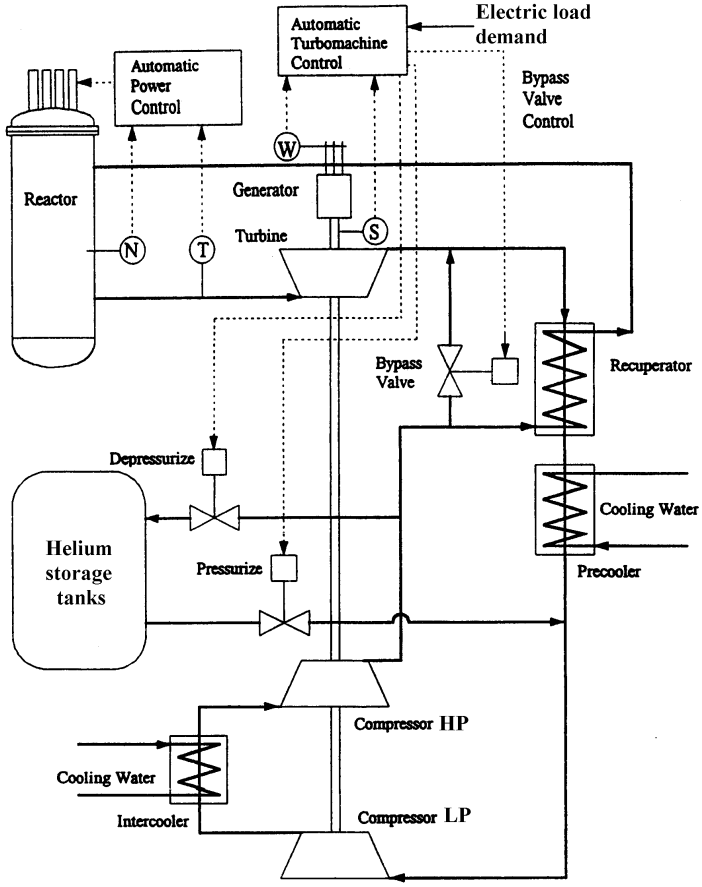

Fig.5. GT-MHR diagram of a single-shaft turbomachine and main controllers.

Generator connected with the turbocompressor by the common shaft and operating in the motor mode from the electric grid through the frequency converter, allows to ensure the required helium circulation through the reactor at startup, for reactor cooldown at planned and emergency shutdowns for repair and refueling. For the case of GT-MHR generator of up to 290 MW, the power of the frequency converter at synchronization of turbomachine speed with the grid and connection of the generator to the grid can amount to up to 5 MW at the shutdown reactor. To ensure sharp synchronization of turbomachine speed with the grid and connection of the generator to the grid at the operating reactor with the help of the turbine, the required power of the frequency converter can be increased to up to 15 MW.

Loading decrease at rates higher than the rate of helium removal from the circuit, emergency turbomachine trips and its prevention from acceleration are ensured simultaneously with removal of helium from the circuit by opening of bypass valves on

helium bypass lines from the high-pressure compressor outlet to the turbine outlet. Opening of valves increases helium pressure at the turbine, outlet, increases helium flowrate through the compressors and reduces the flowrate through the turbine, accordingly, the power of compressors gets increased and the power of the turbine gets decreased. The appropriate opening of valves allows the control of electrical loads on the generator or quickly trip the turbomachine with the generator in case the power supply to the generator gets cut off. This control can be effected at constant reactor power, the balance of which is ensured with the power removed in the precooler and intercooler.

Deficiency of this control mode is the helium temperature increase at the turbine outlet up to the inlet temperature at its emergency trip and heat-up of all the turbine blade system. That's the reason of thermocyclic loading of metal structures on the section behind the turbine outlet up to the recuperator inlet since cold helium mixes with hot helium which is coming out of the turbine. To decrease thermocyclic load, it is necessary to ensure adequate mixing of helium flows.

To avoid such a deficiency and ensure complete turbomachine trip, alongside with bypass of helium through bypass ducts from the high-pressure compressor outlet to the turbine outlet, the consequent quick cut off of helium circulation through the reactor and turbine can be carried out by means of a shut-off device. Its location in the bottom of the reactor is the most preferential from the design viewpoint.

It is known /3,4/, that increasing the turbomachine speed results in increase in efficiency of turbines and compressors and reduction in their dimensions. However, a single-shaft turbomachine requires introduction of the frequency converter between the generator and the grid. The creation of such frequency converter for electric power of 300 MW is problematic. It will be huge and costly, have low reliability and will reduce efficiency of the generator by 2%-3%.

Alternative is the creation of a two-shaft turbomachine with turbine and generator on one shaft and turbine and compressors on the other (Fig. 6). The generator turbine operates at frequency equal to the frequency of the grid, and compressor turbine speed is accelerated. Additional benefits arise, namely: shafts stiffness is augmented because of their smaller

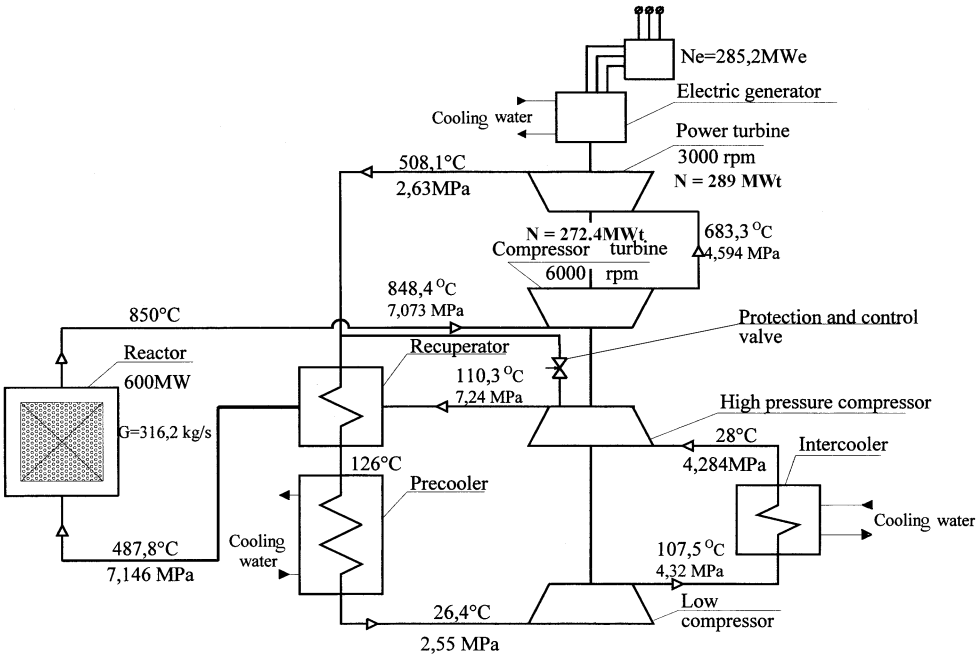

Fig.6. GT-MHR diagram with a two-shaft turbomachine.

length. This ameliorates dynamic performances of rotating shafts. However, applying a two-shaft turbomachine with the improved performances in the plant as contrasted to single-shaft option, calls a set of problems. These are the problems of plant startup, control and protection of the turbomachine.

To provide for helium circulation through the reactor at plant startup, additional devices are indispensable within the turbomachine: either device temporarily connecting two shafts (for example, overrunning clutch), and usage of the main generator operating in the motor mode, or arrangement of the startup electric motor at the bottom of the compressor shaft. None of the alternatives is perfect. The coupling device requires special design development justifying its operability and reliability. The startup electric motor will demand additional hermetic electric inputs in the PCU vessel.

While operating a two-shaft turbomachine it is necessary to have additional controllers to maintain compressor speed within the entire range of loads. Arrangement of additional helium bypasses around compressors, either arrangement of rotatable blades in the turbine or compressors is required for this purpose.

Complex problem at operation of a two-shaft turbomachine is the ensuring of protection from acceleration of the turbine with the generator in case of emergency loss of power supply to the generator. Time of turbogenerator acceleration above admissible speed can amount to ~3 seconds. For this time it is necessary to generate an alarm signal and completely stop helium circulation through the turbine of the generator. It is very difficult from the design viewpoint to stop helium circulation through the turbine of the generator, for example, with the help of bypasses around of it due to high helium temperature. Quick connection of the generator to a power source, for example, air or water cooled resistor heater can be considered as an option of turbomachine braking. The most substantial alternative of preventing from acceleration and ensuring complete trip of the turbogenerator and turbocompressors, as well as at a single-shaft option, alongside with helium bypass through bypass ducts from the high-pressure compressor outlet to the generator turbine outlet, is consequent quick stop of helium circulation through the reactor and turbine by a shut-off device.

3. EFFECTIVE HEAT EXCHANGERS

In order to ensure competitiveness of NPPs with HTGRs in comparison with other NPPs and conventional power plants on fossil fuel, heat exchange equipment of gas turbine cycle should have unique characteristics to provide plant efficiency up to 50%.

The major heat exchangers of gas-turbine cycle are recuperator, precooler and intercooler, which are integrated together with the turbomachine within the PCU vessel with limited dimensions. The recuperator in GT-MHR with direct gas-turbine cycle allows the reactor and the turbine to be operated at high temperatures, whereas the precooler and intercooler ensure operation of compressors at low temperatures, that allows the cycle efficiency to be increased.

The selection of heat exchanger design options is based on the study of effect of their performances on plant parameters and efficiency and taking into account problems of their installation in the PCU.

The heat exchangers must have both high thermohydraulic performances and high compactness and strength, so, for example, the recuperator operates under significant pressure differences between circuits (up to 5 MPa) and at temperatures of up to 600°C.

While integrating the heat exchangers in the PCU high-pressure vessel, the hardest limitations are imposed by the vessel diameter based on fabrication and transportation

considerations and also because of significant influence of the diameter on the vessel wall thickness. This limitation assumes arrangement of heat exchange surfaces along the vessel height. To avoid non-uniform flow distribution through the heat exchange surface, entrance and exit of coolant along the PCU axis are supposed to be more rational. These requirements cause difficulties with providing permissible pressure losses. Pressure losses in the helium circuit influence appreciably on cycle efficiency and parameters (Fig. 7). Therefore, pressure losses are limited in heat exchangers, so, in GT-MHR plant the permissible value of losses in the recuperator is 0.07 MPa on the high pressure side, 0.03 MPa - on the low pressures side, in coolers permissible pressure losses are 0.02 MPa on a helium side, that in total is up to 50% of overall losses.

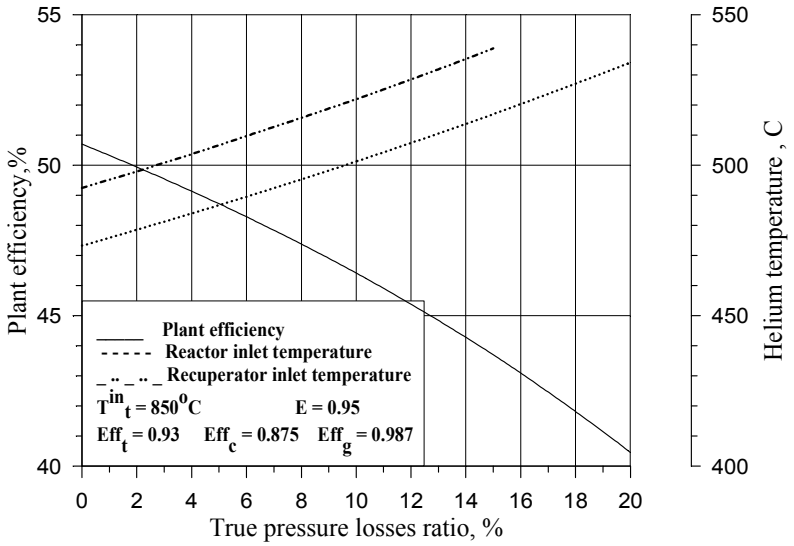

Fig.7. Impact of pressure losses on plant efficiency, reactor and recuperator inlet helium temperature.

Recuperator effectiveness is one of the plant parameters having a significant effect on the plant efficiency (Fig.2), and its operation, as a part of HTGR plant, has required development of a new recuperator design on the basis of compact plate type heat exchangers. Though such compact heat exchangers are characterized by a high ratio of amount of transferred heat to pressure losses, nevertheless pressure losses are great enough. It has required selection of an optimal surface geometry and its optimal arrangement. As it can be seen from Figure 8, while arranging recuperator modules along PCU axis, the optimum (in terms of thermal hydraulic characteristics) was found to be a location of recuperator on two levels with separation of overall helium flow into two parallel ones, that ensures transfer of the set thermal power with admissible pressure losses.

Precooler and intercooler influence on lower temperature in gas-turbine cycle, plant efficiency and plant parameters (Fig. 9). Pressure loss is one of the main problems while compactly arranging the precooler and intercooler on one level along PCU axis.

Both straight tubes and finned tubes with longitudinal and cross flow were evaluated in the thermal-hydraulic analysis of the coolers. It was concluded that externally finned tubes with counterflow scheme provide necessary compactness and heat effectiveness under acceptable pressure loss (Fig. 10). The precooler and intercooler are assembled out of individual modules, i.e. the same modular approach is used as in the recuperator design. Use

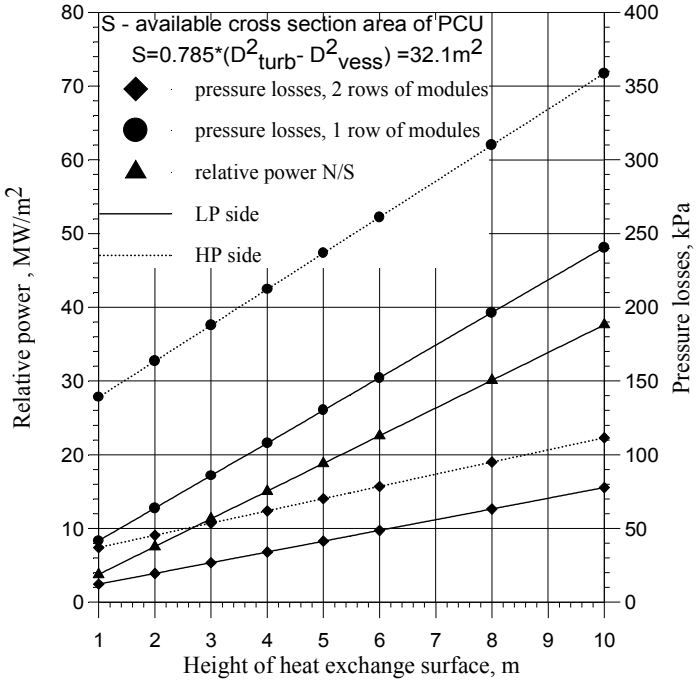

Fig.8. Recuperator thermohydraulic performances.

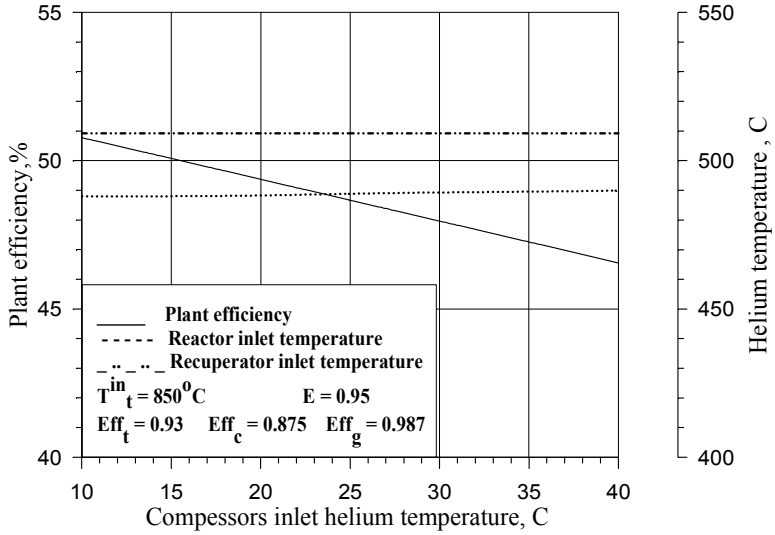

Fig.9. Effect of compressors inlet helium temperature on plant efficiency, reactor and recuperator inlet helium temperature.

of a compact plate surface in the coolers of the same type as in the recuperator can be considered in future as an option to reduce metal consumption and increase compactness and effectiveness. Problems of adapting the heat exchangers for gas turbine cycle are as follows:

- mastering of fabrication technology, design substantiation and experimental testing of thermohydraulic and mechanical characteristics of the developed compact recuperator design;
- selection of materials for heat exchangers to operate at high pressures and temperatures both in normal and emergency shutdown cooling;
- effect of temperature pulsation loads on metal structures due to mixing of helium flows when opening the bypass valve, plugging defective modules or sections.

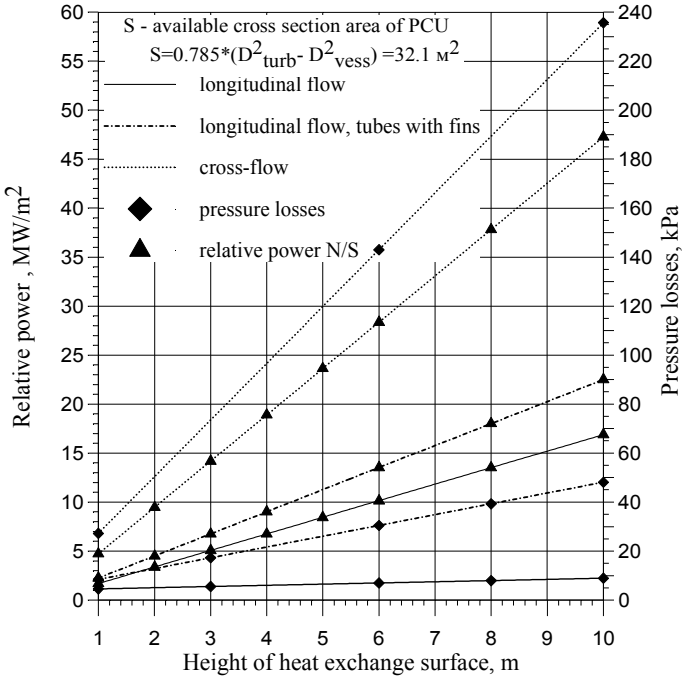

Fig.10. Thermohydraulic characteristics of coolers at helium side.

4. CONCLUSION

(1) For further increase of electricity production efficiency and reduction in overall dimensions of PCU with gas-turbine cycle in the plants with HTGR, it is necessary to provide a capability to raise reactor inlet helium temperature up to 550°C and higher and also have one stage of helium intercooling while pressing in compressors.

(2) From point of view of the plant control and the turbomachine protection against overspeeding at loss of electric load, the most reasonable variant is a single-shaft turbomachine.

(3) For provision of uniform flow distribution at inlet and outlet of heat-exchange surfaces, it is reasonable to arrange the coolant flow along PCU axis. It is possible to meet this requirement in conditions of limited PCU space and pressure losses by arranging a recuperator at two levels and coolers at one level along PCU height.

REFERENCES

[1] Melese G., Katz R., Thermal and Flow Design of Helium-Cooled Reactors, American Nuclear Society, La Grande Park, Illinois USA, 1984.

[2] Kiryushin A.I., Kodochigov N.G., Kuzavkov N.G., N.N. Ponomarev-Stepnoi, E.S. Gloushkov, V.N. Grebennik. Project of the GT-MHR high-temperature helium reactor with gas turbine, Nuclear Engineering and Design 173 (1997) 119-129.

[3] Manushin E.A., Beknev V.S., Osipov M.I., Surovtsev I.G. The gas-turbine nuclear and combined plants. M.: Energoatomizdat, 1993.

[4] Traupel W. Thermal tyrbomachines, Volume 1,2,. translation from German, Moscow. Energomashizdat, 1961.

SYSTEM ANALYSIS

(Session 2)

DYNAMICS OF A SMALL DIRECT CYCLE PEBBLE BED HTR

E.C. VERKERK, A.I. VAN HEEK
NRG,
Petten, Netherlands

Abstract

The Dutch market for combined generation of heat and power identifies a unit size of 40 MW thermal for the conceptual design of a nuclear cogeneration plant. The ACACIA system provides 14 MW(e) electricity combined with 17 t/h of high temperature steam (220^{o}C, 10 bar) with a pebble bed high temperature reactor directly coupled with a helium compressor and a helium turbine. To come to quantitative statements about the ACACIA transient behaviour, a calculational coupling between the high temperature reactor core analysis code package Panthermix (Panther-Thermix/Direkt) and the thermal hydraulical code RELAP5 for the energy conversion system has been made. This paper will present the analysis of safety related transients. The usual incident scenarios Loss of Coolant Incident (LOCI) ans Loss of Flow Incident (LOFI) have been analysed. Besides, also a search for the real maximum fuel temperature (inside a fuel pebble anywhere in the core) has been made. It appears that the maximum fuel temperatures are not reached during a LOFI or LOCI with a halted mass flow rate, but for situations with a small mass flow rate, 1-0.5%. As such, a LOFI or LOCI does not represent the worst-case scenario in terms of maximal fuel temperature.

1. INTRODUCTION

The Dutch market for combined generation of heat and power identifies a unit size of 40 MW thermal for the conceptual design of a nuclear cogeneration plant. The ACACIA system provides 14 MW(e) electricity combined with 17 t/h of high temperature steam (220^{o}C, 10 bar) with a pebble bed high temperature reactor directly coupled with a helium compressor and a helium turbine. The design of this small CHP-unit for industrial applications is mainly based on a pre-feasibility study in 1996, performed by a joint working group of five Dutch organisations, in which technical feasibility was shown.

Previous studies have been performed on the dynamic behaviour of the core of the Dutch conceptual HTR for cogeneration ACACIA [1-3], but these studies have always considered the reactor core as a stand-alone system. The influence of the energy conversion system (ECS) which converts the produced heat to electric power or industrial steam, was not included in the calculations. A fixed coolant mass flow, a fixed temperature and pressure at the reactor core inlet represented the state of the ECS at which the reactor dynamics were analysed. This approximation holds well for the severe transients investigated, such as loss of forced cooling (LOFC) and depressurised loss of forced cooling (DLOFC). In both cases the flow comes to a halt almost completely, thus effectively cancelling the interaction between the reactor core and the ECS. Only in the first minutes of these transients interaction takes place.

However, when studying normal operational transients the mutual interaction between reactor and ECS is governed by the helium mass flow. This flow rate is influenced by essentially two parameters, viz. the helium inventory and the bypass flow around the core and turbine. The helium inventory is the amount of helium circulating in the system and is adjusted each time load following is required. Bypass flow is used in situations of rapid or near-instantaneous power demand reductions and protects the turbine against excessive overspeed.

As the HTR is a very flexible reactor system and capable of load following, the helium mass flow will vary frequently, and a calculational coupling between reactor core and ECS becomes necessary in order to analyse the plant behaviour in sufficient detail. So the code for pebble bed core calculations (Panthermix [4]) and the code for thermal hydraulic calculations for the ECS (Relap5/mod3.2) have been coupled [5]. It should be clear from the beginning, that actually two code couplings were required in order to perform total plant calculations. Firstly, the neutronics code Panther [6] and the pebble bed thermal hydraulic code Thermix-Direkt [7] were coupled for reactor core calculations. This resulted in the HTR-version of Panther, Panthermix. Secondly, this Panthermix code has been coupled to the thermal hydraulic code which describes the ECS, Relap5/mod3.2.

This paper will present the analysis of safety related transients. The usual incident scenarios Loss of Coolant Incident (LOCI, also designated as Depressurised Conduction Cooldown (DCC) or Depressurized Loss Of Forced Cooling (DLOFC)) ans Loss of Flow Incident (LOFI, also referred to as PCC or PLOFC) have been analysed. Besides, also a search for the real maximum fuel temperature (inside a fuel pebble anywhere in the core) has been made.

2. HTR REACTOR DESIGN

The HTR system modelled is the reactor and ECS design of the Dutch ACACIA concept [3], a 40 MWth pebble bed HTR. It's reactor cavity measures 2.5 m in diameter and 4.5 m in height. The active core consists of spherical graphite elements (6.0 cm diameter) filled with TRISO coated fuel particles (0.9 mm diameter). The coating is widely acknowledged to be capable of retaining the fission products even at high temperatures (up to 1600^{o}C). The maximum temperature the fuel can reach in the core - even in case of loss of coolant - is expected to be well below this temperature. Helium flows through this pebble bed and heats up from 500^{o}C to 800^{o}C (at 2.3 MPa), thus extracting 40 MW of thermal power. Initially, the core cavity is only partially filled with pebbles (active core height approximately 1.10 m). New fuel pebbles are added each day in order to remain critical as the depletion proceeds. This is called peu à peu fuelling. After 10 years of operation the core reaches its maximum height and has to be discharged in order to start a new cycle. Due to the minimal over-reactivity in the core, and its low power density, the use of control rods is only required during start up and shutdown. The reactor relies on the feed-back mechanism of the negative fuel temperature coefficient to obtain a critical state during operation, or reach a subcritical state after an incident. Shutdown and recriticality behaviour has been analysed in [8].

3. REACTOR MODELING

The code Panther approximates the 2-D R-Z geometrical structure employed in Thermix-Direkt by a 3-D Hex model with small hexagonal blocks. A radial mesh of Thermix-Direkt is associated with a set of hexagons in the Panther geometry desciption, and power distribution and temperature distribution information is transferred between the two codes. The linear power densities for a set of hexagons associated with a particluar radial mesh are calculated by Panther, averaged and transferred to Thermix-Direkt, whereas the fluid and solid-state temperatures for a radial mesh are calculated by Thermix-Direkt and transferred to all associated hexagons of the Panther model.

The procedure described above is followed for each axial mesh. Axial geometry is modelled in the same way for the two codes.

The nuclear database required by Panthermix containing nuclear data for all reactor materials, depending on local irradiation, (fuel) temperature, xenon density etc. is generated by the WIMS7 code.

More details about pebble bed HTR modelling can be found in [1].

4. ENERGY CONVERSION SYSTEM (ECS)

The direct Brayton cycle is used as thermodynamic cycle for the ECS. It resembles the Rankine cycle for steam cycles, but a single phase gaseous working fluid (helium) is used instead of a condensing fluid. In this design the Brayton cycle can be termed 'direct', because the helium does not transfer its heat to a secondary steam cycle but powers the turbine directly, resulting in a higher efficiency. The system consists of a single-shaft turbine-compressor with a directly coupled electrical generator. A precooler before the compressor and a recuperator further enhance the overall efficiency (nominal 42%). A scheme of this HTR system is shown in figure 1.

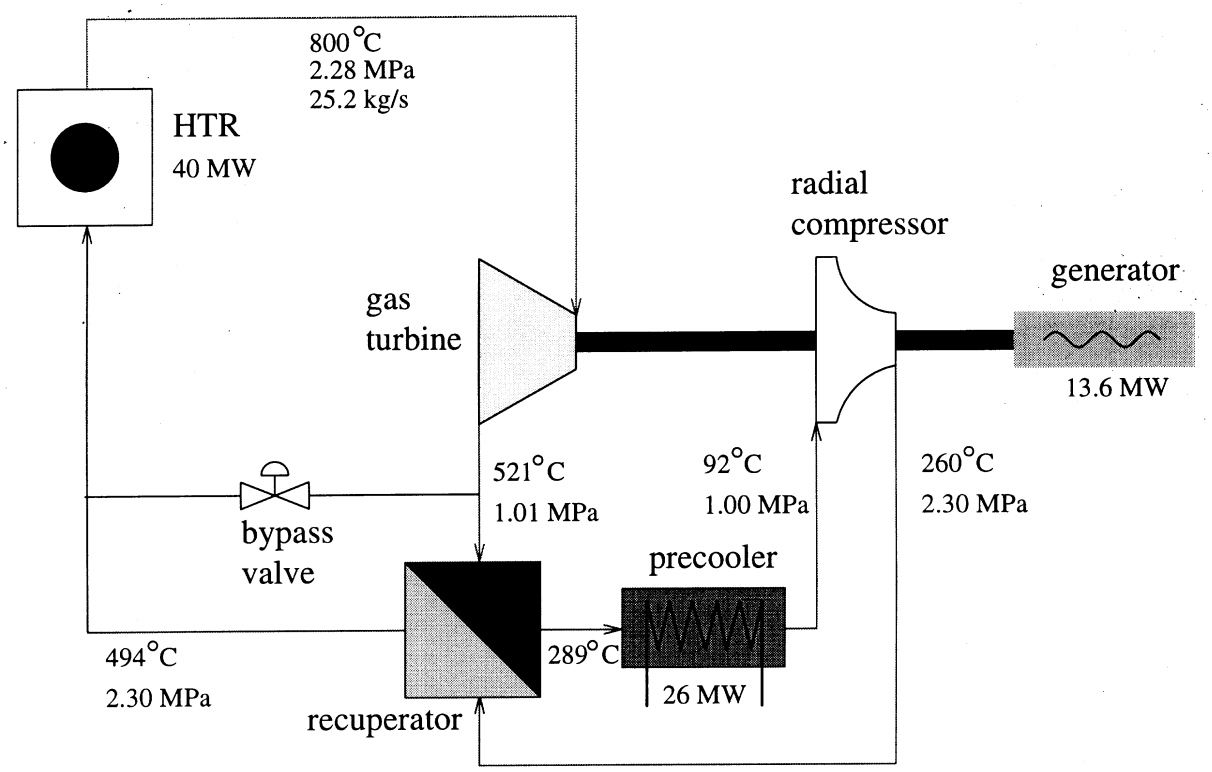

Fig. 1. Cycle diagram of the ACACIA nuclear cogeneration plant.

A detailed computer model of the ECS has been made in Relap5, a code that has as primary purpose to represent the thermal hydraulic cycle of a working fluid, in this case helium in the Brayton cycle. Heat transfer from working fluid to the enveloping structures — so-called heat structures — and the conduction towards an outer environment can be modelled. This model has been coupled to the reactor model and operational transients have been analysed [9, 10].

5. MAXIMUM FUEL TEMPERATURE

5.1. Core heatup incidents

Core heat-up accidents are usually simulated in order to find the maximum possible fuel temperatures for an HTR. The two main scenarios are the loss of coolant incident (LOCI) and the Loss of Flow Incident (LOFI). For these transients the active cooling is absent, and the transport of heat out of the core relies entirely on passive mechanisms: conduction, radiation and free convection. As discussed in the introduction, the fresh core will give the highest decay heat density and consequently the highest fuel temperatures. Figure 2 depicts the results of the calculation with the corrected fuel temperatures. The LOFI and LOCI calculations are shown for two cases, one with unirradiated fuel elements (fresh core), and one with irradiated fuel elements. It should be noted that the conductivity of irradiated graphite is lower and yields higher fuel temperatures than the conductivity of unirradiated graphite.

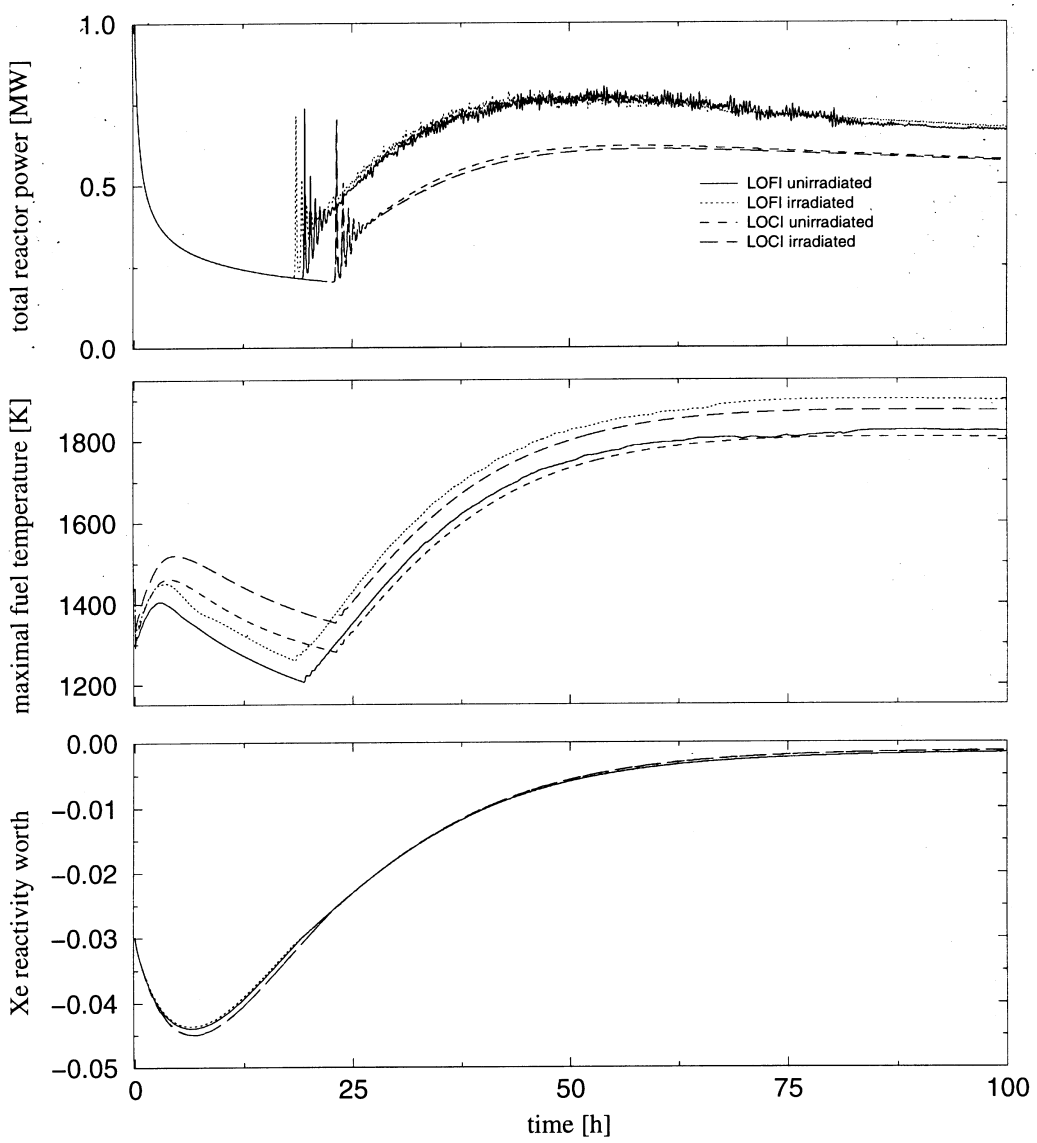

Fig. 2. Reactor power, maximum fuel temperature and xenon reactivity worth for the fresh core (5 days burnup) for the loss of flow incident (LOFI) and the loss of coolant incident (LOCI), each calculated with the heat conductivity of both irradiated and unirradiated graphite. [9].

The fuel temperature steadily increases after recriticality as the fission power slowly returns while xenon further decays. At the point in time that the xenon decay is maximal and in equilibrium with the prompt power, the fuel temperature will reach its maximum. Due to burnup, slowly the power will decrease and with it the temperature eventually will drop.

Figure 2 shows that the maximal fuel temperatures will exceed the 1600^{o}C (or 1873 K) temperature limit for the irradiated LOFI scenario and reach 1900 K. The irradiated LOCI scenario reaches exactly 1873 K. The maximal fuel temperature for the unirradiated scenarios remains under the 1600^{o}C
limit.

5.2. When maximum fuel temperatures really occur

Besides these well-established incident situations the question remains whether fuel temperatures stay with acceptable limits during *all* operational transients. This can be answered by systematically calculating the final states for a large number of load following transients. In the case of a load reduction, the final states of the transient will represent the worst-case situation in terms of fuel and outlet temperature. High fuel temperatures must then compensate the decrease of the negative xenon reactivity.

In order to show the maximal fuel temperature as a function of inlet gas temperature and mass flow rate, a number of load following transients have systematically been calculated for the fresh core. The calculations reflect the steady-state of the load following transient, that is, the stable end situation with the xenon concentration in equilibrium with the power density. In cases of load reduction, these states represent the worst-case scenario in terms of temperature and contain the maximal attainable fuel and outlet gas temperature.

For a fixed mass flow rate the gas inlet temperature has been varied (250, 500, 750 and 1000^{o}C), yielding a power, a gas outlet temperature, and a maximal fuel temperature in the center of the hottest pebble. This has been repeated for a number of mass flow rates. The helium pressures have been scaled with the mass flow rate, with a minimum of 1.0 bar. Figure 3 shows the maximum fuel temperature at a certain mass flow rate as a function of the gas inlet temperature. The 'iso-power' lines show the corresponding power.

For the startup core the maximum in the fuel temperature is normally located at the center of the bottom layer. Figure 3 shows that also a maximum exists in the fuel temperature which is mainly dependent on the mass flow rate. Around 0.25 kg/s the maximal fuel temperature is reached, after which the temperature drops eventually below the 1600^{o}C (1873 K) temperature limit for very small mass flow rates (0.001 kg/s). It can be explained by looking at the temperature distribution in the core; for 0.25 kg/s the heat is still collected and transported towards the bottom of the core, which results in a high pebble surface temperature. In the latter case, however, there is no accumulation of heat at a certain point due to forced convection, and the heat leaks directly away into the side reflectors.

Two important conclusions can be drawn from figure 3: firstly, the LOCI and LOFI do not represent a situation where the maximal fuel temperature is reached, and secondly, according to this ACACIA design the reactor must be prevented from operating in the region below mass flow rates of 1.0 kg/s as the 1600^{o}C limit will then be exceeded. The fact that the maximal fuel temperature is not reached during a LOFI or LOCI, but during low mass flow rate transients, is not specific for this design.

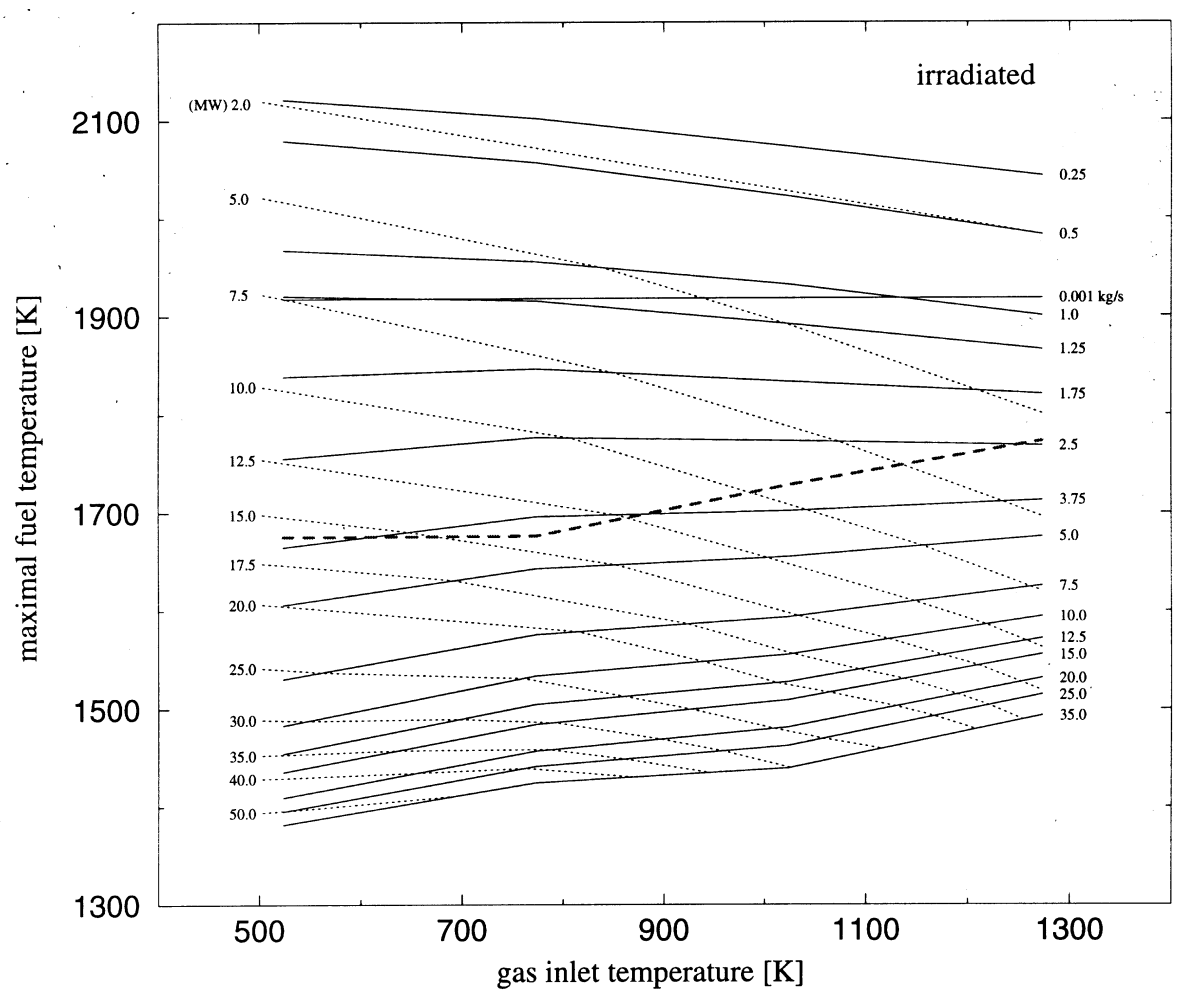

Fig.3. The maximal fuel temperature at certain mass flow rate as a function of the gas inlet temperature (irradiated case). The corresponding iso-power lines for these working points have also been drawn. The calculations reflect the stable end situation of load following transients at xenon equilibrium. Fuel temperatures will exceed 1600^{o}C if a return is made from the reduced mass flow rates in the region above the dashed line to nominal mass flow rate. [9].

Even more severe restrictions must be placed on the range of load following transients if the return to nominal mass flow rate is considered. If for some reason the nominal mass flow rate is restored, 25 kg/s, then the power will rise above nominal because of the relatively low xenon concentration. Especially for the load following cases that remained at low power for a few days, the power rise will be high, around twice the normal value, for a long (day) period of time. The situation that suddenly the nominal mass flow rate returns can arise due to a human error in the control room, or for instance a failure of the valve connecting the helium storage tank to the primary cycle.

The calculation of the maximal fuel temperature during the transient where the mass flow rate returns to nominal has been performed for the stand-alone reactor. This has been done in order to reduce calculation time, but in fact this type of transients demonstrates the value of a coupled reactor and energy conversion system if exact values are required. In the present study the aim is not to present exact values, but more to show that the maximal allowable fuel temperature can be exceeded. Ignoring the feedback of the energy conversion system will result in an underestimation of the fuel temperatures during the transient due to the drop in the

gas outlet temperature. This is the result of the relative increase in mass flow rate being relatively higher than the increase in power, and per kilogram helium less heat is absorbed (more specifically: the heat transfer coefficient does not increase proportionally to the mass flow rate. The energy conversion system reacts by offering a lower reactor inlet temperature due to the recuperative coupling of reactor in- and outlet mass flow rate. This will increase the reactor power and increase the maximal pebble center temperature. Therefore, if it is required to use the correct inlet temperature the energy conversion system should be involved in the calculations.

The return to nominal cooling will for some steady final states result in fuel temperatures over 1600^{o}C. In figure 3 the red line denotes this boundary. If a return to nominal mass flow rate is made from the region above the line, then the fuel temperature exceeds 1600^{o}C in the subsequent
transient.

6. CONCLUSIONS

Linking the Relap5 code with helium as a working fluid to Panthermix through the coupling software Talink opens up the possibility to model the thermal hydraulics and 3-D neutronics of a pebble bed HTR together with its ECS. A more realistic simulation of the entire system can be attained, as the coupling removes the necessity of forcing boundary conditions on the simulation models at the data transfer points.

A loss of flow incident (LOFI) and loss of coolant incident (LOCI) transient have been calculated for the fresh core (5 days old), and when utilising the conductivity for the irradiated graphite (conservative), the LOCI yields a maximal temperature of 1600^{o}C and the LOFI 1627^{o}C.

In order to investigate the maximum fuel temperature during operational transients, the steady final states of load following transients have been calculated for a comprehensive grid of inlet conditions. These final states represent the worst-case state in terms of maximal temperature as the fuel temperature will be maximal in order to compensate the reduction of the negative xenon reactivity by decay. Two conclusions can be drawn from these calculations:

- the fuel temperature can exceed 1600^{o}C for load reduction transients below 20%-10% of nominal power,
- the maximum gas outlet and fuel temperatures are not reached during a LOFI or LOCI with a halted mass flow rate, but for situations with a small mass flow rate, 1-0.5%. As such, a LOFI or LOCI does not represent the worst-case scenario in terms of maximal fuel temperature.

As a continuation of the load following transient, the return to a nominal cooling of 25 kg/s has been calculated. Especially for the load reduction transients to low load (<40%) this can result in fuel temperatures above 1600^{o}C. The xenon concentration is low and the fuel temperature has to rise in order to balance the sudden increase in reactivity due to increased cooling.

REFERENCES

[1] J.C. KUIJPER et al., 'Reactor Physics Calculations on the Dutch Small HTR Concept', Proc. HTGR Technology Development, IAEA-TECDOC-988, pp.407-439, Johannesburg, South-Africa, 13-15 November 1996.

[2] A.I. VAN HEEK (ed.), "INherently safe nuclear COGENeration (INCOGEN)", Pre-Feasibility Study, Netherlands Energy Research Foundation (ECN), Petten (1997).

[3] A.I. VAN HEEK, B.R.W. HAVERKATE, "Nuclear Cogeneration based on HTR Technology", ENC'98, Nice, France, October 1998.

[4] J.OPPE, J.B.M. DE HAAS and J.C. KUIJPER, "Panthermix" (Panther-Thermix) User Manual, Technical Report ECN-1-98-019, Netherlands Energy Research Foundation (ECN), Petten (1998).

[5] E.C. VERKERK, "Coupling Thermal Hydraulics with Neutronics for Pebble-Bed High Temperature Reactor Calculations", Proc. International Conference on the Physics of Nuclear Science and Technology, Long Island (NY), USA, October 5-8, 1998.

[6] P.K. HUTT et al., "The UK core performance code package", Nucl. Energy, 30, No 5, pp291-298 (1991).

[7] S. STRUTH, "Untersuchungen zur Thermohydraulik des Druckentlastungsvorgangs bei Hochtemperaturreaktoren" (Research on thermal hydraulics of the depressurization event with high-temperature reactors), Diplomarbeit (Master's thesis), Section of Nuclear Engineering, Faculty of Mechanical Engineering, Technical University RWTH Aachen, Germany (1988).

[8] H. VAN DAM, 'Role of Neutron Sources, Xenon, and Decay Heat Dynamics in Autonomous Reactor Shutdown and Recriticality', Nucl. Sci. and Eng., Vol. 129, No 30, pp.273-282 (1998).

[9] E.C. VERKERK, "Dynamics of the Pebble-Bed Nuclear Reactor in the Direct Brayton Cycle", PhD Thesis, Delft University of Technology, 2000.

[10] E.C. VERKERK, "Transient Analysis for the High Temperature Pebble-Bed Reactor Coupled to the Energy Conversion System",IAEA Technical Committee Meeting on Safety Related Design and Economic Aspects of HTGR, INET, Beijing, China, 2-4 November 1998.

[11] E.C. VERKERK, 'Helium Storage and Control System for the PBMR", Proc. HTGR Technology Development, IAEA-TECDOC-988, pp.195-203, Johannesburg, South-Africa, 13-15 November 1996.

[12] E.C. VERKERK, "Transient Analysis for the High Temperature Pebble-bed Reactor Coupled to the Energy Conversion System", ECN-RX—98-064, paper presented at the IAEA TCM Safety Related Design and Economic Aspects of High Temperature Gas Cooled Reactors, Beijing, China, 2-4 November 1998.

[13] X.L. YAN, L.M. LIDSKY, "Conceptual Design of the HTR Gas Turbine Cogeneration Plant", Technical Report LPI-HTR- 11019501, LPI, Cambridge USA (1996).

TRANSIENT BEHAVIOUR AND CONTROL OF THE ACACIA PLANT

J.F. KIKSTRA[1], A.H.M. VERKOOIJEN[2], A.I. VAN HEEK[1]

[1] NRG, Petten, Netherlands
[2] Faculty of Mechanical Engineering, Delft University of Technology, Delft, Netherlands

Abstract:

This article deals with dynamic modelling and control of the ACACIA plant. A one-dimensional flow model describing the helium flow and the two-phase water flow is used through the whole plant, with different source terms in different pieces of equipment. A stage-by-stage model is produced for the radial compressor and axial turbine. Other models include the recuperator, water/helium heat exchangers, a natural convection evaporator, valves, etc. The models have been checked by comparison of the transient behavior with several other models, e.g. produced in RELAP. The dynamic behavior of this plant is analysed and a control structure is designed. First the requirements and options for a control system design are investigated. A number of possible control valve positions in the flowsheet are tested with transients in order to make an argued choice. The model is subsequently used to determine the optimal working conditions for different heat and power demands, these are used as set-points for the control system. Then the interaction between manipulated and controlled variables is mapped and based on this information a choice for coupling them in decentralised feedback control loops is made. This control structure is then tuned and tested. It can be concluded that both heat and power demand can be followed with acceptable performance over a wide range.

1. INTRODUCTION

The ACACIA plant (AdvanCed Atomic Cogenerator for Industrial Applications) is a small nuclear gas turbine plant which coproduces steam for industrial use in e.g. beer breweries and paper mills. Figure 1 shows the ACACIA flowsheet; a description of the plant has been previously published, e.g. in references 1 and 2. For a cogenerating plant it is crucial that a range of electricity and power demands can be met. This calls for an advanced control system, since one can not only operate at full load or part-load; operations at different heat-to-power ratios should also be possible. In order to check whether and how this is possible, a dynamic model has been produced. The direct cycle gives a strong influence of the reactor behavior on energy conversion system behavior and vice versa, therefore detailed models of the reactor, the primary cycle, the secondary cycle and the water/steam system have been produced.

2. DYNAMIC MODEL

2.1. Assumptions and Structure

The most rigorous way of modelling the system would be to solve the microscopic mass-, momentum- and energy-balance for the flow path (with a CFD code), the microscopic energy balance of the solid constructions (with a CFD or FEM code), and the neutronics (with a diffusion or Monte Carlo code), all time-dependent and three dimensional. However, the computational effort needed is immense, insufficient information is available for the input of the models, and the level of detail of the information is unnecessarily high. Therefore a strongly simplified model is constructed. The simplifying assumptions are listed in Table 1.

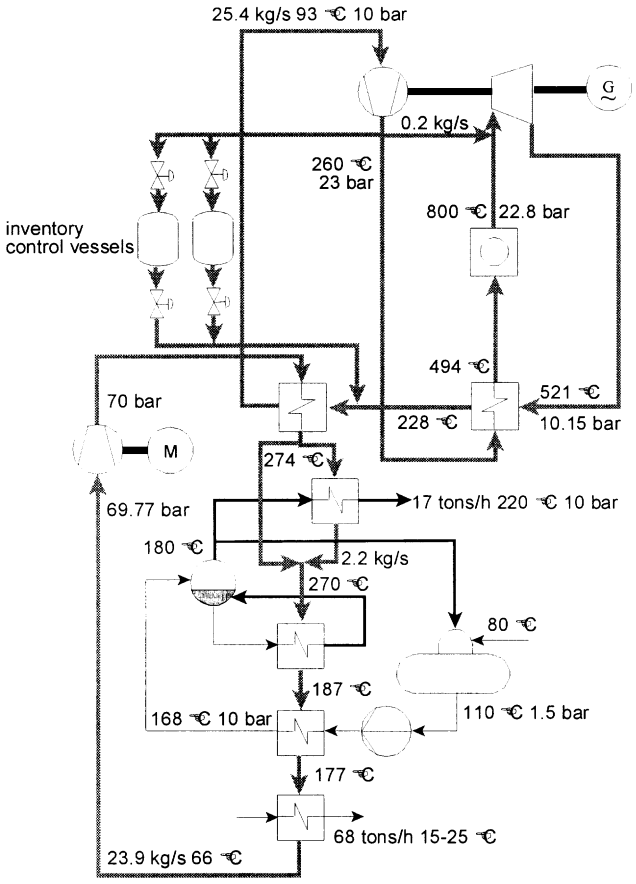

Fig. 1. ACACIA flowsheet.

TABLE I. SIMPLIFYING ASSUMPTIONS

	Modelling assumptions
1	One-dimensional treatment of flow paths
2	Discretisation of flow path with staggered grid and method of lines
3	Point-kinetic neutronics model
4	Two-dimensional model of solid structure
5	Non-homogeneous two-phase flow with single momentum-balance

The division of the total plant into components, which are interconnected with few relations, is analogous to the different pieces of equipment. Modelled components are compressor, recuperator, reactor, turbine, shaft etc. Within each component, sub-systems exist which behave similarly in different components. These sub-systems are:

1) One-phase flow
2) Two-phase flow
3) Neutronics
4) Solid structure.

2.2 Fluids and Solids Model

In the flow model, the flow path in the different components (recuperator, reactor, compressor etc.) is axially divided in a number of so-called thermal nodes, which are small volumes, assumed to be perfectly mixed and to have a constant cross-sectional area [3]. For these thermal nodes, the mass- and energy balances are solved. The mass flow between these volumes is determined by solving the momentum balance for a flow node, which consists of the two halves of neighbouring thermal nodes. This so-called staggered grid is chosen because of its numerical stability. The two-phase water flow in the steam generator is assumed to be at thermal dynamic equilibrium. The water/steam mixture cannot be modelled as a homogeneous fluid, since there can be a considerable difference in velocity between the two phases. Alternatively, one momentum balance for the two-phase mixture is solved and relative velocity of both phases is calculated with an empirical relation. The model allows for negative flows, which is necessary for incident analysis.

The mass and momentum balances are solved with second order central schemes. For the mass balance, this simple scheme may result in a response, which is somewhat slower than in reality in case of large elements, but unlike higher order approximations physically unrealisable behaviour is not possible. In the momentum balance the effects of friction losses, area change, gravitational forces and forces in turbo-machinery and pumps are been taken into account. The discretisation with a second order central scheme is a valid approximation as long as the velocities stay well below the velocity of sound. Choked flow is expected only in the valves connecting the inventory control vessels and the primary system, in the valves connecting high and low pressure plena, and in case of a rupture. For these valves and the ruptures a different model is used.

The energy-balance is be modelled with an upwind scheme. The incoming energy is only influenced by the upstream node, which leads to physically realisable behavior under all circumstances. A total energy-balance is being used, so internal, kinetic and potential energy is considered. Kinetic energy is of importance in the turbo-machinery only, and the potential energy is only relevant in the water/steam cycle. However, in order to keep the models general (in order to reduce the size of the code), all terms are taken into account in all components.

Helium is considered a non-ideal gas, thermal dynamic properties are calculated according to Yan [4]. For the properties of water, the IF-97 water/steam tables are used [5].

The solid construction of most pieces of equipment are also discretised in flow direction only. For the reactor model however, a two-dimensional discretisation is used. The wall model is capable of combining internal heat production, convective heat transport from and to a fluid and heat transfer by conduction to four surrounding wall elements.

2.3 Component Models

Closure of the set of equations describing the interaction between the one-phase and two-phase flow models and solid construction model is reached after insertion of empirical and/or component-specific relations for the source terms. Examples are the energy production in the reactor, heat input and forces in the turbo-machinery, heat transfer and (two-phase) friction in the heat exchangers and a slip-velocity correlation for the two-phase flow.

The heat production in the reactor is calculated using a point-kinetic model. The temperature of a large number of axial and radial sections of the pebble bed and its surrounding reflectors is calculated under the assumption of a constant power profile. The reactivity-feedback of each section is known from its temperature, these contributions are all summed and used in the point-kinetic equation. The parameters of the model have been derived from the full-scope thermal hydraulics and neutronics code Panthermix [6].

The forces and energy transfer in the turbo-machinery are calculated from the two-dimensional gas velocities in each stage. The expressions used do not only hold for normal operation, but also for negative flows and for compressor surge. The work done is calculated from the changes in magnitude and direction of the gas flow, using the Euler equation. Three loss-factors which determine the stator and rotor row efficiency have been implemented with semi-empirical relations: 1) losses over the blade profile, during off-design mainly due to the discrepancy between inlet flow angle and blade angle, 2) due to boundary-layer build-up near the casing and 3) due to leak flows between the rotor and the casing. From the row efficiencies and enthalpy changes the forces are calculated. The compressor, turbine and generator are connected with a shaft, whose acceleration is calculated from the energy balance.

2.4 Implementation

The models have been implemented in the simulation-tool Aspen Custom Modeler (ACM, 1999). All the component models can be combined in a graphical environment, thus allowing the user to built a flowsheet, re-using the predefined models. ACM solves the implicitly formulated set of the algebraic and differential equations. The complete plant model contains approximately 60,000 variables and 1000 state-variables. Because of the implicit formulation, the model can also easily be used for design. For example, instead of calculating the compressor performance from its geometry, the geometry needed to achieve a certain pressure ratio can be found.

2.5 Validation

All component models have been checked with verification of for example macroscopic balances, comparison with other models and codes or sensitivity-analyses with regard to empirical relations.

The compressor map has been produced in order to check its steady-state behavior. It is shown in figure 2 and looks very plausible for this type of radial compressor. Moreover, some surge transients have been simulated, in which the behavior shows the qualitatively expected behavior.

The reactor has been compared to the Panthermix code with a number of transients, resulting in differences of only a few percent. For example, figure 3 shows the response to a step change of the helium inlet temperature of 100^{o}C. One can see that in both time scales, the models agree very well. Most differences are due to the slightly different thermal hydraulic models. In the long run, it is clear that the point-kinetic model (drawn) yields a higher power, since burnup is not taken into account.

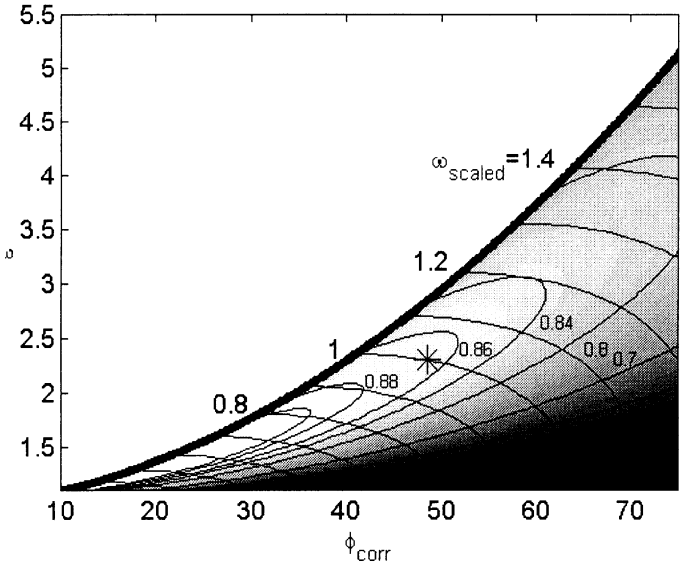

Fig. 2. Compressor map.

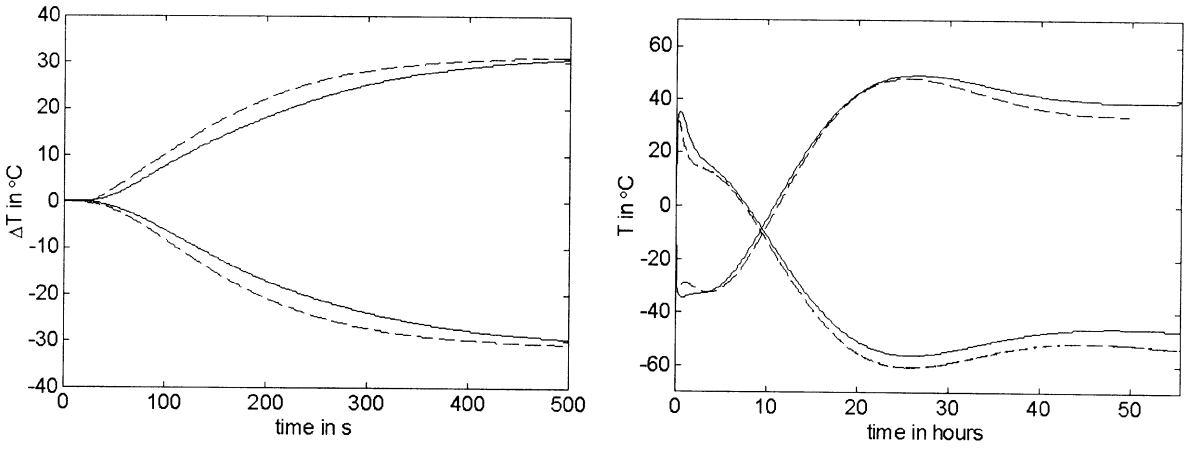

Fig. 3. Comparison of outlet temperature transient on step change of inlet temperature. Drawn: ACM model, dashed: Panthermix model.

The complete primary cycle has been compared to a model made in the code RELAP 5 MOD 3.2. The models yielded very much the same results, differences were mainly due to simplifications made in order to implement compressor and turbine models in RELAP. Figure 4 shows the response after a load rejection, a sudden disconnection of the generator from the grid. The acceleration of the shaft gives an increased pressure ratio and mass flow, which leads to an also increased temperature change over the compressor and turbine. The RELAP turbine model does not perform very well during this strong off-design operation which explains the differences.

3. CONTROL SYSTEM DESIGN

3.1 Goals and Options

A cogeneration plant should be able to meet a range of heat and power demands independently, preferably while maintaining a high efficiency. The variables that have to be controlled and all possible control elements are indicated in figure 5. An asset of the closed cycle is that high part-load efficiency can be obtained by reducing the helium inventory. If at part load the pressure is halved and all temperatures are kept constant, the gas velocities are the same as at full load. The mass flows and the power are also halved. Since the velocity triangles in the turbo-machinery are unchanged, the efficiency stays high. The pressure losses are reduced and the heat exchanger efficiency increases, thus giving a slightly higher efficiency than at full load. The helium inventory can be increased or decreased without need for an extra compressor, if a number of parallel inventory vessels with a pressure between the lower and upper primary system pressure is used. In most designs, the helium inventory is rather large; therefore filling and emptying the system is a slow process [4]. In order to adjust the electricity production quickly the turbine can be bypassed, for this a number of valve positions is conceivable. The mixing with either hot or cool helium when a bypass valve is

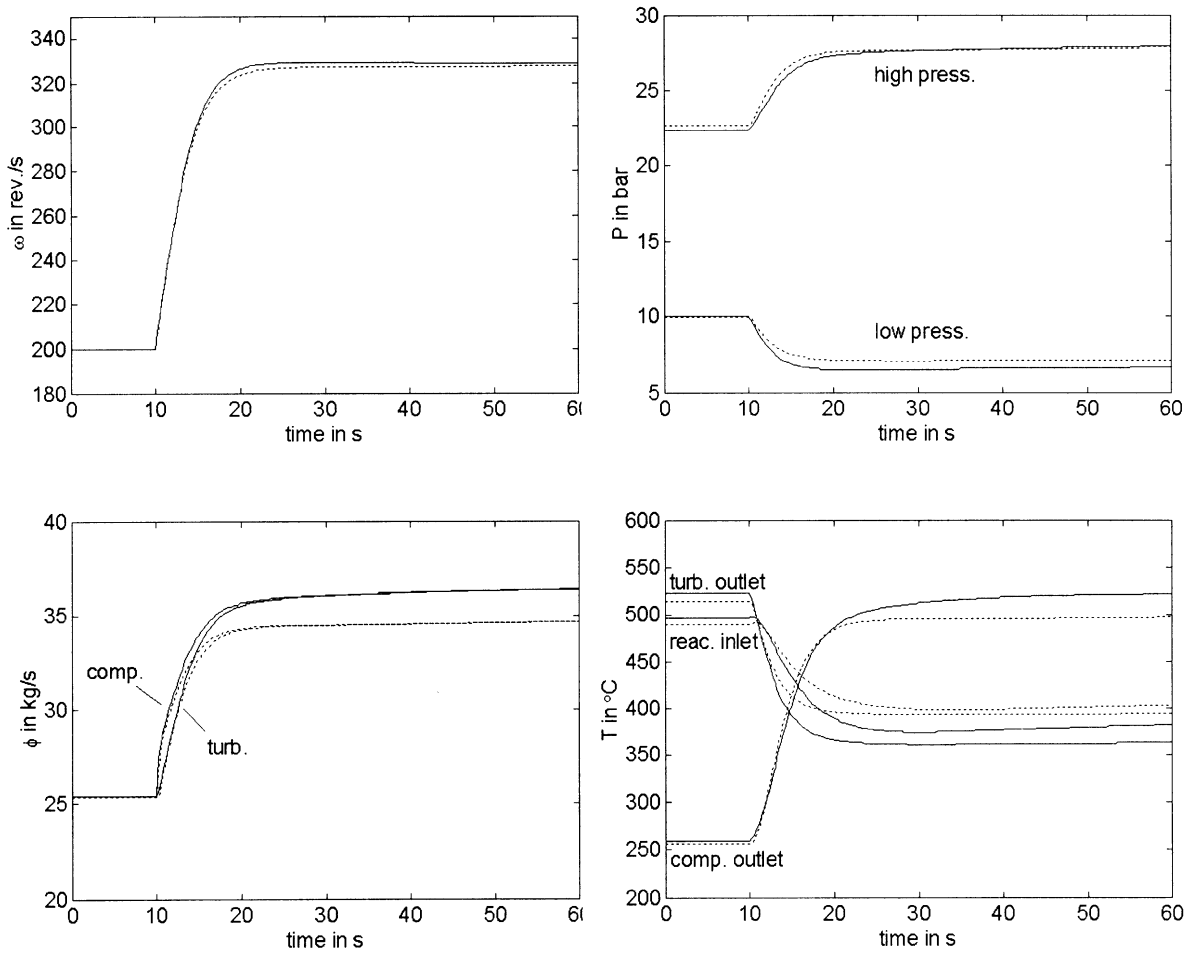

Fig. 4. Comparison of load rejection transient. Drawn: ACM model, dashed: Panthermix model.

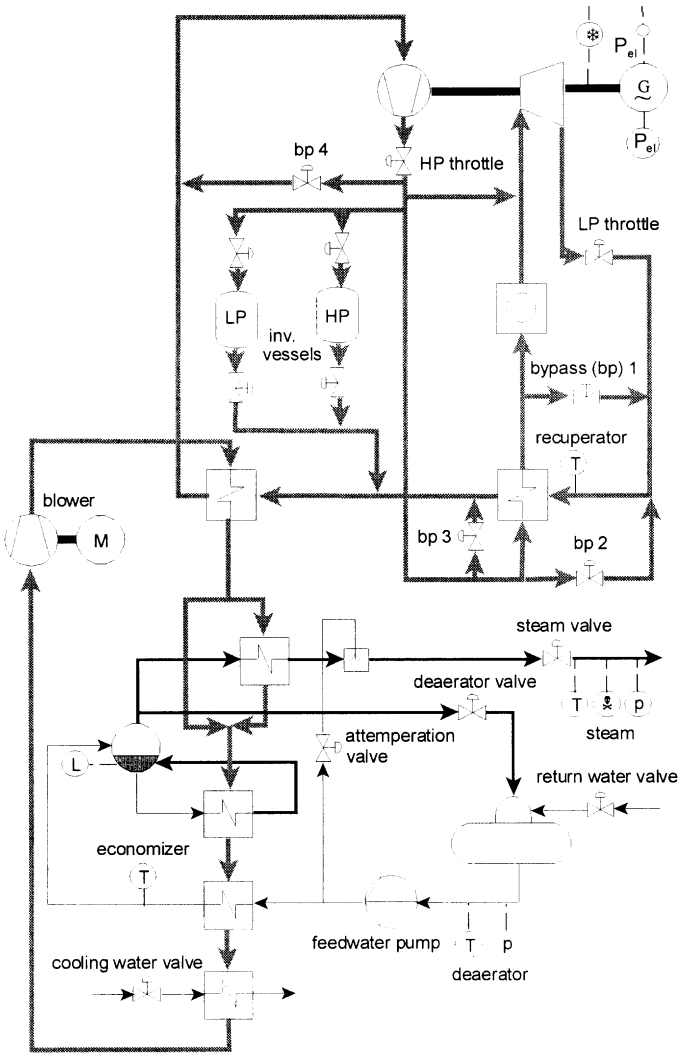

Fig. 5. Controlled variables and possible manipulated variables.

opened will give a strong and fast change of turbine outlet temperature. This results in a thermal shock of the recuperator, which can lead to fatigue or direct failure [7, 8]). A countermeasure could be to use two bypass valves: bypass one (see fig. 5) to control the shaft speed and bypass two to control the temperature [4]. A bypass flow gives a dramatic decrease of efficiency, therefore the bypass valves should be almost closed during prolonged operation at a certain heat and power demand. An alternative for bypass control is to throttle the primary flow [9]. The main disadvantages of throttle valves is that they have to be much larger and that they give a pressure drop and thus a decreased efficiency even when fully opened. Since the generator is a-synchronous, the shaft speed must be actively controlled. The fastest and easiest option is to use the electric load as manipulated variable. The turbine inlet temperature is left uncontrolled, since it is passively controlled by the reactor neutronics. A rise of reactor inlet temperature has a negative impact on the neutron economy, which leads to power reduction, so that the reactor outlet temperature is kept fairly constant.

An inventory reduction with constant temperatures in the primary cycle gives an unchanged heat-to-power ratio. In order to increase the heat-to-power ratio, the temperature in the precooler has to be increased. Reducing the cooling water flow can do this. In order to efficiently transport the energy from the precooler to the steam generator and final cooler the

blower speed must also be adjusted. The temperature and pressure of the industrial steam of course have to be controlled. For temperature control a spray attemperator can be used without a penalty on the system efficiency, because the pinch point in the steam generator lies at the evaporator water inlet. Moreover, the economiser should always remain subcooled, therefore its outlet temperature must be controlled. The drum level and de-aerator conditions also have to be controlled; this can be achieved by manipulating the feed water pump speed and the valves in the steam and water pipes to the de-aerator.

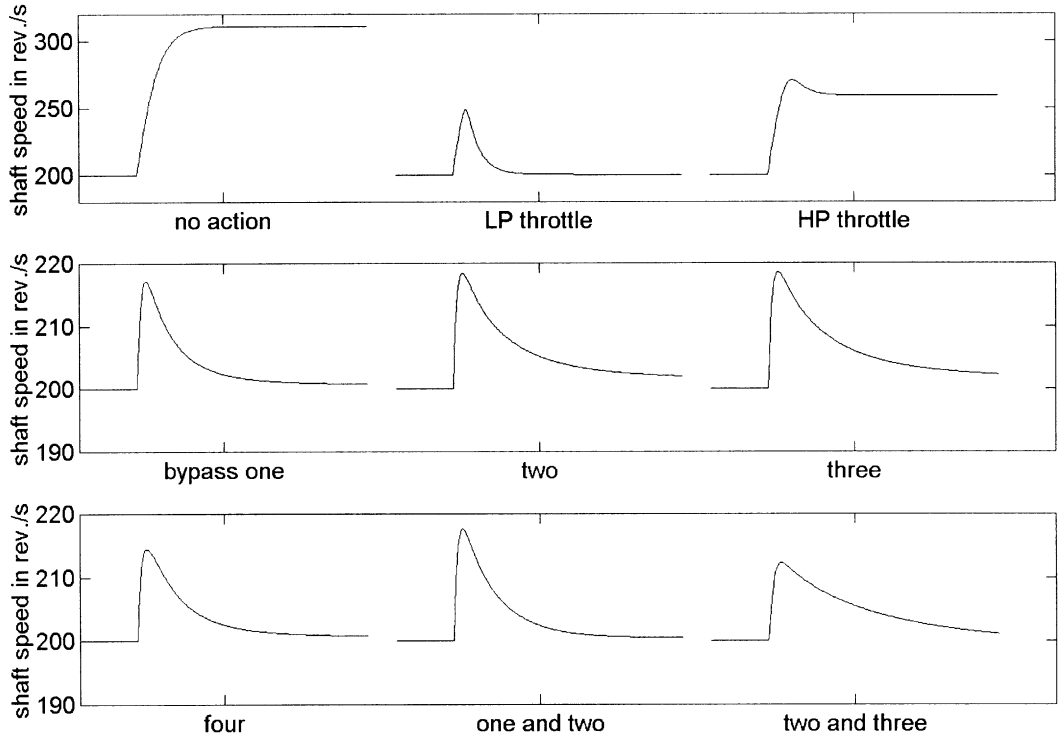

Fig. 6. Shaft speed response on different control actions.

3.2 Control Valve Positions

In fig. 5, a number of alternative bypass and throttle valves are shown. Valves one and two are proposed in similar designs [4, 10]. Valve one is used to reduce the shaft speed, opening leads to a temperature rise of the turbine outlet. To compensate for this temperature rise valve two is opened, which leads to a reduction of the turbine outlet temperature. The bypass valve is situated in a high temperature environment, which might complicate the design. An alternative position for the bypass valve would be between the cold (instead of the hot) inlet and outlet of the recuperator (valve three). Yet another possible position is between compressor outlet and inlet (valve four). Two possible throttle-valves are conceivable, either positioned in the high pressure (HP) or low pressure (LP) side.

The influence of these valves is tested with a model of the primary system only in which the shaft speed is reduced to its nominal speed after a load rejection. The system is operated with constant compressor inlet temperature. In order to assess the different control-possibilities a number of output parameters have been monitored. The shaft speed must be reduced with as little overshoot as possible. Figure 6 shows the transients of the shaft speed during 50 s. Figure 7 shows the original temperature profile of the recuperator (hot and cold helium

temperature) dotted while the profile at the end of the transient (after 50 s) is drawn. The heat transport to and from the primary helium flow in the reactor respectively the precooler are plotted in fig. 8. In order to minimise the disturbance of the secondary system, both the heat flow to it and the precooler hot inlet (recuperator hot outlet) temperature must be as constant as possible. The heat from the reactor becomes equal to the heat supplied to the secondary system; the difference is used to heat the recuperator and precooler core. A small and short deviation between both heat flows proves that the heat exchangers operate at constant temperature.

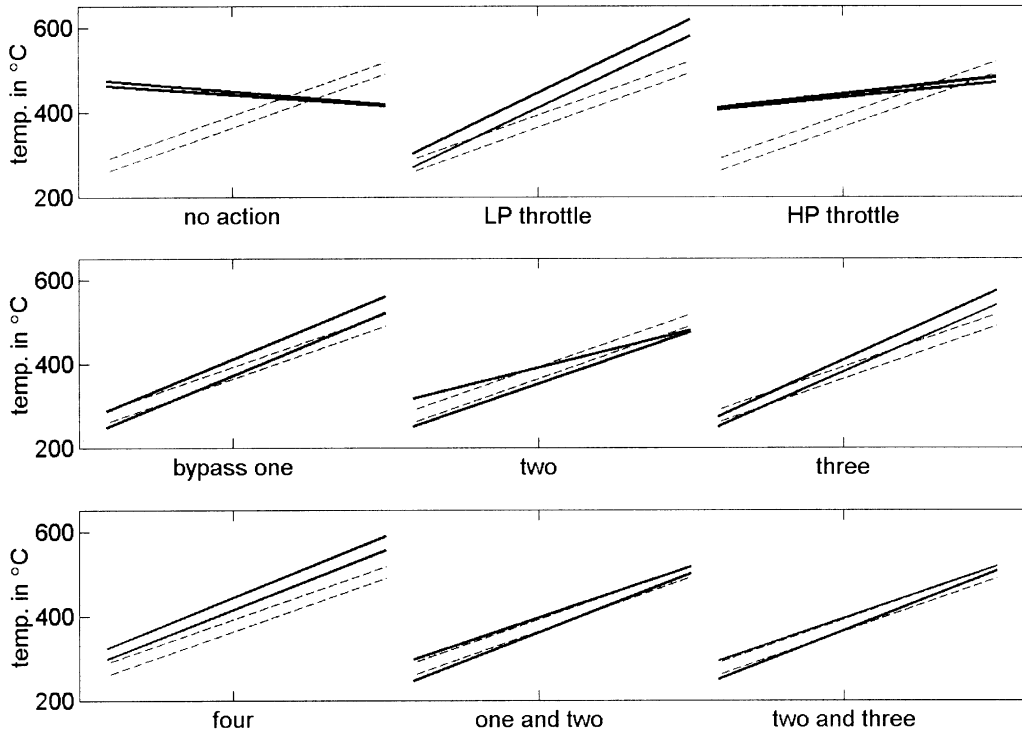

Fig. 7. Recuperator temperature profile response on different control actions. Dotted: profile before transient, drawn: after transient.

It can be seen that in case of a load rejection without control the recuperator actually cools the low-pressure flow instead of heating it. The heat flow to the secondary cycle becomes too large, due to the fact that the compressor inlet temperature is constantly kept low, leading to a poor efficiency. The strong increase of the precooler hot inlet temperature will normally also lead to a rise in compressor temperature and thus to a decrease of the heat transport. If necessary, the temperature can be increased further by reduction of the cooling flow.

With the LP throttle (in the turbine outlet) the mass flow is reduced to 23 kg/s. This leads to a hardly changed energy transport to the secondary cycle and a well-controlled shaft speed. The HP throttle can only limit the increase of mass flow to 29 kg/s (No control gives an increase from 25.4 to 33 kg/s). Throttling further brings the system in an unstable operating. The increased recuperator hot outlet temperature gives a strong increase of heat transport to the intermediate helium loop.

Opening of the bypass valves has hardly any effect on the recuperator cold inlet temperature for valves one, two and three. The reason is that the compressor inlet temperature is kept constant with the large secondary flow through the precooler (simulating perfect control of the

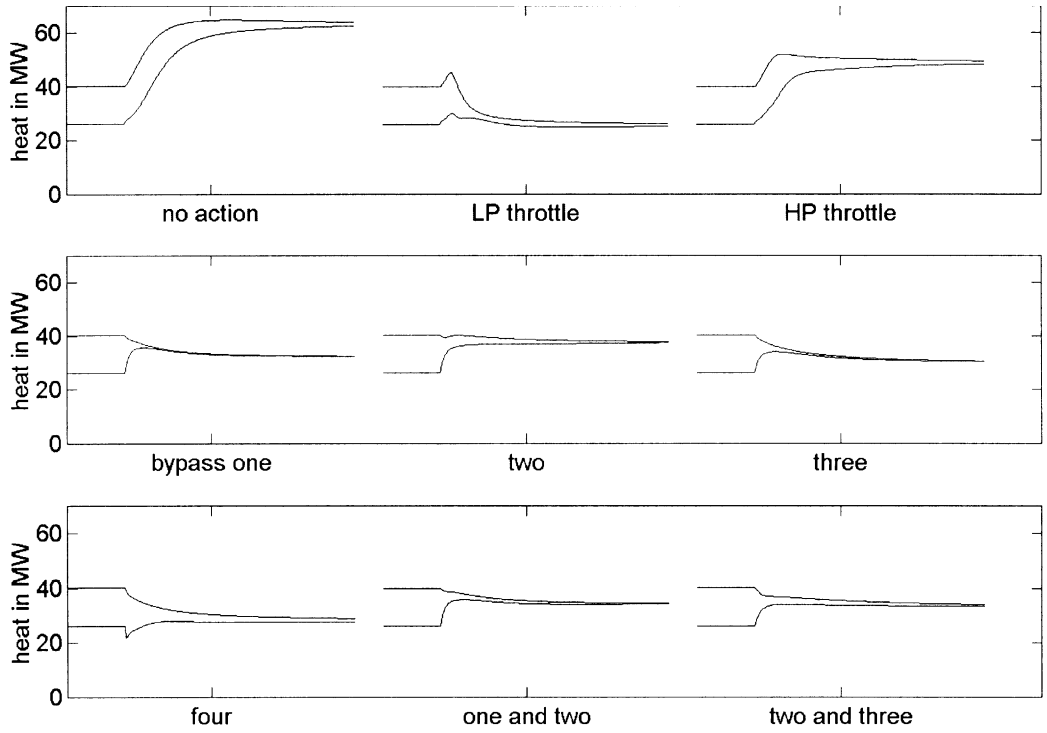

Fig. 8. Heat flow response on different control actions. Upper: heat to primary system in reactor, lower: heat to secondary system.

secondary loop) and the pressure ratio over the compressor does not change very much. When valve four is opened, hot helium is mixed with the compressor inlet flow so the compressor outlet temperature rises. This rise could also be accomplished by decreasing the final cooler water flow. The increase of temperature leads to a decrease of heat transport from the reactor.

For valves one, two and four the mass flow on both sides of the recuperator is equal. This keeps the temperature lines parallel, which is favourable because it keeps the temperature difference and thus the thermal stresses perpendicular to the flow direction small. Opening of valves one, three and four lead to an increase of the turbine outlet temperature. This increase is the smallest with valve one. A load decrease with opening of valve two leads to a decrease of the recuperator hot inlet temperature. This shows that the combination of the bypass and attemperation valve can be used to keep the temperature constant.

Finally the results are shown for a transient in which two bypasses (valve one and two respectively one and three) are opened simultaneously. This can lead to a hardly changed recuperator temperature profile. Figure 8 shows that the energy transport to the secondary cycle is still too high. It can be reduced further with an increase of the compressor inlet temperature. This will again raise the temperature at the cold side of the recuperator. The combination of valve two and three is chosen since it gives good performance with small valves operating at low temperatures.

3.3 Optimal Operating Conditions

The dynamic model can also be used to calculate the optimal steady-state situation for a given heat and power demand. These are subsequently used as set points for the control system. The

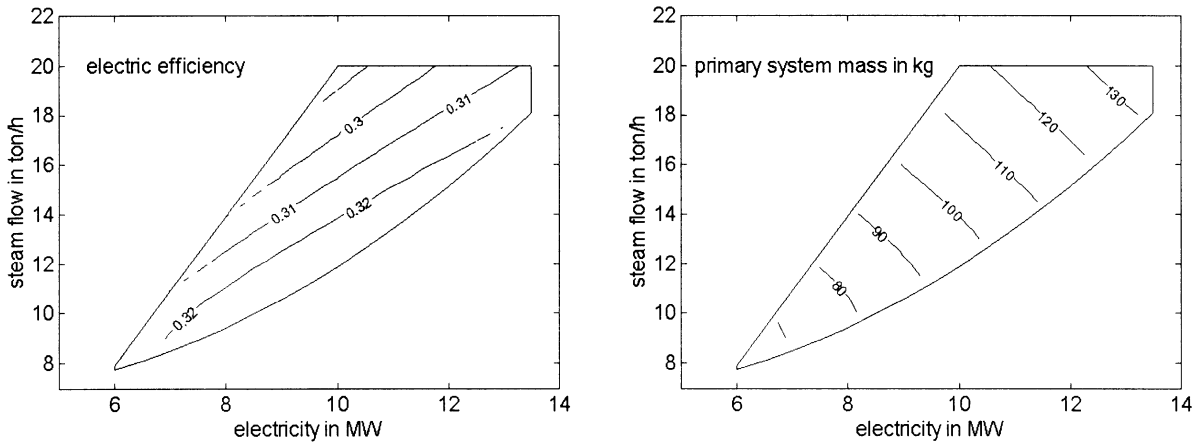

Fig. 9. Attainable efficiency and optimal system inventory.

operational region with optimal conditions is shown in fig. 9. At high electricity and heat production the area is bounded because otherwise the helium inventory and thus the pressure is too high. The 'left' and 'right' boundaries are due to saturation of the cooling valve; at the left boundary the valve is fully closed, whereas it is fully opened at the right boundary. In order to achieve the highest efficiency, the bypass valves should be closed. With the bypass valves open, the plant can operate to the left of the region shown. One can see that the electric efficiency stays high over the operating region. If the inventory is reduced, the both steam and power production decrease proportionally. When the cooling valve is opened, less steam can be produced, but the electric efficiency rises. In order to keep the correct temperature profile in the steam generator (a.o. to keep the economiser water outlet slightly sub-cooled) the blower speed is varied almost proportional to the steam flow.

3.4 Control Structure

The choice for the pairing of manipulated and controlled variables with PI controllers is based on Dynamic Relative Gain Analysis [11] and is elucidated in reference 12. Here only the result will be presented. Figure 10 shows the control structure. The customer gives a set point for the electric power P_{el} and steam flow N_{st}. Using the off-line optimisation the optimal blower speed and primary helium mass (fig. 9) are found. The blower speed is directly adjusted. If the helium inventory is directly adjusted to its optimal steady-state value after a change in electric load, the heat input to the secondary cycle changes quickly. The heat removal in the final cooler cannot be adjusted equally fast, due to its thermal inertia. This results in unacceptably large swings in steam pressure during load changes. The problem can be overcome by first adjusting the helium inventory to such a value that the primary mass flow through the precooler is kept constant. Since the temperatures are also fairly constant due to the operation of bypass valves, the heat flow to the secondary cycle remains in balance. In case of opening of the bypass valve in order to reduce the electricity production, the compressor flow and thus the primary precooler flow increases. To counterbalance this effect the inventory is reduced. This is accomplished by ramping up or down the set point simultaneous with the electricity demand. Subsequently the inventory can be very slowly reduced to the optimal value shown in fig. 9; this is done with a 1000 s ramp. The reduction in heat input into the secondary cycle leads to a steam pressure reduction, which lets the controller close the cooling water valve. The compressor inlet temperature rises which

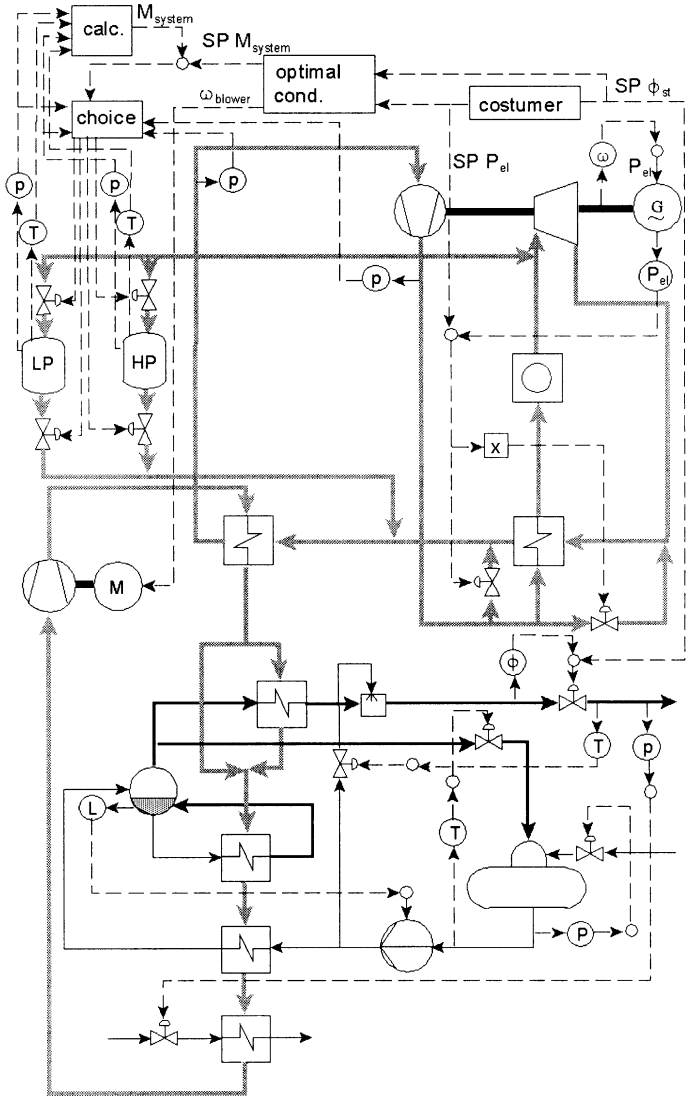

Fig. 10. Control structure of the ACACIA plant.

through an increased power consumption of the compressor gives a reduced electricity production. This is balanced by closing the bypass valves, thus raising the efficiency. The set point for the inventory M_{system} is compared with a value calculated from the helium mass in the vessels, which is known from temperature and pressure measurements. A PI-controller sends a signal to a logic switch which operates the inlet or outlet valve of the LP or HP vessel, dependent on the system upper and lower pressure and the sign of the error. All the controllers use PI-feedback, they have been tuned heuristically with a number of transients.

3.5 Test Transient

The results of a transient in which both power and heat demand are changed is shown in figure 11. Starting At t=10 s the electricity demand is ramped down with 25% in 10 s. As a result, the inventory is directly adjusted and during the next 1000 s ramped down to its optimal value. At t = 2000 s the heat demand is decreased with 15%.

The electricity production exactly meets the demand, while the steam flow and pressure show only small deviations from their set-point (shown as dotted line). The steam temperature and

the de-aerator conditions are almost the same as their set points and therefore omitted in figure 11. Ratio control of bypass valve two cannot keep the recuperator temperature completely constant, but the changes are small. The drum level is kept in the middle of the drum. The controller is not set very aggressively since that would lead to short and large deviations of the steady-state pump speed, which would unnecessarily upset the system. Because of the integrating nature of the drum level response to both the pump speed and disturbances, longer small differences in pump speed work equally well. The bypass valves are almost closed during the heat load following transient. If they are completely closed (as could happen in larger load-swings), either the electricity set-point cannot be attained, or the inventory must be adjusted to secure the electricity production.

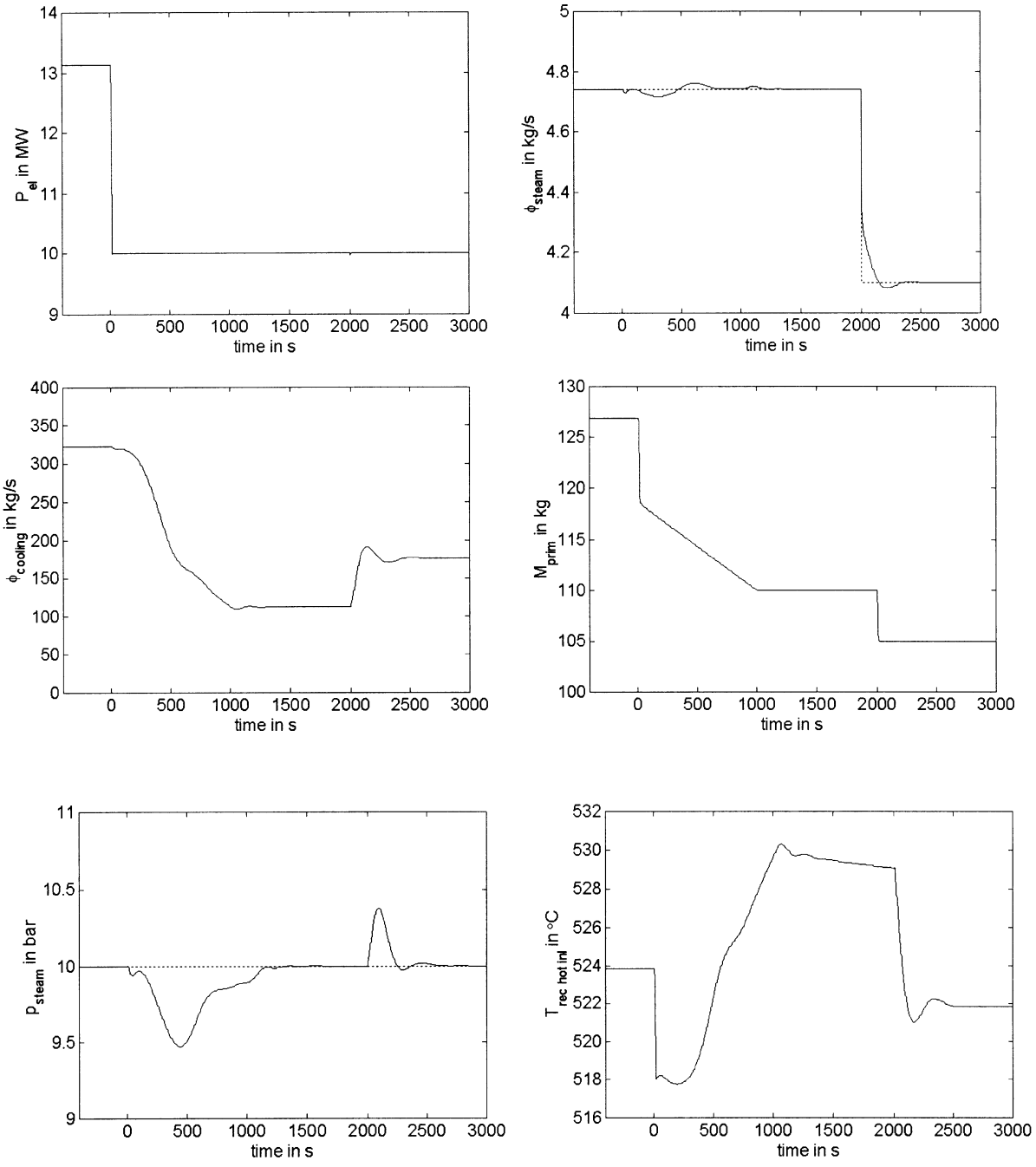

Fig. 11. Results of control system test transient.

4. CONCLUSIONS

A dynamic model of the ACACIA plant has been produced. It is capable of describing a wide range of operating conditions, thus making it a powerful tool both for design and optimisation of a control-structure and incident-analysis. Its level of detail surpasses any model described in literature. The setup of the code allows also for use as a design-code.

It is impossible to prove that a dynamic model correctly predicts the transient behavior under all conditions. However, by logical tests and comparison with analytical solutions and other models and codes, it is made plausible that the model developed gives a correct estimation of the system dynamics over a time-scale varying from fractions of a second to several days.

The dynamic model has proven to be a valuable tool in the system and control system design. It can be used for the assessment of alternative designs and control options and for optimisation of steady-state and dynamic performance. The ACACIA plant can meet a large field of heat and power demands with high efficiency. Its control system can track the set points quickly, without too large temperature swings in the recuperator.

REFERENCES

[1] J.F. KIKSTRA and A.H.M. VERKOOIJEN, "Conceptual Design for the Energy Conversion System of a Nuclear Gas Turbine Cogeneration Plant", accepted for Journal of Energy and Power (2000).

[2] B.R.W. HAVERKATE, A.I. van HEEK and J.F. KIKSTRA, "An HTR Cogeneration System for Industrial Applications", Proceedings of the IAEA TCM on Safety Related Design and Economic Aspects of High Temperature Gas Cooled Reactor, Beijing (1999).

[3] J.F. KIKSTRA and A.H.M. VERKOOIJEN, "Dynamic Modelling of a Closed Cycle Gas Turbine CHP Plant with a Nuclear Heat", ASME 99-GT-002 (1999).

[4] X.L.Yan, "Dynamic Analysis and Control System Design for an Advanced Nuclear Gas Turbine Power Plant", Ph.D. Thesis, MIT (1990).

[5] W. WAGNER and A. KRUSE, "Properties of Water and Steam IAPWS-IF97", Springer, Berlin (1998).

[6] E.C. VERKERK, "Dynamics of the Pebble-Bed Nuclear Reactor in the Direct Brayton Cycle", Ph.D. Thesis, Delft University of Technology (2000).

[7] P. CARTER et al., "Failure Analysis and Life prediction of a Large, Complex Plate Fin Heat Exchanger", Engineering Failure Analysis, **3**, No. 1 (1996).

[8] T. NAKAOKA.et al., "Evaluation of Fatigue Strength of Plate-Fin Heat Exchanger under Thermal Loading", Proceedings of the ASME International Conference on Pressure Vessel Technology, Vol. 1 (1996).

[9] R. ADAMS, Adams Atomic Engines, Inc., U.S. Patent number 5,309,492 (1994).

[10] W.A. SIMON, A.J. NEYLAN.and F.A. SILADY, "Design Features of the Gas Turbine Modular Helium Reactor (GT-MHR)", Technical Report GA-A21351. San Diego: General Atomics (1993).

[11] G. STEPHANOPOULOS, "Chemical Process Control, an Introduction to Theory and Practice", Prentice-Hall, New Jersey (1984).

[12] J.F. KIKSTRA and A.H.M. VERKOOIJEN, "Dynamic Modelling of a Cogenerating Nuclear Gas Turbine Plant Part 1: Modelling and Validation & Part 2: Dynamic Behavior and Control", submitted to Journal of Engineering for Gas Turbines and Power.

PERFORMANCE REVIEW: PBMR CLOSED CYCLE GAS TURBINE POWER PLANT

K.N. PRADEEP KUMAR
Eskom PBMR,
Centurion, Pretoria, South Africa

A. TOURLIDAKIS, P. PILIDIS
Cranfield University, Bedfordshire, United Kingdom

Abstract:

Helium is considered as one of the ideal working fluid for closed cycle using nuclear heat source due to its low neutron absorption as well as high thermodynamic properties. The commercial viability of the Helium turbo machinery depends on operational success. The past attempts failed due to poor performances manifested in the form of drop in efficiency, inability to reach maximum load, slow response to the transients etc. Radical changes in the basic design were suggested in some instances as possible solutions. A better understanding of the operational performance is necessary for the detailed design of the plant and the control systems. This paper describes the theory behind the off design and transient modelling of a closed cycle gas turbine plant. A computer simulation model has been created specifically for this cycle. The model has been tested for various turbine entry temperatures along the steady state and its replications at various locations were observed. The paper also looks at the various control methods available for a closed cycle and some of the options were simulated.

Introduction

It is believed in the power generation circle that a modular gas cooled reactor using helium turbo machineries will have place in the market due to its unique qualities such as inherent safety, short construction time, low operational logistic requirements, efficient part load performance, quick response to sudden load changes, low environmental impact etc.

The PBMR (Pebble Bed Modular Reactor), a subsidiary of the South African Power Utility, Eskom, is engaged in the developmental work for the design and construction of a Closed cycle helium turbine plant using Nuclear heat source. Several local and international companies have shown interest in this exercise and two companies, one from US and one from Europe, have already joined PBMR as share holders. The first proto type, which is a full-scale version of the PBMR having generation capacity of 116 MW of electricity, will be commissioned in 2004.

A team of engineers and scientists in South Africa, identifying and analysing various technical issues associated with the closed cycle gas turbine plants and also coordinating various knowledge bases for finding solutions. Some of the key problem areas are material selection, modular design, testing and commissioning, prediction of plant performance, controllability and control system design etc. The lack of real test data and the inability to make scaled test version of the equipments are real challenges in this project. High levels of computational predictions are being used to help the various phases of this project from detailed design to the commissioning.

Performance prediction is one of the complex issues associated with the gas turbine plants. This is due to the cyclic nature of the plant, where the performance of the compressors

depends on the driving turbines and these turbine's performances depend on the compressors. Hence iterative procedures are required to predict the plant behaviour at any point in time. In this process of iteration either the continuity of the mass flow or the energy balance can used. When using the energy balance, the compressor work is equated to the turbine work for a particular speed along the steady state operation. When the turbine work is more than the compressor work, the shaft accelerates and when it is less, it decelerates. These are transient operations. Any change in load setting will achieve only through a transient operation, which may be very short or long in duration depending on the initial and final points of operation. The steady state and transient performance prediction are important because any load setting or its change can be achieved only through a transient and the control devices which is effecting that load change should be designed based on that knowledge. Performance predictions of conventional power plants are relatively easier because each component's behaviour is independent of others and can be predicted separately. The performances of components are interlinked in the closed cycle plant and a system approach is necessary to predict it.

Nomenclature

N- Rotational speed M- Mach Number K- Kelvin P-Pressure T-Temperature
W -Mass Flow rate ω- Angular speed γ- Ratio of Specific Heats (C_p/C_v)
w -Non Dim: Sp.work τ,θ -Temperature ratios

The PBMR Plant Details

The power conversion unit (PCU) consists of two turbo compressors, power turbine, recuperator, pre-cooler and intercooler. The PCU is designed for any Generator output setting from 2.5 MW to 116.3 MW electricity.

The turbo compressors are placed in a chamber called pressure vessel, which will also be used as the duct between the HPC outlet and the recuperator cold side inlet. Hence there will be an external pressure of 70 bar on the casings of the turbo compressors. All the rotating equipments will be running on magnetic bearings primarily due to the cold welding nature of Helium, which prevents the use of conventional mechanical bearings. Magnetic bearings also improve the rotor dynamics. The total quantity of Helium in the circuit is 2500 kg and same amount is kept in the residual storage as well.

The PCU inventory control strategy is to control the Helium inventory over a range from 20 to 100% of nominal power at the same time ensuring a minimum pressure of 1 Mpa. Lower power levels are obtained by the use of Reactor bypass valve. This valve takes the high-pressure helium from HP compressor outlet and supplies it at the pre-cooler inlet. This can be used for fast acting load variations.

Interrupt valves are placed between HP compressor outlet and the cold side inlet of the recuperator. The interrupt system will be designed for over speed protection and it will act as an emergency stop of the Brayton Cycle. These interrupt valves will be stop valves without much control characteristics

Position Parameter	*Value*
Cycle core mass-flow	140 kg/s
Reactor thermal power	265 MW
Reactor inlet temperature	536ºC
Reactor outlet temperature	900 ºC
Generator electrical output	116.3 MW
Overall pressure ratio	2.7
Generator efficiency	98.5%
Cycle efficiency (generator excluded)	45.3%
System efficiency (generator included)	44.1%
Plant net efficiency	42.7%

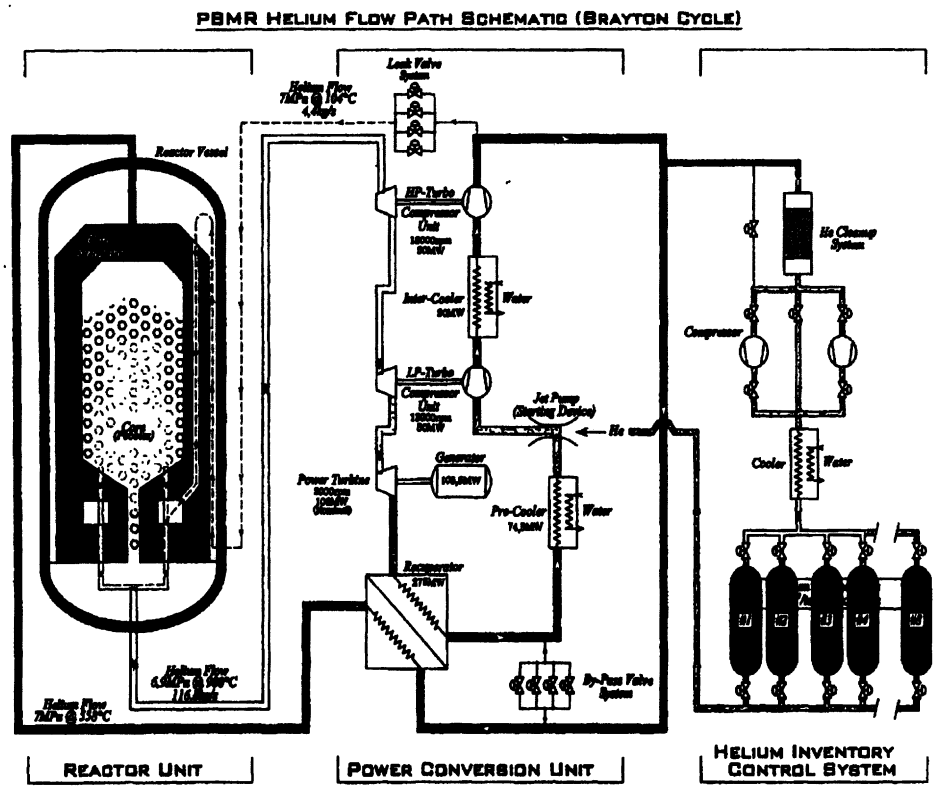

FIG. 1. Flow Diagram of Pebble Bed Modular Reactor with By-pass and Inventory control system.

System Position	P. MPa	T ºC	System Position	P. MPa	T ºC
1	2.59	27.9	4	6.72	900
2A	4.24	104.4	5A	5.46	812
2a	4.23	27.6	5a	4.34	721
2	7.0	104	5	2.61	553
3	6.955	536	6	2.59	138

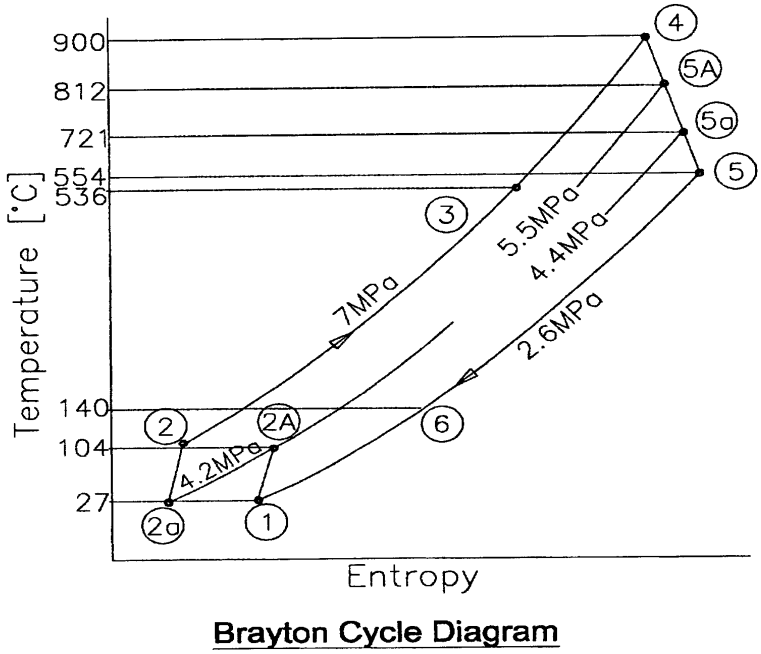

FIG. 2. PBMR Brayton Cycle.

Principle of power control

Closed cycles present unique issues and opportunities for modulating power output from power systems. Two methods, bypass control and inventory control are described and their features discussed here. Temperature modulation is also an option but it has to be done with the reactivity control and hence not described in detail here. These systems have been of interest for use in the nuclear power industry. It is important to be able to produce the part load power at high efficiency and in such a way as to minimize the thermal stress impact on the heat source, especially if the source is a gas-cooled nuclear reactor. For a given machine, the cycle pressure ratio is nominally fixed by the compressor

1. *Heat Source Bypass*
The bypass control is exercised through the bleed of high-pressure gas to short-circuit the heat source and the turbine. The throttling process is obviously a source of irreversibility so that use of such a scheme results in reduced part power efficiency.

The cycle temperatures can be held constant with just the thermal power input matching that required maintaining the cycle temperatures at the reduced mass flow through the reactor. This has the advantage in that stresses associated with temperature gradients in the metals may be held close to constant.

The impact on performance is readily calculated since the cycle temperature may be taken to remain fixed The regenerator will process equal masses on both sides at all times, which implies that the ideal design situation of $T_3 = T_6$ is maintained at part power. This is due to the fact that with constant T_4 and constant compressor pressure ratio, $T_3 = T_5$. The enthalpy balance on the mixer gives the temperature at state 6, which is, for an ideal and perfect gas, trivial. The cycle analysis is merely a work accounting with the full mass flow processed by the compressor and less in the heater and turbine An ideal cycle analysis yields

$$\eta_{th} = \left[1 + \frac{w}{w_{\max}}\left(\frac{\theta_4}{\tau_c} - 1\right)\right]^{-1} \quad \ldots\ldots\ldots\ldots\ldots\ldots 1$$

$$w_{\max} = \left(\frac{\theta_4}{\tau_c} - 1\right)(\tau_c - 1) \quad \ldots\ldots\ldots\ldots\ldots\ldots 2$$

For values of these parameters of 4 and 1.5, respectively, the efficiency is as shown in *FIG. 3.*

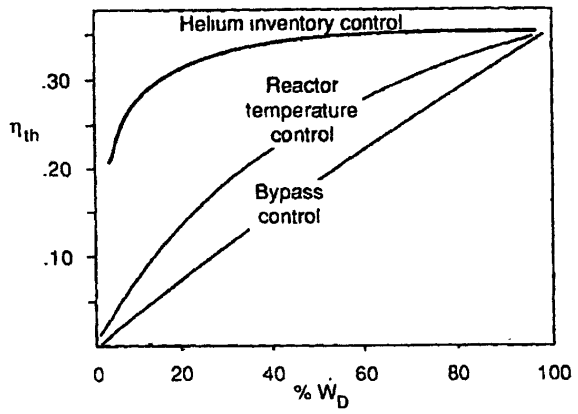

FIG. 3. Performance of the inventory and bypass controlled closed Brayton cycle[5].

The modulation of T_4 in an ideal cycle gives efficiency results that are identical to those of bypass control. The implication is that bypass and peak temperature reduction have the same thermodynamic merit. Temperature modulation and bypass may, therefore, be used together if the resulting performance is acceptable. In practice, accurate part power performance is evaluated with significantly greater consideration of the irreversibilities.

2. *Inventory Control*

A good method of producing part-load power is available to closed cycle engines where the pressure and thus the density of the working fluid may be controlled by connecting the cycle fluid to a storage vessel.

A compressor is used to pump the working fluid out of the system of working components. The reduced mass of the circulating fluid results in a smaller mass flow rate, which, in turn, reduces power output from the system. Means are also provided to allow the return of the fluid to the cycle when power is to be increased. In order to minimize heat transfer in the storage component, the fluid is removed from the lowest temperature point in the cycle with appropriate means for cooling.

The operation of the cycle at reduced mass flow rate allows operation with the same temperatures and pressure ratio This means that the heat engine operates with the same thermodynamic cycle, resulting in approximately constant efficiency and specific work.

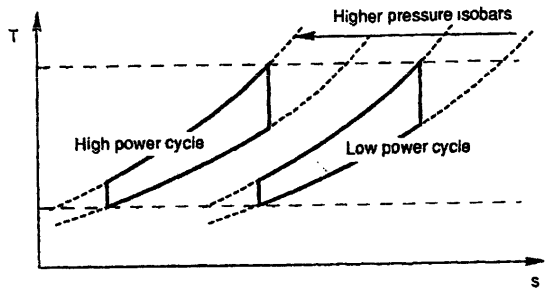

FIG. 4. T-S diagrams for part and full power for the inventory controlled closed cycle [5].

The fact that the temperatures remain invariant, as the mass flow rate is reduced, implies that the local sound speeds are constant. Blading and flow-passage geometric design fix the local Mach numbers so that local flow velocities are everywhere constant to first order. With velocities constant, the mass flow rate is proportional to the density, which, for constant temperature, is also proportional to the absolute pressure. The thermodynamic cycle operating at various pressure levels can be shown as in *FIG. 4*. The variation of cycle performance is a function of the working fluid properties. These properties are insensitive to absolute pressure when the gas is monatomic. For other gases, the effect of changing pressure may be significant in affecting specific work and efficiency.

It is expected, therefore, that the relation between efficiency and fractional power is relatively flat, and a small fractional power output can be obtained by operating at low absolute pressure. In practice, the fluid frictional losses are slightly altered because the decreased density also decreases the flow Reynolds numbers. This increases the importance of viscous losses. The effect is to reduce efficiency slightly as the power output is reduced because component efficiencies are reduced.

The peak and part-power cycle efficiency noted for bypass and temperature modulation control on a realistic analysis are about half the value noted for an idealized analysis for the same temperature extremes, showing the importance of the irreversibilities. Further, the serious degradation of efficiency with bypass control is noted as a disadvantage in relation to inventory control. It should be noted, however, that the severity is important only if the fraction of time spent at less than full power is significant[8].

Theory of Dynamic Behaviour

The physical properties of the dynamic behaviour can be classified into 3 groups according to their velocity.

The first group, which runs with small characteristic times belong to the mass inertia due to the pressure changes caused by gas oscillations. The period of these oscillations amounts to some deciseconds [8]. This can be considered as the running time of the gas particles in passing the turbo machines, heat exchangers and ducts.

The second group is due to the mass storing in the volumes of the gas ducting components and the energy storing of the rotating masses causing a change in rotor speed. This charging time and the machine inertia time are in the range of couple of seconds.

The third group belong to the heat storage in the heat exchangers and the corresponding changes in temperature associated with it. Normally these time constants range at least one-tenth power over those of the second group. Particularly Helium cooled high temperature reactors have great thermal inertias according to their large masses.

There are some other physical phenomenon faster than the above mentioned, like the one caused by the wake dents behind the trailing edges which strike a blade at the frequency of rotor speed time the number of blade per stage. These can be in the order of 10^{-6} seconds. Such dynamic behaviours can be regarded as quasistationery.

With regard to the focus of a calculation, the physical phenomena of one or more groups must be considered [8]. When focusing on the pressure gradient in the hot gas duct during opening or shutting the by-pass valve, the third group, which deal with the heat storage of heat exchangers, can be neglected. Similarly the same third group has to be considered if means for keeping reactor inlet temperature constant during start up. The second group must be considered for the speed control calculations. Here the inclusion of the procedures belonging to the first group can be necessary in case of a greater control operation. The dynamic behaviour of the reactor and the heat exchangers can be neglected based on an assumption that the turbine entry temperature is kept constant by the reactor control. The mass storing in the volumes and the energy storing of shafts have a certain priority and it must be considered for all practical simulation purposes.

Transient Performance Analysis and Control System Design

Transient performance and control system design are inseparable. During transient manoeuvres engine operation is inherently more prone to undesirable events than running steady state. These must be avoided by engine and control system design [6]. Some of the transient operations of a typical power generating unit are load ramping, load rejection, islanding etc. If the unit is connected to a major grid, the frequency has to be maintained to avoid the isolation of the unit from the grid also the unit should keep running for the house load if it isolated from the grid due to trouble in the grid. If it is an independent power producer, not connected to a grid, more rapid power changes are required as there are fewer load devices, which may be switched on and off instantaneously.

The PBMR unit is targeting for a 10% load change in 1 second, which will put heavy target on the control system design. Control system design for a conventional gas turbine or steam turbine driven generator is an established technology and hence it is readily available in the market. But closed cycle gas turbines with helium bringing a different set of issues and hence the transient behaviour of the turbo machineries have to be analysed properly for developing an accurate control system. Various phenomena particular to transient performance are identified and their impact has to be studied [6]. The various phenomena are

a) Heat soakage

During transient operation there are significant net heat fluxes between the working fluid and the engine metal, unlike for steady state operation. This can be up to 30% for acceleration from idling to full load. The impact of the soakage during transient can be very dramatic in this CCGT due to the presence of the heat exchangers. The modelling of the Heat soakage can be done by calculating the heat flux to or from the metal component.

Heat Soakage = f(heat transfer(kW), heat transfer coefficient(kW/m^2K), gas and metal temperatures(K), gas mass flow(kg/s), area of metal(m^2), mass of metal(kg), CP of metal (kJ/kgK)

Heat Soakage, Q = h. A (T_{gas}-T_{metl})
dT_{gas} = -Q/W CP_{gas}
dT_{metal} /dt =Q/ (Mass.metal. Cpmetal)

The T_{gas} and T_{metal} are at time t. Hence for a given heat transfer Q is derived and then dT_{gas} and dT_{metal} are evaluated for the given time step dt as follows

Approximate heat soakage = f(max. heat soakage(kW) , time(s), time constant(s))

$Q = Q_{max}\, e^{(-t/TC)}$

TC , time constant,ranges from 5s for a 200kg engine to 40s for a 2 tonne engine.[6].

The component geometric data, thermal masses and heat transfer coefficients are assumed to be available.

b) Volume packing
During steady state operation the mass flow entering a given volume is equal to that leaving. This is no longer true under transient operation as the pressure, temperature and hence density of the fluid changes with time. This is known as volume packing and can have a notable impact upon an engine's transient performance, especially for the largest volumes such as ducts and heat exchangers. The volume dynamics should be accounted for ducts, the combustor and heat exchangers. The following equation allows the change in mass flow leaving the volume, relative to that entering to be calculated.

Rate of mass storage in a volume (kg/s) = f(γ, Mach number, gas constant (kJ/kgK), mean temperature(K), mean pressure(kPa), volume (m^3))

$$W_{in} - W_{out} = \frac{V\, dP/dt}{RT\left(1 + \left(\frac{\gamma - 1}{2}\right)M^2\right)^{\frac{1}{\gamma - 1}}} \quad \ldots\ldots\ldots\ldots\ldots\ldots\ldots\ldots\ldots\ldots\ldots\ldots\ldots\ldots (3)$$

dP/dt is calculated from the known values of P at time t and time t-1.

Volume packing has a special significance in the PBMR model. The HP compressor is discharging the pressurised helium into a chamber, which houses the turbo machineries. The cold side of the recuperator inlet, where to the gas is flowing, is at the other end of the chamber and hence the gas is taking a complex passage over the pipelines and the equipments. A CFD modelling of this volume with all the internals is planned at a later stage. The output from this CFD analysis will be used in the computer models as an exercise to improve the accuracy.

c) Tip clearance changes
During the acceleration, the thermal growth of the compressor or turbine disc is slower than the pressure and the thermal growth of the casings, causing blade tip clearances to be temporarily increased. The converse is true during a deceleration, which can lead to rubs. This

change in compressor geometry affects its map, the main issue being lower surge lines. There is also second order reduction in flow and efficiency at a speed [6].

This is for the conventional and generic geometrical design. In the PBMR design, the compressors and the turbines are situated in a pressurised chamber and hence the pressure growth of the casings will be different from that of a conventional nature during a transient. Hence the tip clearance change during transient operation has to be modelled or calculated separately to be incorporated in to the computer models. Changing Tip clearances and interstage heating may significantly lower the surge line. The changes to the compressor map are of second order and may be ignored for simple transient performance models.

d) Heat source (Reactor) delay

This is the time delay between the fuel supply and the actual heat rejection. Compared to conventional GTs using liquid or gaseous fuels, gas cooled reactors have more heat source delay due to the slow reaction time and also due to the high heat carrying capacity of the graphite in the reactors. The time delay from reactivity change to the release of heat in the reactor can be obtained from the Reactor designers.

e) Heat transfer within multi-stage components

Where a single map is used to model a multi stage component such as an axial flow compressor, net heat transfer will have a second order effect upon the map during a transient. This is due to its effect upon gas temperature through the component and hence stage matching, as it changes the referred speed and hence flow capabilities of the rear stages.

e) Control system delay and lags

Control hard wares such as valves, variable guide vane actuation rings etc. take a finite time to move to new positions demanded by the controller during a transient. This finite time may comprise a delay, where there is no movement for a given time and or a lag where the device is moving but lagging behind the demanded signal. Control system sensors measuring parameters such as pressures and temperatures will also show delays and lags relative to conditions. The following equations can be used for delays and lags in movement of control system hardware components. The delays and time constants need to be provided by control system component system manufacturers.

Lagged value of parameter = f (lagged value at previous time step, time step, time constant)
*Lagged Value(time = T) = (Lagged value (time = T-DT) + (Actual value (time = T))/(TC + DT) (*e.g.: Actual value of a gas temperature, and lagged value of a thermocouple)

Delayed value of a parameter,
Value (time = T) = Value (time = (T – delay))

More analysis of this aspect should go hand in hand with the suppliers of control hard wares. However a good forecast of the allowable limit of the delay caused by control hardware, for a better transient performance, can be very useful in the detailed design of control hardware. The computer models have to be run for various durations of delays originating from the control system and the effect on the outputs have to be analysed. But a totality of the physics of the transients have to be established by incorporating all the influencing factors mentioned earlier to get a complete picture.

The computer model and the results

A computer model has been developed specifically for this particular project. This is capable for testing the steady state and transient operations. This model carrying only the elementary features at present, but more will be added to it, as detailed designs of the project are available. The various leakages and other pressure losses are based on empirical approximations due to the lack of specific information on the physical design and hence this paper deals with only the steady state performance and detailed transient model will be made available in the future.

Theory of the Simulation Model

To simulate the transient or off design performance of gas turbine engines, the transient period is segmented into time intervals. For each time interval, the calculation of the thermodynamic parameters of the gas path has to be carried out. Once these parameters (temperature, pressures, mass flows etc.) have been found, the power input and output for each component can be calculated. Then a power balance can be carried out for each shaft, and hence the accelerating torque can be calculated. This accelerating torque is then integrated over the time interval, and the change in shaft speeds is obtained. This process of thermodynamic variable calculation and torque integration is repeated over several time intervals as required.

In this procedure, the difficult task of thermodynamic variable calculation can be accomplished by either constant mass flow method (CMF) or inter component volume method (ICV). Inter component volume method is chosen for this exercise. This is the more realistic, since it includes allowance for gas mass storage, which is ignored in the CMF method

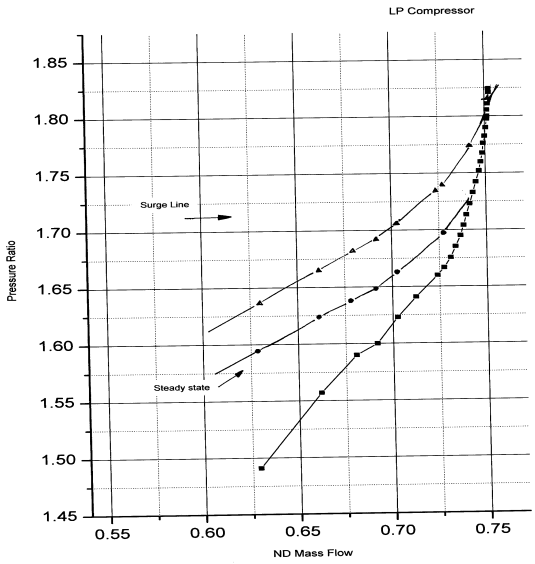

FIG. 5. Compressor performance on a rising TET.

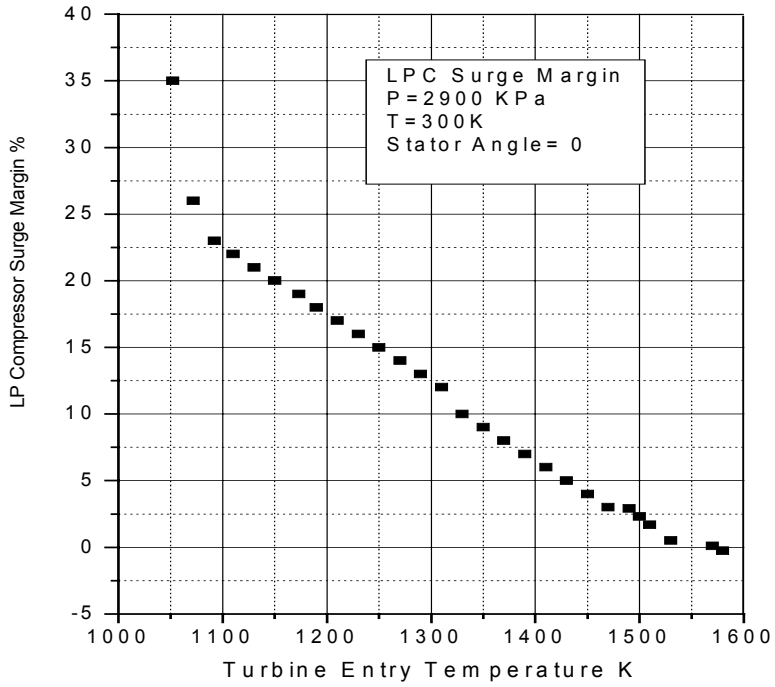

FIG. 6. Change in LP Compressor Surge margin as the TET goes up, keeping the compressor inlet Pressure and Temperature constant.

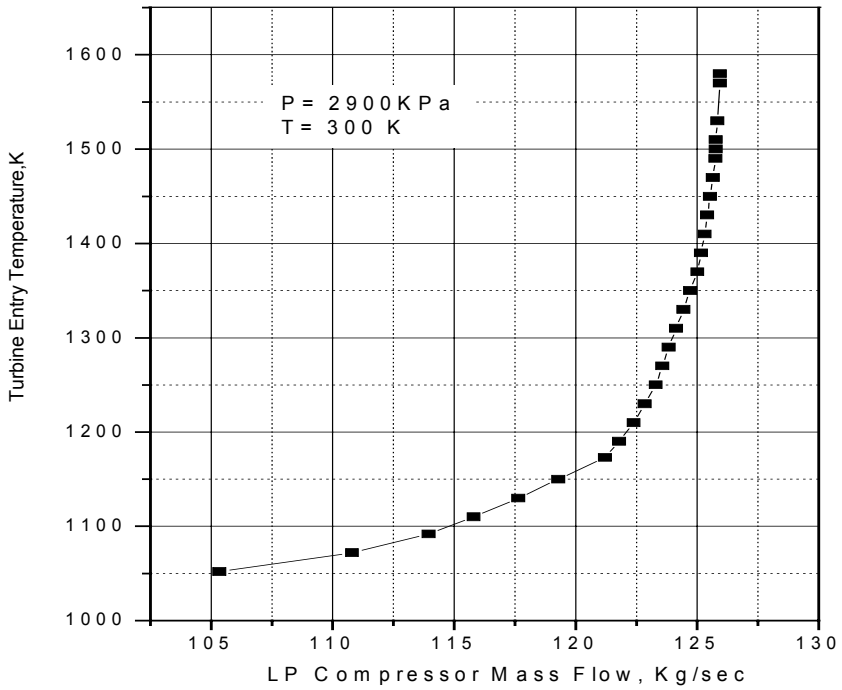

FIG.7. Mass flow through the compressor at various TET.

For each time interval in the segmented transient period, the calculation of the thermodynamic parameters of the gas path has been carried out. Once these parameters have been found, the power input and output of each component can be calculated. Then a power balance has been carried for each shaft and thus accelerating torque can be calculated. This accelerating torque is then integrated over the time interval, and the change in shaft speed is obtained. This process is repeated over several time intervals as required [11].

The method of inter component volume method (ICV) is used in this model. The ICV method is more realistic, since it includes allowance for gas mass storage, which is ignored in the constant mass flow (CMF) method.

The PBMR plan to use the inventory control system to do the load variation at the rate of 10 MW/min. The *FIG. 9* shows that in order to achieve that target the pressure (absolute) change required is around 3.4 bar/min (calculated from the slope). Also the change in mass flow rate is 8 kg/sec/min. This type of information can be useful for the design of Inventory control valves.

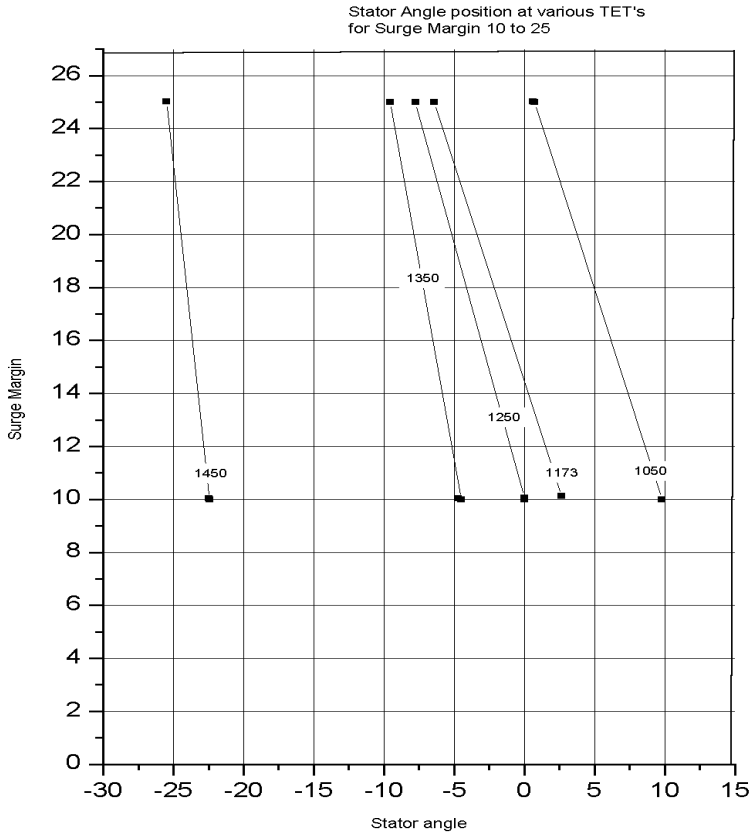

FIG.8. LP Compressor Stator Angles at different TET's for maintaining the Surge Margin between 10% and 25%.

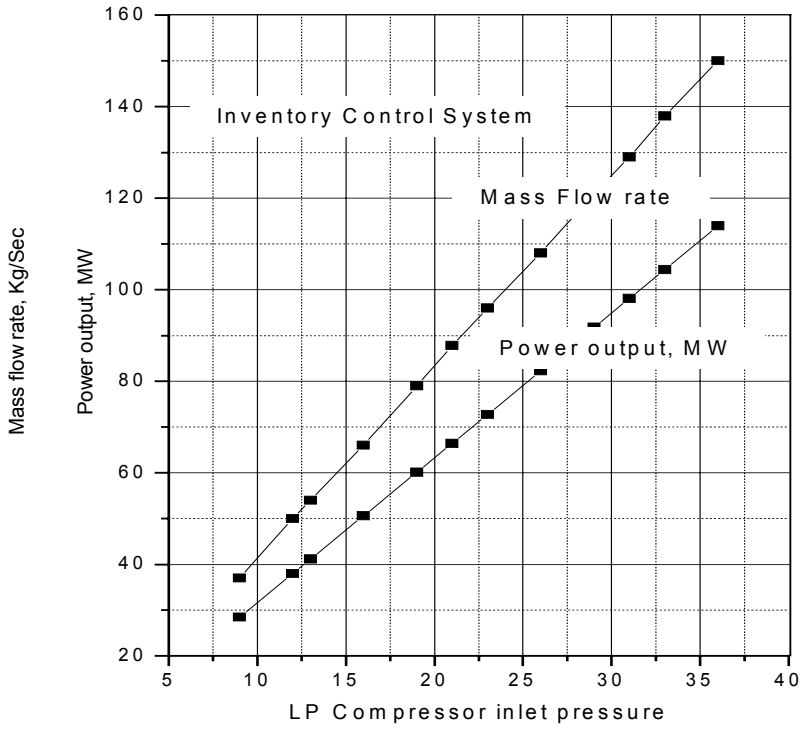

FIG. 9. Effect of change in the system pressure (LPC inlet Pressure shown) on the plant output. The efficiency, Pressure Ratio, TET are theoretically constant for the whole range.

Overall Gas Turbine Performance

The gas turbine part load performance using by pass control is an attractive option due to its rapid action. But an efficiency penalty has to be paid for this. A rough estimate shows that 35% reduction in the flow will be sufficient to bring the unit to synchronous idling. Thesudden decrease in mass flow rate through the reactor may cause in an increase in Turbine Entry Temperature beyond the design value. Another operational problem will be the possibility of surge due to the rising TETs as seen in the *FIG. 5*. However introducing a change of setting for the compressor stator vanes may push the operating line towards the steady state to avoid the surge due to rise in turbine entry temperature. The PBMR high-pressure turbine blades are cooled blades and hence it may have the capability to withstand temperature excursion for a short duration.

Helium inventory control is the most efficient part load control method. The system efficiency will almost same for a wide range of loading from 40% to 100%. The potential for thermal stresses are also minimal. The response time of this method can be considered as moderate and hence it can be used for normal and pre calculated load variations. The drawback of this system is that the logistics required for this method can be space consuming.

Conclusion

The operational performance is subjected to the finding of successful solutions of hard-core technical issues associated with Helium Turbines such as cold welding effects, difficulty in containing helium with the seals etc. More elaborate experimental study coupled with computational work is being carried out to reduce the uncertainty in this area. The future

exercises are planned to focus on the time delay of each control system. The final selection of equipments can only be done after considering the transient effects of each component and the system. However it is convinced that there is a market place for modular high temperature reactor for remote load centres where establishing logistics for conventional power plants is not viable and also for urban load centres where there is a need for efficient part load performance.

REFERENCES

[1] Conceptual design of a 50 MW severe – accident free HTR and the related test program of the HTTR by Kazuhiko Kunitomi, Yukio Tachibana, Akio Saikusa, Kazuhiro Sawa, Lawrence M Lidsky, Page245, Nuclear Technology Sep 1998

[2] ANS topical Meeting. Gas cooled Reactors: HTGR and GCFBR, May 7 –10, 1974, Gatlinburg, Tennessee, Page 401.

[3] PBMR Technical specification Issue 1.0

[4] Design and development of gas cooled reactors with closed cycle gas turbines. Proceedings of TCM held in Beijing, 30 October – 2 November 1995. Page181

[5] Energy Conversion, Systems, Flow physics and Engineering, Reiner Decher.

[6] Gas Turbine Performance, P Walsh and P Fletcher, Blackwell Science

[7] Hosny et al. Turbofan Engine Non recoverable Stall Computer Simulation Development and Validation, AIAA- 85 -1432, 21st Joint Propulsion Conference, Monterey California July 1985

[8] K.Bammert, Dynamic Behaviour and Control of Single Shaft Closed - Cycle Gas Turbines. NASA CASI Report – N7922095

[9] Roos, TH and Bennet M, Simulation of helium turbo machinery for Nuclear Plant, Aerotek Report AER 97/ 298, September 1997

[10] Cumptsy, NA, Compressor aerodynamics, Longman Scientific and Technical, UK, 1989

[11] Cohen H et al Gas Turbine Theory Longman Scientific and Technical UK

[12] A method for predicting the off design performance of closed Brayton Cycle engines, Donald T Knauss NASA / CASI – N7914562

[13] Closed Brayton Cycle system optimisation for undersea, terrestrial and space applications, NASA / CASI – N7922

COMPONENT DESIGN

(Session 3)

STUDY OF FISSION PRODUCT RELEASE, PLATE-OUT AND MAINTENANCE IN HELIUM TURBOMACHINERY

Y. MUTO, S. ISHIYAMA, S. SHIOZAWA
Japan Atomic Energy Research Institute,
Oarai-machi, Ibaraki-ken, Japan

Abstract:

A feasibility study of HTGR-GT has been conducted in JAERI, as an assigned work by the Science and Technology Agency in Japan. So far, the conceptual or preliminary designs of 600, 400 and 300 MW(t) power plants have been completed. The block type core and pebble-bed core have been selected in 600 MW(t) and 400/300 MW(t), respectively. In this plant concept, maintenance of turbine rotor is one of the most important issues. This paper describes the results of preliminary estimation of generation in the fuel, release into coolant and plate out on the components of ^{137}Cs and ^{110m}Ag. In addition, maintenance method of turbine rotor is discussed.

1. INTRODUCTION

A feasibility study of HTGR-GT has been conducted in JAERI, as an assigned work by the Science and Technology Agency in Japan. This paper was prepared based on the results of this feasibility study. So far, the conceptual or preliminary designs of 600, 400 and 300 MW(t) power plants have been completed. The block type core and pebble-bed core have been selected in 600 MW(t) and 400/300 MW(t), respectively. In this plant concept, maintenance of turbine rotor is one of the most important issues. This paper describes the results of preliminary estimation of generation in the fuel, release into coolant and plate out on the components of ^{137}Cs and ^{110m}Ag. In addition, maintenance method of turbine rotor is discussed. In this paper, two power plants, which is a 600 MW(t) plant with pin-in-block type fuel elements and a 300 MW(t) plant with pebble-bed type core are described. In case of 400 MW(t) plant, the amount of fission products can be estimated from the values of 300 MW(t) plant by multiplying 4/3.

In the 600 MW(t) and 300 MW(t) plants, UO_2 fuels with 15 and 10% enrichments are employed, respectively. The average burnup of 100 GWd/ton is reached in both the plants. The maximum systematic fuel temperature is 1300℃ and 1150℃ for the former and the latter plants, respectively. The fission products of ^{137}Cs and ^{110m}Ag are most concerned. The basic features of these fission products are as follows:

^{137}Cs: Directly produced from fission,

half life = 30y, radiation energy = 0.85R/decay

melting point = 28.4℃, boiling point =678.4℃ at the atmospheric pressure

^{110m}Ag: Produced by neutron capture reaction from ^{109}Ag,

half life = 252d, radiation energy = 3.86R/decay

melting point = 961.9℃, boiling point =2210℃ at the atmospheric pressure

The diffusion coefficient of SiC layer is one order larger for Ag than for Cs.

Due to the higher fuel temperature by 150℃, the amounts of fission products in the helium coolant are much larger in the pin-in-block 600 MW(t) reactor than in the pebble-bed 300 MW(t) reactor. In the following, the results of estimation of the fission product amounts existing in both the plants are given.

Regarding the plate-out phenomena, a simple calculation has been conducted under the assumption of steady state phenomenon.

Such processes related to the generation, release, transport and plate-out are schematically shown in Fig. 1.

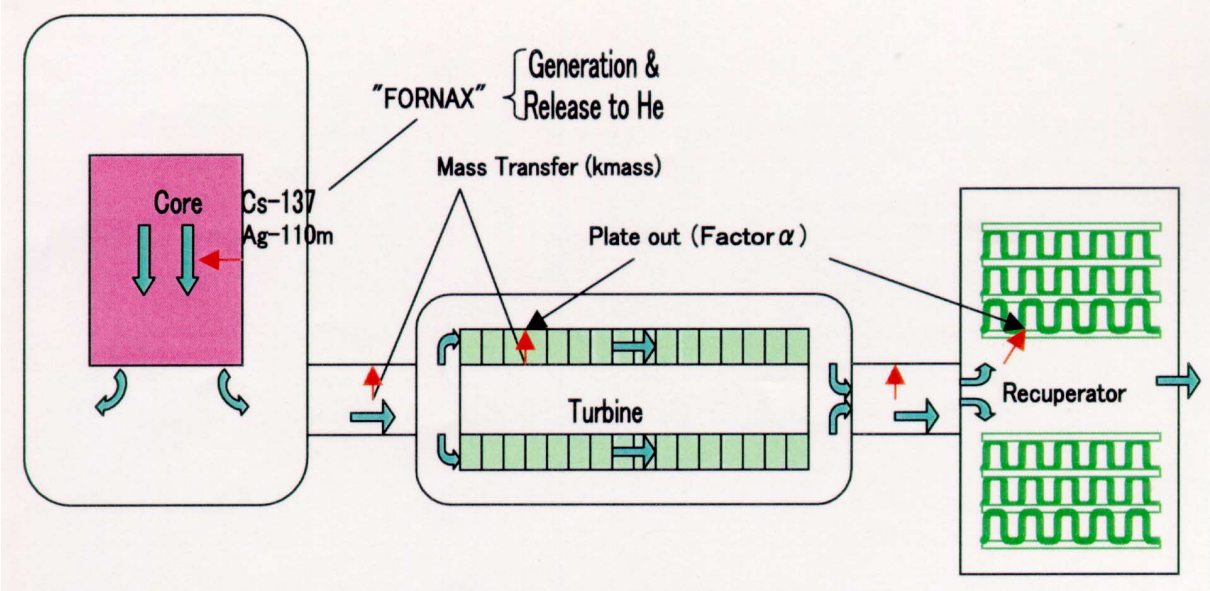

Fig. 1. Outline of fission product generation, release, transport and plate out.

2. THE DESIGN FEATURES OF 600 MW(t) AND 300 MW(t) PLANTS

2.1 600 MW(t) plant

The figures 2 and 3 show the flow diagram and vertical and horizontal cross sections of the reactor, respectively. Table 1 shows the main characteristics of the reactor. The figures 4 and 5 show the power density and systematic fuel temperature distributions in the core, respectively.

2.2 300 MW(t) plant

The figures 6 and 7 show the flow diagram and vertical and horizontal cross sections of the reactor, respectively. The main characteristics of the reactor are given also in Table 1. The figures 8 and 9 show the power density and temperature distributions in the core, respectively. In Fig. 9, both the systematic and nominal temperatures are drawn. The former means a temperature in which a probable temperature increase due to errors included in the analysis and data are taken into consideration.

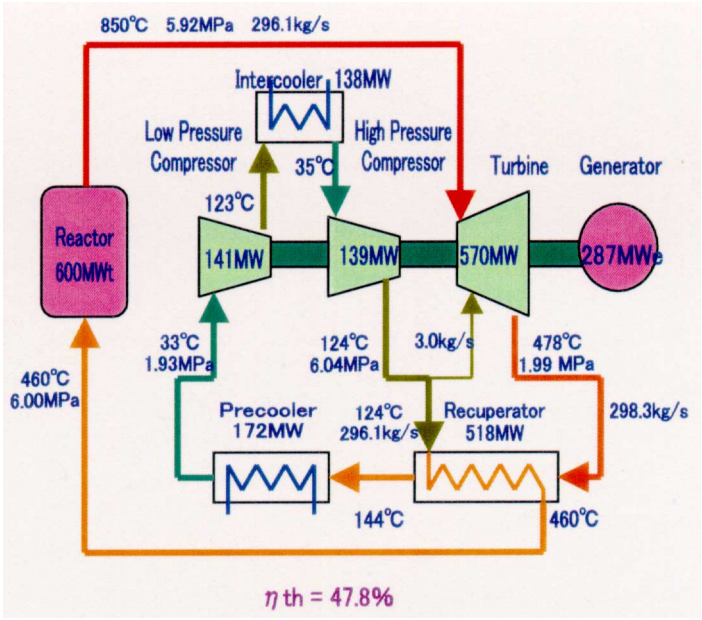

Fig. 2. Flow diagram of the 600 MW(t) plant.

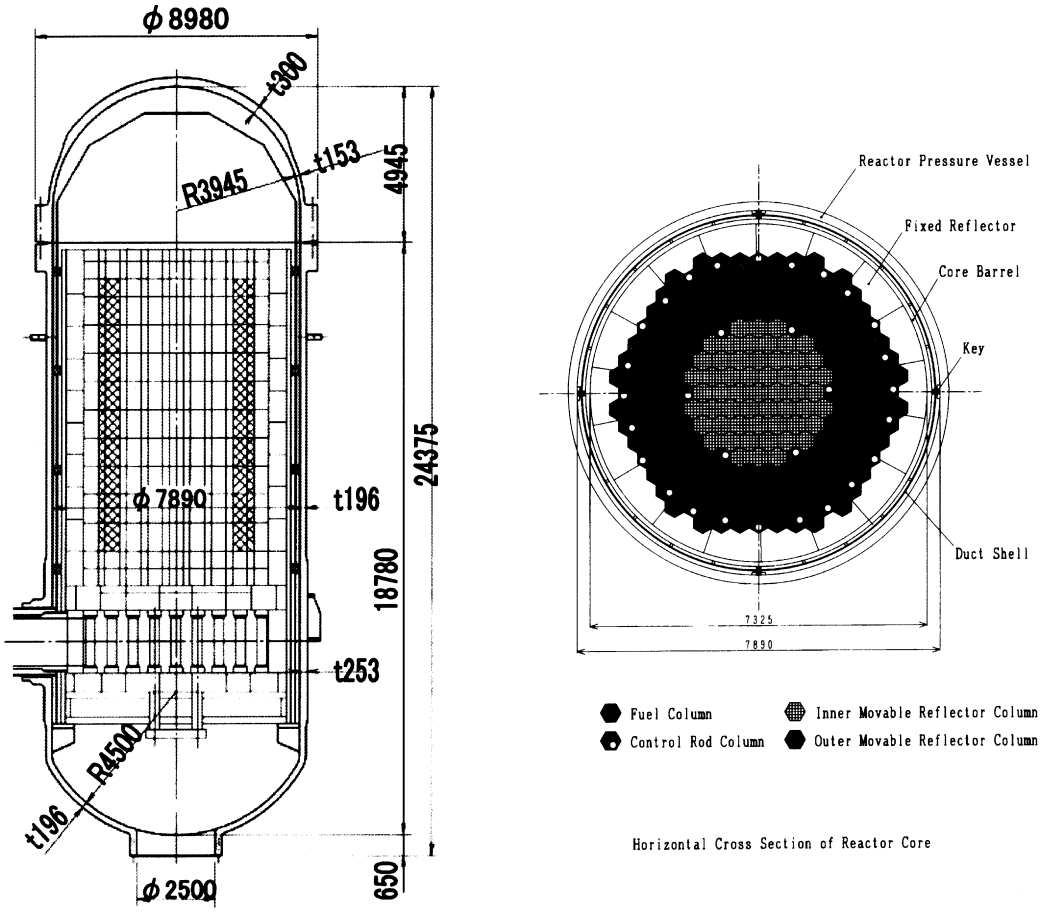

Fig. 3. Vertical and horizontal cross section of the 600 MW(t) reactor.

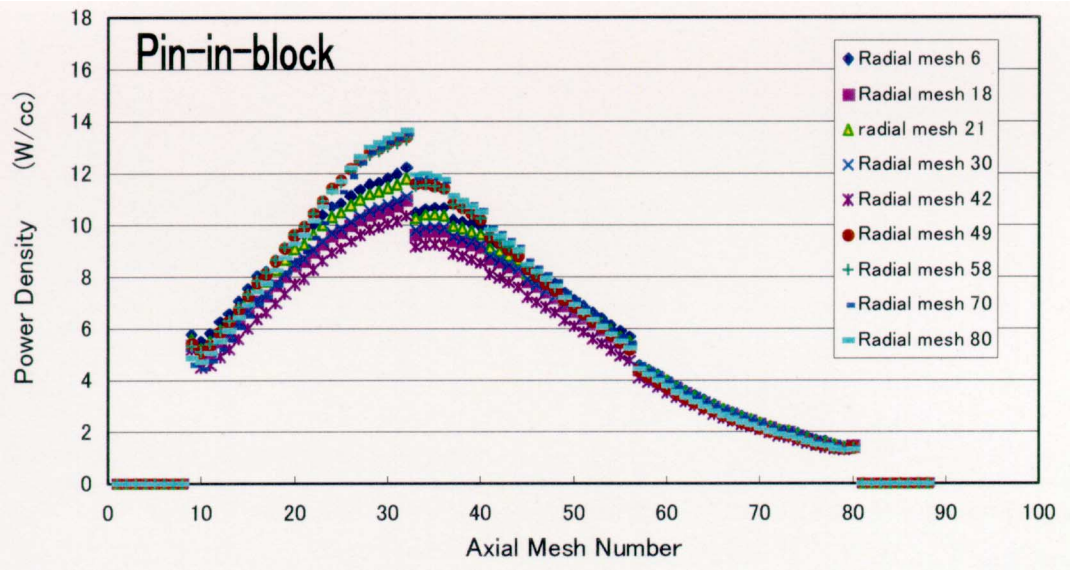

Fig. 4. Axial power distribution (BU=450 days, CR=0/0/0 0/2-/0).

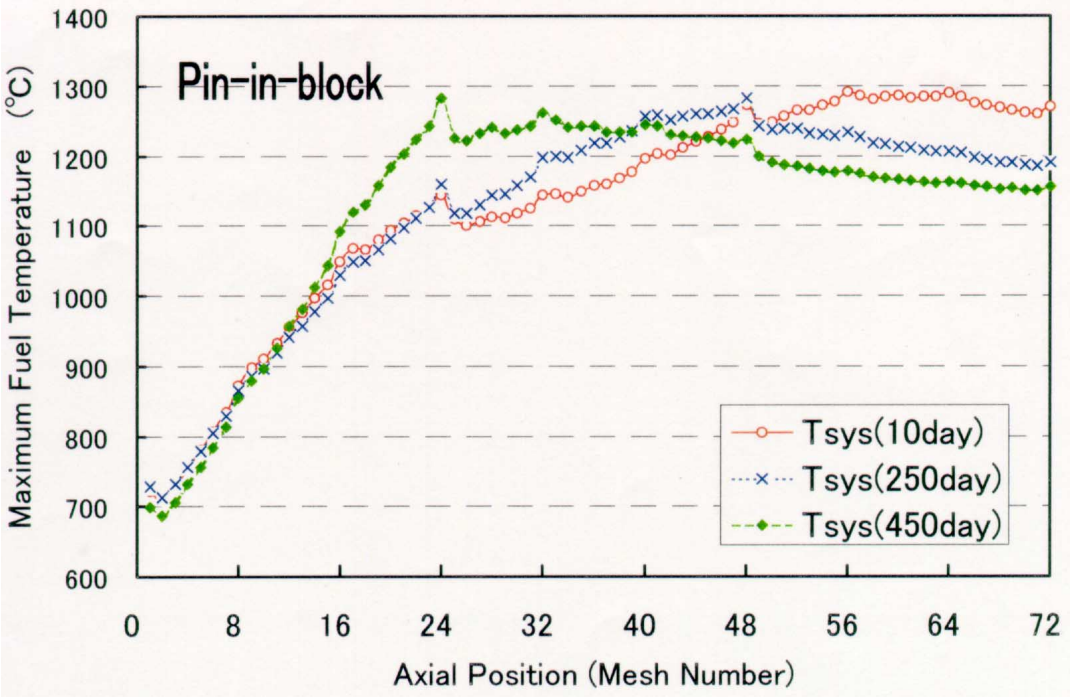

Fig. 5. Axial distribution of the maximum systematic fuel temperature for the 600 MW(t) core.

3. ANALYSIS FOR THE GENERATION AND RELEASE OF FISSION PRODUCTS

3.1 600 MW(t) plant

The generation of fission products in the fuel and the release of them from the particles to the coolant helium gas were analyzed by using the JAERI's in-house code "FORNAX" [1]. This code can take account of four kinds of FP sources and their ratios were assumed as follows:

The ratio of coated particles where their coatings have completely failed = 2×10^{-5}

The ratio of coated particles where only their SiC layer has failed = 2×10^{-5}

The ratio of fission products derived from the contaminated UO_2 into the graphite = 2×10^{-5}

Intact particles = balance.

The material data needed for the analysis are given in Table 2. Here, there are significant uncertainties in the values of diffusion coefficient, in particular, in ^{110m}Ag, in which the value is five times larger in US than that in JAERI.

TABLE 1. MAIN CHARACTERISTICS OF PLANT

Items	600 MW plant (Pin-in-block)	300 MW plant (Pebble bed)
Reactor Thermal Power	600 MW	300 MW
Reactor Inlet Gas Temperature	460℃	550℃
Reactor Outlet gas temperature	850℃	900℃
Helium Gas Pressure	6 MPa	6 MPa
Helium Gas Flow Rate	296 kg/s	165 kg/s
Average Burnup	100 GWd/ton	97 GWd/ton
Fuel Exchange	Daruma-Otoshi 450 day × 3	Multi-Cycle 960 day
Fuel	15w% UO_2	10w% UO_2
Fuel Element	Monolithic Pin-in-block	ϕ 60mm Ball
Coated Particle Type	PyC+SiC+PyC	PyC+SiC+PyC
UO_2 Kernel	500 μ m	500 μ m
Outer Diameter	940 μ m	940 μ m
Packing Fraction	30/ 35%	7.75%
Effective Core Height	8.1m	9.4m
Inner Diameter	3.70 M	2.0 M
Outer Diameter	5.48 m	3.8m
Average Power Density	5.77 MW/m^3	3.89 MW/m^3
Pressure Drop in Reactor	1.42%	4.72%

TABLE 2. INPUT MATERIAL DATA FOR THE CODE ”FORNAX”

Parts	Unit	Diffusion Coefficient D0 & Activation Energy Q0		Dimension & Density	
		Cs-137	Ag-110 M		
UO_2 kernel	D0(m^2/s)	6.7500E-10	6.7500E-10	Diameter（μ）	500
	Q0(J/mol)	1.7710E+05	1.7710E+05	Density(g/cm^3)	10.4
Buffer layer	D0(m^2/s)	6.6900E-06	3.6000E-06	Thickness（μ）	115
	Q0(J/mol)	1.9788E+05	2.1500E+05	Density (g/cm^3)	1.05
I-PyC layer	D0(m^2/s)	6.6900E-09	3.6000E-09	Thickness（μ）	30
	Q0(J/mol)	1.9788E+05	2.1500E+05	Density (g/cm^3)	1.9
SiC layer	D0(m^2/s)	6.7500E-12	6.8000E-11	Thickness（μ）	35
	Q0(J/mol)	1.7710E+05	1.7700E+05	Density (g/cm^3)	3.1
O-PyC layer	D0(m^2/s)	6.6900E-09	3.6000E-09	Thickness（μ）	40
	Q0(J/mol)	1.9788E+05	2.1500E+05	Density (g/cm^3)	1.9
Matrix	D0(m^2/s)	3.6000E-04	1.6000E+00	Diameter（mm）	
	Q0(J/mol)	1.8900E+05	2.5800E+05	Pin-in-block	23
				Pebble-bed	25
				Density (g/cm^3)	1.75
Graphite shell	D0(m^2/s)	9.0000E-06	8.7900E-03	Diameter（mm）	
	Q0(J/mol)	1.5714E+05	1.2270E+05	Pin-in-block	25
				Pebble-bed	30
				Density (g/cm^3)	1.75

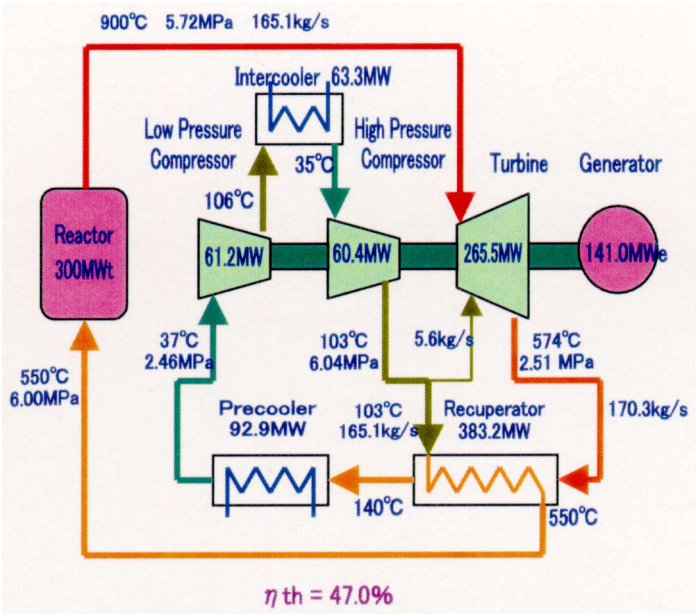

Fig. 6. Flow diagram for the 300 MW(t) plant.

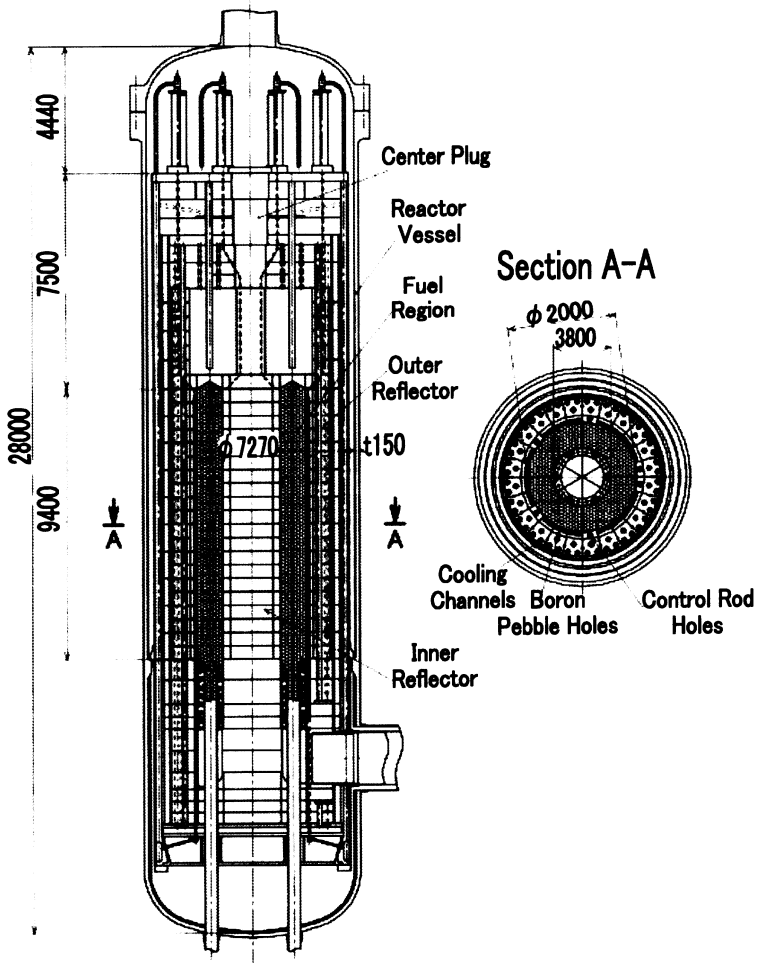

Fig. 7. Sectional view of 300 MW(t) reactor

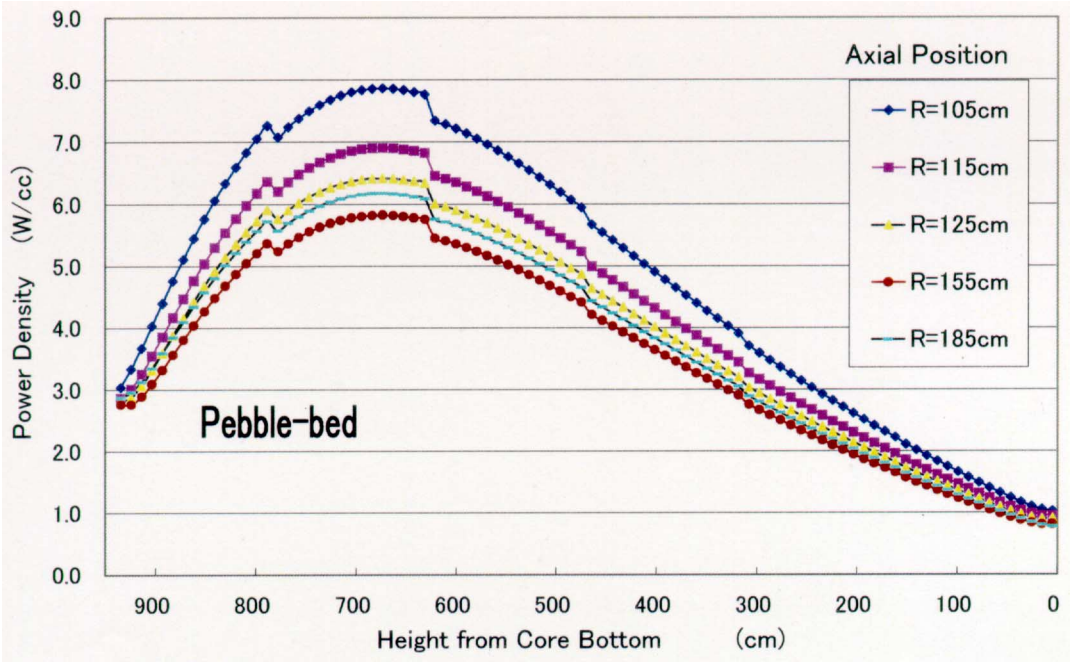

Fig. 8. Power density distribution in the 300 MW(t) core.

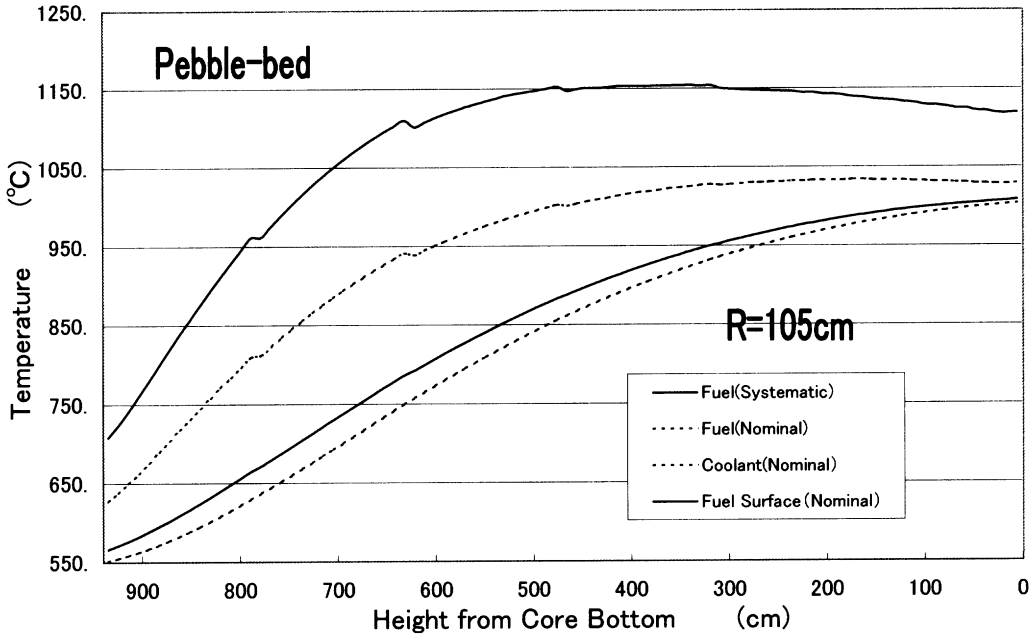

Fig. 9. Temperature distribution in the 300 MW(t) core.

Within the core, there is a distribution in the FPs generation due to the power distribution and the release of FPs is affected by temperature. In addition, these are time dependent. Then, a modeling of core is very complicated. In the block type core, the fuel-loading scheme called "Daruma-Otoshi" is adopted as illustrated in Fig. 10. This scheme is modeled as follows.

Three blocks stacked in the top layers are now considered. These are placed there between 0 to 450 days and moved to the lower stack in the next fuel cycle, that is, 450 to 900 days and finally moved to the bottom in 900 to 1350 days. The time dependent accumulated generation amounts and the accumulated release amounts are calculated for these blocks and the associated

burnup. By subtracting the amounts in the former days from those in the durations of 450 to 900 days and also 900 to 1350 days, the amounts for these cycles can be calculated. The summation for these 3 cycles are tantamount to the total FP amounts in the whole blocks of the 1 column in the each fuel cycle of 450 days for the equilibrium core. In addition, the three blocks are divided into 12 meshes axially and consist of 57 fuel pins horizontally. The one mesh consists of one fuel pin of 1 cm height. These are corrected to the actual height and pin number after the calculation. By this modeling, axial power distribution due to the fuel cycle can be taken into consideration. Regarding the radial power distribution, the core is divided into 3 zones dependent on power peaking factors, which are P.F.=1.24 × 18 columns, P.F.=1.1 × 27 columns and P.F.=1.0 × 45 columns. Here, the power peaking factor stands for a ratio of an axially integrated power in each fuel pin (channel) to the averaged value in the whole core. The values for the burnup of 450 days are illustrated in Fig. 11, where the figures of P.F. mean the maximum in each block. However, this time, the calculation was carried out only for the case of P.F.= 1.24 and the other cases were estimated considering their fuel temperature. This estimation is possible from Fig. 12, which is the result of a simple calculation under the uniform temperature and power. The results of calculation are shown in Tables 3 and 4 for the ^{137}Cs and ^{110m}Ag, respectively.

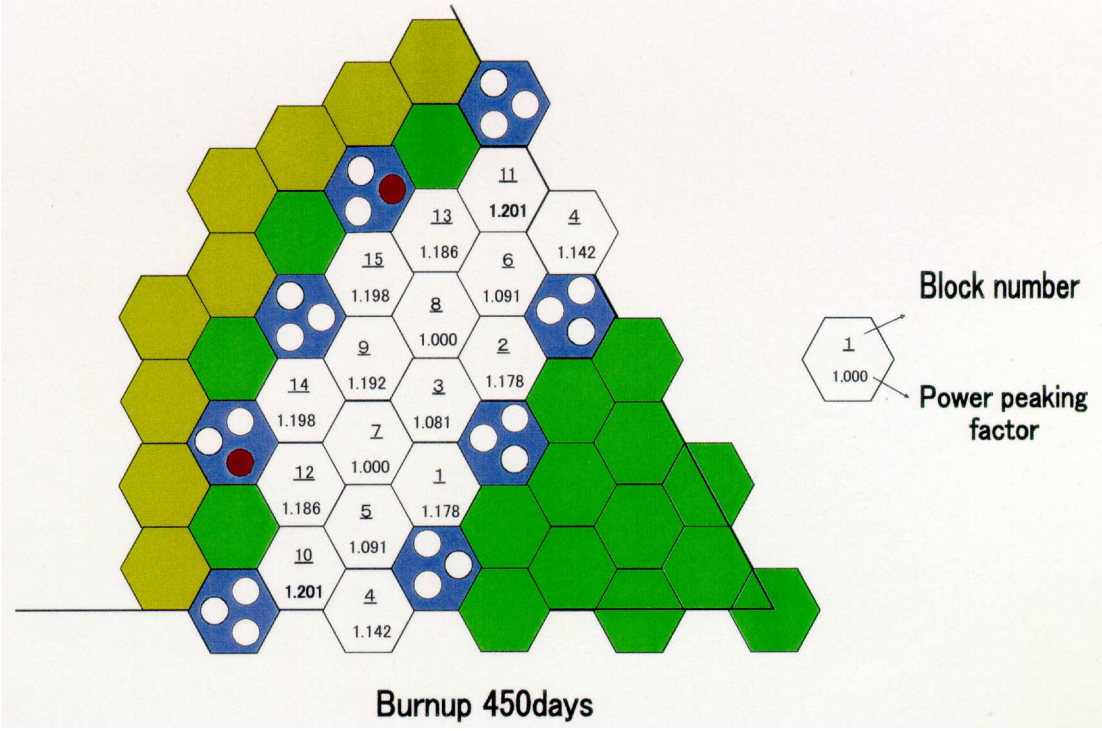

Fig. 10. Fuel loading scheme called "Daruma-Otoshi" for the 600 MW(t) plant.

From the Table 3, the release amount of ^{137}Cs is estimated as follows.

Zone of P.F.= 1.24

The release amount of ^{137}Cs per unit column

$= 8.29 \times 10^{-2}$ Ci/36 cm/pin × 57pin × 85.5 cm/block × 9block

= 101 Ci/column.

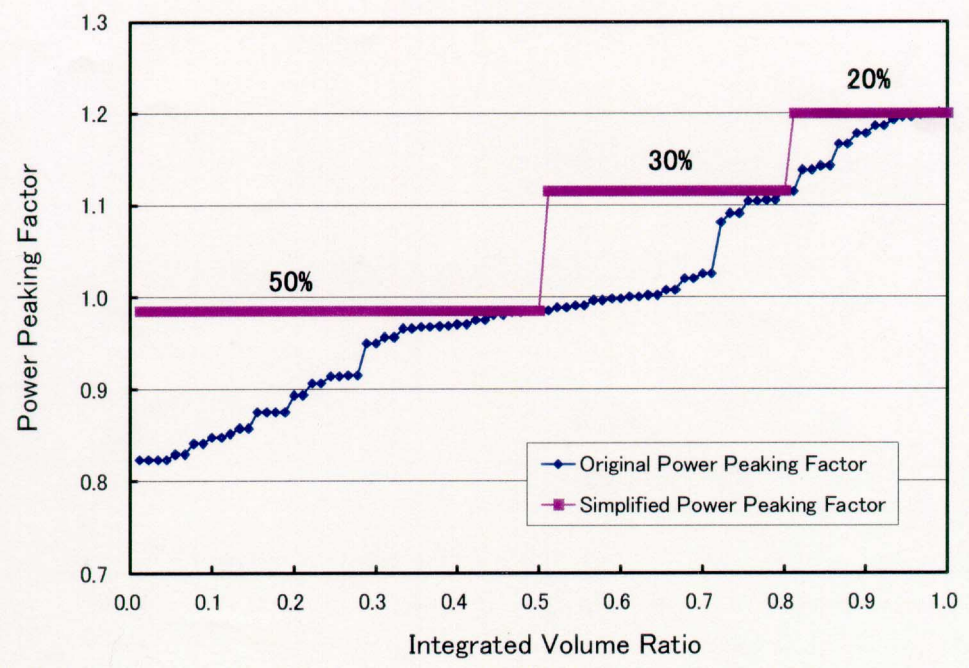

Fig. 11. Power peaking factor distribution and its modeling for the 600 MW(t) core.

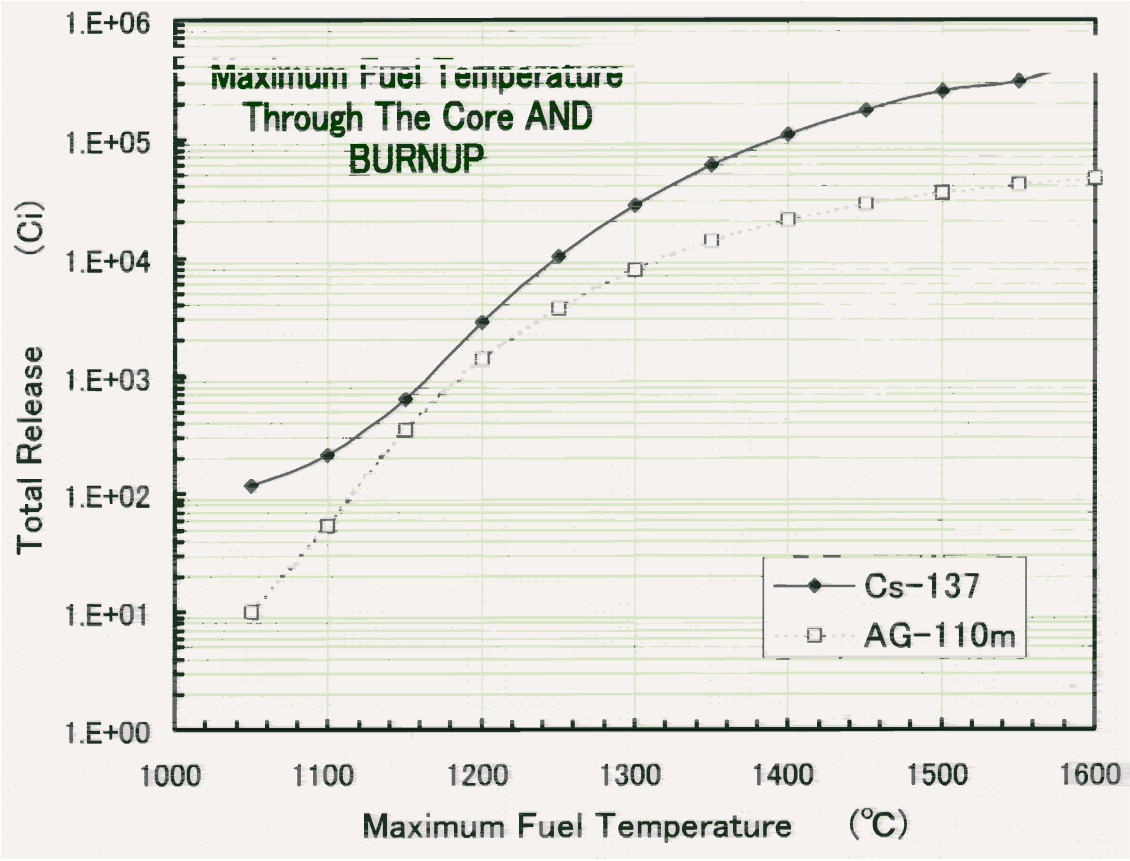

Fig. 12. Effect of the maximum fuel temperature on the total fission product release.

TABLE 3. RELEASE AMOUNT OF ^{137}CS FOR THE 600 MW(T) PLANT（CHANNEL WITH P.F.=1.24 (UNIT: CI

Mesh No.	450 h	900 h	1350 h	900h-450 h	1350h-900 h
Block1, Mesh2	1.73×10^{-10}	1.39×10^{-5}	1.84×10^{-3}	1.39×10^{-5}	1.82×10^{-3}
Mesh 4	2.17×10^{-10}	1.78×10^{-5}	2.88×10^{-3}	1.78×10^{-5}	2.86×10^{-3}
Mesh 6	1.60×10^{-8}	2.17×10^{-5}	3.37×10^{-3}	2.16×10^{-5}	3.35×10^{-3}
Mesh 8	9.41×10^{-8}	5.31×10^{-5}	6.16×10^{-3}	5.30×10^{-5}	6.11×10^{-3}
Block2, Mesh 2	1.97×10^{-7}	5.03×10^{-5}	4.89×10^{-3}	5.01×10^{-5}	4.84×10^{-3}
Mesh 4	4.82×10^{-7}	1.03×10^{-4}	6.17×10^{-3}	1.02×10^{-4}	6.07×10^{-3}
Mesh 6	9.82×10^{-7}	1.48×10^{-4}	6.51×10^{-3}	1.47×10^{-4}	6.36×10^{-3}
Mesh 8	2.36×10^{-6}	4.78×10^{-4}	9.33×10^{-3}	4.76×10^{-4}	8.85×10^{-3}
Block3, Mesh 2	3.38×10^{-6}	5.01×10^{-4}	8.11×10^{-3}	4.97×10^{-4}	7.61×10^{-3}
Mesh 4	5.34×10^{-6}	8.69×10^{-4}	8.91×10^{-3}	8.64×10^{-4}	8.04×10^{-3}
Mesh 6	7.47×10^{-6}	1.37×10^{-3}	9.90×10^{-3}	1.36×10^{-3}	8.53×10^{-3}
Mesh 8	1.13×10^{-5}	3.37×10^{-3}	1.48×10^{-2}	3.36×10^{-3}	1.15×10^{-3}
Sum	3.16×10^{-5}(A)	7.00×10^{-3}	8.29×10^{-2}	6.96×10^{-3}(B)	7.59×10^{-2}(C)
Total	8.29×10^{-2}(A+B+C)				

Zone of P.F.=1.1

The release amount of ^{137}Cs per unit column

= the amount of fission products in the zone of P.F.= $1.24\times10\%$

= 10.1 Ci/column.

Zone of P.F.=1.0

The release amount of ^{137}Cs per unit column

= the amount of fission products in the zone of P.F.= $1.24\times1\%$

= 1.01 Ci/column.

TABLE 4. RELEASE AMOUNT OF ^{110M}AG FOR THE 600 MW(T) PLANT（CHANNEL WITH P.F.=1.24）. UNIT:CI

Mesh No.	450 h	900 h	1350 h	900h-450 h	1350h-900 h
Block1,2	2.09×10^{-12}	7.14×10^{-8}	1.63×10^{-5}	7.14×10^{-8}	1.62×10^{-5}
Mesh 4	1.83×10^{-11}	1.26×10^{-7}	2.17×10^{-5}	1.26×10^{-7}	2.16×10^{-5}
Mesh 6	1.33×10^{-10}	2.16×10^{-7}	2.37×10^{-5}	2.16×10^{-7}	2.35×10^{-5}
Mesh 8	8.44×10^{-10}	1.14×10^{-6}	3.54×10^{-5}	1.14×10^{-6}	3.42×10^{-5}
Block2, Mesh 2	1.79×10^{-9}	9.84×10^{-7}	2.89×10^{-5}	9.82×10^{-7}	2.79×10^{-5}
Mesh 4	4.41×10^{-9}	2.14×10^{-6}	3.28×10^{-5}	2.14×10^{-6}	3.07×10^{-5}
Mesh 6	8.11×10^{-9}	2.81×10^{-6}	3.29×10^{-5}	2.80×10^{-6}	3.01×10^{-5}
Mesh 8	1.40×10^{-8}	7.24×10^{-6}	3.98×10^{-5}	7.23×10^{-6}	3.26×10^{-5}
Block3, Mesh 2	1.74×10^{-8}	6.78×10^{-6}	3.35×10^{-5}	6.76×10^{-6}	2.67×10^{-5}
Mesh 4	1.74×10^{-8}	6.78×10^{-6}	3.35×10^{-5}	6.76×10^{-6}	2.67×10^{-5}
Mesh 6	2.92×10^{-8}	1.23×10^{-5}	3.21×10^{-5}	1.22×10^{-5}	1.98×10^{-5}
Mesh 8	4.99×10^{-8}	2.15×10^{-5}	3.95×10^{-5}	2.15×10^{-5}	1.79×10^{-5}
Sum	1.43×10^{-7}(A)	6.21×10^{-5}	3.70×10^{-4}	6.19×10^{-5}(B)	3.08×10^{-4}(C)
Total	3.70×10^{-4}(A+B+C)				

Whole core

The release amount of ^{137}Cs in the whole core

= 101 Ci/column × 18 columns + 10.1 Ci/column × 27 columns + 1.01 Ci/column × 45 columns

= 1818 Ci + 273 Ci + 45 Ci

= 2136 Ci/450 days,core

If the excessive margin due to the difference between the systematic temperature and the mean temperature (＞100℃) is estimated to be a factor of 5, a realistic release amount of ^{137}Cs becomes 428 Ci/450 days,core.

Regarding the ^{110m}Ag, the release amount is estimated as follows from Table 4.

Zone of P.F.=1.24

The release amount of ^{110m}Ag per unit column

= 3.70×10^{-4} Ci/36 cm /pin × 57pin × 85.5 cm/block × 9block

= 0.451 Ci/column.

Zone of P.F.=1.1

The release amount of ^{110m}Ag per unit column

= the amount of fission products in the zone of P.F.=1.24 × 25%

= 0.113 Ci/column.

Zone of P.F.=1.0

The release amount of ^{110m}Ag per unit column

= the amount of fission products in the zone of P.F.=1.24 × 2.5%

= 0.0113 Ci/column.

Whole core

The release amount of ^{110m}Ag in the whole core

= 0.451 Ci/column × 18 columns＋0.113 Ci/column × 27 columns＋0.0113 Ci/column × 45 columns

= 8.12 Ci＋3.05 Ci＋0.51 Ci

= 11.68 Ci/450 days,core

If the excessive margin due to the difference between the systematic temperature and the mean temperature (＞100℃) is also estimated to be a factor of 5, a realistic release amount of ^{110m}Ag becomes 2.34 Ci/450 days,core.

3.2 300 MW plant

The material data such as failed coating ratios are the same as in the 600 MW(t).

In our pebble bed reactor, the multi-cycle-fuel-loading scheme is employed. Then, the fuel balls pass through the core in 96 days and are circulated 10 times and removed after 960 days. Therefore, a continuous calculation of 96 days × 10 cycles was conducted as illustrated in Fig. 13. To take the reduction of power and temperature dependent on burnup, the total 10 cycles were divided into the first 5 cycles with the maximum power and the maximum temperature of 1155℃ and the second 5 cycles with the average power and the 30℃ reduced temperature of 1125℃.

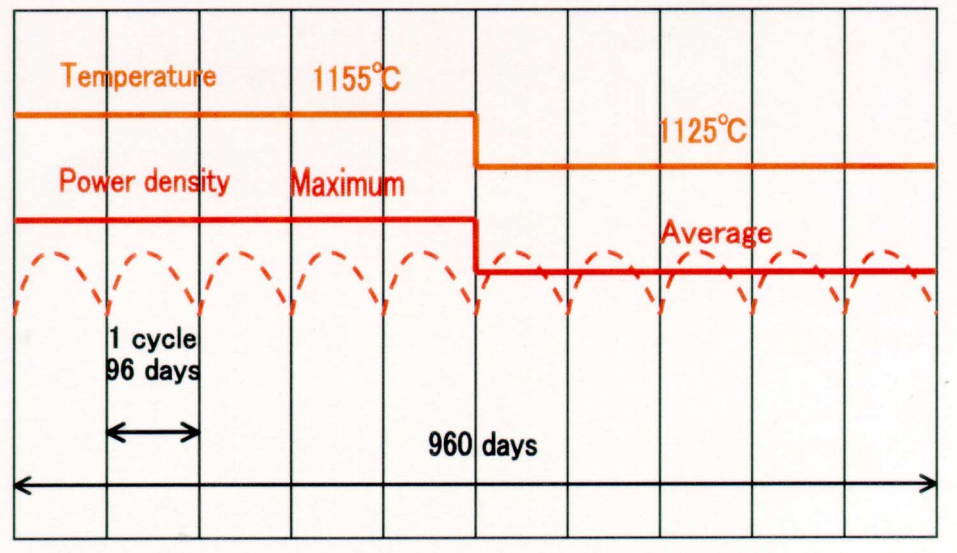

Fig. 13. Fuel loading scheme for the 300 MW(t) plant.

TABLE 5. RELEASE AMOUNTS OF ^{137}CS AND ^{110M}AG IN 300 MW(T) PLANT
UNIT: CI/CM

Time	^{137}Cs		^{110m}Ag	
h	Maximum temperature region	Average temperature region	Maximum temperature region	Average temperature region
96	7.429×10^{-8}	8.789×10^{-9}	2.251×10^{-9}	5.326×10^{-10}
192	3.753×10^{-7}	5.947×10^{-8}	1.326×10^{-8}	3.46×10^{-9}
288	9.625×10^{-7}	1.634×10^{-7}	4.417×10^{-8}	9.692×10^{-9}
384	2.080×10^{-6}	3.242×10^{-7}	1.418×10^{-7}	1.928×10^{-8}
480	4.523×10^{-6}	5.437×10^{-7}	4.025×10^{-7}	3.193×10^{-8}
576	8.023×10^{-6}	7.538×10^{-7}	7.933×10^{-7}	4.342×10^{-8}
672	1.398×10^{-5}	9.844×10^{-7}	1.219×10^{-6}	5.338×10^{-8}
768	2.387×10^{-5}	1.237×10^{-6}	1.772×10^{-6}	6.480×10^{-8}
864	3.953×10^{-5}	1.512×10^{-6}	2.436×10^{-6}	7.676×10^{-8}
960	6.313×10^{-5}	1.810×10^{-6}	3.209×10^{-6}	8.890×10^{-8}

If we consider one fuel ball in a j^{th} cycle, the fission-product-amount released during this cycle becomes Q(j) – Q(j-1), where Q denotes fission-product-amount(Ci). As there exist fuel balls of 1^{st} to 10^{th} cycles equally within the core in every cycle, the sum of these 10 cycles becomes the average fission-product-amounts for ten fuel balls in one cycle. The sum of Q(j) – Q(j-1) for j=1 to 10 equals to Q(10). Then, the requested amounts becomes Q(10)/10 for one fuel ball and one cycle, that is, 96 days. For the 960 days, the amount should be Q(10)/10 × 10=Q(10). Therefore, the requested fission-product-amounts are obtained by Q(10) multiplied by the total number of fuel balls in the core.

As the spherical source cannot be treated in the code "FORNAX", the fuel ball was modeled into a cylindrical pellet of 2.5 cm radius × 1 cm height. As the outer radius of ball is 3 cm and internal radius of compact region including coated fuel particles is 2.5 cm, the ball is equivalent to the cylindrical pellet with 2.5 cm radius × 3.333 cm height. Therefore, by multiplying the calculated data by a factor 3.333, the data for one ball can be obtained. Regarding the radial temperature distribution, the core was divided into two zones, that is, one half with the maximum fuel temperature and the other half with the mean temperature. The results are shown in Table 5.

By multiplying the correction factor of 3.333 and also the total number of fuel spheres in the core, the amount of fission products are estimated as follows:

^{137}Cs:

Zone with the maximum fuel temperature

The release amount of ^{137}Cs $=6.313 \times 10^{-5}$ Ci/cm × 3.333 cm/ball × 697300balls/core × 0.5

$=73.36$ Ci

Zone with the mean fuel temperature

The release amount of ^{137}Cs $=1.810 \times 10^{-6}$ Ci/cm × 3.333 cm/ball × 697300balls/core × 0.5

$=2.09$ Ci

The sum of the release amount of ^{137}Cs =75.45 Ci/core/960 days

If taking the factor of 5 due to the difference between the nominal and systematic temperature into account, a realistic release amount of ^{137}Cs becomes 15.1 Ci/core/960 days.

Similarly, for ^{110m}Ag:

Zone with the maximum fuel temperature

The release amount of ^{110m}Ag $=3.209 \times 10^{-6}$ Ci/cm × 3.333 cm/ball × 697300balls/core × 0.5

$=3.73$ Ci

Zone with the mean fuel temperature

The release amount of ^{110m}Ag $=8.890 \times 10^{-8}$ Ci/cm × 3.333 cm/ball × 697300balls/core × 0.5

$=0.103$ Ci

The sum of the release amount of ^{110m}Ag =3.83 Ci/core/960 days

If taking the factor of 5 due to the difference between the nominal and systematic temperature into account, a realistic release amount of ^{110m}Ag becomes 0.766 Ci/core/960 days.

4. PLATE-OUT

4.1 Analysis method

Simplified analyses were carried out under the assumption of steady state phenomenon to estimate the plate-out amount of fission products on the surface of turbine rotor.

Based on the formula of PAD code［2］of GA, governing equations are written:

$$\frac{\partial C(x,t)}{\partial t} = -\frac{\partial v(x)C(x,t)}{\partial x} - \frac{k_m(x,t)p_L(x)}{A_f(x)}\left(C(x,t) - C_S(x,t)\right) \tag{1}$$

$$\frac{\partial S_c(x,t)}{\partial t} = k_m(x,t)\left(C(x,t) - C_S(x,t)\right) \tag{2}$$

$$k_m(x,t) = \left[\frac{0.023D(x,t)}{d(x)}\right]\mathrm{Re}(x)^{0.83}S_m(x,t)^{0.44} \tag{3}$$

where C(x,t): FP concentration in He(Ci/m^3)

$$C_S(x,t) = F\left\{S_c(x,t)\right\} \tag{4}$$

C_S(x,t) : FP concentration in the boundary He gas layer(Ci/m^3)

Sc(x,t) : FP plate-out on material surface(Ci/m^2)

k_m(x,t) : Mass transfer coefficient (m/s)

P_L(x) : Wetted perimeter (m)

A_f(x) : Sectional flow area(m^2)

D(x,t) : Mass diffusivity(m^2/s)

d(x) : Hydraulic diameter(m)

Re(x) : Reynolds number

Sm(x,t) : Schmit number

F : Function of surface reaction

In addition to the assumption of steady state, C_S is assumed to be zero. Instead of it, a parameter α is introduced which denotes a ratio of an absorbed FP amount to a transported FP amount. If the surface condition is a complete sink, α=1. Under these assumptions, the above equations are simplified to:

$$-\frac{dv(x)C(x)}{dx}-\frac{k_m(x)P_L(x)}{A_f(x)}C(x)\alpha(x)=0 \qquad (5)$$

$$S(x)=\alpha(x)k_m(x)C(x)dt \qquad (6)$$

where $\alpha(x)$: a factor denotes a ratio of a captured FP amount to the transported FP amount from the main flow to the wall.

$$k_m(x)=\left[\frac{0.023D(x)}{d(x)}\right]Re(x)^{0.83}S_m(x)^{0.44} \qquad (7)$$

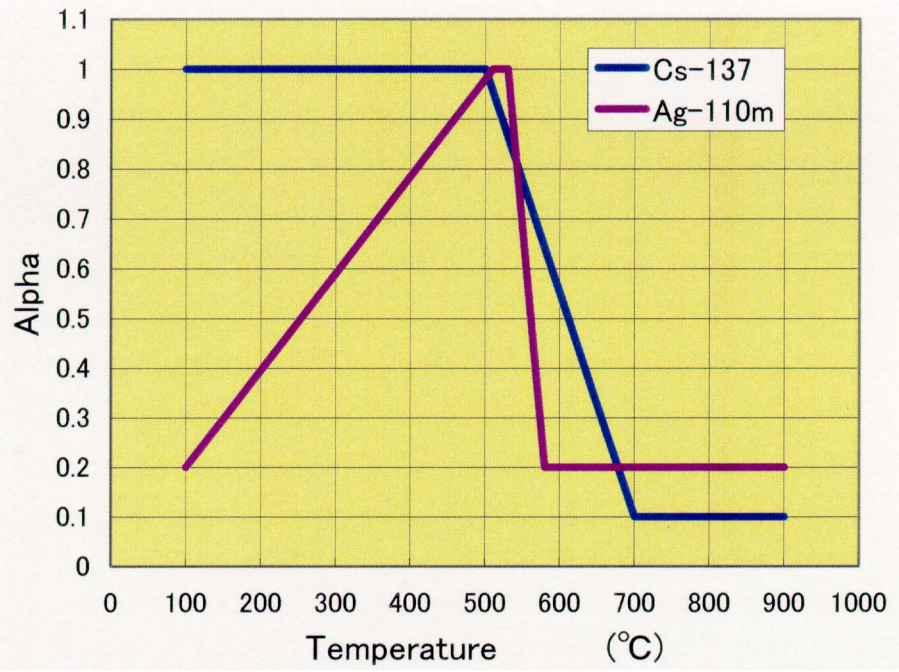

Fig. 14. The assumed values for the factor α.

The value of α was assumed mainly by the engineering judgment as shown in Fig. 14. For the ^{137}Cs, α=0.1 at high temperature and it increases sharply up to 1.0 from 700℃ to 500℃ and at the lower temperature kept constant to be 1.0. This is assumed based on the measurement in the Peach Bottom [3]. As for the ^{110m}Ag, α was assumed referring to the paper of Moormann [4], where the value of α hits the maximum at 510 to 530℃ and sharply decreases both at the higher and lower temperatures. The lowest value was assumed first to 0.1. However, in this value, significant amounts of ^{110m}Ag penetrate the recuperator and reache the precooler. Then, the bottom value of α was assumed to 0.2.

By discretization, these equations result in for the mesh (m):

$$-\frac{C(m)A_f(m)V(m)-C(m-1)A_f(m-1)V(m-1)}{\Delta x(m)}-k_m(m)P_L(m)C(m)\alpha(m)=0 \quad (8)$$

$$\frac{S(m)-S(m-1)}{\Delta t}=k_m(m)C(m)\alpha(m) \qquad (9)$$

$$k_m(m)=\left[\frac{0.023D(m)}{d(m)}\right]Re(m)^{0.83}S_m(m)^{0.44} \qquad (10)$$

As C(0) is a given FP-amount emitted from the reactor to He-gas-flow at the reactor outlet nozzle and $A_f(0)$ and V(0) are assumed to be equal to $A_f(1)$ and V(1), respectively, these equations are solved in turn. In the above parameters, D(m) was calculated by using the equation in Ref. 5. In this equation, the values of Lennard-Jones Parameters σ and ε/κ are needed for He, Cs and Ag. The values for He was found in the reference [5] and those for Cs and Ag are in the reference [6], respectively.

4.1 Plate out in the 600 MW(t) plant

The mesh generation employed is shown in Fig. 15. In the turbine, the either intake scroll and the outlet diffuser was modeled into only one mesh. The blading section was divided into 8 meshes in consistency with the stage number. For the simplification, rotor blades section and nozzle blade section were not separated. As the values of gas velocity, the average velocity (the relative velocity for the rotor blade) was used. This is somewhat not conservative and more exact treatment is needed.

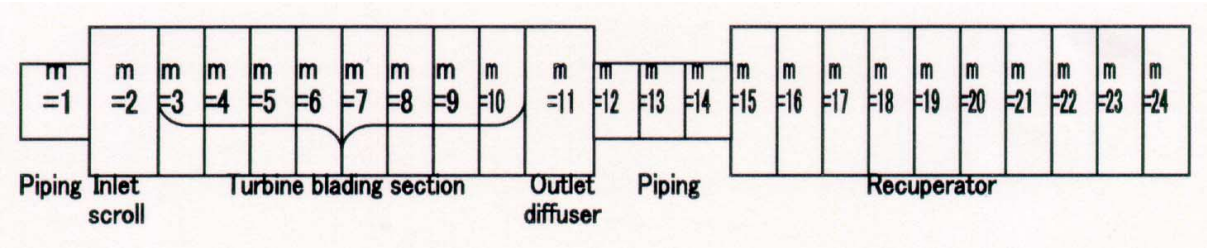

Fig. 15. Mesh generation for the cooling system of 600 MW(t) plant.

The results are shown in Table 6. Due to the high velocity, the mass transfer coefficients are high in turbine blading section. The amounts of FP plate out are concentrated at the lower portion of turbine, which is attributed to the larger value of α. The majority of ^{137}Cs are plated out on the plate-fin surfaces of recuperator due to its vast heat transfer area. In case of ^{110m}Ag, this inclination is also found, but not so remarkable due to the assumed low value of α.

TABLE 6. RESULTS OF PLATE-OUT CALCULATION FOR THE 600 MW(t) PLANT

Component		Mesh	Temperature	Pressure	Gas velocity	Surface area
Piping from reactor		1	850.0	5.914	58.2	51.31
Turbine	Inlet	2	850.0	5.914	44.0	66.87
	1st stage	3	822.8	5.541	402.7	8.04
	2nd stage	4	768.9	4.841	380.2	8.95
	3rd stage	5	717.7	4.229	365.3	9.91
	4th stage	6	669.0	3.695	355.9	10.88
	5th stage	7	622.8	3.229	350.6	11.84
	6th stage	8	578.8	2.821	348.5	12.80
	7th stage	9	537.0	2.465	349.0	13.76
	8th stage	10	497.3	2.153	351.9	14.73
	Outlet	11	478.2	2.008	44.3	95.57
Piping from turbine to recuperator		12	478.2	2.008	68.4	32.35
		13	478.2	2.008	68.4	31.70
		14	478.2	2.008	68.4	31.70
Recuperator		15	461.0	2.005	17.9	4079.30
		16	427.6	2.001	17.1	4079.30
		17	394.1	1.998	16.3	4079.30
		18	360.7	1.995	15.5	4079.30
		19	327.2	1.992	14.7	4079.30
		20	293.8	1.988	13.9	4079.30
		21	260.3	1.985	13.1	4079.30
		22	226.9	1.982	12.3	4079.30
		23	193.4	1.979	11.5	4079.30
		24	160.0	1.975	10.7	4079.30

Component		Mesh No.	α		Mass transfer coefficient		Radioactivity Ci	
			^{137}Cs	^{110m}Ag	^{137}Cs	^{110m}Ag	^{137}Cs	^{110m}Ag
Piping		1	0.1	0.2	0.0488	0.0627	0.91	0.013
Turbine	Inlet	2	0.1	0.2	0.0411	0.0528	1.00	0.014
	1st stage	3	0.1	0.2	0.4991	0.6417	1.40	0.019
	2nd stage	4	0.1	0.2	0.4774	0.6145	1.36	0.019
	3rd stage	5	0.1	0.2	0.4644	0.5987	1.35	0.019
	4th stage	6	0.240	0.2	0.4573	0.5898	3.18	0.018
	5th stage	7	0.447	0.2	0.4539	0.5871	5.81	0.018
	6th stage	8	0.645	0.208	0.4509	0.5888	8.11	0.019
	7th stage	9	0.834	0.798	0.4574	0.5948	10.23	0.069
	8th stage	10	1.0	0.711	0.4634	0.6038	11.85	0.059
	Outlet	11	1.0	0.426	0.0416	0.0543	6.49	0.020
Piping		12	1.0	0.426	0.0571	0.0745	2.99	0.001
		13	1.0	0.426	0.0571	0.0745	2.91	0.001
		14	1.0	0.426	0.0571	0.0745	2.89	0.001
Recuperator		15	1.0	0.269	0.0637	0.0831	196.69	0.583
		16	1.0	0.2	0.0604	0.0791	91.09	0.332
		17	1.0	0.2	0.0571	0.0750	42.37	0.254
		18	1.0	0.2	0.0538	0.0709	19.79	0.195
		19	1.0	0.2	0.0506	0.0668	9.28	0.150
		20	1.0	0.2	0.0472	0.0628	4.37	0.115
		21	1.0	0.2	0.0439	0.0586	2.07	0.089
		22	1.0	0.2	0.0406	0.0545	0.99	0.068
		23	1.0	0.2	0.0373	0.0503	0.47	0.053
		24	1.0	0.2	0.0340	0.0462	0.23	0.041

4.2 Plate out in the 300 MW(t) plant

The mesh generation employed is shown in Fig. 16. In the turbine, the either intake scroll and the outlet diffuser was modeled into only one mesh. The blading section was divided into 11 meshes in consistency with the stage number. For the simplification, rotor blades section and nozzle blade section were not separated. As the values of gas velocity, the average velocity (the relative velocity for the rotor blade) was used.

The results are shown in Table 7.

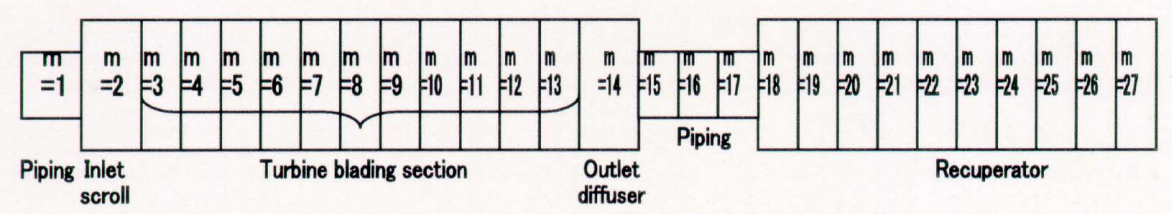

Fig. 16. Mesh generation for the cooling system of 300 MW(t) plant.

4.3 Dose rate

The dose rate is given by the following equations at the location at a distance of 1 m from the radioactive source:

^{137}Cs 3.6mSv/h × S(Ci) (11)

^{110m}Ag 16.5mSv/h × S(Ci) (12)

Then, the results of dose rates for the turbine rotor are given in Table 8. The value for the 600 MW(t) plant with block fuel elements is too large to allow the time for the maintenance work. Then, some countermeasure like ceramic coating of blades is needed. In case of 300 MW(t) plant with pebble bed core, 5.5 hours are available for the maintenance due to the lower fuel temperature. However, 960 days, that is, 2.6 years are very small compared with the expected plant life of 60 years. Then, some countermeasure like decontamination is also needed.

5. MAINTENANCE

In the above estimation, the dose rate at the surface of turbine is concluded to be too high in the 600 MW(t) plant to inspect and repair the turbine blades. In the case of 300 MW(t) plant, some maintenance work seems to be possible as the dose rate is not so high. However, there exist a lot of uncertainties in the above estimation analysis. Then, we had better to take account of the existence of the considerably high radioactivity.

In this case, an indirect cycle is a complete countermeasure for that, but this option seems to be unrealistic due to the introduction of much more difficult problems such as a very expensive intermediate heat exchanger, a higher reactor inlet gas temperature and a control of pressure difference between the 1 ry and 2 ry systems.

TABLE 7. RESULTS OF PLATE-OUT CALCULATION FOR THE 300 MW(t) PLANT

Component		Mesh no.	Temperature	Pressure	Gas velocity	Surface area
Piping from reactor		1	900.0	5.717	58.3	37.05
Turbine	Inlet	2	900.0	5.717	31.1	56.71
	1st stage	3	883.9	5.511	275.4	7.67
	2nd stage	4	849.9	5.114	265.8	8.07
	3rd stage	5	816.9	4.746	258.1	8.47
	4th stage	6	785.0	4.405	252.0	8.86
	5th stage	7	754.0	4.087	247.3	9.26
	6th stage	8	723.9	3.793	243.2	9.66
	7th stage	9	694.9	3.520	240.3	10.05
	8th stage	10	666.5	3.267	238.1	10.45
	9th stage	11	639.2	3.031	236.7	10.84
	10th stage	12	612.6	2.813	235.8	11.24
	11th stage	13	586.9	2.611	235.5	11.64
	Outlet	14	573.5	2.513	26.2	81.08
Piping from turbine to recuperator		15	573.5	2.513	67.2	21.39
		16	573.5	2.513	67.2	21.39
		17	573.5	2.513	67.2	21.39
Recuperator		18	551.8	2.511	15.7	2172.99
		19	508.5	2.507	14.9	2172.99
		20	465.2	2.504	14.1	2172.99
		21	421.8	2.500	13.3	2172.99
		22	378.5	2.496	12.5	2172.99
		23	335.1	2.492	11.7	2172.99
		24	291.8	2.488	10.9	2172.99
		25	248.5	2.485	10.0	2172.99
		26	205.1	2.481	9.2	2172.99
		27	161.8	2.477	8.4	2172.99

Component		Mesh No.	α		Mass transfer coefficient		Radioactivity	
			^{137}Cs	^{110m}Ag	^{137}Cs	^{110m}Ag	^{137}Cs	^{110m}Ag
Piping		1	0.1	0.2	0.0519	0.0666	0.041	0.005
Turbine	Inlet	2	0.1	0.2	0.0342	0.0439	0.041	0.005
	1st stage	3	0.1	0.2	0.3565	0.4571	0.057	0.007
	2nd stage	4	0.1	0.2	0.3464	0.4450	0.055	0.007
	3rd stage	5	0.1	0.2	0.3379	0.4343	0.054	0.007
	4th stag e	6	0.1	0.2	0.3314	0.4263	0.053	0.007
	5th stage	7	0.1	0.2	0.3267	0.4206	0.052	0.007
	6th stage	8	0.1	0.2	0.3227	0.4156	0.051	0.006
	7th stage	9	0.123	0.2	0.3201	0.4125	0.061	0.006
	8th stage	10	0.251	0.2	0.3181	0.4106	0.123	0.006
	9th stage	11	0.374	0.2	0.3171	0.4099	0.178	0.006
	10th stage	12	0.493	0.2	0.3166	0.4095	0.229	0.006
	11th stage	13	0.609	0.2	0.3166	0.4106	0.274	0.006
	Outlet	14	0.669	0.247	0.0289	0.0375	0.185	0.004
Piping		15	0.669	0.247	0.1921	0.2492	0.317	0.008
		16	0.669	0.247	0.1921	0.2492	0.310	0.008
		17	0.669	0.247	0.1921	0.2492	0.302	0.007
Recuperator		18	0.767	0.496	0.0570	0.0740	5.814	0.272
		19	0.962	0.960	0.0537	0.0699	3.532	0.222
		20	1.0	0.301	0.0504	0.0657	1.751	0.049
		21	1.0	0.2	0.0470	0.0616	0.837	0.025
		22	1.0	0.2	0.0436	0.0575	0.402	0.019
		23	1.0	0.2	0.0403	0.0532	0.194	0.015
		24	1.0	0.2	0.0369	0.0490	0.094	0.012
		25	1.0	0.2	0.0335	0.0448	0.046	0.009
		26	1.0	0.2	0.0301	0.0406	0.023	0.007
		27	1.0	0.2	0.0267	0.0364	0.011	0.005

TABLE 8. TOTAL FP PLATE OUT AMOUNT AND DOSE RATE

Plant	600 MW(t) plant		300 MW(t) plant	
Fission product	^{137}Cs	^{110m}Ag	^{137}Cs	^{110m}Ag
FP released into coolant He from the reactor	428 Ci	2.34 Ci	15.1 Ci	0.766 Ci
FP plate out on the turbine rotor	43.29 Ci	0.24 Ci	1.187 Ci	0.071 Ci
Dose rate	155.8mSv/h	3.96mSv/h	4.27mSv/h	1.17mSv/h
Sum of dose rate	159.76mSv/h		5.44mSv/h	
Allowable working time (Note)	11min		5.5h	

Note: Under the assumption of 30 MSv/y for a worker.

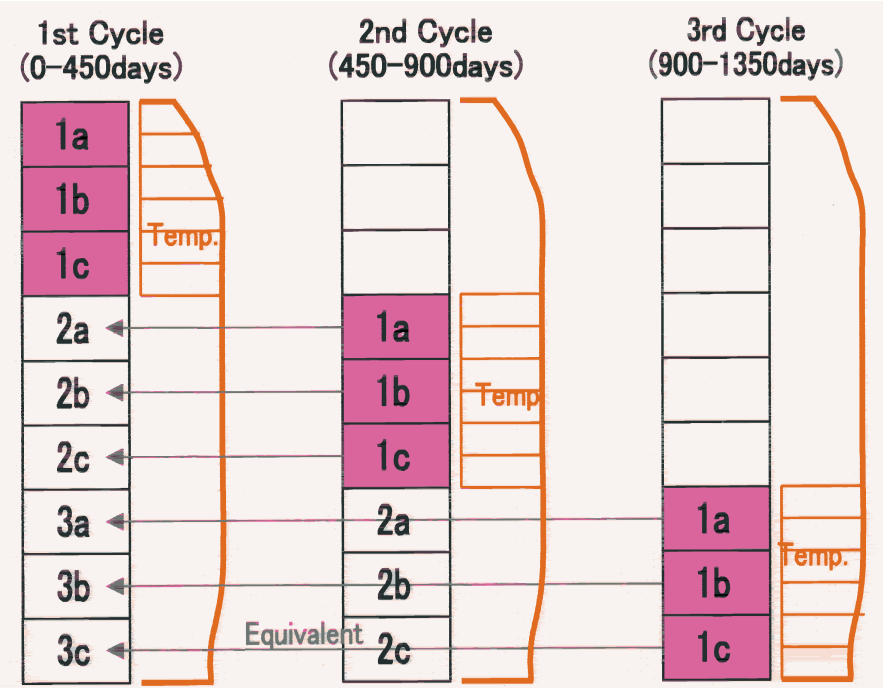

Fig. 17. Schematic view of the 400 MW(t) plant with FP filter apparatus.

The second method is the high temperature filter. This concept seems more realistic and this is employed in the design of 400 MW(t) plant as illustrated in Fig. 17. The filter is made of nickel base alloy called Hastelloy-X manufactured by sintering powder process. The pressure drop through the wall is very small due to its porous structure and thin wall thickness. Though the strength is significantly lower than the forged material, this yields no serious problem because of the small pressure difference load. The drawback is the necessity of additional pressure vessel of diameter of 5m, which requires the larger building space and higher cost.

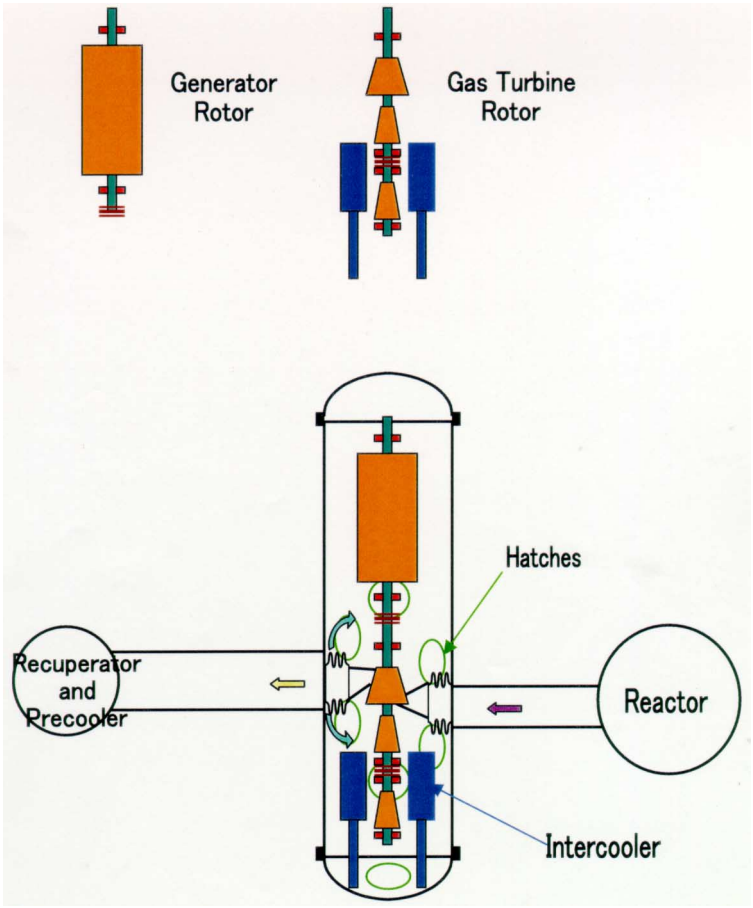

Fig. 18. Replacement method for the gas turbine and generator rotors.

The third method is a coating of turbine blades. As the connection between the metallic fission products and ceramics is considered to be weaker than that between the metallic FPs and alloy, the amount of plate-out will be reduced significantly and then decontamination will be easier. Regarding this, selection of a candidate ceramic material, confirmation of low plate-out of fission products on the ceramic surfaces, confirmation of integrity of the coating, an inspection method of structural integrity and the cost should be clarified.

In the latter two cases, irrespective of their reduced radioactivity, the turbine rotor should be pulled out by remote control from the power conversion vessel. In our design, this is possible by means of the procedure shown in Fig. 18 schematically. After the reactor shut down and sufficient cooling time until the gas temperature becomes nearly ambient temperature, 9 hatches on the turbine vessel are opened. Power manipulators are inserted and bolts of the flange connections between the turbomachinery and piping, the connections of the cooling water pipes for the intercooler and also the diaphragm coupling between the turbine and the generator are disconnected. The cover flange of the vessel at the generator side is opened and the generator is pulled out with its support table on the rail. Then, the generator is moved aside laterally on the cross rail. The support table with the turbomachinery and the intercooler are pulled out similar way. This structure is transported by crane to the neighboring maintenance area. The blades are examined by means of a liquid penetration method. After the inspection and repair if needed, the assembly is returned to the original position by means of the reverse procedure. Though the transmission of thermal expansion load from piping to the

turbomachinery is minimized in this component arrangement, some re-regulation of alignment is needed. For this purpose, man access is necessary at the time of re-assembling. Regarding the field balance, this can be conducted by remote control method.

6. SUMMARY

The fission-product-amounts generated, released, transported and plated out have been estimated for the 600 MW(t) and 300 MW(t) plants, the former is a block type fuel element and the latter is a pebble-bed core. The generation and release of ^{137}Cs and ^{110m}Ag has been calculated using a JAERI's in-house code "FORNAX". The amount of ^{137}Cs is much larger than that of ^{110m}Ag. In comparison between 600 MW(t) and 300 MW(t), the amount of the former is much larger than that of the latter, which reflects the fuel temperature difference between the block fuel elements and the pebble core. The transportation of these fission products from the reactor outlet helium gas to the components has been calculated under the assumption of a steady state phenomenon. The plate out amounts were estimated by introducing a factor α based on an engineering judgment. The values of radioactivity from the plated out fission products mean 11 min and 5.5 h of the allowable working time in the maintenance work for the turbine rotor in the 600 MW(t) and 300 MW(t) plants, respectively. The calculation has large uncertainties in the value of diffusion coefficient of ^{110m}Ag, the mass transfer phenomenon at the turbine blades and the plate out phenomenon. Therefore, more intensified future works are desired in this field. Irrespective of the estimated radiation level, a countermeasure is desired for the easy maintenance work. The leading candidate for this is considered a ceramic coating on the turbine blades. Even in this case, pulling out the turbine rotor by means of remote control is still needed and the replacement procedures of the rotors are shown.

REFERENCES

[1] Sawa, K. and et al., "An Investigation of Cesium Release from Coated Particle Fuel of the High-Temperature Gas-Cooled reactor," Nuclear technology, Vol.118, pp.123-131 (May 1997).

[2] Vanslager, F. E. and L. D. Mears, "PAD: A Computer Code for Calculating the Plateout Activity Distribution in a Reactor Circuit," GA-10460 (1971).

[3] Hanson, D. L., Baldwin, N. L. and Selph, W. E., "Gamma Scanning the Primary Circuit of the Peach Bottom HTGR", GA-A14161 (1976).

[4] Moormann, R., "Source Term Estimation for Small Sized HTGRs", Jul-2669 (1992).

[5] Bird, R.B., Stewart, W. E. and E. N. Lightfoot, "Transport Phenomena, "John Wiley & Sons, Inc. (1960).

[6] Bixler, N.E., "Victoria 2.0: A Mechanistic Model for Radionuclide Behavior in a Nuclear Reactor Coolant System Under Severe Accident Conditions," NUREG/CR-6131 (1998).

FISSION PRODUCT TRANSPORT IN THE PRIMARY SYSTEM OF A PEBBLE BED HIGH TEMPERATURE REACTOR WITH DIRECT CYCLE

A.I. VAN HEEK, N.B. SICCAMA. P.H. WAKKER
NRG, Petten, Netherlands

Abstract:

Transport and deposition of fission products in the primary system of a small pebble bed high temperature reactor with directly coupled gas turbine have been investigated. The reactor has a thermal power of 40 MW and is intended for heat and power cogeneration. Four radionuclides have been identified as most relevant because of volatility and radiotoxicity: ^{137}Cs, ^{90}Sr, ^{110m}Ag, ^{131}I. With the code PANAMA the fraction of failed coated fuel particles has been calculated. The diffusion of the fission products to the fuel element outer surface has been calculated with the FRESCO code. Transport and deposition of the fission products within the primary system has been analysed with the code MELCOR. Under normal operating conditions the release rate of the short-lived ^{131}I reaches a constant level rather quickly, contrary to the longer lived ^{137}Cs and ^{90}Sr which show a steady increase of the release rate during burn-up. Under incident conditions the retention capability of the fuel elements' graphite is strongly reduced. The release from the intact coated particles remains negligible compared to the release from the defect coated particles. After a ten year operation period, the total activity of the released nuclides in the primary system is about 58 GBq. The highest activity is found in the pre-cooler. Other components with high activities are the recuperator and the compressor. These components are contaminated mainly by ^{110m}Ag. The gas ducts in the energy conversion unit are contaminated by ^{110m}Ag and ^{131}I. Contamination as a consequence of incident conditions is difficult to estimate, because it depends on a number of phenomena. Under the assumption that 10 fuel elements are damaged, the activity is about 44 GBq.

1. INTRODUCTION

ACACIA (AdvanCed Atomic Cogenerator for Industrial Applications) is a heat and power cogeneration plant with a small pebble bed high temperature reactor with directly coupled gas turbine [1]. Release, transport and deposition of fission products in the primary system of ACACIA have been investigated. The reactor has a thermal power of 40 MW. The system cycle is depicted schematically in Fig. 1. Initially, the core is loaded with about 28.000 fuel elements with an enrichment of 10%, see Fig. 2. During burn-up, the loss of reactivity is compensated by adding 20% enriched fuel elements. After several years of operation, the core is unloaded and the cycle starts again. At that time the average burnup is 100 GWd/tU, and the core contains about 120.000 fuel elements Four radionuclides have been identified as most relevant because of volatility and radiotoxicity in literature: ^{137}Cs, ^{90}Sr, ^{110m}Ag, ^{131}I [2-5].

For normal operation, the coated particle failure fraction has been assumed to be 10^{-5} consistent with German experience. With the code PANAMA [6-8] the fraction of failed coated fuel particles under incident conditions has been calculated. PANAMA uses models based on measurements on TRISO coated particles. Two failure mechanisms have been taken into account. For temperatures up to 2000^{o}C the pressure vessel model is important: a coated particle fails if the internal gas pressure rises and the tension within the SiC layer exceeds the tensile strength of that layer. At higher temperatures the particles will fail predominantly by dissociation of the SiC layer.

The diffusion of the fission products to the fuel element outer surface has been calculated with the FRESCO code [8, 9]. With FRESCO the diffusion of fission products in the coated

particles during normal operation and under incident conditions is calculated under the assumption that the fission product transport through solid matter can be described by Fick's law.

Transport and deposition of the fission products within the primary system has been analysed with the code MELCOR [10-12]. Within MELCOR, all hydrodynamic material (and its energy) resides in control volumes. Each control volume is characterised by a pressure and a temperature. The control volumes are connected by flow paths through which the hydrodynamic materials may move without residence time, driven by a momentum equation.

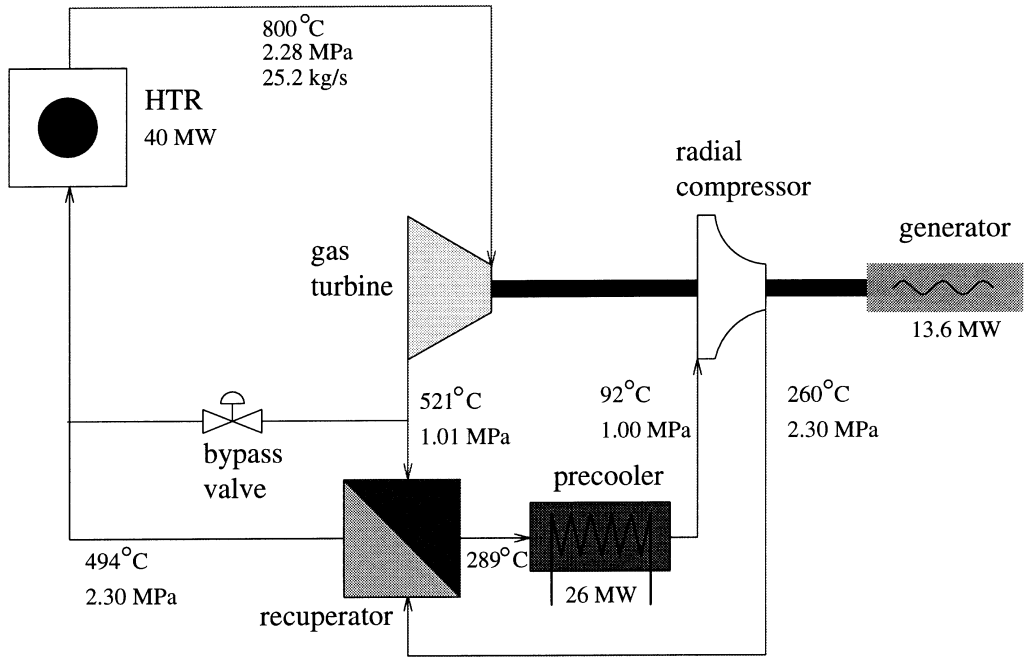

Fig.1. ACACIA cycle scheme.

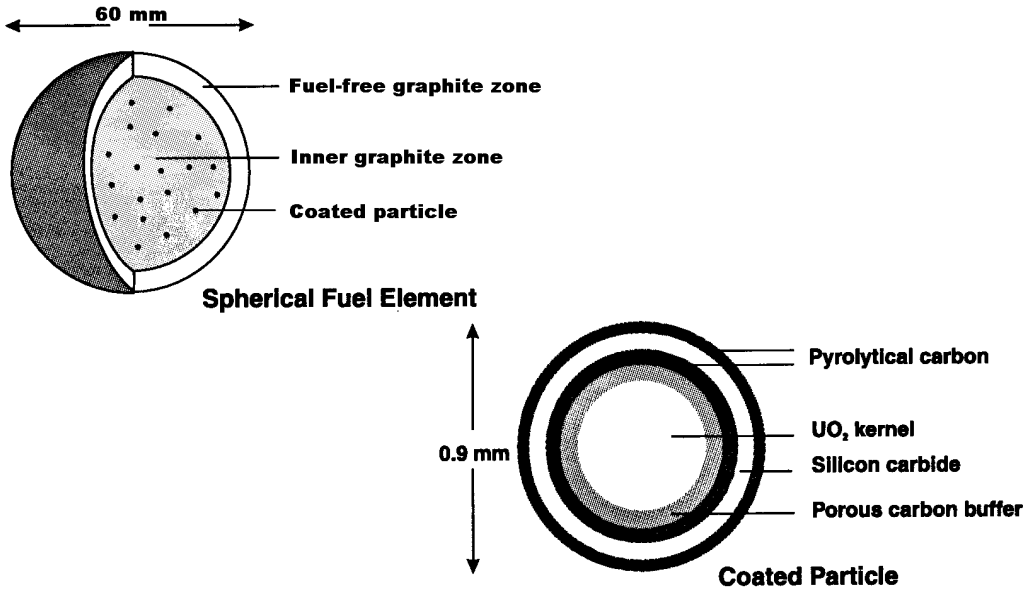

Fig.2. ACACIA fuel element.

2. FISSION PRODUCT RELEASE IN THE ACACIA REACTOR

2.1 Fission product inventory

The ACACIA fuel elements are reaching an average burnup of 100 GWd/tHM. The inventory of the most relevant nuclides used for this study has been estimated with the help of burnup calculations on ACACIA and inventory data on the HTR-Module [2], and is given in Table I.

TABLE I. THE INVENTORY OF THE MOST RELEVANT NUCLIDES USED FOR THIS STUDY, IN AVERAGE NUMBER OF ATOMS PER FUEL ELEMENT [13]

Nuclide	Half life	Average number of atoms per fuel element
^{135}Xe	9.2 h	$7.5 \cdot 10^{16}$
^{131}I	8.1 d	$5 \cdot 10^{18}$
^{134}Cs	2.1 a	$1.1 \cdot 10^{20}$
^{137}Cs	30.2 a	$2 \cdot 10^{21}$
^{90}Sr	28.9 a	$1 \cdot 10^{21}$
^{110m}Ag	249.9 d	$5 \cdot 10^{17}$

2.2 Normal Operating Conditions

In figure 3 the fractional fission product release from all coated particles is plotted. In figure 4 the fractional release from a fuel element under normal operating conditions is shown. This has been done with fractional release figures that are obtained with estimated fast neutron fluence and fission product inventory, so the exact values of the figures have to be treated with caution. The iodine curves are different from those of the other nuclides. This is caused by the relative short half-life of ^{131}I, therefore equilibrium between decay and fission build-up is established rather quickly. Therefore, also the release relative to the inventory at the end of the burn up cycle reaches a constant level rather quickly. Another striking point from figures 3 and 4 is that although the release of cesium and strontium from the coated particies is similar to that of iodine, the release from the fuel element is much less. Especially strontium is almost totally retained in the fuel element's graphite.

For cesium the release from the particles is primarily due to the release from the defect particles. The release from the graphite grains is of the same order of magnitude as the release of the particles.

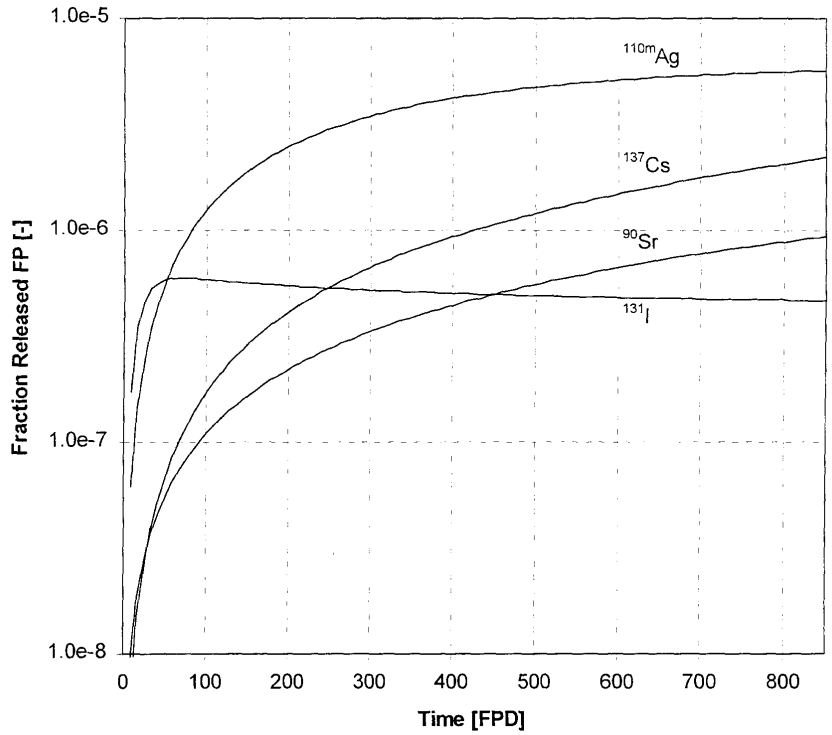

Fig.3. Fractional fission product release from all coated particles under normal operating conditions [13].

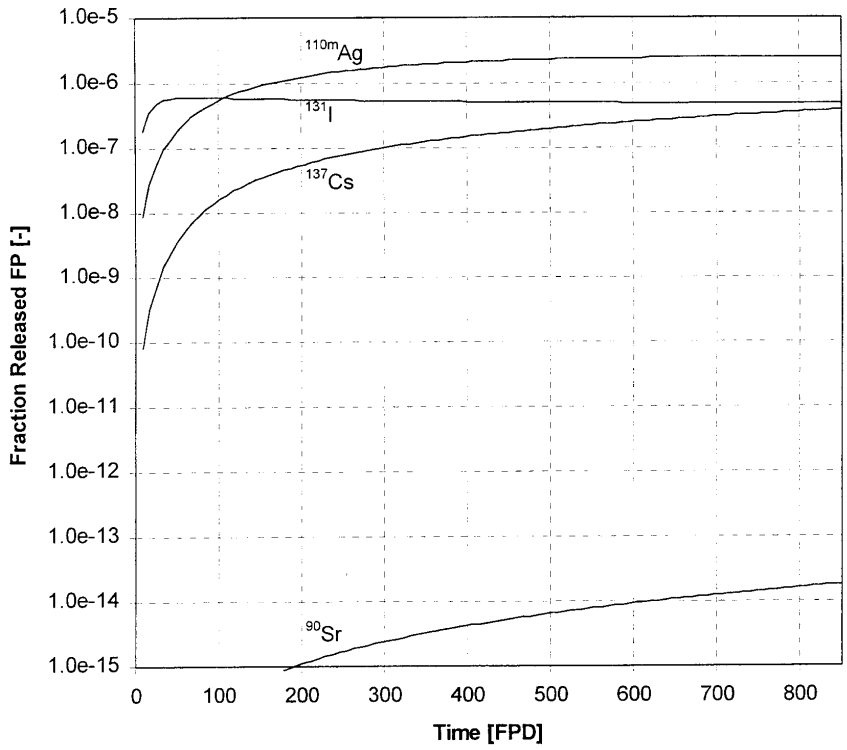

Fig. 4. Fractional fission product release from a fuel element under normal operating conditions [13].

2.3 Incident Conditions

The incident has been assumed to start at the end of the burn up cycle, which is in this case at 848 full power days. In figure 5 the fractional fission product release from a fuel element is given as a function of the time after the start of the incident. In the first thirty to forty hours the release remains about constant, but after that time it increases rapidly because of the increased temperatures and an increasing fraction of failed coated particles.

Comparing figure 5 with figure 4, it can be seen that the retention capability of the graphite matrix is strongly reduced under incident conditions. The release from the fuel element now closely follows the release from the defect coated particles. The release from the intact coated particles is still negligible compared to the release from the defect coated particles. During the incident phase the release from the graphite grains is constant at its maximum of $5 \cdot 10^{-6}$ which is equal to the uranium contamination in the graphite grains.

Figure 6 shows the concentration profile of ^{137}Cs in an intact coated particle. Because of the increased temperatures, the cesium diffuses more easily and the profile flattens out. However, the impenetrability of the SiC layer is still intact and the concentration on the coated particle outer surface is still negligibly small.

From figure 7, which shows the concentration profile of ^{137}Cs in a fuel element, it can be seen that in the first phase of the incident the concentration increases strongly. Later on the concentration profile starts to flatten out in the middle, and to move towards a more static profile.

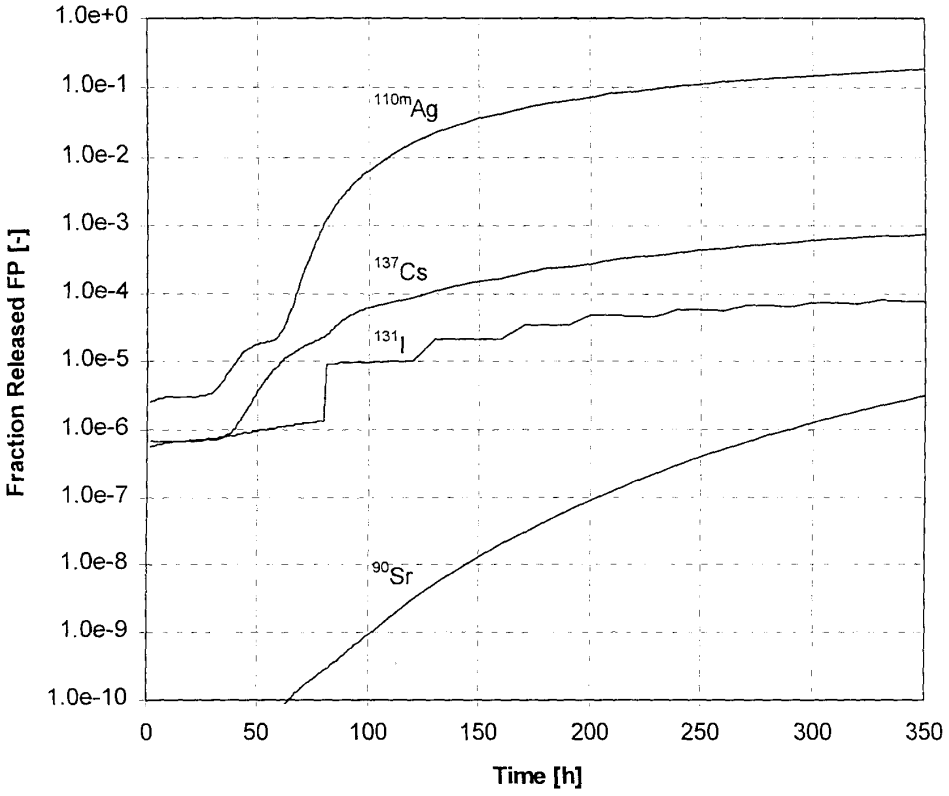

Fig. 5. Fractional fission product release from a fuel element under accident conditions [13].

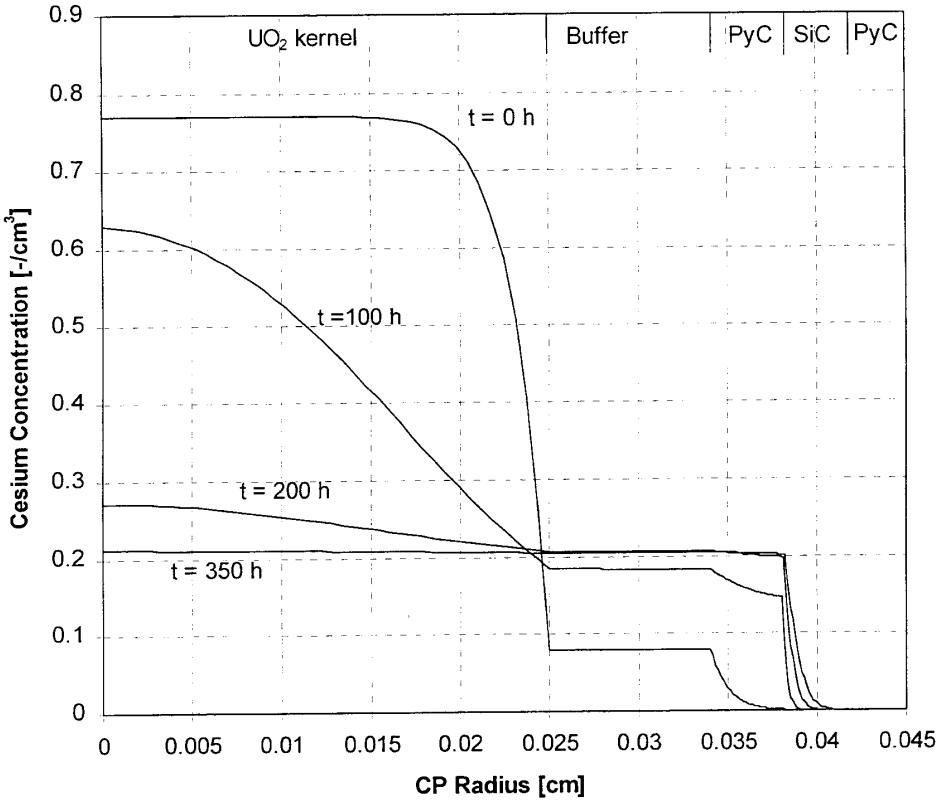

Fig.6. The ^{137}Cs concentration profile in a coated particle at four different points in time after initiation of a core heatup incident [13].

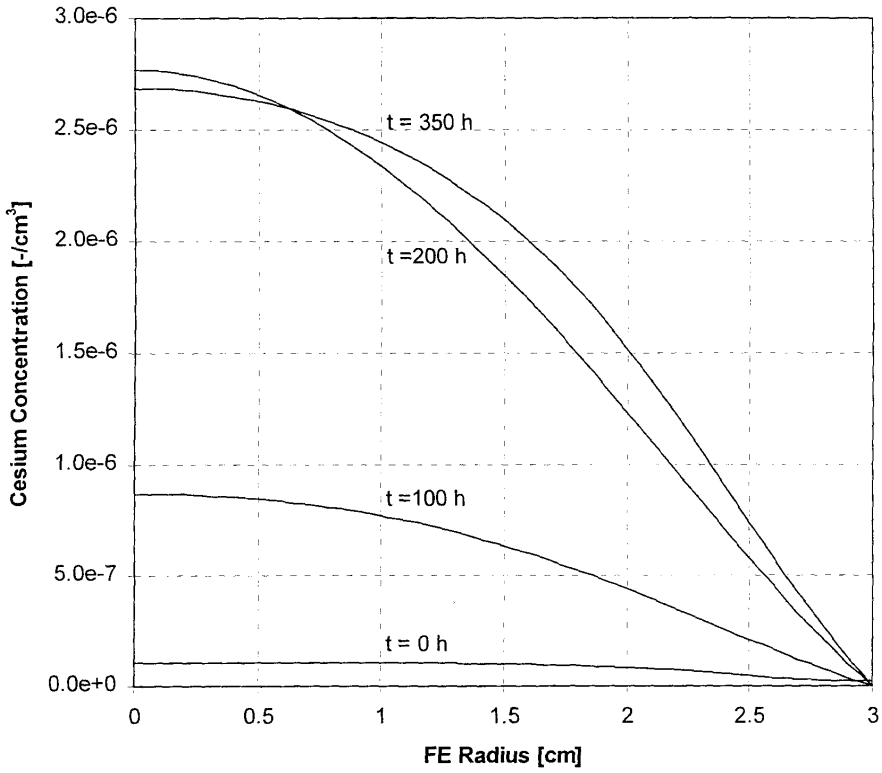

Fig.7. ^{137}Cs. concentration profile in a fuel element at four different points in time after initiation of a core heatup incident [13].

3. FISSION PRODUCT TRANSPORT THROUGH THE ACACIA PRIMARY SYSTEM

3.1. Life cycle of the nuclides

The life of the nuclides in the MELCOR calculation starts at the moment of release from the reactor core in the hot gas plenum in the reactor vessel. In this volume, the released vapour joins with vapours and aerosols that have not yet deposited in the circuit. During the transport in the circuit, the temperature decreases and the vapour pressures of the nuclides decrease. If the partial pressure of a nuclide becomes higher than the vapour pressure, condensation of the nuclide on walls and aerosols starts.

In general, condensation on walls starts first, because the walls are colder than the bulk gas. Further on, the bulk gas is cooled sufficiently, and aerosol formation occurs simultaneously with condensation on walls. This process continues, until the nuclide vapour concentration becomes too low. From this point, only aerosol deposition occurs.

After the precooler, the temperature increases and vapour condensation stops and aerosols start to evaporate. Aerosol deposition continues until all aerosols are evaporated due to the high temperatures. The remaining vapours and aerosols that did not evaporate return and join the freshly released nuclides, and the cycle is repeated.

3.2. Nuclide deposition rates

The behaviour of the nuclides does not influence each other, because the concentration of nuclides is very low. Aerosol growth by agglomeration or condensation hardly occurs: the aerosol size remains at the minimal value of 2 nm. In general, the behaviour of the nuclides can be considered independently.

The transport and deposition of ^{137}Cs occurs by both CsOH and Csl. Since the mass of CsI is much smaller than the mass of CsOH, only the transport of Cs by CsOH is taken into account and the transport of Cs by CsI is neglected.

The deposition of CsOH is driven by condensation. At high temperatures CsOH is a vapour, which condenses on the cold wall in the third part of the precooler. The wall temperature in this part is 312 K. The gas bulk temperature of 368 K is too high for condensation of CsOH into aerosols. Therefore, no CsOH aerosols are present in the ACACIA system.

Deposition of ^{90}Sr occurs by aerosol deposition, because the vapour pressure of SrO is very low. The deposition mechanism is Brownian diffusion. Deposition by gravity and thermophoresis are negligible for small particles.

Deposition of ^{110m}Ag occurs both by condensation and deposition of aerosols. In the middle third of the hot side of the recuperator, silver vapour condenses on the wall. In the next third of the recuperator, the condensation on walls continues, but at the same place, silver vapour condenses as aerosols. These aerosols deposit in subsequent volumes. In the cold side of the recuperator, the silver aerosols evaporate due to the high temperatures, and silver vapour is recirculated to the inlet of the reactor vessel.

Deposition of ^{131}I occurs both by condensation and deposition of aerosols. In the first third of the precooler, CsI vapour condenses on the wall. In the next third, the condensation on walls

continues, but at the same place, CsI vapour condenses as aerosols. These aerosols deposit in the subsequent volume between precooler and compressor. In the turbine, the CsI evaporates due to the high temperature.

3.3. Activity plate-out in components

The total activity caused by the nuclides depend on the average burn-up time. A ten-year operation period corresponds to an average burn-up of 848 full power days. The activity in each component at the end of the ten-year operation period (average burnup of 848 full power days) is given in tabular form in Table II and in a graph in figure 8. This table shows that the total activity is about 59 GBq. The highest activity is produced by ^{137}Cs, followed by ^{131}I and ^{110m}Ag. The contribution of ^{90}Sr is very low.

TABLE II. ACTIVITY OF THE ACACIA COMPONENTS AFTER 10 YEARS OF OPERATION [12]

Description	Activity (Bq) after 10 years of operation				
	^{137}Cs	^{90}Sr	^{110m}Ag	^{131}I	Total
Reactor vessel	-	28	-	-	28
Turbine	-	49	-	-	49
Recuperator	-	1280	$1400 \cdot 10^6$	-	$1400 \cdot 10^6$
Precooler	$52000 \cdot 10^6$	230	$390 \cdot 10^6$	$4000 \cdot 10^6$	$56000 \cdot 10^6$
Compressor	-	4	$7 \cdot 10^6$	-	$7 \cdot 10^6$
Hot pipe from reactor	-	-	-	-	-
Pipe turbine-recuperator	-	6	-	-	6
Pipe recuperator-precooler	-	9	$16 \cdot 10^6$	-	$16 \cdot 10^6$
Pipe precooler-compressor	-	6	$10 \cdot 10^6$	$11 \cdot 10^6$	$21 \cdot 10^6$
Pipe compressor-recuperator	-	6	$10 \cdot 10^6$	-	$10 \cdot 10^6$
Cold pipe to reactor	-	9	-	-	9
Total	$52000 \cdot 10^6$	1600	$1800 \cdot 10^6$	$4000 \cdot 10^6$	$58000 \cdot 10^6$

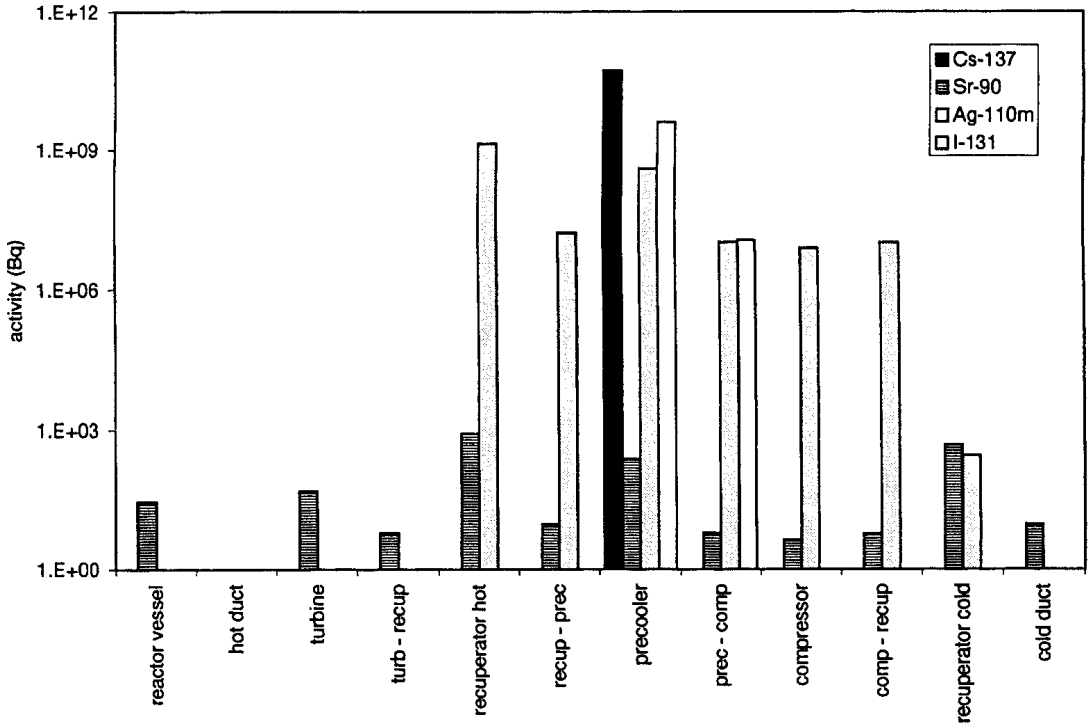

Fig.8. Activity plated out in the components of the ACACIA primary system, in the order of the coolant path from leaving the reactor on the hot side to entering the reactor again on the cold side [12]. (caution: the activity axis has a logarithmic scale).

The highest activity is found in the precooler: 56 GBq. The main reason is the condensation of the volatile species CsOH and CsI in this component. Other components with high activities are the recuperator (1400 MBq) and the compressor (7 MBq). These components are mainly contaminated by ^{110m}Ag. The gas ducts in the energy conversion unit are also mainly contaminated by ^{110m}Ag (43MBq) and by ^{131}I (11 MBq).

3.4. Incident conditions

Contamination as a consequence of a core heatup incident is difficult to estimate. The release of nuclides depend on (among others) the number of damaged fuel elements and the temperature history of the fuel elements. The distribution of the nuclides over the components in the ACACIA system depends on (among others) the helium mass flow rate through the ACACIA plant and the cooling rate of the components in the ACACIA facility.

In [2], an estimation of the fractional fission product release from a damaged fuel element is given. Table III gives the total activity as a function of the number of damaged fuel elements. The following assumptions are used:

- the fractional release given in [2] is used; the incident time is 350 hr, identical to the value used in [2];
- the release rate from the damaged fuel elements is constant during this time.

Table III shows that the activity under incident conditions is equal or higher than under normal conditions. In this incident, ^{110m}Ag produces most of the activity, followed by ^{137}Cs and ^{131}I. Although the activity of ^{90}Sr is high, it is negligible cornpared to the activity of the

other nuclides. The distribution of the nuclides over the components is not considered in view of the large number of uncertainties.

TABLE III. TOTAL ACTIVITY UNDER INCIDENT CONDITIONS [12]

Number of damaged fuel elements	Activity (Bq)				
	^{137}Cs	^{90}Sr	^{110m}Ag	^{131}I	Total
10	$1.2 \cdot 10^{10}$	$2.3 \cdot 10^{7}$	$3.1 \cdot 10^{10}$	$1.4 \cdot 10^{9}$	$4.4 \cdot 10^{10}$
1000	$1.2 \cdot 10^{12}$	$2.3 \cdot 10^{9}$	$3.1 \cdot 10^{12}$	$1.4 \cdot 10^{11}$	$4.4 \cdot 10^{12}$
All elements	$1.4 \cdot 10^{14}$	$2.7 \cdot 10^{11}$	$3.7 \cdot 10^{14}$	$1.7 \cdot 10^{13}$	$5.2 \cdot 10^{14}$

4. DISCUSSION

Transport and deposition of fission products in the primary system of a small pebble bed high temperature reactor with directly coupled gas turbine have been investigated. Although some important input data is not yet available, a rough indication of the release behaviour has been obtained.

Under normal operating conditions the release rate of the short-lived ^{131}I reaches a constant level rather quickly, contrary to the longer-lived ^{137}Cs and ^{90}Sr which show a steady increase of the release rate during burn-up. The retention capability of the fuel elements' graphite with respect to ^{137}Cs and ^{90}Sr is remarkable. Release of ^{137}Cs is primarily due to the release from the defect particles.

Under incident conditions the retention capability of the fuel elements' graphite is strongly reduced. The release from the intact coated particles is still negligible compared to the release from the defect coated particles.

After a ten year operation period, the total activity of the released nuclides in the primary system is about 58 GBq. The highest activity is produced by ^{137}Cs (52 GBq), followed by ^{131}I (4 GBq) and ^{110m}Ag (1.8 GBq). The contribution of ^{90}Sr is very low (1600 Bq).

The highest activity is found in the pre-cooler (56 GBq). The main reason is the condensation of the volatile compounds CsOH and CsI in this component. Other components with high activities are the recuperator (1.4 GBq) and the compressor (0.007 GBq). These components are contaminated mainly by ^{110m}Ag. The gas ducts in the energy conversion unit are contaminated by ^{110m}Ag (0.043 GBq) and ^{131}I (0.011 GBq).

Contamination as a consequence of incident conditions is difficult to estimate, because it depends on a number of phenomena. Under the assumption that 10 fuel elements are damaged, the activity is about 44 GBq. ^{110m}Ag produces most of the activity (31 GBq), followed by ^{137}Cs (12 GBq) and ^{131}I (1.4 GBq). Although the activity of ^{90}Sr is high (0.023 GBq) it is negligible compared to the activity of other nuclides.

REFERENCES

[1] A.I. VAN HEEK, B.R.W. HAVERKATE, "Nuclear Cogeneration based on HTR Technology", ENC'98, Nice, France (1998).

[2] G. BREITBACH et al., "Sicherheitstechnische Untersuchungen zum Störfallverhalten des HTR-Modul" (Safety related research on accident behaviour of the HTR-Module, in German), Jül-Spez-335, Jülich Research Centre, Jülich, Germany (1985).

[3] W. KRÖGER et al., "Festlegung prioritärer Arbeiten zum Spaltproduktverhalten im HTR mit Hilfe von Risiko-Trendanalysen" (Determination of high priority activities on fission product transport in HTR with the help of risk trend analyses, in German), Annual Meeting on Nuclear Technology, Munich, Germany (1985).

[4] R. MOORMANN, K. VERFONDERN, "Methodik umfassender probabilistischer Sicherheitsanalysen für Zukünftige HTR-Anlagenkonzepte; Ein Statusbericht (Stand 1986)" (Method of general probabilistic safety analyses for future HTR plant concepts, a status report (status 1986), in German); Volume 3: "Spaltproduktfreisetzung" (fission product release), Jül-Spez-388/Bd.3, Jülich Research Center, Germany (1987).

[5] INTERNATIONAL ATOMIC ENERGY AGENCY, "Fuel Performance and Fission Product Behaviour in Gas-Cooled Reactors", IAEA-TECDOC-978, Vienna, Austria.

[6] K. VERFONDERN and H. NABIELEK, "PANAMA, ein Rechenprogramm zur Vorhersage des Partikelbruchanteils von TRISO-Partikeln unter Störfallbedingungen" (PANAMA, a calculational code for predicting the failure percentage of TRISO particles under accident conditions, in German), Jül-Spez-298, Jülich Research Center, Germany (1985).

[7] K. VERFONDERN and H. NABIELEK, "The Mathematical Basis of PANAMA-1 Code for Modelling Pressure Vessel Failure of TRISO Coated Particles under Accident Conditions", HTA-IB-03/90, Jülich Research Center, Germany (1990).

[8] P.H. WAKKER, "Beschrijving van de PANAMA en FRESCO codes" (Description of the PANAMA and FRESCO codes, in Dutch), 22884-NUC 98-2101, NRG, Arnhem, The Netherlands (1998).

[9] H. KROHN and R. FINKEN, "FRESCO-II: Ein Rechenprogramm zur Berechnung der Spaltproduktfreisetzung aus kugelförmigen HTR-Brennelementen in Bestrahlungs- und Ausheizexperimenten" (A code to calculate the fission product release from spherical HTR fuel elements in irradiation and heating experiments, in German), Jül-Spez-212, Jülich Research Center, Germany (1983).

[10] R.M. SUMMERS et al., MELCOR Computer Code Manuals. Primer and User's Guides. Version 1.8.3. September 1994, Albuquerque, Sandia National Laboratories, NUREG/CR-6119, SAND93-2185, Vol.1 (1994).

[11] R.M. SUMMERS et al., MELCOR Computer Code Manuals. Reference Manuals. Version 1.8.3. September 1994, Albuquerque, Sandia National Laboratories, NUREG/CR-6119, SAND93-2185, Vol.2 (1994).

[12] N.B. SICCAMA, "Fission product retention in the ACACIA reactor primary system", ECN-R—98-019, NRG, Petten, The Netherlands (1998).

[13] P.H. WAKKER, "Fission Product Release in the ACACIA Reactor", 22951-NUC 98-2644, NRG, Arnhem, The Netherlands (1998).

COMPACT HEAT EXCHANGER TECHNOLOGIES FOR THE HTRs RECUPERATOR APPLICATION

B. THONON
GREThi, CEA-Grenoble, Grenoble

E. BREUIL
FRAMATOME, Lyon

France

Abstract:

Modern HTR nuclear power plants which are now under development (projects GT-MHR, PBMR) are based on the direct cycle concept. This concept leads to a more important efficiency compared to the steam cycle but requires the use of high performance components such as an helium/helium heat exchanger called recuperator to guarantee the cycle efficiency. Using this concept, a net plant efficiency of around 50% can be achieved in the case of an electricity generating plant. As geometric constraints are particularly important for such a gas reactor to limit the size of the primary vessels, compact heat exchangers operating at high pressure and high temperature are attractive potential solutions for the recuperator application. In this frame, Framatome and CEA have reviewed the various technologies of compact heat exchangers used in industry. The first part of the paper will give a short description of the heat exchangers technologies and their ranges of application. In a second part, a selection of potential compact heat exchangers technologies are proposed for the recuperator application. This selection will be based upon their capabilities to cope with the operating conditions parameters (pressure, temperature, flow rate) and with other parameters such as fouling, corrosion, compactness, weight, maintenance and reliability.

1 INTRODUCTION

1.1 Modern HTRs features

The modern HTRs which are now under development (projects GT-MHR, PB-MR) are based on the direct cycle concept. In this case the primary coolant circuit of the nuclear core and the driver circuit of the electric generator is the same circuit. The simple cycle of the helium is called Brayton cycle (figure 1). The hot helium from the core outlet flows directly through the turbine where it is expanded. Then it is cooled before to be compressed and goes back to the core. The turbine drives the electric generator. The high efficiency of the cycle can be still further improved (up to 50%) using a helium/helium heat exchanger called recuperator between the low and high pressures sides. In this case, the remaining gas energy at the turbine outlet is recuperated by this exchanger and is used to preheat the helium at the core inlet. It must be noted that the recuperator can be located inside the pressure vessel and, therefore, is not a containment barrier of the primary coolant.

The recuperator needs to have a high efficiency (95%), but also requires high mechanical characteristics as it operates at high pressure and high temperature. Furthermore, it should be as small as possible to limit the size of the vessel. These constraints lead to evaluate compact heat exchanger technology for modern HTRs recuperator application.

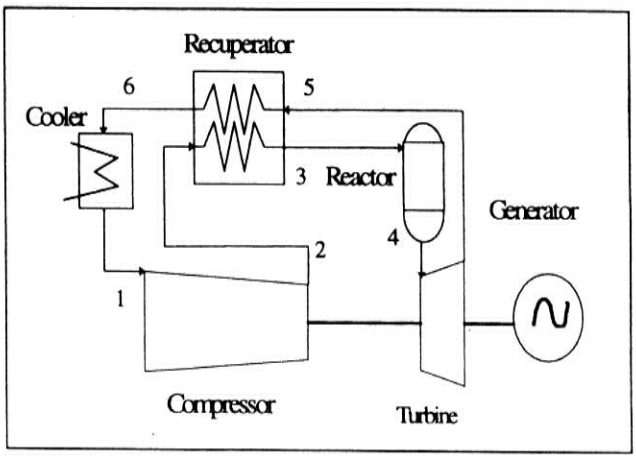

Figure 1. Brayton cycle with recuperator.

1.2 Recuperator operating conditions

For a large power reactor (GT-MHR type) the steady state operating conditions are summarised in the table 1.

TABLE 1. RECUPERATOR TECHNICAL CHARACTERISTICS

Parameter	Unit	Hot side (LP side)	Cold side (HP side)
Thermal capacity	MW	630	630
Inlet temperature	°C	507	107
Outlet temperature	°C	127	487
Inlet pressure	MPa	2.6	7.2
Flow rate	kg/s	320	320

The pressure losses along the HP and LP sides should be as low as possible (<1% of the nominal pressure).

During abnormal events, the recuperator inlet temperature can rise up to 650 °C.

The life time is expected to be the same as the nuclear plant (e.g. 60 years).

The helium contents (H_2O, CO, CO_2, H_2,…) and also solid graphite particles can induce respectively a risk of corrosion and a risk of fouling of the recuperator elementary channels.

1.3 Geometric constraints

The recuperator is located inside the pressure vessel at the turbine outlet. A modular concept is generally proposed to facilitate the maintenance operations (dismantled modules) or repair operations (plugging of leaky modules). These modules can be arranged in an annular space around the turbo-machine rotor.

To limit the size of the primary vessels, compact heat exchangers operating at high pressure and high temperature are attractive potential solutions for the recuperator application.

2 COMPACT HEAT EXCHANGER TECHNOLOGY

2.1 Classification of compact heat exchangers

Heat exchangers could be classified in many different ways such as according to transfer processes, number of fluids, surface compactness, flow arrangements, heat transfer mechanisms, type of fluids (gas–gas, gas–liquid, liquid–liquid, gas–two-phase, liquid–two-phase, etc.) and industry. Heat exchangers can also be classified according to the construction type and process function. Refer to Shah and Mueller [1988] for further details. In the following chapters only non-tubular heat exchangers will be described.

2.2 Plate Heat Exchangers

Plate heat exchangers (PHE's) were formerly used for milk pasteurisation and gradually became the standard choice for heat treatments in the liquid food industry. The facility of dismantling plate heat exchangers is one of the main reasons for their large use in the food industry. Furthermore, as the heat transfer coefficients are high, the fluid path length will be shorter and relatively well defined. Due to the lack of large dead areas in the channels, the corresponding residence time distribution is short and very homogeneous.

Afterwards, with the developments of larger plates, their use began to grow quickly in the chemical, petrochemical, districts heating and power industries, but essentially for single phase duties. The concept of phase change in PHE's started up in the 70's for OTEC applications (Ocean Thermal Energy Conversion) and the working fluids were Freon R22 or ammonia (Panchal and Rabas [1993]). These first studies on evaporation and condensation have been used for the development of PHE's in the refrigeration industry (Kumar [1992], Syed [1992], Navaro and Bailly [1992], Sterner and Sunden [1997], Pelletier and Palm [1997] and Palm and Thonon [1999]). Now PHE's become more often used in the process industry (Patel and Thomson [1992] and Brotherton [1994]), but their use is still not widespread.

In terms of technology, PHE's are made of pack of corrugated plates which are pressed together. The plate size ranges from 0.02 m^2 to over 3 m^2 with conventional pressing technology (figure 2), but can reach up to 15 m^2 for explosion formed plates (figure 3). The hydraulic diameter lies between 2 and 10 mm for most common plates, but free passages and wide gap plates exist for viscous fluid applications. Typically, the number of plates is between 10 and 100, which gives 5 to 50 channels per fluid. Furthermore, the use of high quality metal and the manufacturing techniques lead plate heat exchangers to be less prone to corrosion failure than shell and tube units (Turisini et al [1997]).

To insure the tightness three technologies are available: gaskets, welding and brazing. Gasketed PHE is the most common type, and the gasket material is selected in function of the application (temperature, fluid nature ...). Temperature up to 200°C and pressure up to 25 bars can be achieved by such heat exchangers. For applications where gaskets are undesirable (high pressure and temperature or very corrosive fluids), semi-welded or totally welded heat exchangers are available (figure 4). The last variant is the brazed plate heat exchanger. The plate pattern is similar to conventional gasketed units, but tightness is obtained by brazing the pack of plates. For common applications copper brazing is used, but for ammonia units nickel brazing is possible. This technology leads to inexpensive units, but the plate size is generally limited to less than 0.1 m^2. The counterpart is that the heat exchanger cannot be opened, and fouling will limit the range of application.

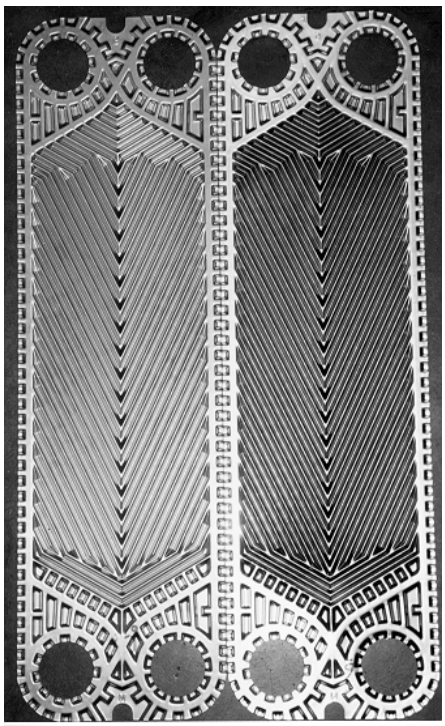

Figure 2. View of corrugated plates(courtesy of Alfa-Laval Vicarb).

Figure 3. Explosion formed plate(courtesy of Packinox).

(courtesy of Ziepack)

(courtesy of Alfa-Laval Vicarb)

Figure 4. View of welded plate heat exchangers

2.3 Spiral Heat Exchanger

The spiral heat exchanger (SHE) consists of two metal sheets that are welded together then rolled to obtain spiral passages. The passages can be either smooth or corrugated, in some cases studs or spacers are introduced between the metal sheets. These devices have two functions, first to adjust the spacing and secondly to induce turbulence that increases heat transfer. The general flow configuration can be crossflow (single or multipass) or counterflow depending on the configuration of the inlet and outlet distribution boxes. The heat transfer surface ranges from 0.05 m² for refrigeration applications up to 500 m² for industrial processes. Spiral heat exchangers are often used for phase change application as the geometry of the hot and cold stream channels can be adapted to the process specifications.

Recent developments in manufacturing technologies (laser welding) allowed to manufacture cost effective recuperators based on a spiral concept (figures 5 and 6) or folded plate recuperator (Oswald et al [1990], Mc Donald [1990] and [2000]).

2.4 Plate and shell heat exchangers

The basic principle of these heat exchangers is to insert a bundle of plate in a shell. On the plate side, the fluids flow inside corrugated or embossed channels (more often in two passes). On the shell side, the flow is similar to shell and tube heat exchangers, and baffles can be inserted. This technology can be used for revamping application as the shell can be kept identical to that of the replaced bundle of tubes.

These heat exchangers are often used in the process industry as boilers (boiling on the shell side) as high pressures can be reached very easily on the shell-side. Furthermore, adopting large gap on the shell side allows using dirty services, as cleaning is possible by removing the bundle of plates.

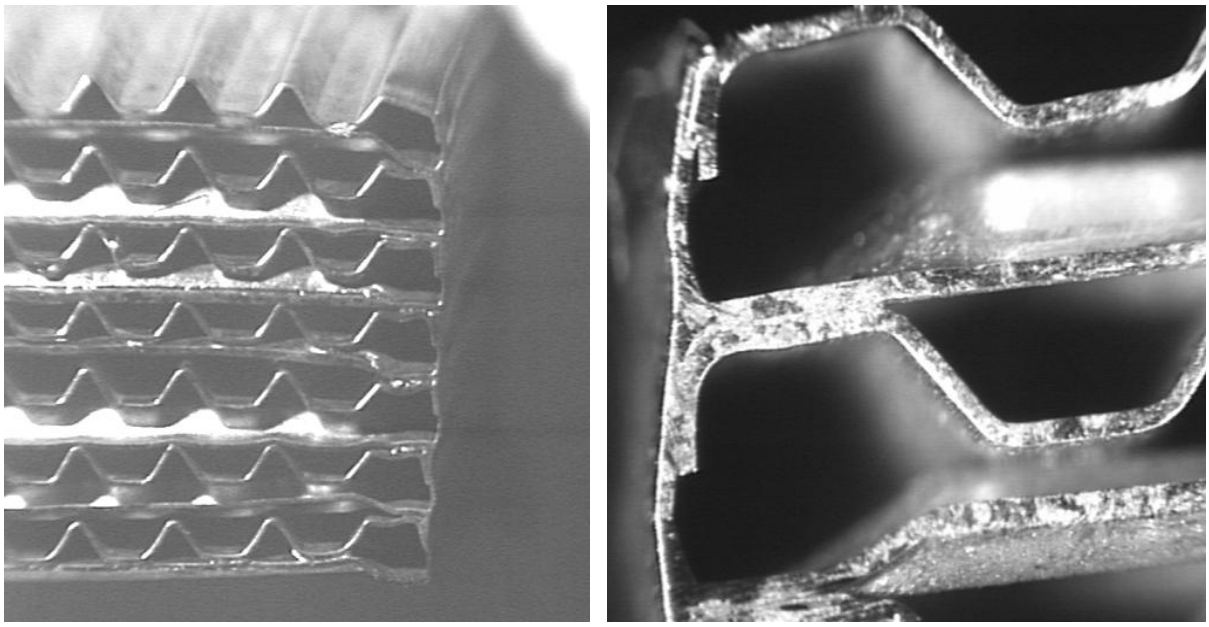

Figure 5. Laser welding of a spiral recuperator (courtesy of ACTE).

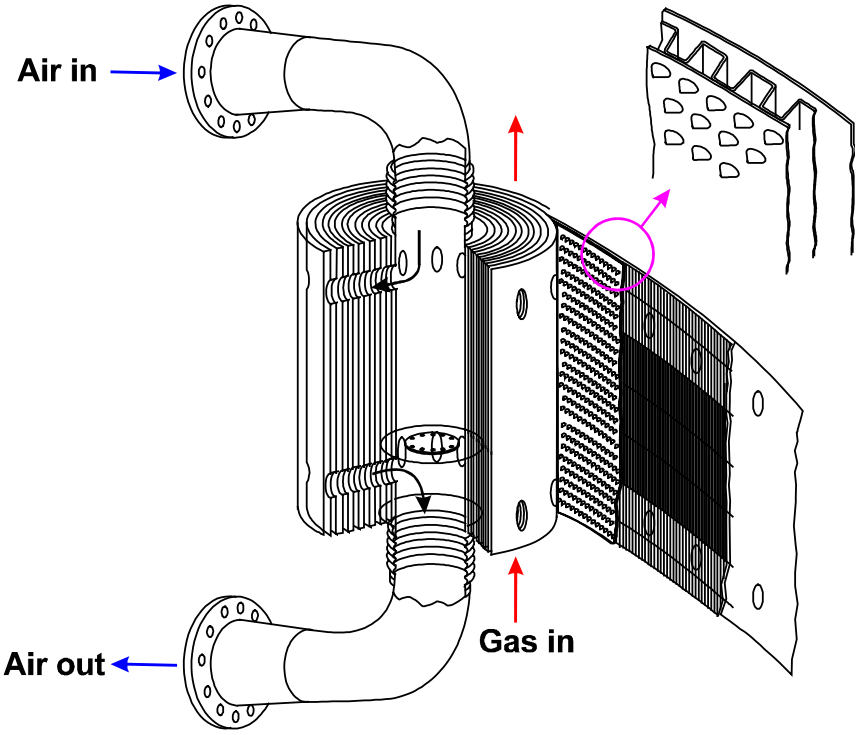

Figure 6. Spiral heat exchanger for gas turbine systems (courtesy of Rolls-Royce).

2.5 Plate-Fin Heat Exchangers

Aluminium plate-fin heat exchangers (PFHE) were initially developed in the 40's to provide compact, light and high efficient heat exchangers for gas/gas applications in the aerospace industry. As the mechanical characteristics of aluminium are increased at low temperatures, this technology has been used since 1950 for liquefaction of natural gases. Nowadays, aluminium plate-fin heat exchangers are extensively used in applications such as air separation, hydrocarbon separation, industrial and natural gas liquefaction (ALPEMA [1994] and Lundsford [1996]). Plate fin heat exchangers offer process integration possibilities (12 simultaneous different streams and more in one single heat exchanger) and high efficiency under close temperature difference (1 to 2 °C) in large variety of geometric configurations.
The brazed plate-fin exchanger consists of stacked corrugated sheets (fins) separated by flat plates, forming passages which are closed by bars, with openings for the inlet and outlet of fluids.

In its simplest form, a heat exchanger may consist of two passages, with the cooling fluid in one passage and the warming fluid in the other. The flow direction of each of the fluids relative to one another may be counter-current, co-current or cross-flow.

The fins and the parting sheets are assembled by fusion of a brazing alloy cladded to the surface of the parting sheets. The brazing operation is made in a vacuum furnace in which the brazing alloy is heated to its point of fusion. All parts in contact are bonded by capillarity action. Once the brazing alloy has solidified, the assembly become one single block. All passages for flow distribution and heat transfer of the streams are contained in the internal geometry of the block. Inlet and outlet headers with nozzles for the streams are fitted, by welding, around the openings of the brazed passages. These nozzles are used for connecting the heat exchanger to existing plant pipe-work.

Numerous fin corrugations have been developed, each with its own special characteristics (figure 7). Straight and straight perforated fins act like parallel tubes with a rectangular cross-section. Convective heat exchange occurs due to the friction of the fluid in contact with the surface of the fin. The channels of serrated fins are discontinuous and the walls of the fins are offset. For air flows, louver fins are extensively used, while for process applications (single and two-phase) continuous or offset strip fins are used.

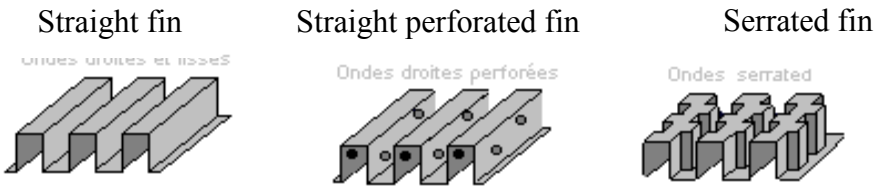

Figure 7. Different fin geometry.

For higher temperature applications or when aluminium is not acceptable, stainless steel (temperature up to 700°C) or copper materials can be used. For very high temperature (gas turbine heat recovery ; T > 1200°C), a ceramic plate fin heat exchanger has also been developed (Ferrato and Thonon [1997]).

For high pressure application in the hydrocarbon and chemical processing industries, a titanium compact heat exchanger has been developed by Rolls-Laval (figures 8 and 9). This heat exchanger consists of diffusion bonded channels that are created by super-plastic forming of titanium plates (Adderley and Fowler [1992]). This heat exchanger can handle high pressure and corrosive fluids and is suitable for marine applications.

2.6 Microchannels Heat Exchangers

Microchannels heat exchangers refer to compact heat exchangers where the channel size is around or lower than 1 mm (Mehendale et al [1999]). Such heat exchangers have been developed for severe environment such as offshore platforms (Johnston [1997]). New applications are also arising for nuclear high temperature reactors (Takeda et al [1997]). To manufacture such small channels several technologies are available (Tonkovitch [1996]). chemical etching, micromachining, electron discharge machining ...

The processing technique is as flexible as for plate-fin heat exchangers, and crossflow and counterflow configurations are employed. The main limitation of microchannel heat exchanger is the pressure drop, which is roughly inversely proportional to the channel diameter. For high pressure applications, the pressure drop is not a constraint, but for other fields of application it will be the main barrier to the use of such heat exchangers.

The most common one is the printed circuit heat exchanger developed by the Heatric Company. The channels are manufactured by chemically etching into a flat plate. The plates are stacked together and diffusion bonded, these heat exchangers can support pressure up to 500-1000 bar and temperature up to 900°C. The typical size of the channels is 1.0 by 2.0 mm (figures 10 and 11), and the plate size can be up to 1.2 × 0.6 m.

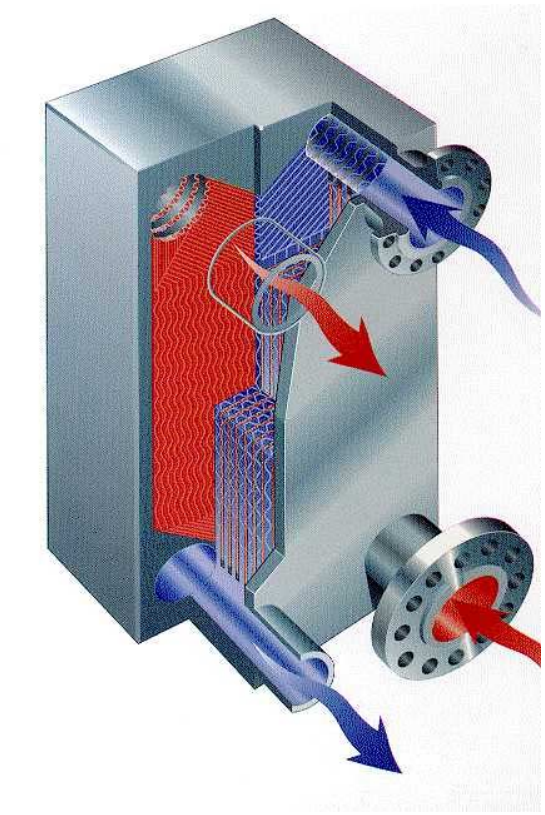

Figure 8. Schematic view of the heat exchanger (Rolls-Laval).

Figure 9. Picture of a titanium compact heat exchanger (Rolls-Laval).

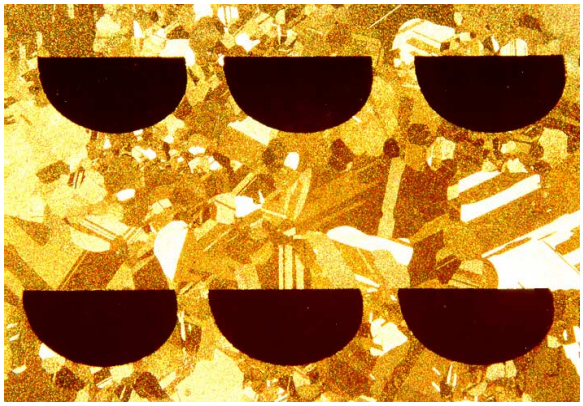

Figure 10. Detail of the bonded plates.

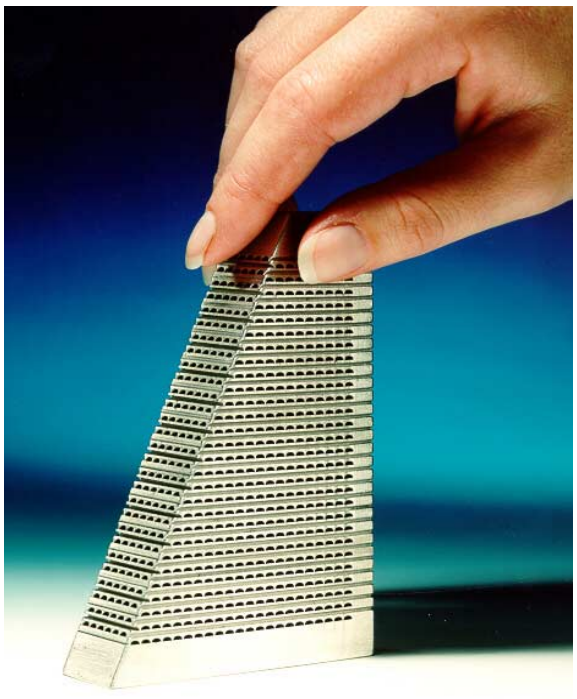

Figure 11. Printed circuit heat exchanger (courtesy of Heatric).

After diffusion bonding, the blocks are welded endplate to endplate to suit duty, then the headers are welded to the blocks to cover inlet and outlet. Headers are in rolled plate, cast or HIP (Hot Isostatic Pressing).

Diffusion bonded heat exchangers are often used for gas compressor cooling in the oil and gas processing industries. A typical 24.4 MW unit operates at 70 bar for both gas/gas and gas/condensate duties.

Recently, Chart-Marston has developed the Marbon heat exchanger (Watton et al [1997]). This heat exchanger is made of stacked and bonded together stainless steel plates. Several configurations are possible. (1) shell and tube or (2) plate fin. So far only small units can be manufactured. The use of such heat exchanger as a chemical reactor is under consideration, and the thermal and hydraulic characterisation is undertaken in the framework of a European funded project.

2.7 Matrix heat exchangers

Perforated or matrix heat exchangers are highly compact heat exchangers and consist of a stack of perforated plates made of high thermal conductivity material such as copper or aluminium, alternating with spacers of low thermal conductivity such as plastic of stainless steel. The pack of alternate low and high thermal conductivity plates are bonded together to form leak free passages between the streams. The main assembly technique adopted is diffusion bonding, more information can be found in Krishnan et al [1997].

Such heat exchangers have been developed for cryogenic and low temperature application (Nilles et al [1993]) and for fuels cells (Ahuja and Green [1998]). These heat exchangers are suitable for a large range of operating conditions, but there is only little information on their thermal and hydraulic behavior. Furthermore, as the heat is transferred by conduction in the plate, the temperature distribution is not homogeneous.

2.8 Flat tube and fins heat exchangers

The concept of flat tube and fins in heat exchangers has been developed in the automobile industry for engine cooling and air conditioning (Cowell and Achaichia [1997], Trauger and Hughes [1993] and Webb [1998]). In such application one of the two fluids is air and the other is either water or an other coolant. The non equilibrium of the heat capacities of the two fluids leads to adopt different enhancement technologies for both fluids. Generally on the air side the surface is finned (plain or louver fins) and on the other side the fluid flows in small diameter channels. The technology is based on assembling aluminium elements either by mechanical expansion or brazing. For conventional applications, the pressure can be up to 20 bar. Recently for car air-conditioning systems using carbon dioxide as coolant, heat exchangers with operating pressure up 140 bar have been manufactured (Pettersen et al [1998]).

2.9 Selection of heat exchanger technology

The selection of compact heat exchangers technology depends on the operating conditions such as pressure, flow rates, temperature but also on other parameters such as fouling, corrosion, compactness, weight, maintenance and reliability. Table 2 summarises the major limits for the different types of compact heat exchangers. In most of the cases, the maximum pressure and temperature cannot be reached simultaneously.

TABLE 2. OPERATING CONDITIONS OF COMPACT HEAT EXCHANGERS

Technology	Maximal pressure	Maximal temperature	Number of streams	Fouling
Aluminium plate fin heat exchanger	80-120 bar	70-200°C	>10	no
Stainless steel plate fin heat exchanger	80 bar	650°C	>2	no
Ceramic plate fin heat exchanger	4	1300°C	2	no
Diffusion bonded heat exchanger	500 bar	800-1000°C	>2	no
Spiral heat exchanger	30 bar	400°C	2	yes
Matrix heat exchanger	1000 bar	800°C	>2	no
Flat tube and Fin heat exchanger	200 bar	200°C	2	no
Brazed plate heat exchanger	30 bar	200°C	2	no
Welded plate heat exchanger	30-40 bar	300-400°C	>2	yes/no
Plate and shell heat exchanger	30-40 bar	300-400°C	2	yes/no
Gasketed plate heat exchanger	20-25 bar	160-200°C	>2	yes
Plastic plate heat exchanger	2 bar	200-250°C	>2	yes/no

TABLE 3. HEAT EXCHANGER SELECTION FOR THE HTR RECUPERATOR

Technology	**Pressure**	**Efficiency***	**Reliability***
Spiral	30 bars	good	good
Plate-fin	80 bars	very good	good
Welded plates	30-40 bars	good	good
Diffusion bonded	500 bars	good	very good

*based on manufacturers information.

3 CONCLUSION

Within the HTR context and due to the high pressure difference for the recuperator (≈ 45 bar) only welded, brazed or diffusion bonded heat exchangers could be used (table 3).

Today, the diffusion bonded heat exchangers with micro-channels appear to be the more promising concept for the recuperator application. In spite of a more important pressure drop, this concept is best rated compared to the other concepts in particular in terms of reliability, mechanical resistance and compactness. This concept has been proposed as alternative solution in the frame of the GT-MHR and PBMR projects.

BIBLIOGRAPHY

Adderley C.I. , Fowler J.O. "High performance titanium plate fin exchanger using a novel manufacturing process", *Design and Operation of Heat Exchangers* , Springer-Verlag , 1992

Ahuja V. and Green R., "Application of matrix heat exchangers to thermomechanical energy recovery from liquid hydrogen", *Cryogenics*, Vol. 38, No.9, pp.857-867, 1998

Alpema, "The standards of the barsed aluminium plate-fin heat exchangers, Association Alpema, Houston, 1994

Brotherton F., "Evaporation in plate heat exchangers", *Heat Recovery Systems and CHP*, Vol 14, No 5, pp 555-561, 1994

Cowell T. and Achaichia N., "Compact Heat Exchangers in the Automobile industry", in Compact Heat Exchangers for the process industries', pp 11-28, Editor R.K. Shah, Begell House Inc, 1997

Ferrato M. and Thonon B. "A compact ceramic plate-fin heat exchanger for gas turbine heat recovery" *Compact Heat Exchanger for the Process Industry*, Editor R.K. Shah, Begell House Inc, 1997

Johnston N. "Development and applications of printed circuit heat exchangers", *communication at the Compact heat exchangers for the process industry conference*, Snowbird, June 1997

Krishnan et al "Manufacture of a matrix heat exchanger by diffusion bonding" *Journal of Material Processing Technology*, Vol 66, pp 85-97, 1997

Kumar H. "The design of plate heat exchangers for refrigerants", *Proceedings of the Institute of Refrigeration*, 1991-92, 5-1 to 5.5, 1992

Lunsford K., "Understand the use of brazed heat exchangers", *Chemical Engineering Progress*, pp 44-53, November 1996

Mc Donald C., "Gas turbine recuperator renaissance", *Heat Recovery Systems & CHP*, Vol. 10, No. 1, pp 1-30, 1990

Mc Donald C., "Low-cost compact primary surface recuperator concept for microturbines", *Applied Thermal Engineering*, Vol 20, pp 471-497, 2000

Mehendale S., Jacoby A. and Shah R., "Heat exchangers at micro and meso-scale", *Compact Heat Exchangers and Enhancement Technologies for the Process Industries*, Editor R.K. Shah et al, pp .55-74, Begell House, 1999

Navarro J.M. and Bailly A. "Compact brazed plate heat exchanger", in *Recent developments in heat exchanger technology*, Elsevier, Paris, 1994

Nilles M., Calkins M., Dingus M. and Hendricks J., "Heat transfer and flow friction in perforated plate heat exchangers", Aerospace Heat Exchanger Technology, R.K. Shah and A. Hashemi editors, pp.293-313, Elsevier1993

Oswald J., Dawson D. and Clawley L., "A new durable gas turbine recuperator", paper 99-Gt-369, ASMR Int. Gas Turbine & Aeroengine Congress, Indianapolis, USA, June 7-10, 1999

B. Palm and B. Thonon "Thermal and hydraulic performances of compact heat exchangers for refrigeration systems", Compact Heat Exchangers and Enhancement Technology for the Process Industry, pp. 455-462, Begell House, 1999

Panchal C.B. and Rabas T.J., 'Thermal performance of advanced heat exchangers for ammonia refrigeration systems', Heat Transfer Engineering, Vol.14, No.4, pp.42-57, 1993

Patel N. and Thompson, "Plate heat exchangers for process evaporation and condensation", *Heat Exchange Engineering*, E.A. Foumeny et P.J. Heggs ,Ellis Horwood Series in Chemical Engineering, Volume 2 Compact Heat Exchangers. Technique of size reduction, 1992

Pelletier O. and Palm B., 'Condensation and boiling of hydrocarbons in small plate heat exchangers, Nordiske kôle-ogvarmepumpedager, Reykavik, Island, 19-22 June 1997

Pettersen J., Hafner A., Skaugen G. and Rekstad H. "Development of compact heat exchangers for CO2 air conditioning systems", Int J. of Refrigeration, Vol. 21, No. 3, pp. 180-193, 1998

Shah, R.K. and Mueller, A.C.: Heat exchange, in *Ullmann's Encyclopedia of Industrial* Chemistry, Unit Operations II, Vol. B3, Chapter 2, 108 pages, VCH Publishers, Weinheim, Germany, 1988.

Sterner D. and Sunden B., 'Performance of some plate and frame heat exchangers as evaporators in refrigeration systems', Proc of the 5th UK Heat Transfer Conference, IMechE, 1997

Syed A. "The use of plate heat exchangers as evaporators and condensers in process refrigeration", *Heat Exchange Engineering*, E.A. Foumeny et P.J. Heggs ,Ellis Horwood Series in Chemical Engineering, Volume 1 Design of Heat Exchangers, Chapter 10, 1992

Takeda T., Kunitomi K., Horie T. and Iwata K. "Feasibility on the applicability of a diffusion welded compact intermediate heat exchanger to next generation high temperature gas-cooled reactor' *Nuclear Engineering and Design*, Vol 168, pp 11-21, 1997

Tonkovich A. L; et al, "Microchannel heat exchanger for chemical reactors", *AICHE symposium series*, Vol 92, No 310, pp119-125, 1996

Trauger P. and Hughes G.G., 1993. Construction and Performance Characteristics of the PFE Evaporator, SAE paper, n° 930155

Trom L., 'Heat exchangers. Is it time for a change ?', *Chemical Engineering*, pp 70-73, February 1996

Turisini et al, 'Prevent corrosion failures in plate heat exchangers', *Chemical Engineering Progress*, pp.44-50, September 1997

Watton B., Symonds K. and Symonds S. "Heat Exchanger", International Pattern, WO 97/21064, June 1997

Webb R. L., 1998. Advances in Air Cooled Heat Exchanger Technology, Proceedings of the Heat Exchanger for Sustainable Developments Conference, paper IL.6, pp.677-692, Lisbon, June 1998

HIGH TEMPERATURE ALLOYS FOR THE HTGR GAS TURBINE: REQUIRED PROPERTIES AND DEVELOPMENT NEEDS

R. COUTURIER
CEREM, CEA-Grenoble, Grenoble

C. ESCARAVAGE
FRAMATOME-NOVATOME, Lyon

France

1. INTRODUCTION

Recent advances in the design of turbomachinery, recuperators and magnetic bearings provide the potential for the use of the High Temperature Gas Reactor (HTGR) with a closed cycle gas turbine. The reactor size has been reduced in developing the passively safe module design and the size of industrial gas turbine has increased to accommodate the energy released from a HTGR module. Highly effective compact recuperators have been developed, they are a key requirement for achieving high efficiency. The availability of large magnetic bearings has also eliminated the potential problem of coolant contamination by the oil of lubricated bearings.

National and international R&D programs are under way to explore areas where technical development is needed [1]. Among these programs, the closed-cycle gas turbine concept is investigated in several industrial projects [2]:

- The Pebble Bed Modular reactor (PBMR) in South Africa, with a gross electrical generation of 117 MWe. The project schedule has been established, with a deployment of a first unit in 2006.
- The Gas Turbine Modular Helium Reactor (GT-MHR) developed by an international consortium, with a targeted 286 MWe generation per module, a prototype single unit is scheduled in Russia in 2009.
- Test Reactors are being commissioned in Japan (High Temperature Test Reactor HTTR) and China (HTR10) to evaluate the safety and performance of HTGR. These reactors are designed with an indirect conversion cycle, but they will support R&D activities like electricity generation via the gas turbine and high temperature process heat applications.

A common European approach to the renewal of HTR technology through the direction of a European HTR Technology Network (HTR-TN) has also been established to enable and encourage work-shared structures within this nuclear R&D field.

Among these recent R&D programs, Framatome and CEA are involved in the materials development for the key components of the HTGR. The development of advanced HTGR concepts requires materials data and understanding of materials behaviour under reactor operating conditions and environment. The components for the primary circuit operate at temperatures above 600°C and up to 850°C in order to reach high efficiencies. For these materials and components, considerable data and know-how exists, but industrial and technical feasibility are not well established for the most recent designs. For example, a significant effort is needed for the turbine components, for which the expected working conditions are beyond the today's industrial capabilities. The fundamental technologies required for the design of the turbomachine have been proven for aerospace and industrial gas turbines. However, the HTGR gas turbine requires a design that includes high temperature capability and long term endurance. The required design properties, associated with the large sizes of components, can be seen as a major issue.

In this work, a review with a selection of most relevant materials and processes is presented, for both turbine blades and disks. The focus of this work is to discuss the choice of high temperature materials in accordance with the recent HTGR design specifications. The GT-MHR turbine design is used as a reference for high temperature materials selection. Also an evaluation of recent advances in materials for industrial gas turbine is presented, with a brief overview of associated fabrication processes.

2. HTGR TURBINE DESIGN SPECIFICATIONS

The GT-MHR module consists of a nuclear source of heat (reactor system) and the Power Conversion System. Details of the general design can be found in [2] and [3].

The Power Conversion System (PCS) receives about 600 MW of thermal energy from the reactor system and converts 286 MW of net usable electrical energy, with an overall efficiency of about 47%. The PCS includes the turbomachine, the precooler and intercooler, and connecting pipelines. The turbomachine consists of the turbocompressor, the electrical generator, bearings and seals. The turbocompressor includes the turbine and two compressor sections (low pressure and high pressure compressor).

The helium is received by the PCS from the hot gas duct. The helium then expands trough the gas turbine which is coupled to the electrical generator. From the turbine exhaust, the helium flows trough the hot side of the recuperator, transferring heat to helium returning to the reactor. The helium leaving the hot side of the recuperator is cooled (precooler) before passing trough the low-pressure compressor, intercooler and high-pressure compressor. The helium then passes in the cold side of the recuperator where it is heated for return in the reactor system.

The entire assembly is installed in a vertical orientation and is rotating at 3000 rpm (50Hz). The turbine design is based on the technology available for large industrial engines. Substitution of helium for air in this nuclear gas turbine modifies aerodynamic requirements by removing Mach number limitations. As the rotational speed is fixed (synchronous generator), the size of the turbine is dictated by the choice of blade speed. The highest blade speed is desirable to limit the number of stages, but it is limited by the high temperature stress limits for the blades. In the GT-MHR concept, a 12 stages turbine with very high efficiency was established. With turbine inlet temperature of 850°C, blade and disks cooling are not considered as necessary in the design. Salient features of the GT-MHR turbine are given in table 1.

3. CRITERIA FOR MATERIAL SELECTION

For the material selection, the key points are the first stages turbine disks and blades where the stresses and temperatures are the highest. Table 2 summarizes the thermal and mechanical loads for the turbine disks and blades. The materials for these components should ensure a safe operation for at least 60000 hours. Therefore, a ground rule for the material selection of the most critical parts was proposed as following [5]:

- for the blade alloy $\sigma_{60000h}^{850°C} \geq 225 MPa$
- for the disk alloy $\sigma_{60000h}^{850°C} \geq 180 MPa$

TABLE 1. GT-MHR TURBINE CHARACTERISTICS AT FULL POWER [4]

Power, MW	560
Rotational speed, rpm	3000
number of stages	12
Expansion coefficient	2.67
Adiabatic efficiency, %	93
hub diameter, mm	1400
Inlet parameters	
temperature, °C	848
pressure, MPa	7.0
He mass flow, kg/s	320
pressure losses, MPa	0.007
blade height, mm	170
Outlet parameters	
temperature, °C	510
pressure, MPa	2.62
pressure losses, MPa	0.02
blade height, mm	225

TABLE 2. PRELIMINARY STRESS ANALYSIS FOR THE GT-MHR TURBINE [5]

	Stage 1 (850°C)	**Stage 12 (510°C)**
Blade root section area, mm^2	827	827
blade height, mm	170	225
centrifugal force created by a blade, N	85400	117110
Blade root section stresses, MPa		
Radial stress	92	118
Bend stress	68	82
Total stress	160	200
Stesses in the disk (rotor), MPa		
Annular	150	165
Radial	116	131

The use of high temperature materials for nuclear systems will require an extension of material design rules and codes currently used. From the designer side, increasing the temperatures means a change from time-independent to time-dependent characteristics (creep, creep-fatigue).

Figure 1 illustrates the maximum temperature of metallic components in current and future reactor systems. In addition, figure 1 indicates the maximum temperature considered in the design codes. Although some existing codes use time-dependent properties in design (ASME Code Case N47 now incorporated as subsection NH of section III and RCC-MR), the temperature limits of materials included in the design codes available to day are significantly lower compared to HTGR needs and therefore a significant step forwards is required.

The first criteria being high temperature tensile strength and stress to rupture, other properties as resistance to thermal fatigue must be considered in design. Notch sensitivity is also probably detrimental to the high cycle fatigue of rotating parts of complicated shapes.

Possible corrosion effects of environment should also be considered for the materials' choice as helium impurities can influence the metallic material properties in service via carburisation and oxidation mechanisms. Part 6 will discuss the corrosion performance of several alloys in term of weight gain that can be related to the reduction of effective load bearing thickness.

However, for the complete assessment of structural integrity, the combined effect of different failure modes must be considered and particularly the following:

- creep-fatigue: it is generally considered that the amount of fatigue endurance reduction by creep or relaxation is increased when the material has low creep strength. Creep ductility can also be considered as a limiting parameter in creep-fatigue.
- fatigue and environment effect: initiation of cracks particularly in case of thermal fatigue takes place at the surface of the material and can be influenced by the effects of the environment on the material surface as pointed out at the end of section 6.
- creep-fatigue and environment effect: the effect of environment can be important in creep-fatigue and in thermal fatigue, and experiments have shown that the reduction of fatigue life by hold times in relaxation can be quite different in vacuum from what is observed in air. The corresponding mechanisms are difficult to clarify for a quantitative prediction, the helium effects being suspected to be intermediate between vacuum and air effects.

As long term service is needed, long term stability of material properties must be assessed: this point is discussed in part 7. When the optimum strength is obtained by a heat treatment at temperature lower or nearly equal to the service temperatures, there are some doubts about the stability of the corresponding microstructure.

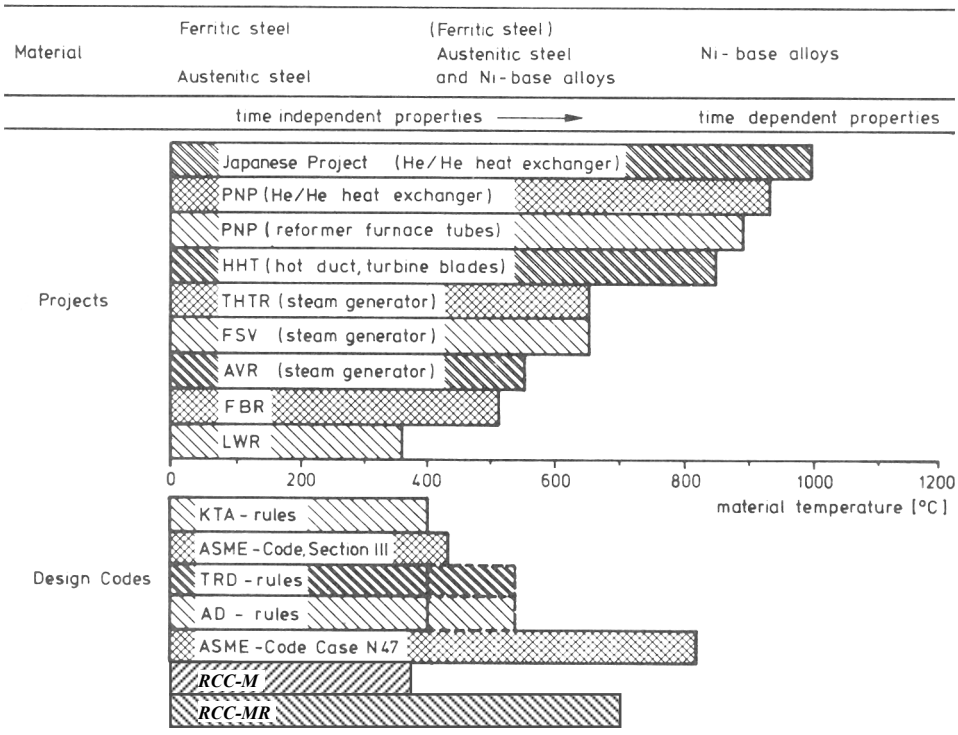

FIG.1. Material temperature and design codes for metallic components in nuclear applications (partly from [6]).

Based on these requirements, the selection of metallic materials for blades and disks is discussed in the next sections. The chemical compositions of alloys that are evaluated is given in appendix 1.

4. MATERIALS FOR THE TURBINE DISKS

At this stage, it remains unclear if alloys containing substantial additions of cobalt or tantalum would be selected for use in the turbine of a HTGR. In some past studies, alloys containing more than residual levels of these elements have often been excluded from the list of reference alloys for the primary circuit, because of potential radioactive contamination. However, many of the high temperature alloys with Cobalt have the highest mechanical properties and they are examined in the case of further acceptability [7,8].

Inconel alloy 718 was selected for the HTGR turbine disks in recent studies [8]. Alloys IN718 is a nickel-based precipitation hardened material. It has the necessary strength, short term creep and corrosion resistance only in the case of active cooling of the disk. With a turbine inlet temperature of 850°C, IN718 will require cooling to lower the temperature of the disks to around 650°C. Alternatively, alloys containing cobalt may be better in terms of high temperature strength (like Udimet 720 with $\sigma_{1000h}^{850°C}$=245MPa).

From the GTMHR design reports issued from OKBM, classical nickel-base superalloys used for industrial gas turbines (IN 718, Waspaloy) do not achieve the long term stress level requirements [5]. For OKBM, the only existing alloy that could be envisaged for a non-cooled first stage disk is the alloy MA 6000. MA 6000 is an Oxide Dispersion Strengthened (ODS) superalloy that offers very high strength and microstructural stability. The creep strength of this grade could reach values higher than 185 MPa for 60000 hours at 850°C. This grade is produced by mechanical alloying of powders and subsequent Hot Isostatic Pressing or hot extrusion [9]. The main difficulties with using ODS grades are that the process route is not mature and that much work is needed to produce large ingots with homogeneous mechanical properties.

Among the cast alloys that could serve as a basis for further grades optimisation, OKBM proposes ZhS6F and VZhL12U grades, VZhL12U chemical composition being very close to that of IN 100 alloy.

In the frame of the Dragon project, Graham has proposed A286 and IN 706 as reference grades for the disk production. These are Fe-Ni-Cr precipitation hardened grades with sufficient forgeability for large disks production but medium high temperature properties. Again, these grades can only be envisaged in the case of cooled turbine disks [7].

In the case of large components as the GT-MHR turbine disks, the manufacturing capability is closely related to the strength of the alloy. In the case of nickel-base superalloys, the two major issues are the following:

- to obtain large ingots (~5-10 tons) without solidification porosities and macro-segregations. For recent superalloys, manufacturing route includes a vacuum induction melting, a vacuum arc remelting and/or electro-slag remelting. The powder metallurgy would allow to produce high quality ingots with highly alloyed grades. In this case, microstructural inhomogeneities would be limited to the size of the powder particle.

- to forge these ingots which usually offer a very low hot-workability. Isothermal forging is used, but with the most recent superalloys (like Udimet 720), the maximum forgeable size is much lower than the GT-MHR disk diameters. Again, elaboration of near-net shapes components by Hot Isostatic Pressing of powders appears promising for these large disks, as hipping furnaces with large diameters are available (~1.4 m).

5. MATERIALS FOR TURBINE BLADES

Materials selection and testing for HTGR turbine blades has been extensively studied. Essentially 2 types of metallic materials were investigated:

- Nickel-base cast superalloys.
- Molybdenum-base grades.

5.1. Ni-base cast superalloys

In several past R&D programs, selected alloys were ranked by their high temperature strength, castability and cobalt content. Most promising alloys for the blades are therefore:

- 713LC [6,7,8,10,11,12,13]
- M21 [7,10,12]
- MAR-M 004 [7,13,12]

Alloy 713 LC is a cast nickel base precipitation hardened alloy that combines superior castability and creep resistance. Alloy 713LC has the advantage of wide industrial experience in conventional gas turbine (turbine housings, case, stator) [8]. Alloy 713 LC neither contains Co or Ta and should therefore not present any contamination problems. In HTGR environment, alloy 713LC can be susceptible to carburisation and sulfidation problems, and coatings have to be envisaged. Alloy 713LC is well suited for the turbine blades required specifications, except for the first row of blades where cooling would be necessary to achieve the required lifetime [8]. Directionally Solidified (DS) or Single Crystal (SC) blades would solve this problem, but alloys commonly used for DS or SC blades contain about 10% cobalt (DS Mar M 247, SC René N4).

Alloy 713LC was used for the fabrication of the turbine blades in the HHV project [11]. During this project held in Germany, a full-scale test turbine driven by HTGR–type helium was built. During the short high temperature lifetime experienced (~325 hours at 850°C), no material problems appeared with the working blades.

Alloy M21 is a low chromium nickel base alloy that combines precipitation hardening and solid solution hardening (~10% tungsten addition). It was selected for its superior corrosion resistance in impure helium.

Alloy MM004 has been developed from alloy 713LC and is claimed to have a better toughness because of Hafnium addition [13].

Among alloys that were also studied for a potential use as HTRG turbine blades, there are:

- IN 100 grade with good corrosion resistance [10]. IN 100 is the reference alloy for PBMR power-turbine cooled blades [1].

- Nimonic 80A with medium creep rupture strength which is envisaged for the last row of blades (lower temperature) [6,13].
- Alloys Nimonic 90, 105 and 115, Udimet 520 et 700, IN 591, IN738, IN 792, René 80, M22, MAR-M 247, Nx 188 were also proposed in various studies [7,13,14]. FIS 145 alloy was developed in Germany for HTGR applications. It combines precipitation and solid solution hardening (~13.5% tungsten) with a high castability [13].

In figure 2, a comparison of several blade alloys properties is shown, for creep rupture performed in both air and helium. Jakobeit pointed out the sharp decrease in creep strength for long times at 850°C, except for the Mo-base alloy. This decrease is less pronounced at lower temperatures, supporting the idea of a design with cooled blades to increase the blade lifetime [13]. L-TZM is the strongest alloy in figure 2, this Mo-base grade is presented in the next section.

Alloys proposed by OKBM in the GT-MHR project include precision investment cast Ni-base alloys (ZhS6K, CNK8M) and single crystal alloys (ChS-120M that is close to CSMX-2 grade) [5].

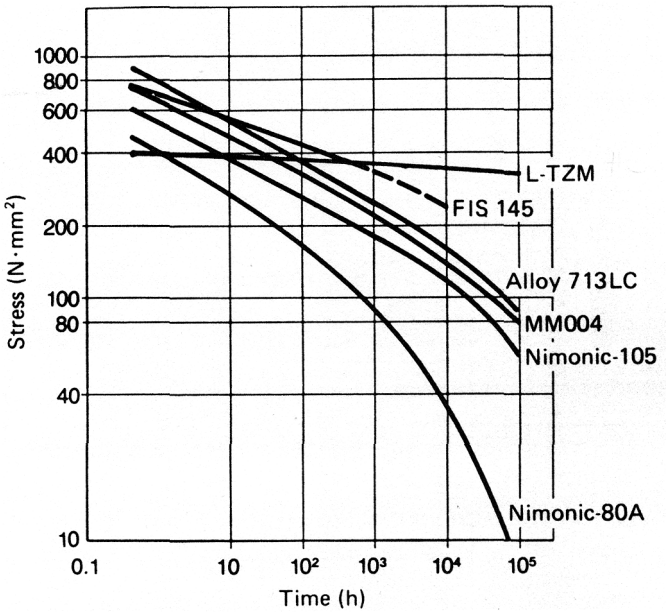

FIG. 2. Creep rupture strength of different turbine blade materials at 850°C [13].

5.2. Molybdenum-base alloys

The molybdenum-base alloy TZM (Mo-0.5Ti-0.08Zr) has not been used in industrial gas turbines because of its poor oxidation resistance in air. However, R&D efforts performed in German HTGR programs have demonstrated a promising application for this alloy for helium turbine blades. As shown in figure 2, Mo-TZM exhibits a completely different creep-resistance behaviour as compared to the nickel-base alloys, mainly because of its high melting point (2607°C) [15]. Almost flat creep curves make a 100 000h life time appear possible with an uncooled blade, as shown in figure 3 [12].

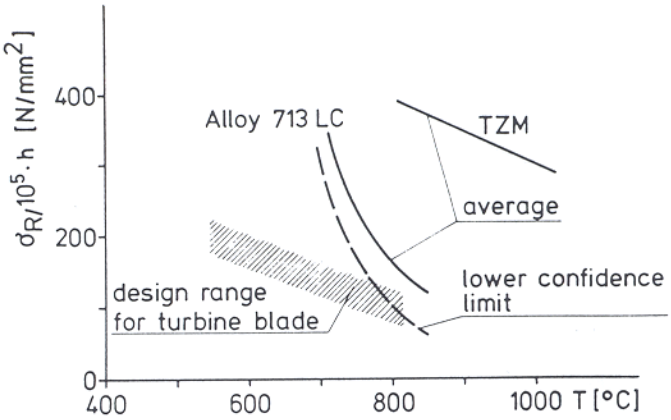

FIG.3. Stress for rupture in 10^5 h versus design temperature for HTGR turbine blade [12].

Precision forged blades were fabricated, starting from vacuum-arc-melted or powder metallurgy ingots. These blades showed a very high corrosion resistance in impure helium, but several fabrication difficulties and inherent drawbacks were encountered, and efforts for further development are almost abandoned today:

- Mo-TZM is brittle at temperatures up to 360-440°C and the notch sensitivity remains high at HTGR service temperature.
- in case of air ingress in the circuit , this alloy will suffer a massive oxidation.
- microstructure is heterogeneous in the blade, as a result of locally non uniform deformation state during hot forging. Low strength areas were found in fatigue and creep, especially in the airfoil/root transition zone [15].

6. EFFECT OF HELIUM ENVIRONMENT

The main corrosion effects of metallic materials in HTGR helium environment have been extensively studied, especially for high temperature materials. Corrosion derives from the presence of low partial pressures of H_2O, CO, and CH_4 in helium. Hydrogen also plays a role in controlling the oxygen potential trough the H_2/H_2O ratio. A recent review has given the following general trends [16]:

- below 850K (577°C), corrosion is limited. Only mild steels can suffer decarburisation. Steels with additions of chromium are slightly oxidized.
- from 850 to 1173K (577-900°C), creep resistant alloys form a chromium rich oxide scale. Internal microstructural changes are observed (precipitate free zones, carburised zones), especially when the surface scale is porous.
- under 1173K, rapid carburisation or decarburisation can occur, the dominant mechanism being controlled by the environment chemistry.

Concerning the high temperature alloys for blades and disks, the mains conclusions are:

- Mo-TZM alloy is almost insensitive to He environment up to 1000°C [7]. Jakobeit has observed a 30 μm thick MO_2C surface scale formed after 36000 hours at 850°C. This surface modification does not influence the creep resistance [13].
- 713 LC alloy and more generally nickel-base superalloys develop an oxide surface scale (Cr_2O_3) with an internal oxidation (Al_2O_3) and carburisation ($Cr_{23}C_6$). The

carburised zone is depleted in γ' precipitates. Creep tests with 713LC specimens performed from 500 to 850°C in HTGR helium and air show virtually no environment effect on rupture time for test durations up to 55 000 hours [13].

The first way of optimisation to deal with corrosion problems is the optimisation of alloy composition, as shown in figure 4. Several chemical ratios were proposed as controlling parameters for the formation of stable protective surface scales:

- Alloys with high Al/Cr ratios (M21, IN591) are much more sensitive to corrosion than alloys with the same Al content and a reduced Cr content (Mar-M004, 713LC). Alloys with low Cr and high Ti develop a stable oxide scale. For this reason, alloys IN 100 and IN738 appear promising for HTGR applications if the constraints on cobalt contents are lowered [7].
- Alloys with a ratio Al/Ti around unity develop more stable surface oxides than alloys with Al/Ti<1 (as 713LC, M21) [10].

The second way to prevent corrosion problems is to apply a coating on the surface. An industrial experience exists for aluminide coatings for alloy 713LC, which then offers a stable continuous Al_2O_3 film [8].

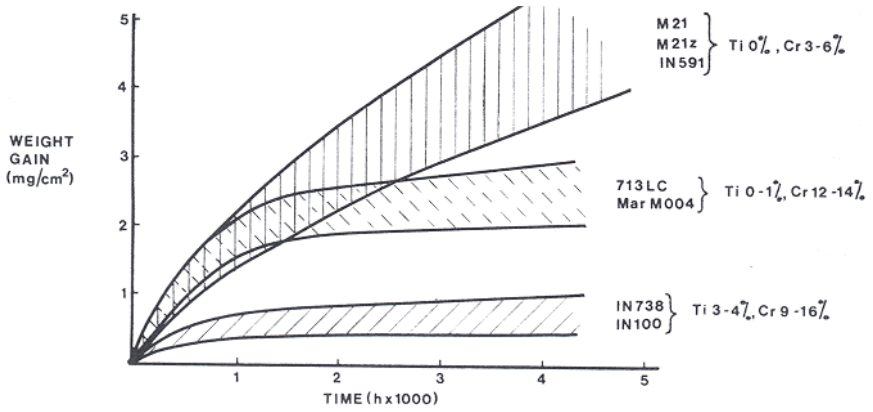

FIG.4. Weight gain of cast Ni-base alloys in HTGR environment at 900°C [Graham76].

The main concern with design of high temperature alloys in impure helium is whether the surface corrosion influences the strength (and lifetime) of the components. From the literature available on creep rupture properties, it appears that degradation of mechanical properties after elevated exposure in helium is similar to degradation experienced in air [8,13]. Therefore the degradation is mainly due and thermally activated structural changes rather than corrosion. However, when dealing with crack propagation properties, a study on cast Ni-base alloys has shown that environment effects are not similar in fatigue and creep crack propagation [14]. Complex mechanisms can occur at the crack tip (oxidation/plasticity interactions) which are difficult to model and predict.

7. LONG TERM MATERIALS PROPERTIES

Most of Ni-base superalloys investigated for turbine blades and disks are heat treated before use for maximum strength, usually with a solution treatment followed by aging treatments. They are strengthened by a very fine dispersion of coherent precipitates (γ' or γ'') with some

carbides and borides. They are therefore inherently subjected to structural instabilities in high temperature service. Microstructural changes are of fundamental importance for HTGR material selection as most of the foreseen grades were developed for aeronautical turbines with much shorter lifetimes. For example, precipitation of hard brittle phases must be controlled for component lifetimes greater than 50000 hours.

Figure 5 shows an example of large microstructural changes of 713LC alloy after a creep test at high temperature. For the HTGR turbine, blade and disks alloys will endure thermal aging and there will be a strong need to understand the induced changes in strength, creep ductility and remaining life [17].

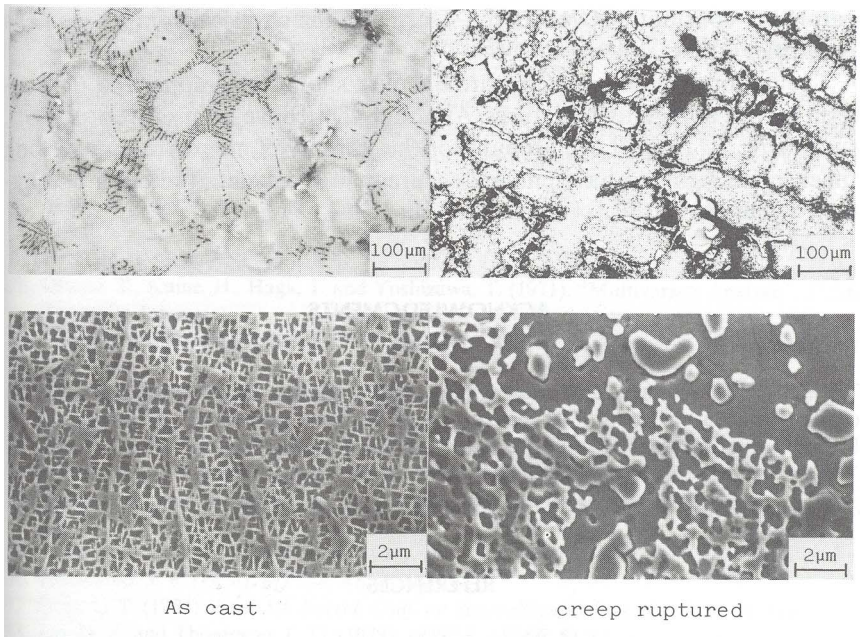

FIG 5. Optical (upper) and scanning electron (lower) micrographs of alloy 713LC before (left) and after (right) a creep test at 1000°C for ~50000 hours [17].

8. POTENTIAL BENEFIT OF RECENT ADVANCES IN GAS TURBINE MATERIALS

8.1 Evolutions in turbine technology

There has been a considerable development in natural gas fired advanced land-based turbines with combined cycles (reaching 60% thermal efficiency). These units are intended for base-load operations, with power continuously increasing: from 60-70 MW in the 70's to 280 MW today and around 500 MW in the next years (GE MS 7001H turbine in 2001). Reviews of recent achievements in turbine technology and associated materials developments can be found in [18,19].

The need to increase engine combustion temperature to increase the efficiency of gas turbines has resulted in a large increase in Turbine Inlet Temperature (TIT), for both land-based and aero turbines. In the last 50 years, the TIT has risen from around 800°C to nearly 1600°C [18,20]. This increase has been accompanied by several changes in the materials for the hottest parts. Recent advances in material processing and strength capability are now presented, as they certainly offer new possibilities to achieve the HTGR requirements.

8.2. Advances in disk materials

This increase in TIT has a significant impact on turbine disks technology. Turbine disks rim temperatures have risen to 680°C and will exceed 700°C in future aero-engines. In the past, Waspaloy has been used extensively, and Alloy 718 and Udimet 720 are now replacing it. However, even U720 approaches its limits. Therefore, major efforts are made to produce disks with temperature capabilities above 700°C [20].

Alloy 718 has a large propensity for segregation during casting. For aero-engines, melting technology advances have allowed to produce the required disk diameters of largest engines.

However, for power generation, turbine disks can be typically 1.5 meters or more in diameter. Such large components require the production of around 10 tons ingots with subsequent forging. This has not been possible with 718 alloy because of low castability, and a new grade with less Mo and Nb was developed (IN 706). This grade allows the production of large disks with modest diminution in mechanical properties. However, melting technology of large 706 ingots remains complex, and the alloy reaches today the limits of its performance. Again, large efforts are put to produce large disks in more resistant 718 grade, and also Udimet 720 for the future [21].

Large segregation during solidification of highly alloyed grades has forced to move to powder metallurgy processing for which segregation is not an issue. Alloys such as Merl 76 (Pratt &Whittney), René 88DT (General Electric) and N18 (Snecma) represent the current state of the art for aero-engines [22].

In the past, hipped powder compacts yielded excellent static properties, however low-life fatigue failure occurred in service. These failures were initiated at defects on powder particle boundaries due to powder contamination. To overcome these problems, atomisation and handling of the powders were improved, and post-HIP isothermal forging used to mitigate the influence of contamination. Today, powder metallurgy offers two interesting perspectives [21]:

- Production of Ni-base superalloy grades that are almost not castable (due to excessive segregation) and alloys with a low forgeability.
- Production of net shape parts with minimum final machining.

Recently, there has also been interest in the development of HTGR ceramic turbine disks in Japan [2]. Achieving a rotor of lightweight and high strength could indeed facilitate the turbine design. With the HTGR helium environment, C/C composite was chosen, and the fabrication of a representative disk was achieved in 1998. Tests showed poor rotating properties, but further fabrication and tests are under way. Many technical problems still need to be resolved for this long-term solution of disk fabrication.

8.3. Advances in blade materials

The rise in TIT has been met by replacing the forged blades by cast blades ($T^{100000h}_{140MPa} \approx 805°C$ and $\sigma^{850°C}_{100000h} \approx 175MPa$ for IN 738 [18,22]), and the subsequent introduction of directionally solidified (DS) and single crystal (SC) blades ($T^{100000h}_{140MPa} \approx 870°C$ [18]). Today peak metal temperatures of over 1100°C are experienced in some turbine parts, with service lives around 10 000 hours achievable [20]. The DS process allows blades to operate at temperatures about 25K higher than conventional blades. An additional temperature increase of about 25K is achieved by using blades made of single crystal materials (no grain boundaries). Thermal

barriers coatings are extensively used in aircraft turbines, allowing another temperature increase of about 100K [23].

9. CONCLUSION – FUTURE DEVELOPMENTS

Future developments in materials will be associated with new turbine designs. Multi-structure disks, optimised for low cycle fatigue in the bore and creep resistance in the rim, are today under development [24]. This process route is likely to be more expensive, but it offers the designer to optimise independently the properties of the bore and the rim. This will result in better performance and disk endurance [20].

Oxide Dispersion Strengthened alloys (ODS) like MA6000 are promising for their high temperature strength and stability. These grades are indeed more suited for static components (vane, combustion chambers) than for rotating parts . This is because the strength advantage of ODS occurs at stresses which are lower than the stresses in the blades. ODS alloys only become superior where a large microstructural stability is required, at medium stresses and temperatures higher than the γ' coarsening temperature: $\sigma^{850°C}_{100000h} \approx 250MPa$ for MA 6000, compared to $\sigma^{850°C}_{100000h} \approx 175MPa$ for IN 738[25].

The modelling of production processes will need further development, essentially for cost savings. In fact, typically 70% of the price of semi-finished parts of blades and disks is the input material cost. Then, the final machining doubles the component cost. Therefore, cost savings can only be done by producing net-shape components to reduce the material input weight. This will be done by precise modelling of the production steps: solidification, hot working or Hot Isostatic Pressing [20].

The development of large land-based turbines like in HTGRs also requires progress in material mechanical testing and life modelling [25]. The total lifetime required for the hot components will be greater than in the past: around 100 000 hours instead of 20 000 hours. Low cycle and thermal fatigue will still be life determining failure modes, but high temperature oxidation and creep rupture may become more important. In service degradation of the alloy microstructure will lead to a reduction in the creep rupture strength, and it will be needed to predict accurately the life of "degraded" components. This will be possible by developing experimental tests to quantify and to evaluate the interaction between creep damage mechanisms and microstructural evolutions.

REFERENCES

[1] INTERNATIONAL ATOMIC ENRGY AGENCY, Design and development of gas cooled reactors with closed cycle gas turbines, IAEA-TECDOC 899, Vienna, (1996).

[2] INTERNATIONAL ATOMIC ENRGY AGENCY, Current status and future development of modular high temperature gas reactor technology, IAEA-TECDOC (new), Vienna, (2000).

[3] OKBM, Conceptual Design report, Task PL9, Prod. PL9-4, Rev.0, (1998).

[4] OKBM, Turbocompressor Design performance (draft report), Task PCS 4, Prod. PCS 4-4, Rev.0, (1996).

[5] OKBM, Report on turbocompressor materials (Final report), Task PCS 4-8, Prod. PCS 4-8-3, Rev.0, (1997).

[6] NICKEL H., SCHUBERT F., SCHUSTER H., Evaluation of alloys for advanced High Temperature Reactors systems, Nuclear engineering and design 78 (1984) 251-265.

[7] GRAHAM L.W., Materials for advanced high temperature reactors, Rev. Int. Htes Temp. et Refract., T13, (1976), pp. 190-203.
[8] KOHLER B., GT-MHR turbocompressor Design Report, Allied Signal report n°41-14039, (1995)
[9] BENN R.C., MC-COLVIN G.M., The development of ODS superalloys for industrial gas turbines, Superalloys 1988, Ed. S. Reichman, D.N. Dhul, G. Maurer, S. Antolovitch and C. Lund, The Metallurgical Society, (1988), pp. 73-80.
[10] JOHNSON W.R., THOMPSON L.D., LECHTENBERG T.A., Design of wrought nickel-base alloys for advanced high temperature gas cooled reactor applications, Nuclear Technology vol. 66, (1984), pp. 88-101.
[11] WEISBRODT I.A., Summary report on technical experiences from high temperature helium turbomachinery testing in Germany, IAEA-TECDOC 899, (1996), pp. 177-248.
[12] SCHUSTER H., JAKOBEIT W., High temperature alloys for the power conversion loop of advanced HTRs, Proceedings of the symposium "Gas-Cooled Reactors with emphasis on advanced systems", Julich, vol. 1, (1976), pp. 401-418.
[13] JAKOBEIT W., PFEIFER J.P., ULLRICH G., Evaluation of high temperature alloys for helium gas turbines, Nuclear technology vol. 66, (1984), pp. 195-206.
[14] SHAHINIAN P., SADANANDA K., Creep and fatigue crack growth behaviour of some cast nickel-base alloys, Materials Science and Engineering A108 (1986) 131-140.
[15] JAKOBEIT W., PM Mo-TZM turbine blades-Demands on mechanical properties, Refractory and Hard Metals, Sept. 1983, (1983), pp.133-136.
[16] GRAHAM L.W., Corrosion of metallic materials in HTR-helium environments, Journal of Nuclear materials, vol. 171, (1990), pp. 76-83.
[17] MONMA Y., Creep and stress-rupture / long term, Superalloys, Supercomposites and Superceramics, Ed. Tien and Caulfield, Academic Press, (1989), pp. 339-361.
[18] VISWANATHAN R., SCHEIRER S., STRINGER J., Materials advancements in land based gas-turbines, Proceedings of PowerGen International, Orlando, 1998 (1998).
[19] MATERIALS SOLUTIONS 98, Gas turbine materials technology, Conference proceedings from Materials Solution'98, Pub. ASM International, (1998).
[20] WINSTONE M.R., PARTRIDGE A., BROOKS J.W., The contribution of advanced materials to future aero-engines, Proceedings of the fifth international Charles Parsons Turbine Conference, July 2000, (2000), pp. 779-797.
[21] OAKES G., SHAW L.H., COULSON W., The use of aerospace materials and manufacturing technology for power generation gas turbines, presented at the fifth international Charles Parsons Turbine Conference, July 2000, (2000).
[22] THOMAS M., Materials Development in aero gas turbines, Proceedings of the fifth international Charles Parsons Turbine Conference, July 2000, (2000), pp. 710-723.
[23] BECKER B., Potential Benefits of advanced Materials for performance and life cycle cost of large industrial gas turbines, Proceedings of the fifth international Charles Parsons Turbine Conference, July 2000, (2000), pp. 658-670.
[24] BURLET H., LUTHI T, MC-COLVIN G., GALLET S, OLSCHEWSKI J., PETEVES S, RAISSON G., VOGEL F., Development of Bi-metallic Gas Turbine Components, presented at the fifth international Charles Parsons Turbine Conference, July 2000, (2000).
[25] SINGER R.F., Advanced materials and processes for land-based gas turbines, Materials for advanced power engineering part 2, ed. D. Coutsouradis et al., (1994), pp. 1707-1729.
[26] STRINGER J., VISWANATHAN R., Gas turbine hot section materials and coatings in electric utility applications, Proceedinds of ASM 1993 congress materials, Pittsburgh, (1993), pp. 1-21.

Appendix 1

CHEMICAL COMPOSITION OF INVESTIGATED ALLOYS

Possible alloys for blades (weight %).

Alloy	process	Ni	Cr	Co	Mo	Al	Ti	W	Nb	others
713LC	C	b	12.0	0.04	4.65	5.82	0.74	-	2.0	0.07C, 0.1 Zr, 0.009B
MAR-M 004	C	b	11.86	-	4.42	5.95	-	-	1.6	1.3Hf, 0.065C, 0.3Ta
IN 738	C	b	16	8.5	1.75	3.4	3.4	2.6	0.9	1.75Ta, 0.11C, 0.04Zr, 0.01B
IN 792	C	b	12.15	9.25	1.8	3.45	4.10	3.78	-	3.75Ta, 0.52Hf, 0.11C, 0.012B, 0.09Zr
René 80	C	b	13.8	9.4	3.9	3.15	5	3.8	-	0.16C, 0.017B, 0.04Zr
M21	C	b	6	-	2	6	-	10.5	1.5	0.1C, 0.02B, 0.1Zr
M21Z	C	b	6	-	2	6	-	10.5	1.5	0.1C, 0.02B, 0.5Zr
IN 591	C	b	3	12	-	5.7	-	19	-	0.1C, 0.03B, 0.37Zr, 3Ta
IN 100	C	b	10	15	3	4.7	3	-	-	0.18C, 0.014B, 0.06Zr, 1V
Udimet 700	C	b	15	18.5	5.2	4.3	3.5	-	-	0.08C
MAR-M 247	C, DS	b	8.5	-	-	5.5	1	10	-	0.15C, 3.0Ta, 1.3Hf
Nx-188	C	b	-	-	18	8	-	-	-	0.04C
Nimonic 80A	F	b	20	0.17	-	1.32	2.45	-	-	0.04C, 1.86Fe, 0.045Zr
Nimonic 90	F	b	19.5	16.5	-	1.4	2.35	-	-	0.09C
Nimonic 105	F	b	15.4	20.25	4.72	4.69	1.00	-	-	0.14C, 0.051Zr
FIS 145	F	b	7.44	9.90	-	5.28	-	13.46	-	0.11C, 0.88Hf
Nimonic 115	F	b	14.2	13.2	3.2	4.8	3.7	-	-	0.16C
Udimet 520	F	b	19	12	6	2	3	1	-	0.05C, 0.005B
René N4	C, SC	b	9	8	2	3.7	4.2	6	0.5	4Ta
Mo-TZM	C, P	-	-	-	b	-	0.45	-	-	0.015C, 0.09Zr

F : wrought or forged, C : as Cast, P : Powder Metallurgy, DS : Directionally Solidified, SC : Single Crystal.

Possible alloys for disks (weight %).

Alloy	process	Ni	Cr	Co	Mo	Al	Ti	W	Nb	others
A 286	F	26	15	-	1.3	0.2	2.0	-		Fe base, 0.05C, 0.015B
IN 706	F	41.5	16	-	0.5	0.2	1.0	-	2.9	Fe base, 0.03C,
Waspaloy	F	b	19.5	13.5	4.3	1.3	3.0	-	-	0.08C, 0.006B, 0.06Zr
Udimet 720 (PER 72)	F, P	b	17.9	14.7	3.0	2.5	5	1.3	-	0.03C, 0.033B, 0.03Zr
Merl 76	P	b	12	18.5	3	5	4	-	1.5	0.02C, 0.5Hf
René 88DT	P	b	16	12.7	4	2.15	3.7	4	0.7	0.05C, 0.05Zr
N18	P	b	11.2	15.6	6.5	4.4	4.4	-		0.13Fe, 0.03Zr, 0.5Hf, 0.015B, 0.018C
IN 718	F	b	19	-	3	0.6	0.8		5.2	19Fe
MA6000	P	b	15	-	2.0	4.5	2.5	4.0	-	2.0Ta, 0.05C, 0.01B, 0.15Zr, 1.1Y2O3
ZhS6F	C	b	5.5	9.4	0.9	5.3	1.0	12.0	1.6	0.11C, 0.9V, 0.9Hf
VZhL12U	C	b	9.5	13.5	3.1	5.4	4.4	1.4	0.75	0.17C, 0.75V

F : Forged, C : as Cast, P : Powder Metallurgy.

NUCLEAR GRAPHITE FOR HIGH TEMPERATURE REACTORS

B.J. MARSDEN
AEA Technology,
Risley, Warrington, Cheshire,
United Kingdom

Abstract:

The cores and reflectors in modern High Temperature Gas Cooled Reactors (HTRs) are constructed from graphite components. There are two main designs; the Pebble Bed design and the Prism design, see Table 1. In both of these designs the graphite not only acts as a moderator, but is also a major structural component that may provide channels for the fuel and coolant gas, channels for control and safety shut off devices and provide thermal and neutron shielding. In addition, graphite components may act as a heat sink or conduction path during reactor trips and transients. During reactor operation, many of the graphite component physical properties are significantly changed by irradiation. These changes lead to the generation of significant internal shrinkage stresses and thermal shut down stresses that could lead to component failure. In addition, if the graphite is irradiated to a very high irradiation dose, irradiation swelling can lead to a rapid reduction in modulus and strength, making the component friable.The irradiation behaviour of graphite is strongly dependent on its virgin microstructure, which is determined by the manufacturing route. Nevertheless, there are available, irradiation data on many obsolete graphites of known microstructures. There is also a well-developed physical understanding of the process of irradiation damage in graphite. This paper proposes a specification for graphite suitable for modern HTRs.

HTR graphite component design and irradiation environment

The details of the HTRs, which have, or are being, been built and operated, are listed in Table 1. A feature of the present designs is that to optimise the power output, an annular core is proposed. This annular core configuration tends to increase the dose to the graphite reflector. The fast neutron flux reduces exponentially with distance into the reflector thus increasing the thermal flux.

During reactor operation, neutron flux and thermal gradients in the graphite components, including the reflector, can lead to component deformations, bowing and the build up of significant shrinkage and thermal stresses.

TABLE 1. HIGH TEMPERATURE GAS COOLED REACTORS

Reactor	Type	MW(t)	MW(e)	Helium Pressure (bar)	Inlet Temperature	Outlet Temperature	Criticality	Shutdown
Dragon	Prism	20		20	350	750	1966	1976
Peach Bottom	Prism	115	40	24	340	715	1967	1974
Fort St, Vrain	Prism	842	330	48	405	780	1974	
HTTR	Prism	30		40	395	950	1999	
GT-MHR	Prism	600		71	288	704		
AVR	Pebble	46	15	11	260	950	1967	1988
THTR	Pebble	750	300	40	250	800	1985	1989
HTR-10	Pebble	10		30	300	900		
PBMR	Pebble	265	110	70	560	900		

In addition the operation of these reactors at high temperature for many years could lead to degradation of the graphite material properties.

The design of the HTR graphite cores must account for these thermal, irradiation conditions. Some of the issues are common to both the prism and pebble bed designs, others are specific to the type of reactor. These design issues are discussed below.

HTR core — prism design

The prism design is best illustrated by the Fort St. Vrain design as described by Neheig, (1972). The main features are the permanent reflector, surrounded by boronated carbon shielding, a replaceable graphite reflector and the hexagonal graphite fuel elements.

Permanent reflector

Although the irradiation fast neutron flux is significantly reduced from the peak value by the time it reaches the permanent reflector, these components must last for the life of the reactor. Therefore the dose the permanent reflector sees may be significant towards the end of life.

The permanent reflector components have to be designed in such a way that the structure remains "gas tight" and that thermal and neutron streaming are minimised. This has to remain the case throughout life and during all thermal and pressure transients, for both normal and emergency operation.

Most designs use graphite keying systems and dowels to keep the components located together. The columns of graphite bricks are usually free standing as individual columns of blocks. This is important as it avoids gapping due to differential thermal expansion and irradiation growth between columns arising from variations in material properties and irradiation behaviour that would occur in a "brick wall" type bonded system.

It is important to provide side restraints for the columns using systems of springs or garters or other support systems. The first major issue connected with the restraint system is the low coefficient of thermal expansion of graphite compared with steel ($\sim 4 \times 10^{-6}\ K^{-1}$ for graphite compared with $\sim 18 \times 10^{-6}\ K^{-1}$ for steel). The second is the large axial and radial temperature distributions within the graphite components that would cause the columns to bow outwards if no radial restraint were provided. The third is the irradiation shrinkage and growth that also leads to column bowing. As changes in the dimensions of graphite components due to thermal gradients and irradiated-induced dimensional changes cannot be prevented, the result of restraining the distortion leads to column kinking which could lead to gas leakage and thermal and neutron streaming if the design did not take this into account. It was small movements of the reflector and fuel element in Fort St. Vrain that led to redistribution of the coolant flow. These resulted in significant changes in fuel outlet temperatures and steam generator inlet temperatures that in turn caused power fluctuations that prevented the achievement of full power operation. To resolve this problem constraining devices were installed on the upper elements (Brey et al., 1982).

In the prism type of reactor design, the permanent reflector receives much less dose than the replaceable reflector. For this reason lower grade graphites were used in Fort St. Vrain and in the HTTR. However, care must be taken in selecting these lower grade graphites as the higher levels of impurities may lead to an increase in decommissioning costs, as discussed later.

Replaceable reflector

The replaceable reflector is normally constructed from blocks of graphite of similar dimensions to the fuel elements. The grade of graphite used in Fort St. Vrain was of a lower grade than that of the fuel. The side replaceable reflector elements were solid, but the upper and lower replaceable reflector had coolant holes and control rod holes. As these components have large flux, and possibly large temperature gradients, across their width and length it is possible that they will become significantly distorted and bowed after several years of operation. This may require prompt replacements, as it was bowing of the replaceable reflector and delaying its replacement that caused problems with fuel removal in the final years of the DRAGON project.

In deciding on the graphite grade for the replaceable reflector, it is important not only to consider the implications for activation of the graphite, but also to consider the cost of obtaining irradiation data to sufficient dose for use in life extension and safety cases. This exercise may be so costly that use of good quality fuel element graphite for the replaceable reflector may be a cheaper option in the long term.

For early permanent moderator prism reactor designs (no longer considered) Blackstone (1969) gives a peak dose of 200×10^{20} n/cm^2 EDND for a 30 year life time at temperatures between 450-800^{o}C. Clearly a reflector element changed once during its lifetime could only see one quarter of this dose on the side against the fuel.

Fuel elements

There have been various fuel element designs for prism fuel. The behaviour of the individual fuel particles and the compact material in which they are encased are not considered here. However, it should be noted that although the graphite technology associated with the particles and compact is related to that of the main moderator graphite there are differences as non-graphitised materials and possibly natural graphites are used in these fuel items.

The graphite fuel moderator blocks remain in the reactor for much shorter periods than the reflector. However the temperature and flux that they see is more onerous. The blocks may contain passages for the coolant gas and the control rods, as well as holes for the fuel elements and possible burnable poisons.

The large temperature and flux gradients between holes can give rise to significant shrinkage and thermal stresses leading to cracking. For this reason the design and through-life stressing of the graphite prism fuel blocks is important. Three –dimensional assessments are required due to possible end effects in the length of the blocks.

Table 2 gives the doses and temperatures quoted for the lifetime of HTR prism fuel taken from various sources.

Upper and lower graphite structures

Fort St. Vrain is supported on keyed support blocks and post structures in the lower gas outlet plenum. However modifications were suggested for later designs to better resist seismic loading and thermal strains (Peinado, 1982). Above the core there is an upper plenum for the inlet gas, however there is no graphite lining for this structure.

TABLE 2. DOSES AND TEMPERATURES FOR HTR PRISM FUEL

Reactor	Temperature Range ^{o}C	Dose × 10^{20} n/cm^2 EDND
UK Mark II		
Fort St. Vrain Maxiumum[#]	1150	53.6
Fort St. Vrain Median[#]	700 – 950	16.75
Peach Bottom[***]	400-800	30-40 (max)
NP-MHTGR[*]	200 and 1300	30
HTTR[**]	800-1000	10

[*]Graphite data requirement for the whole of the reactor.
[**] Ishihara et al (1998)
[***] Everett et al. (1969)
[#] Nehrig et al. (1972)

HTR – Pebble bed design

A typical design of a pebble bed reactor is described by Lohnert and Reutler (1982).

Side reflector

In the pebble bed design the main graphite component to consider from a life-time point of view is the side reflector only. In some earlier designs, as in AVR, there were also graphite "noses" which protruded into the core. The purpose of these noses was to house the control rods, allowing them to be positioned some distance into the core. These noses are no longer a feature of the latest pebble bed designs which have annular core configurations. One of the reasons for the removal of the noses from the design was the high dose environment that they would operate in would probably lead to the need to replace them several times during the reactor life.

The replacement of the reflector in a pebble bed design would be a major undertaking. However, this is being considered in some of the latest designs. The following information is reported on the lifetime dose for pebble bed type cores:

1. From the Dragon programme 140.0 × 10^{20} n/cm^2 EDND with a peak temperature of 900^{o}C for a 30 year life (Blackstone, 1969)
2. For the AVR reflector 50 × 10^{20} n/cm^2 EDND at 650^{o}C, 12 × 10^{20} n/cm^2 EDND at 1000^{o}C (Haag et al, 1986)
3. For the later designs of German pebble bed reactors 300-400 × 10^{20} n/cm^2 EDND at 730-880^{o}C (Schmidt, 1979).

In AVR the coolant flow was upwards with the return flow passing outside the reflector blocks as was the case in the THTR, where the flow was downwards. However, in the concept for the modular HTR (Lohnert and Reutler, 1982) very large blocks of graphite are used for the reflector, containing holes for the return coolant flow, control rods and small absorber spheres (KLAK-system). The control rod holes are very close to the core boundary where the flux and temperature gradients are high. This can lead to unacceptable shrinkage and stresses at these holes. Various ways have been investigated of overcoming this problem, including slitting the hole, through to the core, to avoid component failure (Schmidt, 1979). This may necessitate the use of graphite sleeves to prevent bypass of the control rod coolant gas. In

addition graphite sleeves may be used in the return gas holes to prevent large temperature gradients and excessive cooling of the large graphite reflector blocks. Another feature of the blocks in the pebble bed design is saucer shaped indentations in the reactor side face of the lower core. These indentations act as “disturbances” to prevent bridging of the outer layers of fuel that may cause these layers to stay longer in the reactor than would be desirable.

The blocks are joined together by a system of graphite dowels and keys and have similar restraint problems related to thermal expansion and dimensional change as discussed for the prism reactor core as discussed above.

The high dose at the surface of the reflector block may cause some of the graphite to be irradiated through shrinkage and “turn-around” until the swelling is much greater than the original volume. At this stage the graphite structure will have started to disintegrate and it is possible that some of the graphite will become so friable that the fuel balls will rub the surface away. Several solutions have looked into solving this problem including sacrificial layers. Another way may be to return to the single zone core with noses and replace the noses at regular intervals.

Lower core, inlet and outlet plenum

The present modular pebble bed designs have both the inlet and outlet ducts at the bottom of the reactor pressure vessel. This arrangement avoids any chimney effect in the extremely unlikely event that the inlet/outlet duct should shear and allow air ingress.

Although the irradiation dose is low at the bottom of the core, there may be large temperature gradients that have to be accounted for. In addition there are gas outlet holes, or slots, that may be subject to compressive loading from the pebbles.

Deeper into the lower core structure the inlet and outlet plenum may pose design problems related to the temperature differences between the inlet and outlet gas. In addition the many paths through the graphite taken up by the inlet and outlet holes, the KLAK systems and the control rod holes can also lead to design problems.

Reflector roof and upper inlet plenum

The irradiation dose to the upper structure is low, however there may be stressing problems related to temperature gradients.

The present pebble bed designs use graphite components for the roof structure and the upper plenum. Roof designs have been either cantilevers as in the HTR module or structures hung from upper structures by metal hangers as in THTR. Both designs have advantages and disadvantages related to component reliability, connectivity with the side reflector and the many holes required for the inlet gas and the control mechanisms.

Graphite manufacture

The starting point in production of graphite is the selection of a suitable coke. These cokes are produced as by-products from the petroleum or coal industry or from naturally occurring pitch sources. These cokes vary considerably in their structure, size and purity.

After production the cokes are broken up and calcined at temperatures between 900-1300^{o}C to drive off volatile material and reduce the amount of shrinkage in the later processes. The calcined cokes are then crushed, milled and graded before being supplied to the graphite manufacturer. It is the choice of the particular coke size, purity and structure that decides the virgin and irradiated properties of the final product.

A suitable blend of coke grades are then mixed with a binder, usually a coal tar pitch. In addition a crushed graphite flour may be added. The coke particles are often referred to as filler particles.

The mixture is then formed into blocks often referred to as the "green article". Various methods of forming are used and the method chosen has an influence on the properties of the final product. The methods are discussed below:

1. The most common method of production is by extrusion. In this method the mixture is forced through a die under pressure. This method can be used to produce blocks of various sections and of reasonably long lengths. Blocks of the order of 500 mm square by 3600 mm long can be produced in this way. It is important that the extrusion pressure and rate is carefully controlled in order to maintain the desired quality. Graphites produced in this way have anisotropic material properties due to alignment of the filler particle grain, however it is possible to produced reasonably isotropic using this method.
2. Moulding or pressing. This method is used to produce a very isotropic product. The blocks are moulded or pressed from one or two directions at the same time. The AGR graphite moderator blocks were produced using this technique.
3. Iso-static moulding is a more sophisticated method in which the coke and binder mixture is contained in a rubber bag and external pressure applied to give a uniform pressure from all sides.
4. Finally there is vibration moulding. In this method the graphite mixture is placed in a mould, which is vibrated to compact the mixture. Next the graphite mixture is pressed from one side and vibrated again whilst under load.

There are other variations on these methods.

Having formed the 'green article', which is reasonably soft, it is rapidly cooled by immersion in water. The green article is then baked at a temperature of around 800^{o}C to drive off more volatile material and 'coke' the binder. To prevent oxidation, the blocks are encased in a granular packing, usually a coke. This allows for expansion and helps to support the shape of the green article. This is a long process and may take 30-70 days. One difficulty that arises at this stage is that the thermal conductivity of the graphite is very low, ~30 W/m/K and on cooling thermal gradients in the blocks may lead to internal cracking. One method of overcoming this problem is to add crushed scrap graphite to the mix. However, this has implications for the irradiation behaviour of the final product as discussed later.

The baking process will produce gas evolution pores throughout the structure as volatile gases are driven off. Much of this porosity will be open. To increase the density the baked blocks may be impregnated with a pitch under vacuum in an autoclave. This pitch is much less dense than the binder pitch. To help with this process the surface of the block may be broken by rough machining or by grit blasting. This allows the pitch to enter the open porosity more readily. After impregnation the blocks are re-baked for a much shorter period. There may be up to four impregnations used; however the gain in density for each subsequent impregnation is much less. The product can now be regarded as carbon blocks, which can be used as an

insulation material or furnace liner. However for this application they are usually baked at a higher temperature ~1100^{o}C.

The carbon blocks are now ready for graphitisation. There are two methods of graphitisation commonly used. The original method is to use an Acheson furnace. This is a large open furnace, which may be up to 7 m wide by 20 m long, into which the carbon blocks are stacked and covered in an electrical conducting coke. A large electric current is applied to each end of the bed through water-cooled electrodes and the blocks are taken through a temperature cycle to ~3000^{o}C. This process can take about 15 days.

Another, more modern, quicker and cheaper method of graphitisation is to stack the carbon blocks in long lines so that they touch. Again the blocks are covered in coke to prevent oxidisation, but this time the current is applied directly through the carbon blocks and not through the packing material. This method can only be used for blocks of similar cross-sections.

During this graphitisation period the graphite crystals are formed and the material becomes much softer and more easily machined. The electrical and thermal conductivity dramatically improve and many more impurities are driven off.

If a more pure product is required the graphite blocks can be reheated to ~2400^{o}C in an Acheson furnace with a halogen gas passed through it. However, this final process could add up to 30% to the cost of the graphite. This process of graphite production is summarised in Fig. 1

Polycrystalline graphite microstructure

As discussed above, the final polycrystalline microstructure is determined by the structure of the coke and the binder phase and also by the manufacture process.

At the crystallite level the graphite has strong hexagonal basal planes with much weaker bonding between the planes. For perfect graphite crystals the ‘d’, or inter-layer, spacing has been measured to be 3.3539 Å (0.33539 × 10^{-9}m) with an ‘a’ spacing of 2.46 Å (0.246 × 10^{-9}m). The ‘c’ spacing is twice that of the ‘d’ spacing.

The size of the crystallites can be measured by x-ray diffraction and has been found to give values of between 400 and 800 Å for L_a and L_c is well graphitised material (Reynolds, 1968).

In the ‘c’ direction the size of the crystallite is limited due to so call “Mrozowski” cracks which are formed during cooling from the graphitisation temperature (~3000^{o} C), see Fig. 2. The mechanism, which leads to the formation of these cracks, is due to the large difference in the coefficient of thermal expansion in the two crystallographic directions (α_a =~26.5 × 10^{-6} K^{-1} , α_c =~-1.5 × 10^{-6} K^{-1}). At a temperature of around 1800^{o}C the structure hardens and the much larger shrinkage in the ‘c’ direction coupled with the restraining affect of the rest of the structure leads to horizontal cracking in the basal planes. Various estimates of the size of Mrozowski cracks have been given, however, in practice there are probably cracks of a variety of widths ranging from less than 250 Å upwards.

It is this cracked structure that gives graphite its good thermal shock resistance, allowing large crystal expansion in the ‘c’ direction without leading to inter-crystalline cracking. These

cracks also provide accommodation spaces that can be taken up by irradiation-induced crystal growth and play an important role in determining component property changes in reactor.

Beyond this scale, the cracked crystallite structures are jointed together and follow the general shape of the coke particle. There are also many larger cracks and fissures which also tend to follow the coke particle shape. Examples of this are illustrated in Figs 3. It can be envisaged that the general alignments of the 'a' axis is with the "flow" of the coke particle with the 'c' axis perpendicular to this direction. It can also be envisaged that the shape, size, distribution and orientation of the coke particles will strongly influence the material property of the final graphite component.

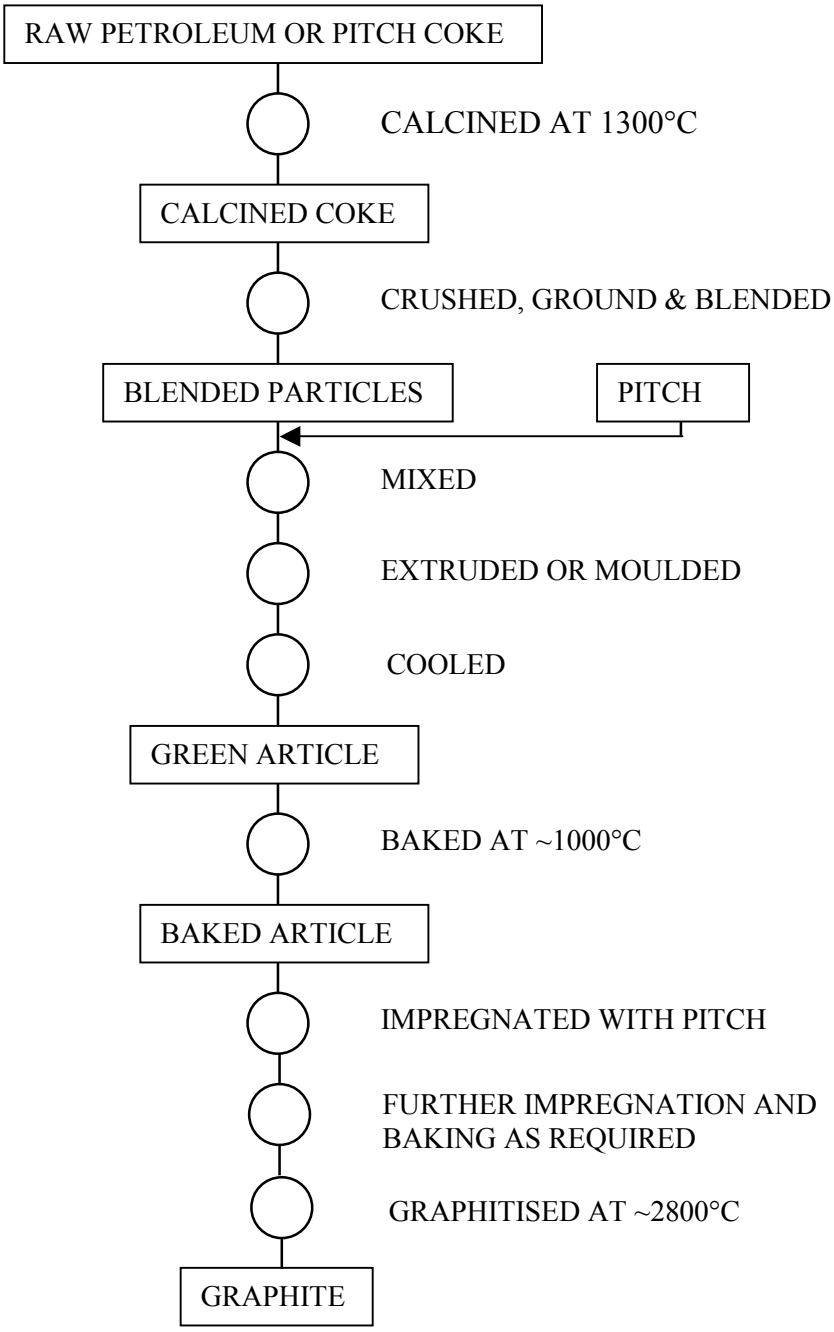

FIG. 1. Graphite manufacturing process.

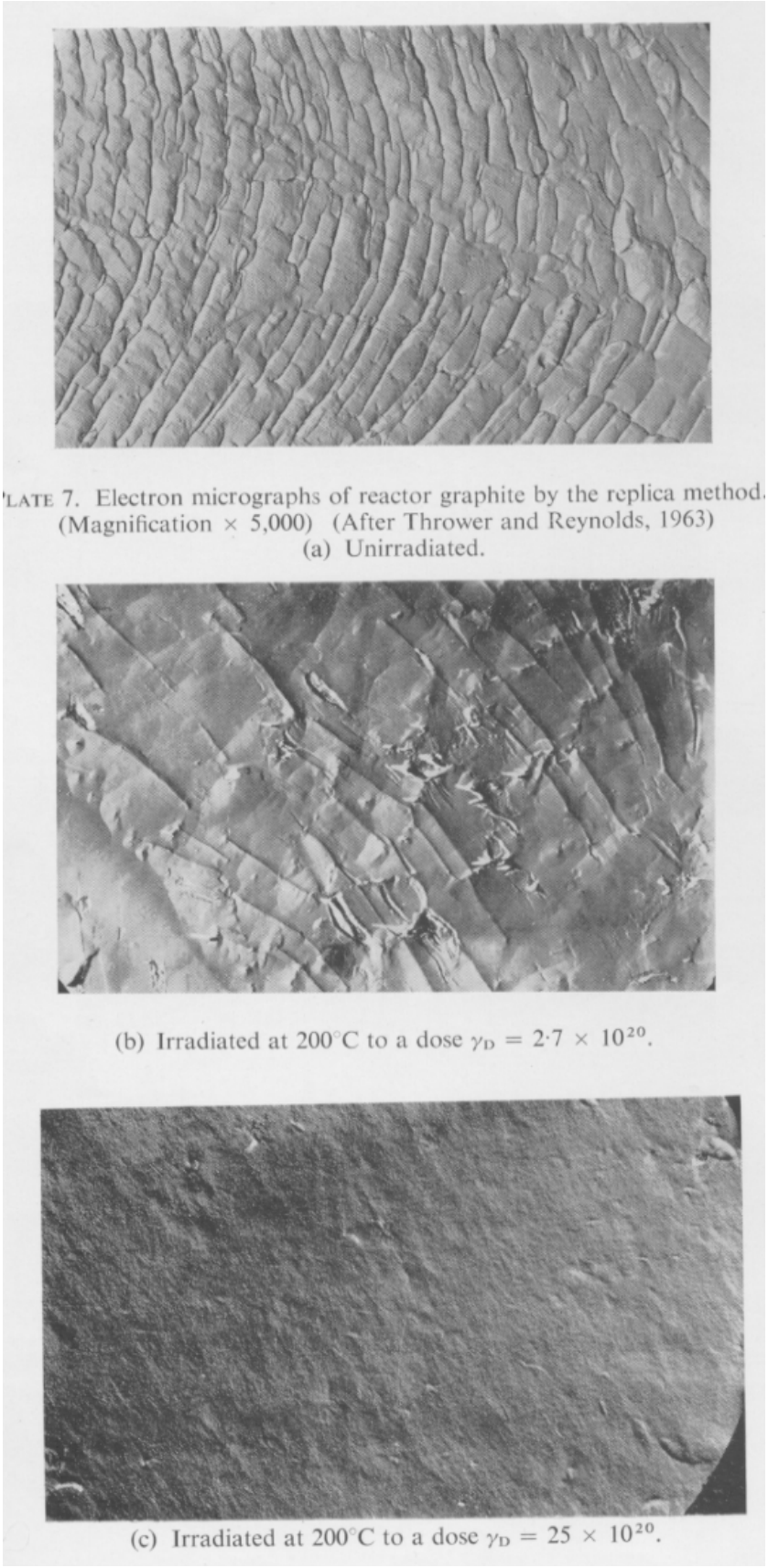

PLATE 7. Electron micrographs of reactor graphite by the replica method.
(Magnification × 5,000) (After Thrower and Reynolds, 1963)
(a) Unirradiated.

(b) Irradiated at 200°C to a dose $\gamma_D = 2{\cdot}7 \times 10^{20}$.

(c) Irradiated at 200°C to a dose $\gamma_D = 25 \times 10^{20}$.

FIG. 2. Microcracks in the graphite crystallite structure.

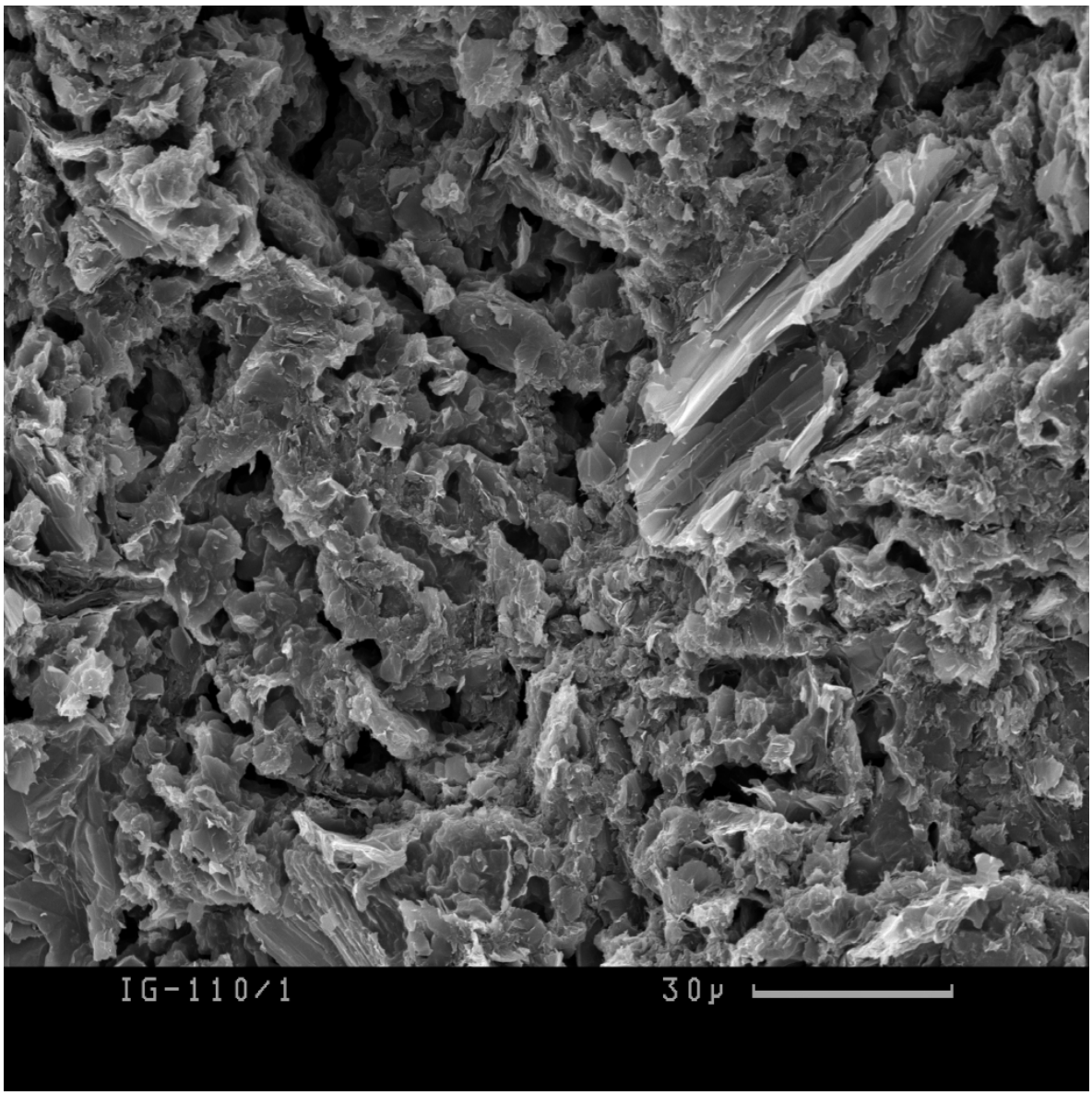

FIG. 3. Micrograph of pitchcoke graphite.

During manufacture the graphite coke particles may have been ground and blended to give a uniform mix. They may be lenticular or needle like in shape or in some special cases spherical. In the UK the Pile Grade A graphite, used in the Magnox reactors was manufactured from a needle coke. Graphite produced from these needle type coke particles is very anisotropic with an anisotropy ratio in the region of 2. The most famous of the graphites with spherical structures is Gilsocarbon graphite which as manufactured from naturally occurring pitch found in remote parts of Utah in the USA. These coke particles formed spheroids with the 'c' crystallographic direction lying mainly in the radial direction and the 'a' crystallographic direction mainly in the hoop. Graphites formed from Gilsocarbon coke had semi-isotropic properties.

Some modern graphites are manufactured from finely ground coke particles, this also can produce semi-isotropic properties.

The coke particles are usually bound together using a pitch binder. The binder itself will probably be mixed with a "flour" consisting of finely ground coke and possibly scrap

graphite. The baked structure may have also have been impregnated once or twice to increase the overall density. Features that are of interest are the randomly ordered, well-structured, small particles and the large gas evolution pores.

The orientation of the coke particles in the bulk product is strongly influenced by the forming process. Many types of graphite are manufactured by extrusion which tends to align the coke particles. Other processes described above that can give more isotropic structures are compression moulding and isostatic moulding.

Graphite requirement specification

Density

For a given amount of output, the higher the density of the moderator, the smaller the volume of the core, thus a high-density graphite is desirable. The theoretical density of graphite crystals is 2.265 g/cm^3, however polycrystalline graphites have a much lower density due to inter-crystalline porosity. Early nuclear graphites had typical densities of 1.6 g/cm^3, the second generation of graphite moderated reactors used graphites with densities around 1.72 g/cm^3 and the third generation 1.82 g/cm^3. Modern nuclear graphites have not improved over this latter figure.

The importance of crystallinity

In theory, from a nuclear point of view, any carbon could be used as a moderator if it could be packed to the required density in the required nuclear configuration. However, the availability, and structural properties, of relatively pure artificial graphite led to its use as a moderator in the first graphite moderated nuclear reactors.

These artificial graphites were essentially electrodes used in the steel industry and their purity relied on the choice of raw materials (filler coke and binder) and the manufacturing process and heat treatments to drive off unwanted volatile impurities.

The method used by the graphite manufacturers to determine the degree of crystallinity (or graphitisation) is to measure the electrical resistivity. At room temperature the electrical resistivity can be directly related to the thermal conductivity by the Wiedemann Franz law:

$$\text{Thermal conductivity (kcal/m.h.}^{\circ}\text{C)} = \frac{0.1116 \times 10^6}{\text{Resistivity}(\mu\Omega\text{cm})}$$

The importance of good crystallinity to the nuclear industry is that it gives an indication of:

a) a high virgin thermal conductivity
b) lower crystallite irradiation induced growth than would be the case in poorly graphitised material
c) lower irradiation induced material property changes (this follows from above)
d) high purity levels
e) good machinability.

Nuclear graphite should have a thermal conductivity of around 140 W/m/K, when measured at room temperature.

Dimensional stability

In addition to good crystallinity, polycrystalline graphite components have another requirement to ensure dimensional stability. This is related to the way the randomly orientated crystals in a porous material interact as they grow and shrink with irradiation. Simmons (1965) demonstrated that there was an empirical relationship between dimensional change rate and the Coefficient of Thermal Expansion (CTE) (The higher the coefficient of expansion the less the dimensional change rate). He also derived a theoretical relationship between dimensional change rate and the coefficient of thermal expansion (Marsden, 1998). However this relationship breaks down at comparatively low doses.

It was also found that extruded course grain graphites that have anisotropic material properties tended to have lower CTEs than more isotropic graphites. However, it was also observed that some isotropic graphite with very high CTEs expanded with irradiation.

From experience it is desirable to choose a graphite with a coefficient of expansion between 4.0 and 5.5×10^{-6} K^{-1} measured over the range 20-120^{o}C.

Air reactivity (thermal oxidation in air)

In the unlikely event of an incident involving air ingress, it is important that the air reactivity, that is the rate at which graphite can oxidise in air, is as low as possible. Irradiation increases the air reactivity rate in graphite, however this effect is minimal compared to the increase in air reactivity caused by catalytic impurities.

For the AGRs the mean reactivity in air of samples was specified as not exceeding 3×10^{-6} g/g/k at 400 ^{o}C (Hutcheon and Thorne, 1965).

Absorption cross-section

For the particular HTR design the nuclear physics considerations will lead to the values of absorption cross sections required. However, historically there has been no systematic effort put into determining a specification for the absorption cross-section in graphite.

The early plutonium production reactors built in the UK used various graphites with nuclear abortion cross-sections of between 4.7 and 5.1 mbarn. The later military and civil carbon dioxide cooled reactors used Pile Grade A (PGA) graphite with an absorption cross-section of 4.0 mbarn. For this reason an upper limit for boron of 0.2 ppm was specified. The method used to measure the absorption cross section was to place graphite samples, or whole blocks in some cases, in a test reactor such as GLEEP in the UK.

Later when the AGRs were designed it was recognised that the major impurity atom contributing to the absorption cross section in graphite was ^{10}B which burnt up rapidly early reactor life. For these later reactors the absorption cross-section was calculated from the chemical inventory, however the value arrived at depended on what impurities were measured and the choice of measurements was somewhat arbitrary.

As previously discussed it is clear that in the past no systematic effort has been made to define a specification related to the impurity levels related to absorption cross-section. The author considers that a list of elements with significant absorption cross-sections should be identified

as part of a graphite specification. The graphite manufacturer could then be asked to analyse their product for these elements.

Impurities related to operational and decommissioning problems

The radioactivity associated with graphite components arises from initial impurities and from subsequent contamination within the reactor circuit.

Probably the most important isotopes related to initial contamination will be ^{60}Co, ^{154}Eu, ^{3}H, ^{36}Cl, ^{41}Ca and ^{14}C , however this is not an exhaustive list and a more rigorous approach is required as discussed below.

An IAEA TechDoc (Marsden, 2001) is being prepared at present on the subject of decommissioning graphite reactors which gives much more detail concerning the problems related to disposal of nuclear graphite.

Releases during operation

In the UK, graphite reactors such as the AGRs and Magnox have to monitor the release of certain isotopes. Some of these radionuclii, such as ^{36}Cl, ^{14}C and ^{3}H, may be related to the release of products from the graphite core. Again a definitive list of undesirable isotopes, which may be released from graphite, is required, taking account of regulations in the country where the reactor is to be constructed. The likely origins of these radionuclii can then be determined to give a list of undesirable impurities from an operational point of view. Information will also be required as to how easily these radionuclii can be released from the graphite structure during operation.

Decommissioning

Similarly a list of the most undesirable radionuclii with regard to the long-term risks associated with waste disposal can be obtained from the appropriate authorities, such as NIREX in the UK. Then the route that can produce these radionuclii can be determined to give a comprehensive list of undesirable elements from a decommissioning point of view.

Strength

In a modern reactor, the strength of the graphite is important, as it may be subjected to shrinkage and thermal stresses, as well as restraint loads and possible seismic impact loads during the life of the reactor. Irradiation modifies graphite strength, as does thermal and radiolytic oxidation.

Graphite is stronger in bend than tension and stronger in compression than bend. As with many brittle polycrystalline materials, the failure strength depends on the component geometry, loading configuration and component size. Unfortunately at present there is no satisfactory failure model for unirradiated, or irradiated, graphite which makes it difficult to predict the behaviour of graphite components in the future.

Proposed Specification for HTR Graphite

1. The graphite should be reasonably dense ~1.8 g/cm^3.

2. It should be well graphitised as indicated by a thermal conductivity of ~145 W/m/K measured at room temperature.
3. It should have a low absorbtion cross-section, between 4 and 5 mbarns. (This can be calculated from knowledge of the chemical impurities).
4. Impurities that could possibly lead to operational problems and high decommissioning costs must be kept to a minimum.
5. The graphite must have a high irradiation dimensional stability. This is indicated by a relatively high CTE(20-120^{o}C) between 4.0 and 5.5 × 10^{-6} K^{-1}.
6. The irradiation time, over the irradiation temperature of interest, for the graphite to return to its original volume should be as long as possible. (In the long term a Material Test Reactor (MTR) programme can only confirm this.)
7. The graphite must have a moderately high strength (A tensile strength of about ~20 MPa).
8. The air (moisture) reactivity should be measured to ensure that the rates are acceptable (0.2 to 0.01 mg/g-h).
9. A suggested list of chemical impurities that should be minimised is given in Table 6. This list is based on past experience and should be reviewed in the light of local requirements for decommissioning and operation.

TABLE 6. GRAPHITE IMPURITIES THAT ARE CONSIDERED TO BE INCOMPATIBLE FOR REACTOR OPERATION AND FINAL DECOMMISSIONING AND DISPOSAL

Element	**Symbol**	**Element**	**Symbol**
Aluminium	Al	Mercury	Hg
Antimony	Sb	Manganese	Mn
Arsenic	As	Molybdenum	Mo
Beryllium	Be	Nickel	Ni
Barium	Ba	Chlorine	Cl
Boron	B	Potassium	K
Bismuth	Bi	Phosphorous	Pb
Cadmium	Cd	Platinum	Pt
Caesium	Cs	Selenium	Se
Calcium	Ca	Samarium	Sm
Chromium	Cr	Silver	Ag
Cobalt	Co	Silicon	Si
Copper	Cu	Sodium	Na
Gold	Au	Tantalum	Ti
Indium	In	Tin	Sn
Hafnium	Hf	Sulphur	S
Lead	Pb	Titanium	Ti
Dysprosium	Dy	Tungsten	W
Europium	Eu	Vanadium	V
Iron	Fe	Zinc	Zn
Gadolinium	Gd	Strontium	Sr
Lithium	Li	Halogens	
Magnesium	Mg	Rare earth metals	

Conclusions

Unirradiated and irradiated graphite material properties depend strongly on the choice of the raw materials and the manufacturing process. Suitable graphite for modern HTRs can be designed based on the choice of coke, binder and manufacturing technique. However a compromise is always necessary. A suggested specification for HTR graphite is given.

BIBLIOGRAPHY

Blackstone R, Graham L W, Everett M R, Delle W. Irradiation data on Gilsocarbon graphites for high temperature nuclear reactors. DP Report 646. April 1969.

Brightman F G. Development of sampling and assay methods for WAGR radwaste. CEC Report EUR 13254, 1991

Brey H L, Olson H G. The Fort St. Vrain quality assurance programme. Gas Cooled Reactors Today, BNES Conf. Bristol, Vol. 1, pp. 103-105, 1982.

Brey H L. Fort St. Vrain experience. Gas Cooled Reactors Today, BNES Conf. Bristol, Vol. 1, pp. 35-39, 1982.

Engle G B. Assessment of Grade H-451 graphite for replaceable fuel and reflector elements in HTGR. GA-A14690, UC-77, 1977.

Everett M R, Blackstone R, Graham L W, Manzel R. Graphite materials data for high temperature nuclear reactors. DP Report 699, 1969

Haag G, Delle W, Kirch N, Nickel H. Results of visual in-pile inspection of the inner graphite reflector of AVR. IAEA Specialist's meeting on Graphite Component Structural Design. Japan, July 1986

Hutcheon J M, Thorne R P. Improved graphite for nuclear purposes. Second conference on Industrial carbon and graphite. Soc. Chem. Ind. pp. 441-445, London 1965.

Ishihara M, Hanawa S, Iyoku T, Mogi H. Study on structural integrity of core graphite components in nuclear reactor. Int. Sym. Carbon 1998, Tokyo.

Lohnert G H, Reutler H. A new design of a HTR pebble bed reactor. Gas Cooled Reactors Today, BNES Conf. Bristol, Vol. 1, pp. 265-269, 1982.

McKee D W. The catalysed gasification reactions of carbon. Chemistry and physics of carbon. Vol. 16, 1965

Marsden B J, Arai T, Hopkinson K L. Validation of a model on irradiation induced porosity evolution in gas cooled reactor graphites. AEAT-3212, 1998 (unclassified).

Marsden B J. Characterisation, treatment and conditioning of radioactive graphite from decommissioning of nuclear power plants. IAEA TechDoc. To be published 2001.

Nehrig D A, Neylan A J, Winkler E O. Design features of the core and support structures for the Fort St. Vrain nuclear generation station. Graphite Structures for Nuclear Reactors. Inst. Mech. Eng. March 1972.

Peinado C O, Wunderlich R G, Simon W A. HTGR nuclear heat source component design experience. Gas Cooled Reactors Today, BNES Conf. Bristol, Vol. 1, pp. 107-112, 1982.

Reynolds W N. Physical Properties of Graphite. Elsevier 1968.

Schmidt A. Analysis of the stresses in a side reflector block of the Pebble reactor. IAEA Specialist meeting on mechanical behaviour of graphite for HTRs. France June 1979.

Simmons J H W. Radiation damage in graphite. Pergamon Press. 1965.

White I F, Smith G M, Saunders L J, Kaye C J, Martin T J, Clarke G H, Wakerley M W. Assessments of management modes for graphite from nuclear reactor decommissioning. EUR 9232 En., 1984

AUXILIARY BEARING DESIGN CONSIDERATIONS FOR GAS COOLED REACTORS

S.R. PENFIELD, Jr.
Technology Insights,
Carthage, Tennessee

E. RODWELL
EPRI,
Palo Alto, California

United States of America

Abstract:

The need to avoid contamination of the primary system, along with other perceived advantages, has led to the selection of electromagnetic bearings (EMBs) in most ongoing commercial-scale gas cooled reactor (GCR) designs. However, one implication of magnetic bearings is the requirement to provide backup support to mitigate the effects of failures or overload conditions. The demands on these auxiliary or "catcher" bearings have been substantially escalated by the recent development of direct Brayton cycle GCR concepts. Conversely, there has been only limited directed research in the area of auxiliary bearings, particularly for vertically oriented turbomachines. This paper explores the current state-of-the-art for auxiliary bearings and the implications for current GCR designs.

1. INTRODUCTION

With continued progress in power electronics and controls technologies, magnetic bearings are finding increased acceptance in specialized applications where their unique characteristics offer particular advantages. One such application is high-temperature gas-cooled reactors (GCRs), which employ high-purity helium as the working fluid. In GCRs, magnetic bearings provide a practical means for eliminating the necessity of rotating seals and for avoiding the potential contamination associated with conventional bearing lubricants. Well-designed magnetic bearing installations are also demonstrating high reliability in large conventional turbomachinery applications, such as pipeline compressors and turbo-expanders.

Given the above, there are compelling incentives for magnetic bearings in GCRs. However, a consequence of their selection is the need to provide backup support to mitigate the consequences of primary bearing failures. Further, while auxiliary bearings are a common feature in all machines with magnetic bearings, there is little in the present literature addressing their design and implementation. In addition, GCR applications pose particular challenges for the following reasons:

1. The tribological characteristics of materials in dry helium tend to be more difficult due to the potential for self-welding
2. The more recent evolution of direct Brayton cycle GCR's has increased the size of the turbomachinery and, thus, heightened the technical challenges associated with both magnetic and auxiliary bearings.
3. GCR designs with vertical turbomachines pose even greater demands on the axial auxiliary bearing.

With increasing worldwide interest in GCR's, EPRI has launched a supporting initiative with the initial objective of exploring areas where focused research could best facilitate

GCR development. The technology of catcher bearings is one such area, and this paper summarizes preliminary results of the EPRI sponsored evaluation. While current GCR turbomachine designs include both horizontal and vertical variants, the focus of the preliminary evaluation has been on vertical machines, due to their more demanding technical requirements and the relative timing of the associated project initiatives.

The remainder of the paper begins with a review of key parameters that will drive the design of auxiliary bearings for the two commercial-scale GCR projects. Next, the principal design considerations associated with auxiliary bearings are outlined and various auxiliary bearing types are described, along with their advantages and disadvantages. With this background, the requirements for GCR auxiliary bearings are compared with the existing experience base. Finally, some preliminary observations are offered regarding an integrated approach to bearing design and the need for additional research and development.

2. TURBOMACHINE CHARACTERISTICS IN CURRENT GCR PROJECTS

At present, the two active GCR projects of commercial scale are the Pebble-Bed Modular Reactor (PBMR) Project, based in South Africa and the US/Russian Federation Gas-Turbine Modular Helium Reactor (GT MHR) Project, which is largely being developed in Russia. The designs being advanced by both of these projects apply the direct gas-turbine (Brayton) cycle for power conversion, with the primary coolant, helium, serving as the working fluid. Additional details of the PBMR and GT-MHR designs have been reported elsewhere in Refs. [1] and [2].

Key parameters of the PBMR and GT-MHR turbomachines are provided in Table I. Note that, where the GT-MHR utilizes a single shaft turbocompressor-generator (TC-Gen), the PBMR incorporates separate low-pressure (LP) and high-pressure (HP) turbocompressors (TC), plus a power turbine-generator (PT-Gen). Common features include the vertical orientation of the machinery, the working fluid, dry helium, and the use of magnetic bearings for support. Both the GT-MHR's turbocompressor-generator and the PBMR's power turbine-generator rotate at the 50 Hz synchronous speed of 3000 rpm; however, the PBMR's turbocompressors will operate at higher speeds. As would be expected from the relative configurations and power outputs of the two designs, the mass of the GT-MHR TC-Gen is substantially larger than that of the PBMR PT-Gen.

TABLE I. SUMMARY OF TURBOMACHINE CHARACTERISTICS IN THE PBMR AND GT-MHR

Parameter	**PBMR** [3]			**GT-MHR** [4]
Nominal Power (MWt/MWe)	265/110			600/285
Component	LP TC	HP TC	PT-Gen	TC-Gen
Orientation	Vertical	Vertical	Vertical	Vertical
Speed (rpm)	15,000	18,000	3000	3000
Mass (ton)	[TBD]	[TBD]	[~50]	105

3. AUXILIARY BEARING DESIGN CONSIDERATIONS

The requirements for auxiliary bearings evolve from a number of interrelated considerations. These include the basic characteristics of the machine in which they are installed and the characteristics of the system of which the machine is a part. In addition, there may be external environmental considerations (e.g. seismic) that affect both the machine and the system. In many cases, the considerations related to auxiliary bearing design are iterative in nature. That is, particular features of a machine or system may influence the selection of a particular auxiliary bearing concept and, conversely, the selection of a particular auxiliary bearing concept may significantly influence the design of the machine. A summary of some of the important considerations in auxiliary bearing design is given in Table II.

3.1. Auxiliary Bearing Options

As evidenced by Table II, auxiliary bearing design involves many diverse and often competing technical issues, which must be balanced in the requirements for any given application. The diversity in both requirements and applications has led to the development of several auxiliary bearing concepts, each having its own advantages and disadvantages. In general, the auxiliary bearing concepts in use today fall into four general categories. These are plain bearings, rolling element bearings, planetary bearings and zero-clearance auxiliary bearings.

3.1.1. Plain Auxiliary Bearings

Plain bearings represent the simplest and, potentially, the least expensive of the auxiliary bearing options. In their most basic form, they might comprise interfacing surfaces on the rotor and stator, which are configured to come into first contact in the event that electromagnetic bearing (EMB) support is lost or the capacity of the EMB's is exceeded.

More commonly, plain auxiliary bearings incorporate a tribologically compatible and replaceable wearing surface on either the rotor or stator or on both. This can be as simple as a plain bronze sleeve (radial) or thrust washer (axial), or can be much more sophisticated, involving highly engineered material pairs, and/or the use of compliant mountings to mitigate rotordynamics effects. Depending upon the characteristics and/or requirements of the application, lubrication provisions can be met by the working fluid, built into the materials themselves or provided from external sources.

An example of a sophisticated plain auxiliary bearing system is the rotor delevitation system (RDS) developed by Federal-Mogul (F-M) [5]. The F-M RDS employs special sintered bearing alloys that are impregnated with various lubricants, selected on the basis of particular design requirements. For smaller, simpler machines, the sintered components are mounted on sleeves or thrust washers. For larger and more complex machines, such as the 23MW motor-compressor developed for NAM (a partnership of Exxon and Shell in the Netherlands), the sintered material is mounted on individual bushing pads that comprise sectors of the auxiliary bearing (Fig. 1). In turn, the auxiliary bearing sectors are mounted on compliant springs (for damping) within an outer retaining ring that may be split for ease of maintenance. If required, the bushing pads in the corresponding axial auxiliary bearing (Fig. 2) may also be compliantly mounted.

TABLE II. AUXILIARY BEARING DESIGN CONSIDERATIONS

CHARACTERISTIC	CATCHER BEARING (CB) IMPLICATIONS
Machine Related	
Rotor Mass	Primary influence on CB sizing. Also affects CB design via rotordynamics and rundown times.
Shaft Orientation	Gravitational loads shared by multiple radial CBs in horizontal machines, usually concentrated in a single axial CB in vertical machines. Smaller influence on rotordynamic loads. Becomes more significant as size of machine increases.
Speed (rpm)	High speeds, particularly when combined with large shaft diameters, may reach DN (bore diameter x rpm) limits of CBs. Also influences rundown times.
Rotordynamics	Rotordynamics must be acceptable both on the EMBs and CBs, plus any combination of the two within the design basis (see Reliability/Risk Criteria).
EMB Limitations	When capacity of EMBs is exceeded, CBs must absorb excess loads.
System Related	
Reliability/Risk Criteria	Significant influence on the EMB design and the likelihood of partial vs. full EMB failures. This, in turn, is a primary determinant of the number and type (related to full vs. partial EMB failure) of demands on the CB during its lifetime. May determine the design objectives of the CB (i.e. to avoid vs. mitigate damage to the machine). Also potentially influences CB margins.
Number of Drops	Related to reliability/risk criteria. Likely to be the primary factor limiting life of CBs and potentially lead to need for in-service evaluation and/or replacement provisions.
Operating Environment	Includes temperatures, pressures and characteristics of working fluids, including contaminants. These factors would potentially impact CB materials selections. Also includes limitations placed by environmental requirements on CB options, e.g. lubricant limitations in GCRs.
Overspeed Criteria	Would affect CB design if an assumption of coincident EMB failure were imposed or if overspeed events result in loads that exceed the capacity of the EMBs.
System Induced Loads	These include mostly dynamic loads induced by operation of the system that might be a factor during a rundown event. An example would be unbalanced pressure loads across a turbine, which could potentially exceed the weight of the rotor.
Externally Induced Loads	Examples would be seismic requirements and shock loads from external explosions.
Rundown Time	In large applications, such as GCRs, primarily determined by the system response to EMB failure, plus active braking provisions. Absent system influences, rundown time would be determined by inertial energy stored in the rotor, plus deceleration forces, such as those associated with internal machine friction and windage.
Maintenance Criteria	For example, the extent to which CBs are available for inspection and/or replacement in standby service or following a rundown event.
Bearing Related	
Heat Generation and Dissipation	For a given application, the CB type would have an important influence on the heat generated during rundown and the provisions that are required to manage it.
Lubrication	Lubrication provisions for a given CB design will have a significant influence on heat generation during a rundown event. They may also influence the applicability or desirability of specific bearing design for a given application
Materials Characteristics	The characteristics of materials will influence the size of the CBs and the compatibility of the CBs with the machine and system.
Cooling Provisions	CB cooling provisions would allow higher loads and/or extended rundown periods.
Gap Control	In a zero clearance design, the capability exists to actively control the gap between the auxiliary bearings and supported shaft, providing additional control over machine rotordynamics during rundown.

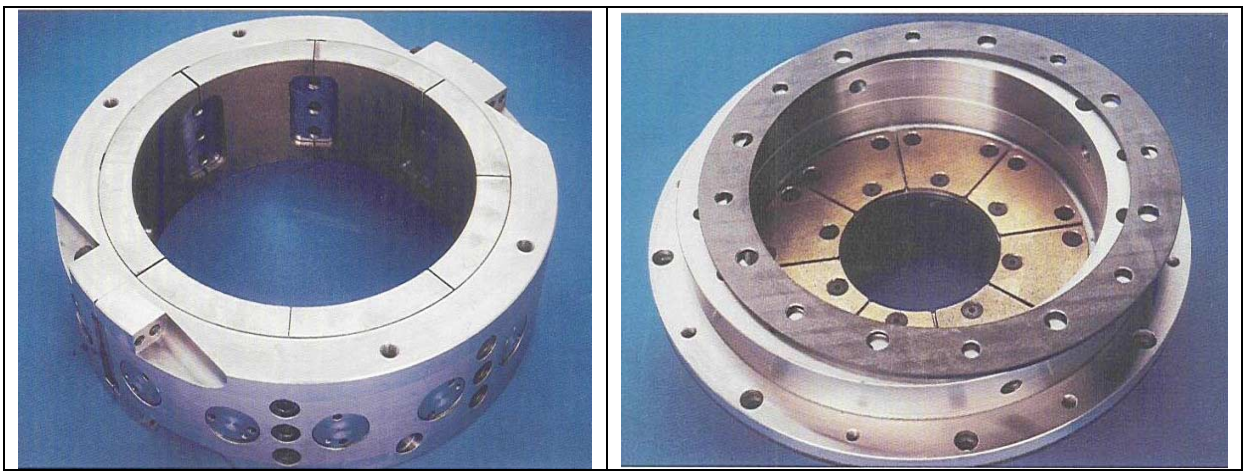

Figure 1. NAM Radial Auxiliary Bearing [5] Figure 2 NAM Axial Auxiliary Bearing [5].

3.1.2. Rolling Element Auxiliary Bearings

At present, the majority of large machines supported on EMB's incorporate rolling element auxiliary bearings for backup. The most common configuration is dual full-complement angular contact ball bearings mounted in a face-to-face preloaded configuration in order to prevent windage-induced motion under standby conditions. The angular contact design supports both radial and axial loads. Balls are preferred over rollers in such backup applications to minimize the potential for skidding during acceleration. Full-complement bearings (which are cageless) avoid the issue of cage-related failure modes, which were observed in earlier qualification tests for a GCR circulator (see Section 4.2.). In some applications, a clutch- or plain bearing-like material is provided at the rotor-bearing interface to moderate the initial acceleration and/or avoid rotor damage.

3.1.3. Planetary Auxiliary Bearings

In planetary auxiliary bearing concepts, an external ring surrounding the rotating shaft serves as a carrier for three or more individual rolling elements (planets) (Fig. 3). The number of planets and the type of rolling element depend upon the requirements of the specific application. The corresponding interface on the rotating shaft might be a hardened sleeve or a tribologically engineered surface, similar to that used in a plain bearing design, also depending on application requirements. The primary uses of planetary designs are with large diameter shafts and/or applications in which the rated speed (DN rating) of the bearing becomes an issue. This is because the planetary configuration reduces the effective DN requirement in accordance with the following formula:

$$\mathbf{DN = Rotor\ OD\ (mm) \times rpm \times \left[\frac{Bore}{OD}\right]_{Roller}}$$

In practice the ratio reduces the effective DN speed of the bearing by 0.5 or more [6].

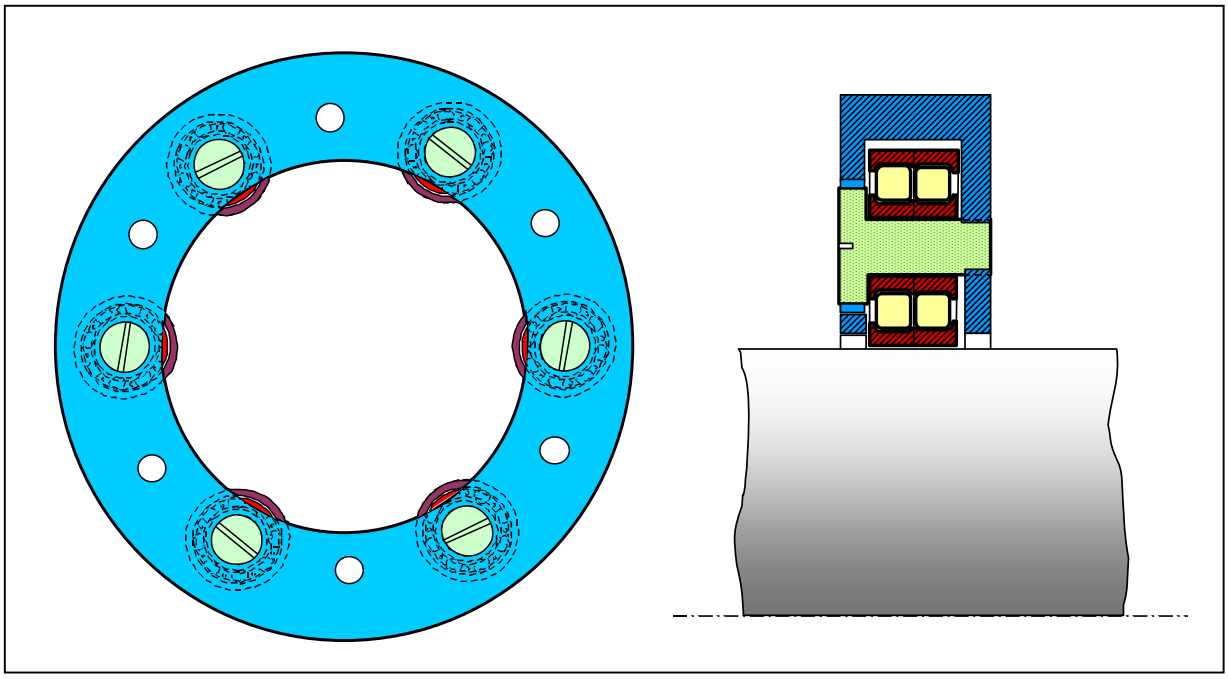

Figure 2. Planetary Auxiliary Bearing.

3.1.4. Zero-Clearance Auxiliary Bearing (ZCAB) [6][7]

The zero clearance auxiliary bearing (ZCAB), developed by Mohawk Innovative Technology Inc. (MITI) (Fig. 4), is a specialized variant of the planetary auxiliary bearing concept. Its particular objectives are to support the shaft with zero clearance when the auxiliary bearing is actuated and to provide a "get home" capability for certain defense-related aviation and marine applications.

In the ZCAB design, the azimuthal position of the planetary elements (typically five to eight) is maintained by a pair of drive rings, incorporating radial slots. The slots engage the individual shafts upon which the planetary elements are mounted and allow limited movement of the planetary elements toward and away from the machine rotor. The drive rings along with their planetary elements are, in turn, mounted within a separate support assembly that incorporates two support plates with spiral circumferential slots. These spiral circumferential slots also engage the individual shafts upon which the planetary elements are mounted. As the support plates are rotated relative to the drive rings, the planetary elements are moved closer to or further from the shaft. Through this means, the nominal clearance between the machine rotor and auxiliary bearings is closed when the auxiliary bearings are actuated. By reversing the process, control can be returned to the magnetic bearings upon their restoration. As is the practice with other auxiliary bearing designs, the support assembly is usually compliantly mounted to provide an additional measure of damping.

The relative movement between the drive rings and support plates and, thus, the clearance between the auxiliary bearings and machine rotor can be actively or passively controlled in either direction. In the specific example depicted in Figure 4, the ZCAB is held in the open position by a spring mechanism (F_s). In the event of failure of the radial EMB, or a loading in excess of its capacity, the rotor will impact one or more of the planetary elements. This results

in a tangential force (F_t), which moves the planetary element(s) and, thus, drive rings in the direction shown. This, in turn, causes the planetary elements to move inward and engage the rotor.

In instances where both axial and radial loads must be reacted, the outer ring of the planets can be modified to an elliptical form, which acts in conjunction with a corresponding groove in the shaft to withstand axial loads. An example of such an interface is provided in Fig 5 [8].

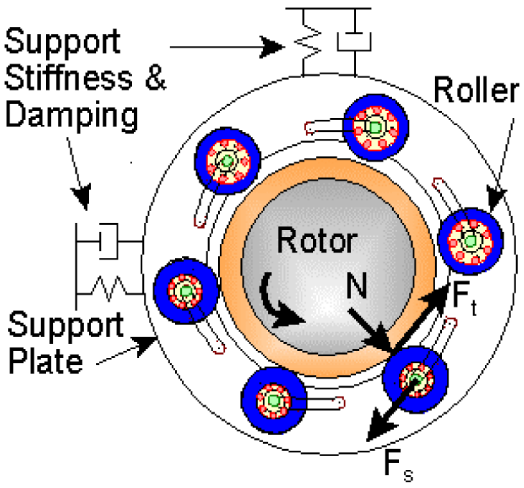

Figure 3. Zero-Clearance Auxiliary Bearing (ZCAB) [6].

Figure 4. ZCAB Providing Both Axial and Radial Support [8].

3.1.5. Hybrid Bearings

In addition to the individual bearing types described in the Sections 3.1.1 through 3.1.4, various permutations and/or combinations of these concepts can be considered. For example, one bearing type can be used for axial support while another is used for radial support. Additionally, the materials associated with the plain bearing types could be utilized in the interface between the rotating shaft and the various rolling element or planetary designs.

3.2. Advantages And Disadvantages Of Auxiliary Bearings

Each of the auxiliary bearing designs described in Section 3.1 has its own set of advantages and disadvantages. These are summarized in Table III.

Note that there is a fundamental tradeoff between plain auxiliary bearings and the low friction bearing types, which include both simple rolling elements and planetary configurations. The plain bearing types have significant advantages in terms of their simplicity, durability in standby service over extended periods of time and the ability to assess their condition without direct access or removal. However, these advantages come at the cost of greater friction and heat generation, which must be managed during rundown. The significance of this issue increases with higher loads and stored energy (primarily driven by rotor mass and speed). Furthermore, the tribological characteristics of plain auxiliary bearings have not yet been verified for the dry helium environment of the GCR designs.

By contrast, the low friction bearing types, and particularly the planetary designs, minimize the additional heat generated during a rundown event. However, the initial acceleration of the bearing is a very violent event, potentially leading to bearing damage or even failure. In addition, these bearings must survive long periods of standby service, prior to being called into service. During this period, undesired motion of the bearings must be prevented and damage by corrosion and/or contamination must be avoided. Furthermore, there is only limited potential for assessing the condition of the bearings, either as a preventative maintenance measure or following their use. One positive factor specific to GCR's is that the dry helium environment will tend to limit corrosion in standby service.

The advantages and disadvantages of planetary auxiliary bearings are similar to those for simple rolling element bearings, but with the additional advantage that the DN rating required of the individual planetary bearing elements is reduced. This desirable feature must be weighed against their additional complexity and cost.

The tradeoffs associated with the ZCAB concept are similar to those for other planetary designs; however, the ZCAB concept provides an additional capability to eliminate the rotor-bearing gap and allow enhanced control over shaft rotordynamics during a rundown event. As previously noted, the ZCAB design has also been developed to provide an extended runtime or “get home” capability in critical aviation and marine applications. However, both the extended runtime feature and the potential for ZCAB auxiliary bearings to provide axial support would need further evaluation in the context of GCR requirements.

4. AUXILIARY BEARING EXPERIENCE BASE AND IMPLICATIONS FOR GCR'S

As of the present, there are several hundred large turbomachines operating on magnetic bearings, with a cumulative experience base well in excess of 5 million operating hours [9]. The majority of these large machines are industrial compressors and turboexpanders, which are used in both the production and transportation of liquid and gaseous fuels. The size of these machines ranges up to 29 MW, with rotational speeds (not coincident) as high as 70,000 rpm.

While the existing experience base is substantial, there is little actual experience with vertical machines. Further, there is no field experience and only limited research specific to the conditions found in GCR's. To date, the largest vertically oriented machine on magnetic bearings is Korea Electric Power Company's Yoshino hydropower installation. The Yoshino machine is a 6 MW Francis turbine driving a generator, operating at 600 rpm [10, 11]. The weight of the rotor is 35 tons, about 2/3 of the weight of the PBMR rotor (~50 tons) and 1/3 of the weight of the GT-MHR rotor (105 tons).

There have been two related experimental programs specifically addressing auxiliary bearing issues for GCR's. James Howden Company conducted both of these programs, which supported both a proposed retrofit of the Fort St. Vrain power plant gas circulators with magnetic bearings and the gas circulator design for a modular steam cycle high temperature gas-cooled reactor (MHTGR)[12,13].

TABLE III. ADVANTAGES AND DISADVANTAGES OF AUXILIARY BEARING CONCEPTS

Technology	Advantages	Disadvantages
Plain Auxiliary Bearings	• Low-cost • Passive, no moving parts in bearing • Reduced potential for deterioration in standby mode • Condition, wear may be assessed by measuring clearance with EMB's	• Higher friction coefficients, heat generation during rundown
Rolling Element Auxiliary Bearings	• Low-cost • Low friction coefficients, heat generation during rundown • Potentially minimum volume with combined radial/thrust bearing	• Potential for bearing/cage damage during acceleration • Potential for deterioration in standby mode; contamination must be avoided • Windage induced rotation must be prevented in standby mode
Planetary Auxiliary Bearings	• Reduced DN for given rotor diameter and speed • Low friction coefficients, heat generation during rundown	• Greater complexity and cost • Contamination must be avoided • Windage induced rotation must be prevented in standby mode • Potential for acceleration damage (reduced relative to rolling element bearings)
Zero Clearance Auxiliary Bearings	• Eliminates rotor-bearing gap during rundown • Extended run time capability • Reduced DN for given rotor diameter and speed • Low friction coefficients, heat generation during rundown	• Greatest complexity and cost • Actuation failures should be considered • Contamination must be avoided • Windage induced rotation must be prevented in standby mode • Potential for acceleration damage (reduced relative to rolling element bearings)

4.1. Applicability of Experience in Horizontal Machines

For the auxiliary bearing, the primary difference between horizontal and vertical machines is the direction and distribution of loads. In a horizontal machine, the weight of the rotor is distributed over at least two radial auxiliary bearings if a complete failure of the magnetic bearing system occurs. In a vertical machine, the entire weight of the rotor is usually concentrated on a single axial auxiliary bearing. This concentration of load affects both the initial impact on the auxiliary bearing and the heat generated during the rundown, both of which must be sustained at one location.

By contrast, rotordynamic differences are likely to be of secondary importance, when comparing otherwise identical horizontal and vertical machines. Since rotordynamic response is determined by the physical characteristics of the shaft and the stiffness and damping of the supports, there would be little change in key dynamic parameters, such as critical speeds, if the location and characteristics of the auxiliary radial supports were comparable. One notable orientation-related difference is the reduced potential for backward whirling in horizontal machines that results from the stabilizing influence of gravity. However, experience indicates that the tendency for backward whirling in vertical machines can be controlled by appropriate design of the auxiliary bearings (See Section 4.2).

Given the rotordynamic similarities between horizontal and vertical machines, the sophisticated rotordynamic analysis tools now used to predict the behavior of horizontal machines can also be used for vertical applications. This includes the ability to predict and avoid the incidence of backward whirl. One caveat that applies to both orientations, however, is that the physical characteristics of the rotor components must be well understood. This can be problematical in some instances, such as accurately predicting the effective stiffness and internal damping of compressor, turbine, generator and coupling design features.

4.2. Howden Catcher Bearing System Development Tests

Initial design work by James Howden & Co. in the 1985 timeframe [14] resulted in the selection of rolling element bearings to back up the magnetic bearings in the gas circulator for the MHTGR. Balls were chosen over cylindrical rolling elements to avoid the potential for skidding at the ends of the rolling elements in the dry helium environment. The upper auxiliary bearing, which was required to provide both axial and radial support employed an angular contact design. The radial auxiliary bearing at the lower end of the circulator was of a deep groove ball bearing design that would provide radial support only. To moderate the initial acceleration transient imposed by axial loads on the upper auxiliary bearing, a graphite ring was incorporated at the rotor-bearing interface. The resulting radial/axial auxiliary bearing design for the MHTGR is schematically depicted in Figure 6.

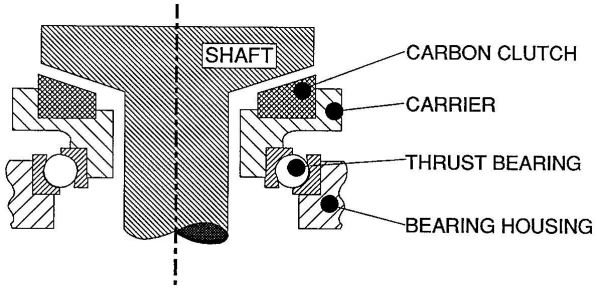

Figire 5. MHTGR Axial Auxiliary Bearing Configuration.

Given the lack of experience with auxiliary bearings in vertical machines, two separate research programs were conducted between 1988 and 1991, addressing the axial and radial support characteristics of the bearings, respectively. These are described in the following sections.

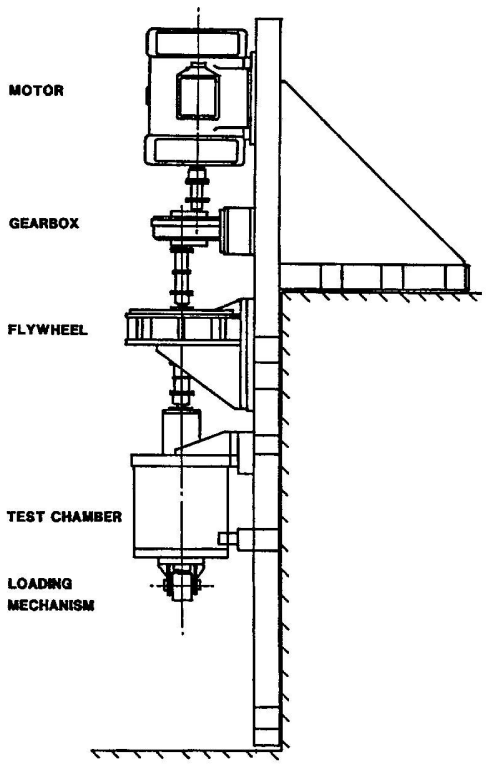

Figure 6. Axial Auxiliary Bearing Test.

4.2.1. Axial Support Tests [12]

In addition to the MHTGR circulator, the axial support tests were initially intended to support the prospective retrofit of the Fort St. Vrain High-Temperature Gas-Cooled Reactor (HTGR) circulators with magnetic bearings. On this basis, the maximum loads selected for the tests were 100 kN impact and 33 kN steady-state. Also the maximum speed for the tests was initially set at 10,500 rpm, based on Fort St. Vrain requirements. However, this was subsequently reduced to 6000 rpm, following the permanent closure of the Fort St. Vrain plant. A further objective of the tests was to achieve 20 drops on the axial auxiliary bearing from a height of 0.5 mm. This represented a factor of two margin relative to the MHTGR circulator design criteria, which was 10 drops.

The rig utilized for the axial bearing tests is graphically depicted in Figure 7. The test shaft was driven by an inverter/motor combination through a speed-up gearbox. A flywheel was incorporated to provide some inertia on the shaft and, when combined with continued operation of the motor, was adequate to represent the energy input during the bearing acceleration transient. The catcher bearing assembly test article was enclosed in a hermetically sealed enclosure, which contained dry helium corresponding to the MHTGR requirements.

A total of 7 test series were run with the number of drops in each ranging from six to thirty. The test series explored various options for the axial auxiliary bearing design, which are identified along with test results in Table IV. The significant conclusions of the axial auxiliary bearing tests are summarized in Table V.

4.2.2. Radial Support Tests [13]

While the axial tests were primarily concerned with the initial acceleration of the combined radial/axial auxiliary bearing at the upper end of the circulator, the radial tests were focused on the potential for backward whirling instabilities in the lower radial bearing. Simplified mathematical models of such instabilities had predicted the potential for very high dynamic loadings associated with movement of the rotor within the nominal clearance of 0.5 mm provided at the interface between the rotor and auxiliary bearings.

Based on preliminary scaling calculations completed during 1989, a suitably designed quarter-scale model was deemed adequate to model the behavior in the MHTGR circulator. The analytical evaluation also included a full assessment of the conditions required to initiate the feared orbital motion in the model. Paradoxically, it was found that initiation of the orbit motion could not be assured unless artificially induced.

The quarter-scale model developed through the analytical study is depicted in Figure 8. It comprises a rotor driven by an air motor located at the top of the rig, connected by a double universal drive. The rotor is initially spun up on ball bearings at the top and bottom of the rig. A release mechanism is provided that removes lateral support from both the top and bottom bearings simultaneously. Following release, the upper bearing support continues to provide axial support. A permanent magnet device is incorporated to ensure that the orbit motion is always initiated.

Initial tests quickly revealed that the orbit frequency quickly reached 38 Hz and was independent of shaft speed over a range of 5-20 Hz. It was concluded that the orbit frequency was unrelated to the dynamic characteristics of the system, but instead arrested by a balance between friction-induced acceleration forces and damping. However, the level of damping observed was substantially higher than expected. The source of the excess damping was at first a mystery, but finally identified as being the result of rolling friction, a normally negligible component in a linear system. However, it was subsequently shown that when the shaft is rolling within a track that has been “rolled up into a circle”, the normally small rolling resistance force becomes amplified by a factor equal to R/(R-r), where R is the hole radius and r is the shaft radius. The amplification factor in the model was approximately 200, and accounted for the excess damping. With this revelation, the results of the quarter-scale tests can be summarized as in Table VI.

5. DISCUSSION AND CONCLUSIONS

The large size and vertical orientation of the PBMR and GT-MHR turbomachines pose particular challenges in the design and development of auxiliary bearings. Field experience is limited, with only one large vertical machine, incorporating a 35-ton, 600-rpm rotor, presently operating on magnetic bearings. That compares with the ~50 ton PBMR rotor and the 105 ton GT-MHR rotor, both of which will operate at 3000 rpm. The remaining experience is derived from EMB-equipped flywheels and limited testing in support of GCR circulators, both of which relate to smaller, albeit higher speed machines.

TABLE IV. HOWDEN AXIAL AUXILIARY BEARING TEST SUMMARY

Feature	Options Tested	Test Results
Bearings	RHP 7224 • 25 degree contact angle • Inner ring centered solid brass cage	Series 1: Bearing failure attributed to lubrication breakdown. Series 2: Severe cage wear after 27 drops. Evidence of local heating at cage/inner race interface. However, bearing remained functional.
	SKF 7224BM • 40 degree contact angle • Rolling element centered solid brass cage	Series 3: Bearing undamaged after 30 drops. Series 4-7: Cage cracking or fracture after 6-18 drops, however, running elements of bearing remained undamaged, functional. Cage fractures attributed to difference in processing vs. bearing in Series 3.
Lubricants	Kluber Barrierta 1MI	Lubrication failure, discontinued after first test series
	Dupont Krytox 250AC (High temperature grease)	Acceptable in remaining test series
Rubbing Materials	Electrographite (Morganite EY308	Cracking observed after first test series (10 drops), severe cracking after 3 test series, totaling 67 drops
	Carbon fibre reinforced graphitized carbon (Dunlop CB7 or similar)	No observable damage after two test series (16 drops)
Cone Angle	15.0 degrees	Insignificant radial support
	27.5 degrees	No significant improvement in radial support. Increased angle resulted in faster acceleration, greater damage potential

TABLE V. SIGNIFICANT RESULTS AND CONCLUSIONS OF HOWDEN AXIAL AUXILIARY BEARING TESTS

1. Axial auxiliary bearing design for the MHTGR circulator successfully qualified for 10-drop criteria.
2. Both of the angular contact ball bearings tested were found acceptable
• Rolling element-centered cage (SKF bearing) judged to be preferable
• Sand blasting of cage in Series 3 bearing apparently reduced residual stresses from manufacture, avoided cracking seen in other test series with SKF bearings
• Higher strength cage materials should be considered
3. Clutch cone angles do not provide significant radial support. Higher cone angles may aggravate acceleration-related damage.
4. The observed friction coefficients in the carbon based clutch materials were significantly lower than expected. It is possible that carbon debris generated at the interface forms a rolling lubricant, reducing the friction.
5. Both graphite and carbon reinforced carbon clutches were satisfactory, with the latter preferred.

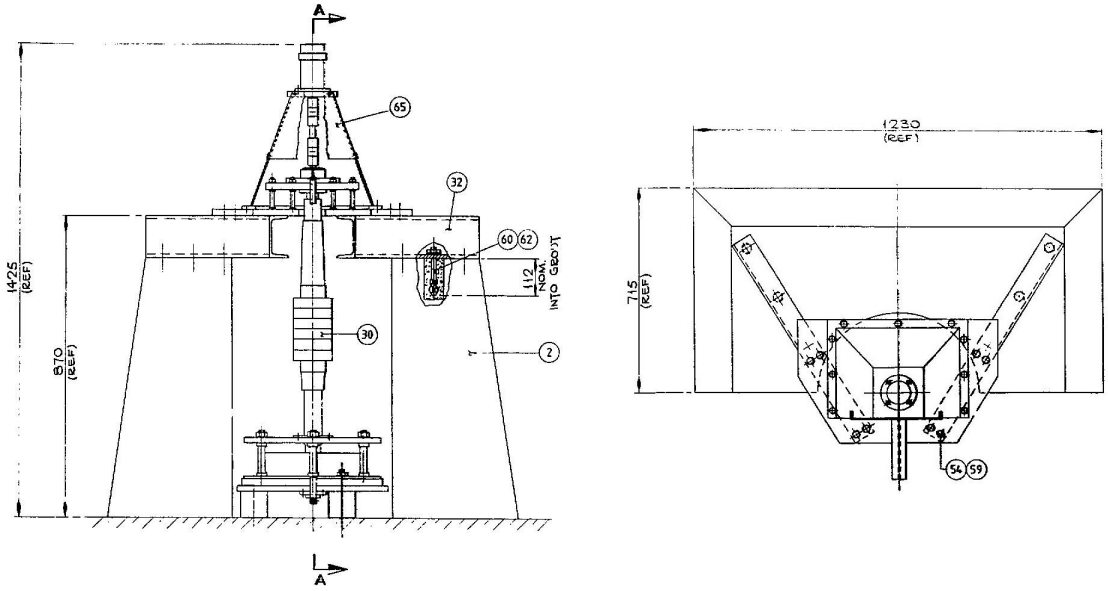

Figure 7. Radial Auxiliary Bearing Test Rig.

TABLE VI. SIGNIFICANT RESULTS AND CONCLUSIONS OF HOWDEN RADIAL AUXILIARY BEARING TESTS

1. Orbital motion of the rotor is a real phenomenon that can be induced for a wide range of operating conditions.
2. Arrestment of orbital speed was unrelated to any dynamic phenomenon; rather, the orbital speed would increase rapidly until damping energy balanced the input energy due to friction.
3. Energy loss due to structural and shaft damping processes by themselves cannot limit the orbit speed and resulting radial loads to tolerable levels, unless the bearing friction coefficient is impracticably low or an extraordinary level of damping is incorporated.
4. Orbit arrestment speeds were consistently below that explained by structural damping alone. Follow-up analyses indicated that rolling resistance at the shaft-bearing interface accounted for the unexplained energy absorption.
• Normally negligible, but becomes the dominant factor in a close conformity rolling geometry
• Resulting force scales with the ratio of bearing diameter to bearing clearance
5. Rolling resistance loss can limit the orbit speed and radial forces to tolerable levels and can provide an engineering basis for control of rotor behavior on failure of the magnetic bearing system.

Not withstanding the above, the technical basis for radial auxiliary bearings in large vertical machines appears to be established. Over 5 million hours of operation have accumulated in large horizontal machines on magnetic bearings, and the rotordynamic issues that are the principal concern with the vertical radial bearings are common to both horizontal and vertical machines. Rotordynamic analysis tools presently available are believed to be adequate for either orientation. Further, the Howden vertical rotor tests, described in Section 4.2, provide additional assurance that the rotordynamic responses in a large vertical machine can be adequately managed by appropriate design. For the radial auxiliary bearings, there appears to

be no compelling advantage for either the plain bearings or low-friction designs that are likely to be considered for this size application. The principal tradeoff will be in terms of minimal heat generation (low friction) vs. low maintenance (plain).

The axial auxiliary bearing, however, remains a significant challenge, due to the high loads and associated heat generation that are likely to be encountered during the rundown process. This is aggravated by the fact that the generator must be disconnected from the grid at the start of the rundown transient and that provisions for dynamic braking are both difficult and expensive. These factors clearly favor low-friction designs, and it is likely that development and testing of the axial auxiliary bearings will be required.

Finally, the reliability of magnetic bearings continues to improve, leveraging on the continuing major advancements in both computers and power electronics. Given a level of redundancy appropriate to the size of the GCR machines, it should be possible to develop a bearing support system that would place minimal demands on the auxiliary bearings. In this context, the number of rundowns and the criteria for success (e.g. damage avoidance vs. damage mitigation) are open to further discussion.

Consideration of the above leads to the following conclusions:

1. The design of the primary EMB support system should be such that the likelihood of a rundown on the auxiliary bearings is minimized, preferably being not likely to occur within the lifetime of the plant.
2. The technical basis for rotordynamic design of the radial auxiliary bearings is presently in hand and is adequately supported by computer modeling techniques. While it appears that either plain or planetary auxiliary bearing designs could be applied, management of the heat generated during rundown must be addressed for either type.
3. The key to the design of the axial auxiliary bearings in the GCR designs will be management of the heat generated during the rundown process. This is presently viewed as problematical in these machines. Of the auxiliary bearing designs described in this paper, this would tend to favor the rolling element concepts, given their lower friction coefficients. Active cooling provisions are likely to be required during the rundown process.
4. Testing of axial auxiliary bearing design alternatives is recommended, preferably at full-scale.

REFERENCES

[1] Nicholls, D.R. “Status of the Pebble Bed Modular Reactor”, Presented at the EPRI Helium Gas Reactor Workshop, Palo Alto, CA, December 7-8, 1999.

[2] Simon, W. “Status and Current Activities of the International GT-MHR Program”, Presented at the EPRI Helium Gas Reactor Workshop, Palo Alto, CA, December 7-8, 1999.

[3] http://www.pbmr.com/pebbed3/Simulate/800.html, October 2000.

[4] Rodwell, E. “Helium Gas Turbine Reactor Technical Challenges”, TP-114690, EPRI, Palo Alto, CA, January 2000.

[5] *Federal Mogul News Update*, Federal-Mogul Magnetic Bearings, Mystic, CT, Number 4, 1999.

[6] Chen, H.M. Walton, J. Heshmat, H. “Test of a Zero Clearance Auxiliary Bearing”, *Proc. of the MAG ’97 Industrial Conference and Exhibition on Magnetic Bearings*, MITI, Albany, NY, August 21-22, 1997.

[7] "Zero Clearance Auxiliary Bearing Developed", http://www.albany.net/~miti/feb99.htm, downloaded, October 20, 2000.
[8] "Auxiliary Bearing Developed for 140mm Shaft with 1000 Pound Load at 18,000 RPM", http://www.albany.net/~miti/sep99.htm, downloaded October 20, 2000.
[9] *Turbomachines Reference List*, S2M, St. Marcel, France, June 9, 2000.
[10] "35 Tons Load Capacity", *Actidyne News*, S2M, St. Marcel, France, September 1998, p. 3.
[11] Yamaishi, K. "Applications and Performance of Magnetic Bearing for Water Turbine and Generator", Nippon Koei Co. Ltd. Yokohama, Japan, Circa 1997.
[12] Rennie, J.A. *Catcher Bearing System Development and Test, Thrust Bearing Tests – Final Report*, TR7404, Prepared by James Howden & Co. Renfrew, Scotland for EPRI, Palo Alto, CA, June 14, 1991.
[13] Fraser, W.M, Catcher Bearing Development and Test, Final Report on Dynamic Behaviour of a Gas Circulator Rotor During Run-Down in Catcher Bearings, TN7411, Prepared by James Howden & Co. Renfrew, Scotland for EPRI, Palo Alto, CA, May 30, 1991.
[14] Lewis, M.W.J. "Helium Gas Circulator Catcher Bearing Selection and Design", NCT Report 2585/451 prepared for James Howden & Co. Renfrew, Scotland, August 1985.

LIST OF PARTICIPANTS

R. Ballinger	Massachusetts Institute of Technology, United States of America
E. Breuil	Framatome, France
H. Brey	United States of America
A. Chudin	MINATOM, Russian Federation
R. Couturier	CEA, E.E.N., France
D. Favet	Framatome, France
P. Florido	Comision Nacional de Energia Atomica, Argentina
V. Golovko	OKBM, Russian Federation
A. Heek	NRG, Netherlands
J. Hufnagel	Exelon, United States of America
P. Karcz	US Department of Energy, United States of America
J. Kendall	International Atomic Energy Agency
N. Kodochigov	OKBM, Russian Federation
P. Kumar	PBMR, South Africa
M. Lecomte	Framatome, France
L. Loflin	Electric Power Research Institute, United States of America
B. Marsden	AEA Technology, United Kingdom
Y. Muto	JAERI, Japan
S. Penfield	Technology Insights, United States of America
E. Rodwell	Electric Power Research Institute, United States of America
P. Roebuck	US Department of Energy, United States of America
W. Roscoe	PBMR, South Africa
A. Shenoy	General Atomics, United States of America
Y. Sun	INET, Tsinghua University, China
M. Tanihira	Mitsubishi Heavy Industries, Japan
Y. Tsuchie	Japan Atomic Power Co., Japan
J. Wong	US Department of Energy, United States of America
X. Yan	JAERI, Japan